USGS
science for a changing world

Water Availability and Use Science Program

Volcanic Aquifers of Hawai‘i—Hydrogeology, Water Budgets, and Conceptual Models

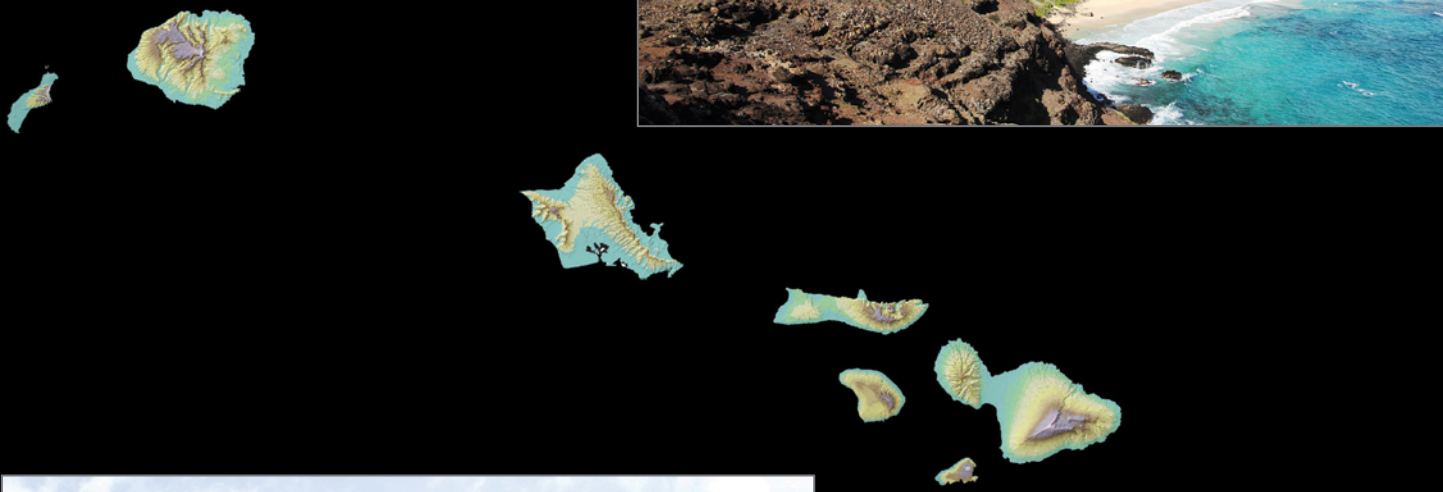

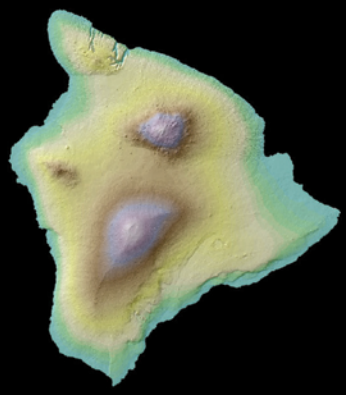

Scientific Investigations Report 2015–5164
Version 2.0, March 2018

U.S. Department of the Interior
U.S. Geological Survey

Cover. Shaded-relief map of the main Hawaiian Islands and photographs of thin shield-stage lava flows exposed in eroded cliffs of the Ko‘olau volcano (upper right) and dikes cutting across shield-stage lava flows exposed in an eroded cliff of the Wai‘anae volcano, O‘ahu (lower left). Photographs by Scot Izuka, U.S. Geological Survey.

Volcanic Aquifers of Hawai‘i—Hydrogeology, Water Budgets, and Conceptual Models

By Scot K. Izuka, John A. Engott, Kolja Rotzoll, Maoya Bassiouni, Adam G. Johnson, Lisa D. Miller, and Alan Mair

Water Availability and Use Science Program

Scientific Investigations Report 2015–5164
Version 2.0, March 2018

U.S. Department of the Interior
U.S. Geological Survey

U.S. Department of the Interior
RYAN K. ZINKE, Secretary

U.S. Geological Survey
William H. Werkheiser, Deputy Director
exercising the authority of the Director

U.S. Geological Survey, Reston, Virginia
First release: 2016, online
Revised: March 2018 (ver. 2.0), online

Suggested citation:
Izuka, S.K., Engott, J.A., Rotzoll, Kolja, Bassiouni, Maoya, Johnson, A.G., Miller, L.D., and Mair, Alan, 2018, Volcanic aquifers of Hawai'i—Hydrogeology, water budgets, and conceptual models (ver. 2.0, March 2018): U.S. Geological Survey Scientific Investigations Report 2015-5164, 158 p., https://doi.org/10.3133/sir20155164.

ISSN 2328-0328 (online)

Geographic and Geologic Names

Geographic names in this report are largely consistent with the U.S. Geological Survey (USGS) Geographic Names Information System (GNIS) (http://geonames.usgs.gov/), including the use of the ʻokina (ʻ) and kahakō (¯) diacritical marks in Hawaiian names. The diacritical marks are not used, however, in anglicized derivations from Hawaiian names (for example, the ʻokina appears in the name "Hawaiʻi" but not in the derivation "Hawaiian"), or where a place name appears without the diacritical marks in an established proper noun or title in a cited reference. Names of geologic formations and features are consistent with the State geologic map by Sherrod and others (2007).

The entire group of Hawaiian Islands and the largest island in the group are named "Hawaiʻi." To avoid confusion, the island group is referred to as "Hawaiʻi" and the largest island is referred to as "Hawaiʻi Island." Other islands (for example, Oʻahu, Maui, and Kauaʻi) are simply referred to by their names because there is no potential for confusion with other geographic entities.

State Well Numbers

Since 1971, Hawaii's well-numbering system has contained seven digits. The first digit distinguishes the island, which is then followed by a dash separator. The next four digits represent the grid system, with the first two digits representing minutes of latitude and the second two digits representing minutes of longitude for that grid (using leading zeroes for minute values less than 10). To distinguish wells within a minute grid, two digits were added following the 4-digit minute-grid numbers with a dash separator, and are sometimes referred to as a sequence number.

In 2012, Hawaii's well-numbering system was modified to accommodate more wells than the previous numbering system would allow. The sequence number was changed from two digits to three digits, allowing for a grid to have 100 or more wells. If the sequence number is less than 100, the new numbering system places a zero in front of the 2 digits. References to wells in this report will only use a two-digit sequence number when the sequence number is less than 100.

Acknowledgments

The authors are grateful to the following people who contributed expertise and data to this study: Tui Anderson (Maui County Department of Water Supply), Robert Chenet (Commission on Water Resource Management [CWRM]), Abby Frazier (University of Hawaiʻi at Mānoa), Neal Fujii (CWRM), Thomas Giambelluca (University of Hawaiʻi at Mānoa), Stephen Gingerich (USGS Pacific Islands Water Science Center), Samuel Gon, III (The Nature Conservancy), Jim Jacobi (USGS Pacific Island Ecosystems Research Center), Heather Jeppesen (USGS Pacific Islands Water Science Center), Jim Kauahikaua (USGS Hawaiian Volcano Observatory), Tracy Nishikawa (USGS California Water Science Center), Lenore Ohye (CWRM), Delwyn Oki (USGS Pacific Islands Water Science Center), Joel Robinson (USGS Volcano Science Center), Scott Rowland (University of Hawaiʻi at Mānoa), Carolyn Sawai (Honolulu Board of Water Supply), David Sherrod (USGS Cascades Volcano Observatory), Norris Uehara (Hawaiʻi Department of Health), Dean Uyeno (CWRM), Norman Verbanic (Hawaiʻi Electric Light Company), Anela Whisenhunt (USGS Pacific Islands Water Science Center), and Robert Whittier (Hawaiʻi Department of Health).

Contents

Figures

Tables

Conversion Factors

[Inch/pound to International System of Units]

Multiply	By	To obtain
inch (in.)	25.4	millimeter (mm)
foot (ft)	0.3048	meter (m)
mile (mi)	1.609	kilometer (km)
acre	4,047	square meter (m^2)
square foot (ft^2)	0.09290	square meter (m^2)
square mile (mi^2)	2.590	square kilometer (km^2)
gallon (gal)	3.785	liter (L)
cubic inch (in^3)	16.39	cubic centimeter (cm^3)
cubic foot (ft^3)	0.02832	cubic meter (m^3)
foot per day (ft/d)	0.3048	meter per day (m/d)
million gallons per day (Mgal/d)	0.04381	cubic meter per second (m^3/s)

Temperature in degrees Celsius (°C) may be converted to degrees Fahrenheit (°F) as follows:

°F=(1.8×°C)+32

Temperature in degrees Fahrenheit (°F) may be converted to degrees Celsius (°C) as follows:

°C=(°F-32)/1.8

Horizontal coordinate information is referenced to the North American Datum of 1983 (NAD 83).

Altitude, as used in this report, refers to distance above mean sea level.

Concentrations of chemical constituents in water are given in milligrams per liter (mg/L).

Volcanic Aquifers of Hawai‘i—Hydrogeology, Water Budgets, and Conceptual Models

By Scot K. Izuka[1], John A. Engott[1], Kolja Rotzoll[2], Maoya Bassiouni[1], Adam G. Johnson[1], Lisa D. Miller[1], and Alan Mair[1]

Abstract

Hawai‘i’s aquifers have limited capacity to store fresh groundwater because each island is small and surrounded by saltwater. Saltwater also underlies much of the fresh groundwater. Fresh groundwater resources are, therefore, particularly vulnerable to human activity, short-term climate cycles, and long-term climate change. Availability of fresh groundwater for human use is constrained by the degree to which the impacts of withdrawal—such as lowering of the water table, saltwater intrusion, and reduction in the natural discharge to springs, streams, wetlands, and submarine seeps—are deemed acceptable. This report describes the hydrogeologic framework, groundwater budgets (inflows and outflows), conceptual models of groundwater occurrence and movement, and the factors limiting groundwater availability for the largest and most populated of the Hawaiian Islands—Kaua‘i, O‘ahu, Maui, and Hawai‘i Island.

The bulk of each of Hawai‘i’s islands is built of many thin lava flows erupted from shield volcanoes; the great piles of lava flows form highly permeable aquifers. In some areas, low-permeability dikes cutting across the lava flows, or low-permeability ash and soil horizons interlayered with the lava flows, can substantially alter groundwater flow. On some islands, sedimentary rocks form thick semiconfining coastal-plain deposits, locally known as caprock, that impede natural groundwater discharge to the ocean. In some regions, thick lava flows that ponded in preexisting depressions form aquifers that are much less permeable than aquifers formed by thin lava flows.

Fresh groundwater inflow to Hawai‘i’s aquifers comes from recharge. For predevelopment conditions (1870), estimates of groundwater recharge from this study are 871, 675, 1,279, and 5,291 million gallons per day (Mgal/d) for Kaua‘i, O‘ahu, Maui, and Hawai‘i Island, respectively. Estimates of recharge for recent conditions (2010 land cover and 1978–2007 rainfall for Kaua‘i, O‘ahu, and Maui; 2008 land cover and 1916–1983 rainfall for Hawai‘i Island) are 875, 660, 1,308, and 6,595 Mgal/d for Kaua‘i, O‘ahu, Maui, and Hawai‘i Island, respectively. Recent recharge values differ from predevelopment recharge values by only a few percent for all islands except Hawai‘i Island, where changes in forest cover affected recharge. Spatial distribution of recharge mimics the orographic rainfall pattern—recharge is high on windward slopes and mountain peaks below the top of the trade-wind inversion. Human activity such as irrigation also contributes to recharge in some areas.

Outflows from Hawai‘i’s aquifers include withdrawals from wells and natural groundwater discharge to springs, streams, wetlands, and submarine seeps. Under predevelopment conditions, groundwater withdrawal is assumed to be negligible and natural groundwater discharge probably was equal, or close, to recharge. Under recent conditions (2000–2010), groundwater withdrawal averaged 19, 209, 104, and 103 Mgal/d on Kaua‘i, O‘ahu, Maui, and Hawai‘i Island, respectively. If recent withdrawal and recharge rates are maintained until steady state is achieved, natural groundwater discharge will be reduced by an amount equal to the withdrawal rate. Total recent withdrawal for the four islands is only about 5 percent of total recharge, but about half of the withdrawal comes from O‘ahu, whereas O‘ahu receives only 7 percent of the total recharge. Effects of high withdrawals on O‘ahu cannot be mitigated by the lower withdrawals on other islands because no freshwater flows between islands. Even within an island, high withdrawals from one area cannot be completely mitigated by recharge in another area. Water-level, saltwater/freshwater-transition-zone, spring, and stream base-flow data indicate an overall reduction in storage for most areas where groundwater has been developed.

Groundwater occurrence and movement in Hawai‘i’s volcanic aquifers can be described in terms of four conceptual models: (1) fresh groundwater lenses in high-permeability lava-flow aquifers, (2) aquifers with groundwater impounded by dikes, (3) thickly saturated low-permeability aquifers, and (4) perched aquifers. In Hawai‘i, most fresh groundwater withdrawn for human use comes from freshwater lenses in the dike-free high-permeability lava-flow aquifers where the principal limiting factor to groundwater availability is saltwater intrusion, but impacts of reduced natural groundwater discharge may also limit availability. Dike-impounded groundwater is common near the center of Hawaiian shield volcanoes, where water moves and is stored in permeable lava flows between the dikes; groundwater availability in these aquifers is primarily limited by storage depletion and reduction of flow to adjacent aquifers and natural groundwater discharge. Thickly saturated low-permeability aquifers have been identified on Kaua‘i and Maui; groundwater availability is primarily limited by streamflow depletion and water-table decline. Perched groundwater is postulated to exist in some areas of Hawai‘i, but store much less water than other modes of

[1]U.S. Geological Survey.

[2]Water Resources Research Center, University of Hawai‘i.

groundwater occurrence. Limits on groundwater availability in perched aquifers include the potential of reducing inflow to other groundwater settings and reducing natural discharge and stream seepage. Some groundwater bodies in Hawai‘i are enigmatic; consequences of groundwater development in these bodies and their relation to groundwater availability are not completely understood.

Introduction

The eight main islands in the Hawaiian archipelago—Ni‘ihau, Kaua‘i, O‘ahu, Moloka‘i, Lāna‘i, Kaho‘olawe, Maui, and Hawai‘i Island (fig. 1)—are the emergent tops of enormous basaltic shield volcanoes that rise from the floor of the Pacific Ocean. An island may be formed by one or more shield volcanoes (table 1). The volcanoes form the principal aquifers on which 1.36 million residents (U.S. Census Bureau, 2011), diverse industries, and a large component of U.S. military presence in the Pacific rely upon for freshwater. Natural discharge from the aquifers feeds springs, wetlands, and base flow (groundwater discharge to streams) that are used for cultural practices, aesthetics and recreation, and habitat for aquatic biota, including some endangered species. Groundwater also discharges at and below sea level near the coast, providing freshwater to near-shore ecosystems.

Hawai‘i volcanic aquifers have limited capacity to store fresh groundwater because the islands are small and isolated from each other by seawater. Saltwater also underlies much of the fresh groundwater (fig. 2). Fresh groundwater resources in Hawai‘i are therefore particularly vulnerable to the effects of human activity, short-term climate cycles, and long-term climate change.

Because of their importance to humans and natural ecosystems, the Hawai‘i volcanic aquifers are considered among the principal regional aquifers in the United States (Reilly and others, 2008), and have been part of periodic national groundwater assessments by the U.S. Geological Survey (USGS) since the 1920s. The last assessments prior to this study were the Regional Aquifer System Analysis (RASA) of the 1980s–90s (Nichols and others, 1996), and the Hawai‘i chapter in Segment 13 of the Groundwater Atlas of the United States (Oki and others, 1999a). Since then, rates of groundwater use have changed as a result of population growth, changing agricultural needs, and improvements in conservation and management. Rates of groundwater recharge have also changed as a result of changes in irrigation practices, vegetation cover, and climate. New data, technologies, methods, and studies have advanced our understanding of climate, geology, and hydrology in Hawai‘i, and indicate that early concepts of groundwater occurrence do not describe all parts of Hawai‘i. An updated evaluation of Hawai‘i’s groundwater resources is needed to address questions about the availability of fresh groundwater for human use now and into the future.

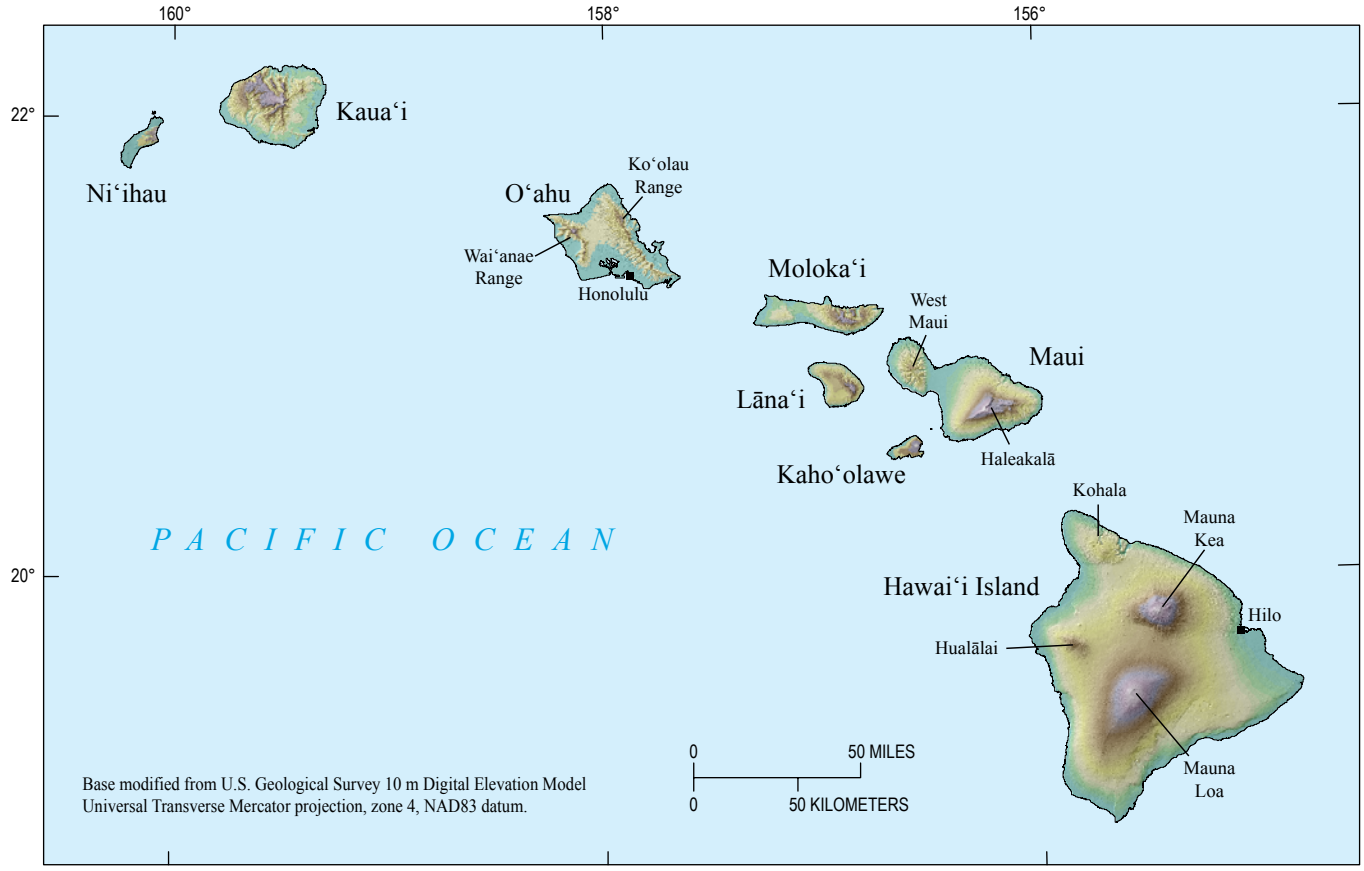

Figure 1. Map of the main Hawaiian Islands.

Table 1. Summary of geographic data for the main islands of Hawai'i.

[Shield volcanoes listed are only for subaerial part of island; submarine volcanoes that may be part of an island's massif are not listed. Population from U.S. Census Bureau, 2011; land area and highest altitude from Juvik and Juvik, 1998]

Island	Population		Land area		Population density (persons per square mile)	Highest altitude (feet)	Shield volcanoes
	Persons	Percent of total	Square miles	Percent of total			
Hawai'i	185,079	13.6	4,028	63	46	13,796	Kohala Hualālai Mauna Loa Mauna Kea Kīlauea
Maui	144,444	10.6	727	11	199	10,023	West Maui Haleakalā
Lāna'i	3,135	0.2	141	2	22	3,366	Lāna'i
Kaho'olawe	0	0	45	1	0	1,483	Kaho'olawe
Moloka'i	7,345	0.5	260	4	28	4,970	West Moloka'i East Moloka'i
O'ahu	953,207	70.1	597	9	1,597	4,025	Wai'anae Ko'olau
Kaua'i	66,921	4.9	552	9	121	5,243	Kaua'i
Ni'ihau	170	<0.1	70	1	2	1,281	Ni'ihau
Total	1,360,301		6,420				

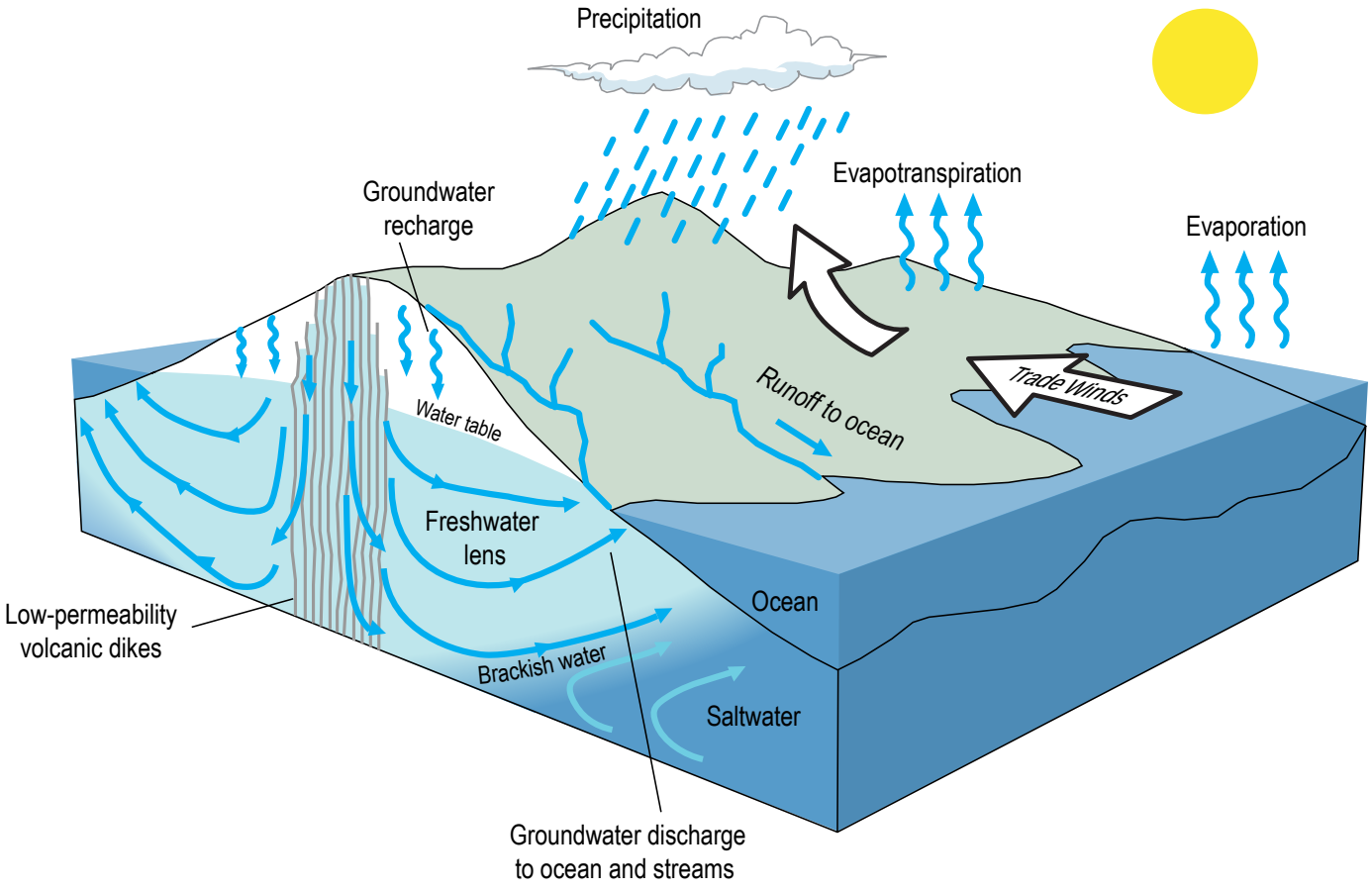

Figure 2. Relation of fresh groundwater to precipitation, evapotranspiration, runoff, and saltwater from the ocean in the Hawaiian Islands.

Groundwater Availability—Any groundwater withdrawal by humans affects the resource to some degree; even withdrawing water at a small fraction of the inflow (recharge) rate will have an impact. Groundwater availability for human use is limited by the impacts that are deemed acceptable by the community or those to whom water-resource management has been delegated. Assessment of groundwater availability thus requires, to the extent possible by analysis of available data, identification and quantification of the impacts of withdrawals. Four principles are fundamental to understanding the effects of withdrawing groundwater (fig. 3):

1. The groundwater system is dynamic—groundwater in the aquifer is constantly flowing from inflow points (recharge areas) to outflow points (natural discharge to springs, streams, wetlands, and submarine seeps, as well as artificial withdrawals at wells).

2. Prior to groundwater development (withdrawal by wells), the aquifer is in a steady-state condition (fig. 3*A*), that is, the long-term average inflow rate balances the long-term average outflow rate:

$$\text{Inflow} = \text{Predevelopment Natural Outflow}. \quad (1)$$

3. Artificial groundwater withdrawal (pumping from wells) adds another outflow component and upsets the predevelopment balance (fig. 3*B*). The system will adjust toward a new balance—the water withdrawn from the wells initially comes from storage, but as time progresses, more and more of the withdrawal is compensated by reductions in groundwater discharge to springs, streams, wetlands, and submarine seeps. During this adjustment period, the aquifer is in a transient condition, and the mass balance of water is given by:

$$\text{Inflow} = \text{Natural Outflow} + \text{Withdrawal} + \text{Change in storage}. \quad (2)$$

4. If withdrawals are not too excessive, the system will eventually achieve a new steady-state condition, storage reduction will cease, and the outflow rate will again equal the inflow rate:

$$\text{Inflow} = \text{New Natural Outflow} + \text{Withdrawal}. \quad (3)$$

The new steady-state storage volume will be smaller than the original volume (fig. 3*C*); the difference in the volumes is known as groundwater-storage depletion.

These principles were presented in a classic paper by Theis (1940) and are universal, but application of the principles differs between Hawai‘i’s aquifers and continental aquifers in two important ways. First, Theis (1940) wrote that withdrawing water from a well could increase recharge into the aquifer by inducing seepage from perennial surface-water bodies (for example large lakes and rivers). Although theoretically true in Hawai‘i, few large perennial bodies of fresh surface water exist in the islands; thus, well withdrawals in most cases cannot induce more recharge—they can only reduce natural outflows to achieve a new balance between inflows and outflows. Second, in noncoastal continental aquifers, fresh groundwater storage depletion resulting from withdrawal from wells is manifest in a decline in groundwater levels. In coastal and island aquifers, however, depletion of fresh groundwater storage also results in a rise of saltwater—in other words, the freshwater body in the aquifer shrinks from above and below (fig. 4). Therefore, any artificial groundwater withdrawal in Hawai‘i will cause a lowering of water levels and a rise of saltwater until the rate of artificial withdrawal is compensated by an equivalent reduction in the natural discharge rate to springs, streams, wetlands, and submarine seeps. In a given location, the magnitude of each of these impacts depends on the rates and distribution of recharge, rates and distribution of withdrawal, and the geologic structure and distribution of hydraulic properties of the aquifer. Fresh-groundwater availability for human use is limited by the impacts that a community deems acceptable.

An extreme case of groundwater storage depletion would result from withdrawing more freshwater than the aquifer receives from recharge or other inflows. This situation, sometimes referred to as “groundwater mining,” is not sustainable and eventually will result in the complete depletion of the resource. Groundwater mining will not be considered further in this report because it is primarily a problem in heavily pumped aquifers in arid regions (Reilly and others, 2008). In coastal aquifers, where the freshwater resource overlies saltwater, steady state could theoretically be achieved even if withdrawal exceeds freshwater recharge, but in this case, at least part of the water withdrawn from wells would be salty. Although it can happen in Hawai‘i, management strategies are in place to protect Hawai‘i’s principal aquifers from such overdraft (see, for example, Wilson Okamoto Corporation, 2008).

Besides water quantity, water quality can also limit groundwater availability. Contamination can make groundwater unavailable for some uses. In particular, saltwater that naturally underlies much of Hawai‘i’s fresh groundwater resources can mix with the freshwater, making it undesirable for uses such as drinking water or irrigation. A study of groundwater quality by the USGS National Water-Quality Assessment Program in 1999–2001 found anthropogenic contamination—for example, fumigants, solvents, herbicides, and elevated concentrations of nutrients—in water from public-supply and monitoring wells on O‘ahu (Anthony and others, 2004). In the present study, water quality is discussed only with regard to encroachment of saltwater and brackish water on the freshwater resource. Assessment of the limitations to groundwater availability related to anthropogenic contamination is not within the scope of this study.

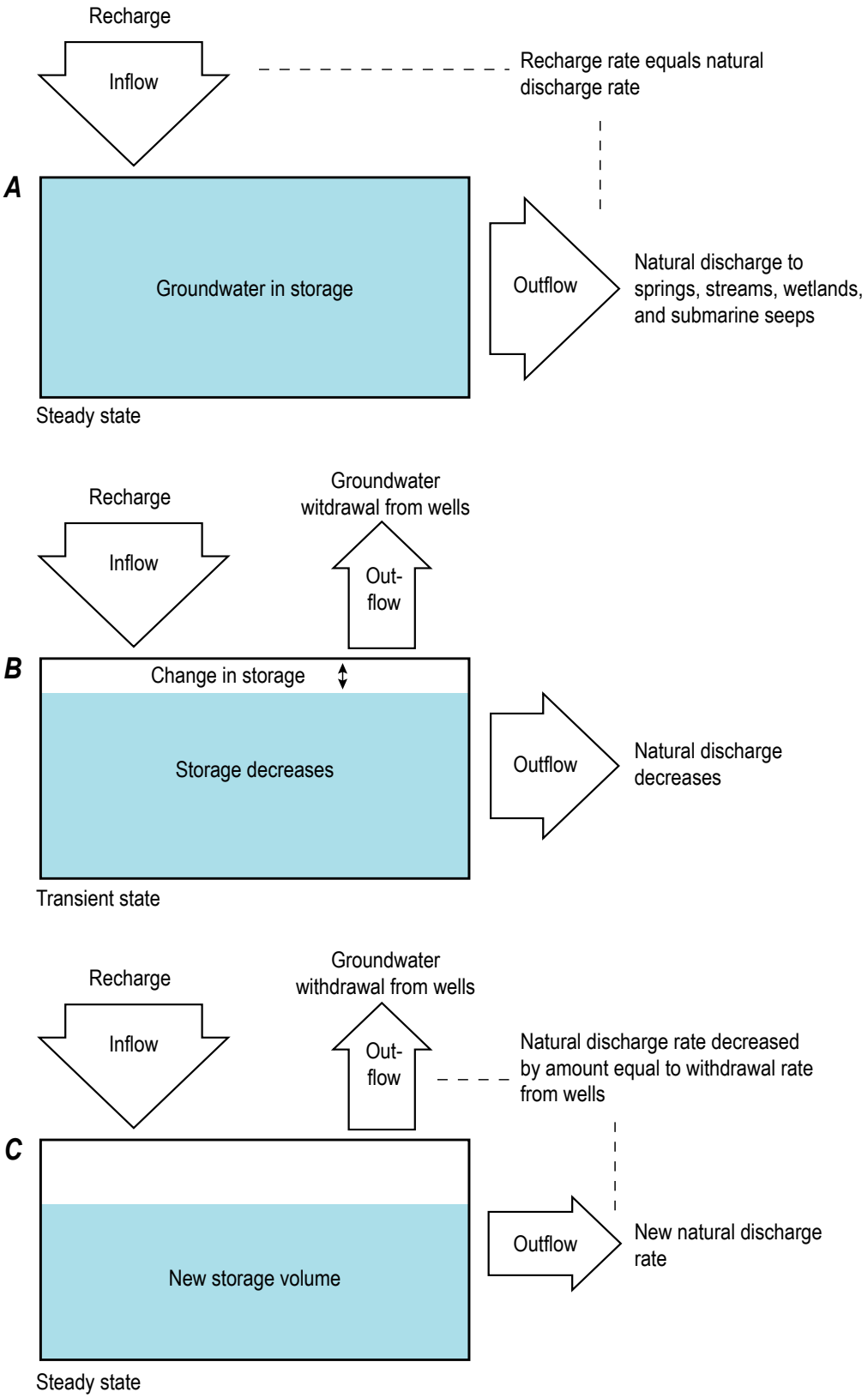

Figure 3. Effects of groundwater withdrawal from wells. (*A*) Steady state before groundwater withdrawals. (*B*) Transient state as aquifer adjusts to newly introduced withdrawals. (*C*) New steady state after aquifer has adjusted to the withdrawals.

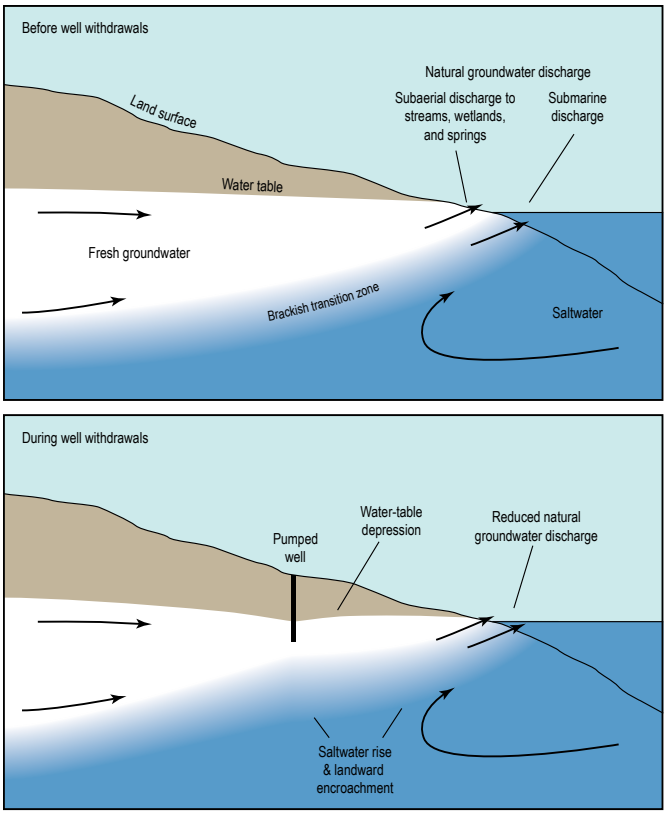

Figure 4. Effects of withdrawing water from a coastal aquifer.

Purpose and Scope

The USGS Water Availability and Use Science Program seeks to update and advance understanding of groundwater availability of the nation's principal aquifers. This report presents the results of a study of Hawai‘i's volcanic aquifers that partly fulfills this objective. The study included:

1. Review and revision of the hydrogeologic framework—the hydraulic properties and distribution in three-dimensional space of the rocks through which groundwater moves and is stored, and the structures that affect groundwater flow.
2. Updated assessment of the groundwater budget—accounting of inflows to, and outflows from, the groundwater system.
3. Development of updated conceptual groundwater models—conceptual models describe groundwater flow and occurrence in the islands and are developed on the basis of the hydrogeologic-framework and groundwater-budget information.
4. Identification of the limitations of current data.

Practical constraints limited the scope of the study to Kaua‘i, O‘ahu, Maui, and Hawai‘i Island. These islands constitute 92 percent of the land area and 99 percent of the population of Hawai‘i, and thus represent a large fraction of groundwater use and potential resource (table 1).

The resource assessment in this report is limited to freshwater, but freshwater resources in ocean-island aquifers are associated with and limited by saltwater in the aquifers. Freshwater that mixes with saltwater to form brackish groundwater is part of the freshwater budget (fig. 2). Also, brackish water may be important to some coastal ecological systems, and some brackish water and saltwater is used by humans. The occurrence and movement of saltwater therefore are discussed briefly. For the purposes of this study, freshwater is defined as water with a total-dissolved-solids concentration of 1,500 mg/L (approximately equal to a mixture of 2 percent seawater with 98 percent pure freshwater); this broad definition includes some water that is suitable for irrigation but undesirable for use as drinking water.

Study Area

The eight main islands in the State of Hawai‘i have a total land area of 6,420 mi^2 (table 1). The four islands in this study (Kaua‘i, O‘ahu, Maui, and Hawai‘i Island) have a total land area of 5,904 mi^2. Major industries in Hawai‘i include tourism, government (including military), and agriculture (State of Hawai‘i, 2011). About 70 percent of the state's population of 1.36 million lives on O‘ahu (U.S. Census Bureau, 2011). O‘ahu also has the capital city of Honolulu, as well as the large military installations Joint Base Pearl Harbor-Hickam, Wheeler Army Air Field, Schofield Barracks, and Marine Corps Base Hawaii.

Throughout Hawai‘i's history, the impact humans have had on the landscape has had implications for groundwater resources. Not only does groundwater withdrawal from wells decrease storage and natural discharge, but changes in land use—such as expanding urbanization, deforestation and reforestation, replacement of native forests by nonnative species, and agricultural irrigation—can affect groundwater recharge. Even before the first modern well was drilled in 1879, land cover in Hawai‘i had already been substantially altered by human activities. Comparison of land-cover maps from 1870 and 2010 (figs. 5 and 6) shows how humans have transformed the landscape even further in the last 140 years.

Archaeological evidence indicates that the Hawaiian Islands were first colonized by humans from Polynesia around A.D. 300–700, and that the population had grown to several hundred thousand by about the 1600s to 1700s (Kirch, 1998, 2000; Ziegler, 2002). Early effects of humans on the landscape included introduction of nonnative plants and animals, forest clearing for agriculture and other human activities, and surface-water diversion for irrigation of crops, particularly taro (Newman, 1972; Kirch, 1982). Europeans arrived in Hawai‘i in the late 18th century. Over the decades that followed, Hawai‘i's population declined sharply to less than 100,000 by the middle to late 19th century, primarily due to introduced diseases (Schmitt, 1998). Subsistence agriculture gave way to production of food and materials for trade or export, particularly with people from the United

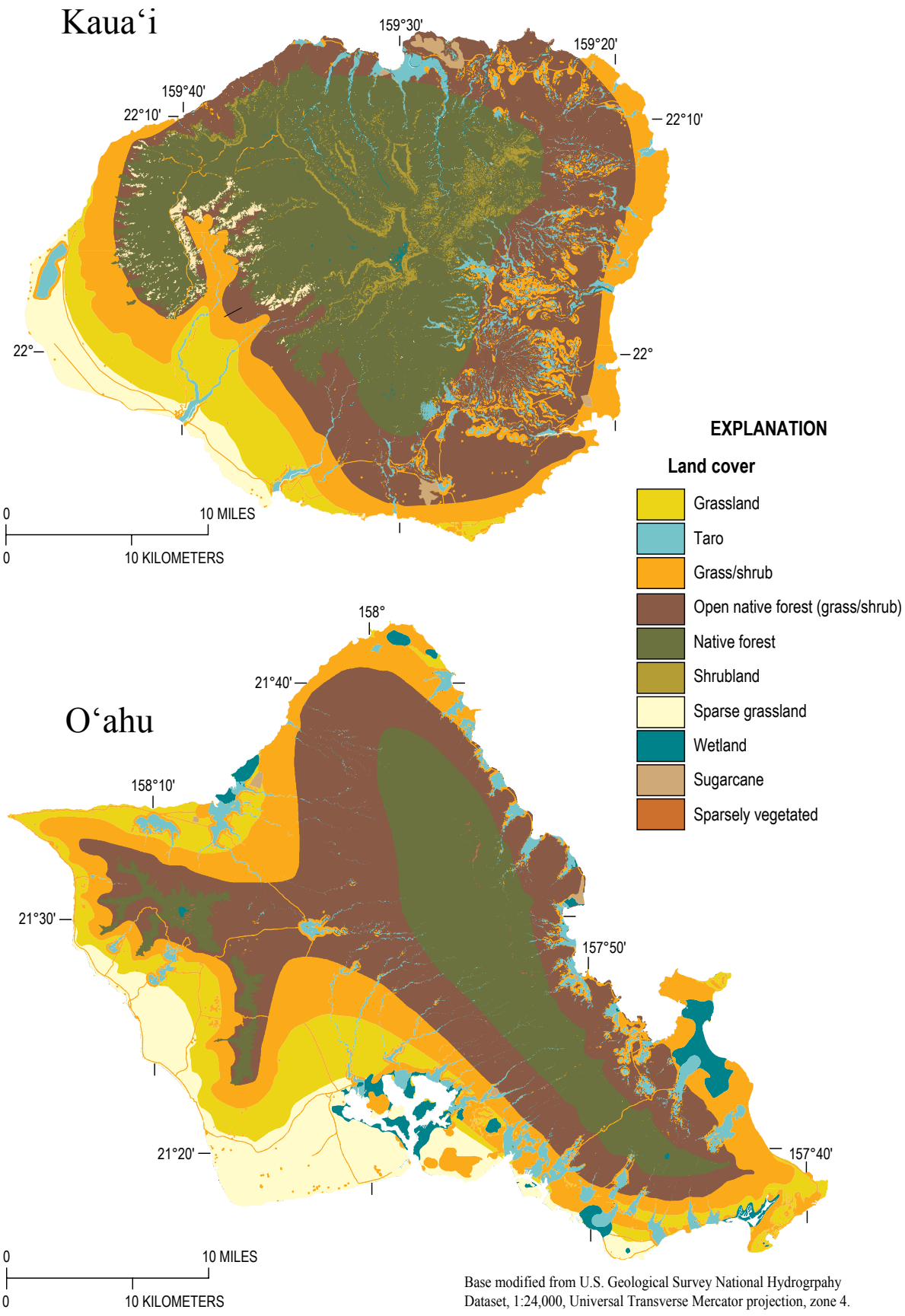

Figure 5. Maps of land cover in 1870 on Kauaʻi, Oʻahu, Maui, and Hawaiʻi Island.

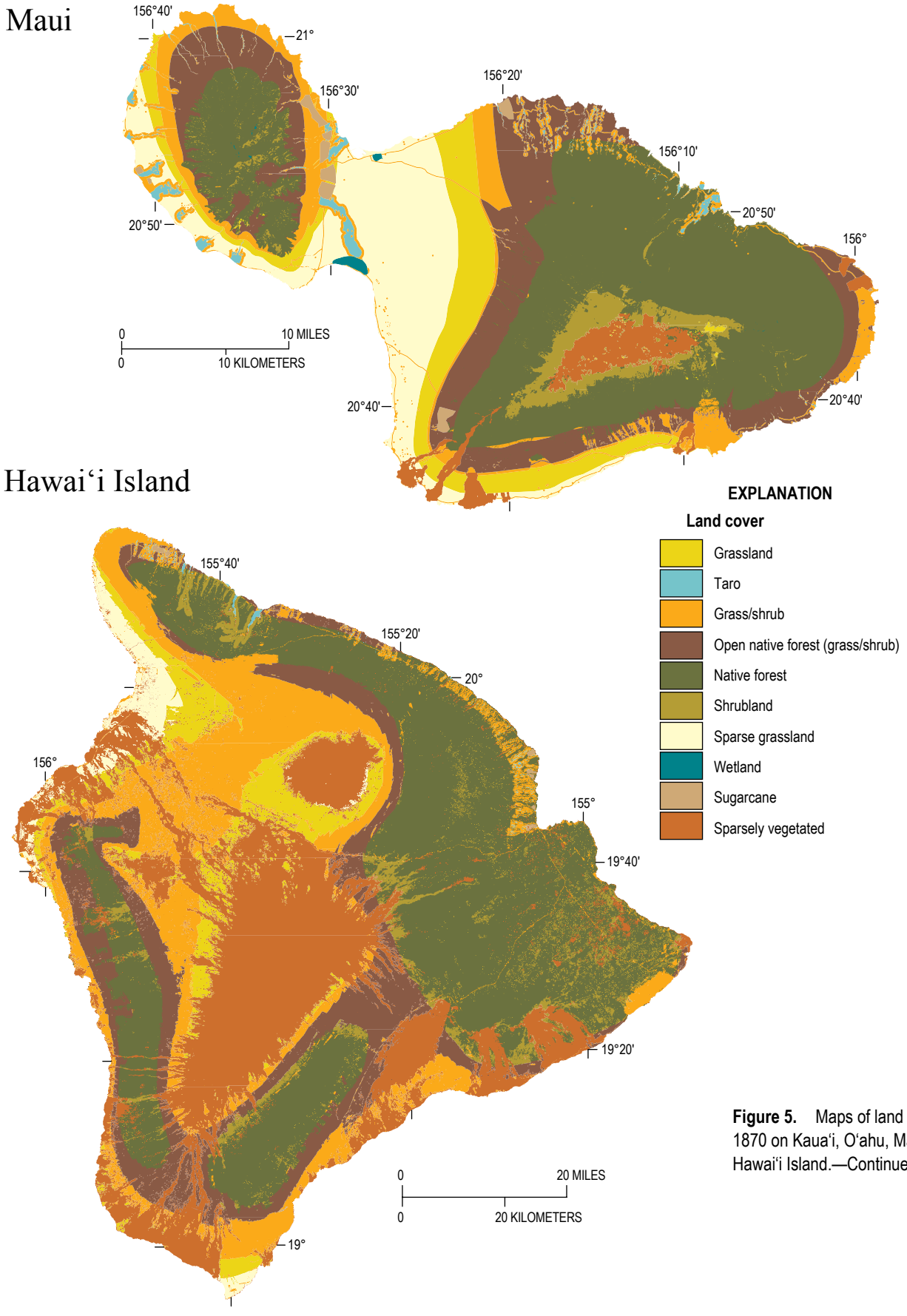

Figure 5. Maps of land cover in 1870 on Kaua‘i, O‘ahu, Maui, and Hawai‘i Island.—Continued

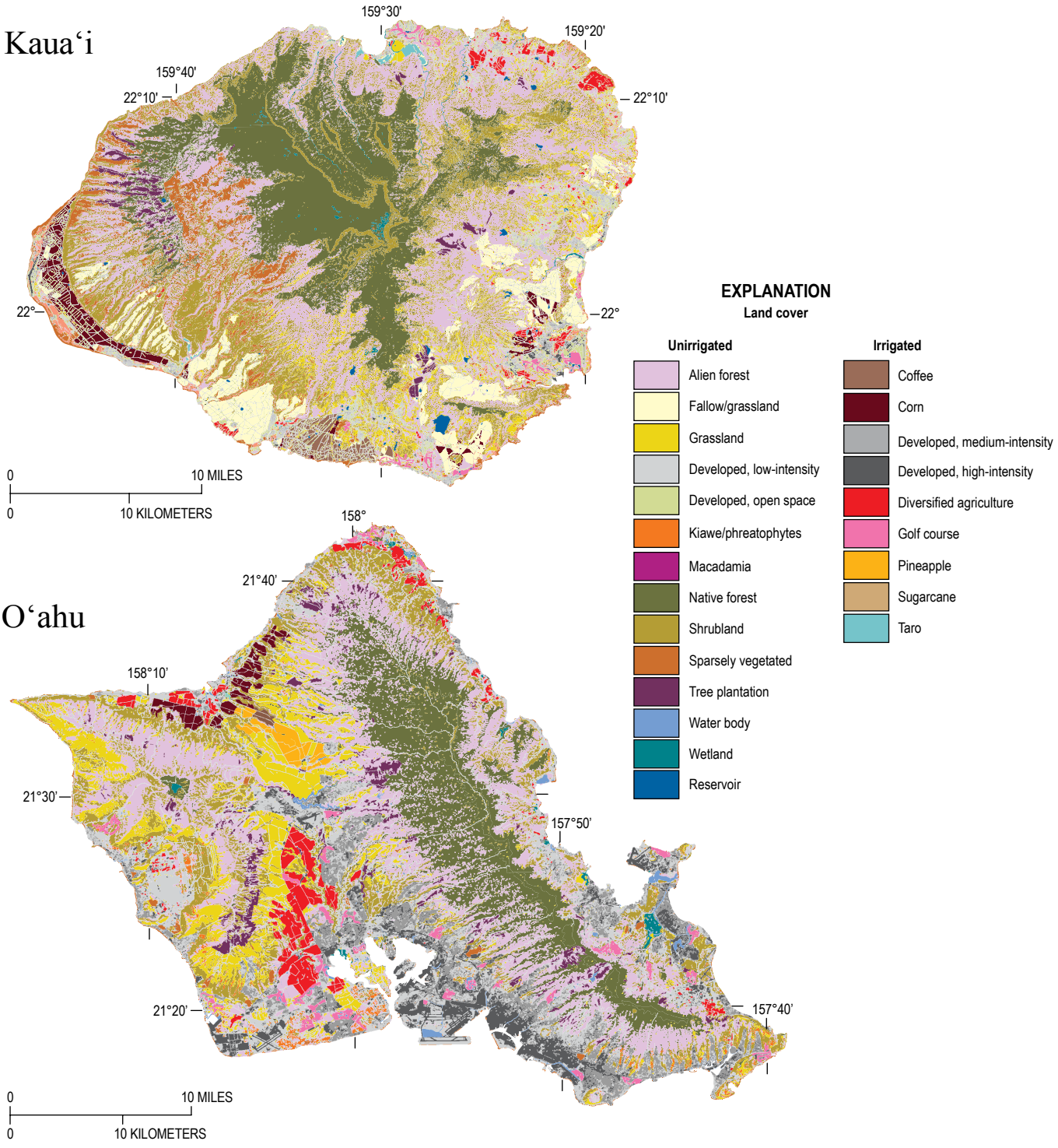

Figure 6. Maps of land cover in 2010 on Kaua‘i, O‘ahu, and Maui, Hawai‘i. Land cover for Hawai‘i Island is shown by Engott (2011); because it uses different land-use categories, it is not reproduced here.

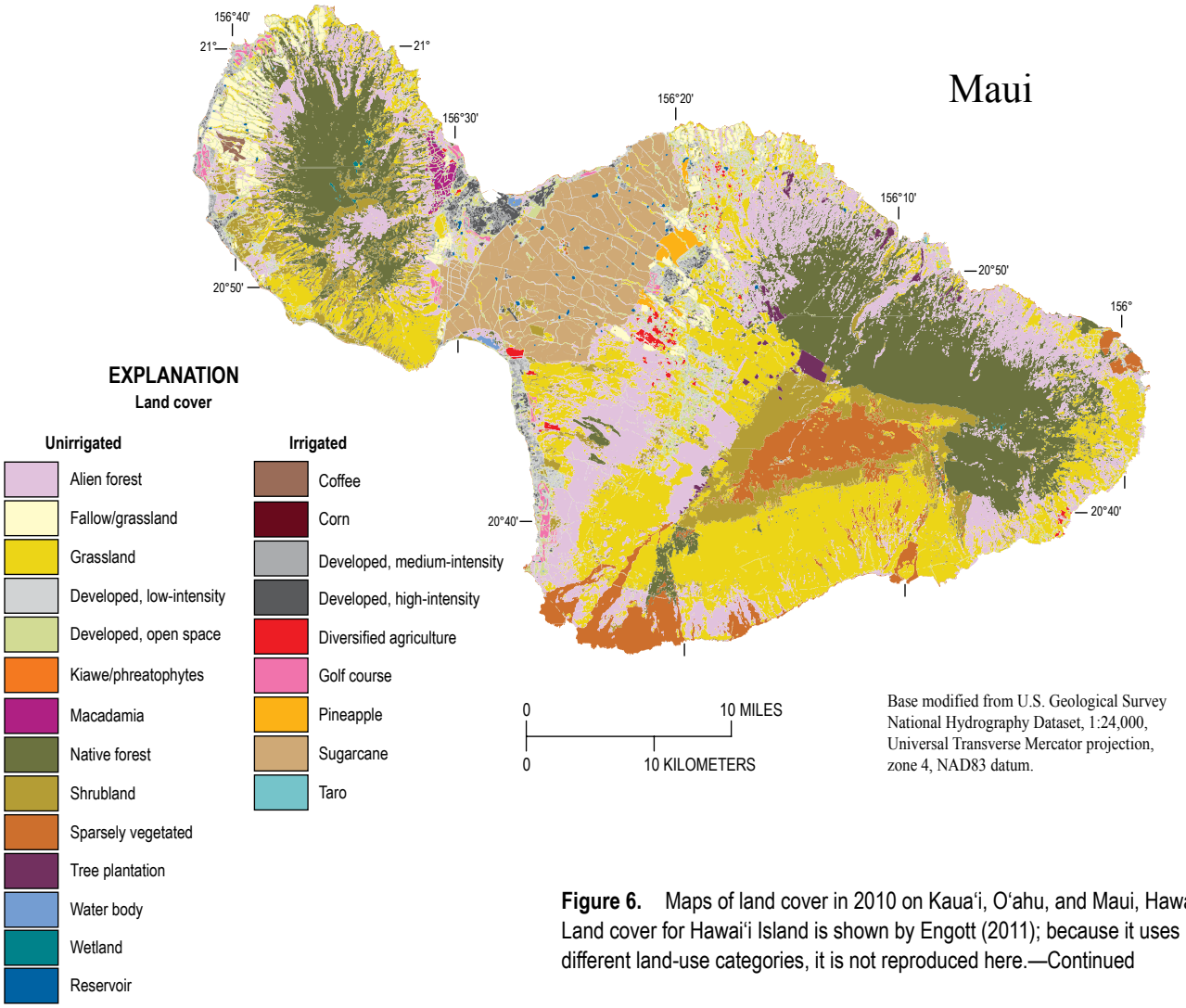

Figure 6. Maps of land cover in 2010 on Kaua‘i, O‘ahu, and Maui, Hawai‘i. Land cover for Hawai‘i Island is shown by Engott (2011); because it uses different land-use categories, it is not reproduced here.—Continued

States, resulting in the harvesting of some native plants (such as sandalwood) and animals from the forests and oceans, and the introduction of more nonnative plants and animals (Cuddihy and Stone, 1990; Langlas, 1998). Cattle, goats, and sheep brought to Hawai‘i in the late 18th century formed large feral populations that contributed substantially to deforestation through much of the 19th century until ranching curbed their numbers (Cuddihy and Stone, 1990; Ziegler, 2002). Pigs were brought to Hawai‘i by the early Polynesians and later by other people; feral populations of pigs continue to thrive and affect upland forests today (Ziegler, 2002). Concern over the degraded state of Hawai‘i’s forests and the perceived connection to watershed health led to the establishment of forest reserves and reforestation efforts—mostly using nonnative trees—in the early 1900s (Woodcock, 2003).

From about the middle of the 19th century, large-scale agriculture, particularly sugarcane and to a lesser extent pineapple, began to emerge in Hawai‘i. The sugarcane industry built extensive networks of ditches, flumes, tunnels, and reservoirs, and diverted hundreds of millions of gallons of water per day from streams for irrigation and processing (Wilcox, 1996). The irrigation systems not only diverted water to irrigate nearby fields, but also transferred water across drainage divides, for example from wet windward areas to dry leeward areas. The need for water to support sugar production spurred the drilling of the first modern well in 1879 on O‘ahu (Stearns and Vaksvik, 1935; Wilcox, 1996). This well, which had strong artesian flow, initiated development of Hawai‘i’s extensive groundwater resources, not only for agriculture, but also for other industries and for public supply. By the early 20th century, sugarcane producers were withdrawing hundreds of millions of gallons of water per day from Hawai‘i’s aquifers (Wilcox, 1996). The sugar industry also had an effect on population growth by importing labor, beginning in the 1850s but especially after the Reciprocity Treaty in 1856 allowed duty-free export of sugar to the United States (Langlas, 1998). With immigration and the stemming of disease-related deaths, the population of Hawai‘i rebounded to 423,000 by 1940, spiked to 859,000 during World War II, and was 622,000 when Hawai‘i became a state in 1959 (Schmitt, 1998).

The sugar and pineapple industries in Hawai‘i began declining in the latter decades of the 20th century. By the end of the 1960s, tourism had surpassed agriculture as the dominant industry in Hawai‘i (State of Hawai‘i, 2012a; Hawaii Agriculture Research Center, 2014). U.S. military spending has also become a major source of income for the state (State of Hawai‘i, 2014a). Fifty-five sugar plantations were in production statewide in 1990, but only two plantations (one on Kaua‘i and one on Maui) remained in production in 2002 (Cai and Leung, 2004). By 2009, sugarcane production had ceased on all islands except Maui, and pineapple canneries throughout Hawai‘i had closed. Some former sugarcane and pineapple fields have been converted to other forms of agriculture and some have been urbanized, but much former agricultural land is currently covered by grass and shrub.

Climate

Hawai‘i lies in the tropics, in the trade-wind belt of the North Pacific anticyclone. The climate for most of the islands is characterized by mild temperatures, moderate humidity, and prevailing northeasterly trade winds (Giambelluca and Schroeder, 1998). Hawai‘i’s climate is diverse, however, and includes deserts, tropical rain forests, and snow-capped mountains. Climate distribution is influenced by the prevailing northeasterly trade winds and their interaction with the islands’ volcanic mountains. Rain is generated by the orographic effect—trade winds blow against the mountain slopes and air carrying moisture from the ocean is forced to rise and cool adiabatically. The cooling causes condensation of water vapor; as a result, rainfall amounts are high over mountain crests and on northeast-facing (windward) slopes, and low in leeward areas (fig. 7). The contrast between dry leeward areas and wet windward slopes and mountain peaks is substantial—mean annual rainfall ranges from less than 10 in. on some leeward coasts to more than 400 in. on the windward slopes of Maui, and can vary by more than an order of magnitude within 5 horizontal miles (Giambelluca and others, 1986, 2013). The interaction of trade winds and mountains thus provides a voluminous and persistent influx of freshwater to Hawai‘i; without the orographic effect, rainfall would be less than 30 in/yr, similar to that of the open ocean in this region of the Pacific (Giambelluca and Schroeder, 1998).

The orographic effect and the rainfall it generates are limited to about 7,200 ft altitude by the trade-wind inversion (a temperature inversion), thus the climate at the peaks of the highest mountains—Haleakalā on Maui, and Mauna Kea and Mauna Loa on Hawai‘i Island (fig. 1)—is dry and includes the lowest mean annual rainfall values in Hawai‘i (fig. 7; Giambelluca and others, 2013). The southwest-facing slopes of Hawai‘i Island, although sheltered from the trade winds, receive air flow as the trade winds wrap around Mauna Loa and from sea breezes generated by the diurnal heating and cooling of the

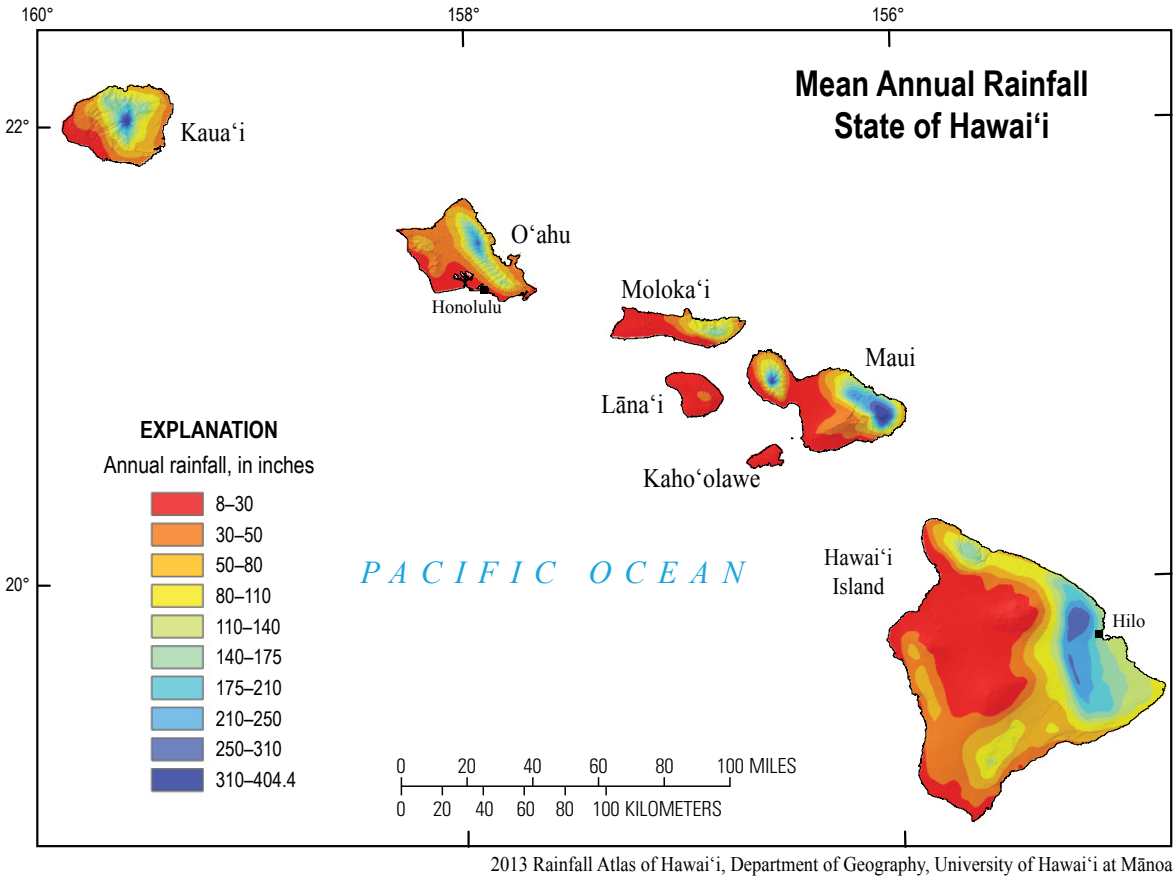

Figure 7. Map of mean annual rainfall in Hawai‘i. Modified from Giambelluca and others (2013).

large land mass of Hawai‘i Island; these winds produce a band of higher precipitation on the middle-altitude slopes (Giambelluca and others, 1986, 2013). Hawai‘i also receives rain from occasional migratory storm systems unrelated to the orographic effect. These storms can bring heavy rain to any part of an island, and are the main source of rainfall in the dry leeward areas and on mountain tops above the trade-wind inversion (Giambelluca and others, 2013).

Interception of fog by vegetation is an important source of water for high-altitude forests in Hawai‘i, particularly during the drier summer months (Juvik and Nullet, 1995). Mountain fog in Hawai‘i commonly occurs during periods of onshore, up-sloping winds and is associated with rainfall. However, it can also occur in the absence of rainfall, especially during the summer when the more frequent presence of the trade-wind inversion limits the vertical development of orographic clouds. This type of fog can persist with relatively high wind velocities, resulting in large volumes of water passing near the ground (Juvik and Ekern, 1978).

Hawai‘i’s climate varies seasonally, but the seasonal pattern differs from one location to the next (Giambelluca and others, 1986, 2013). In drier leeward areas, where most rainfall comes from storms, mean monthly rainfall is highest in December and January and lowest in June and July (fig. 8*B*). In wet windward areas that receive abundant orographic rainfall, mean monthly rainfall tends to be more evenly distributed throughout the year (fig. 8*A*). On the southwest-facing slopes of Hawai‘i Island, rainfall tends to be highest in the summer when the sea breezes generated by the diurnal heating and cooling of the large land mass are strongest (fig. 8*C*).

Precipitation in Hawai‘i also varies with multi-year cycles linked to ocean/atmosphere climate cycles such as the El-Niño-Southern Oscillation (ENSO), which repeats at a frequency of about 3 to 7 years and has events that last about 0.5 to 1.5 years, and the Pacific Decadal Oscillation (PDO); these cycles cause some years to be wetter or drier than the long-term average (fig. 9; Chu and Chen, 2005). Rainfall in Hawai‘i is typically lower during El Niño conditions (Giambelluca and others, 2013).

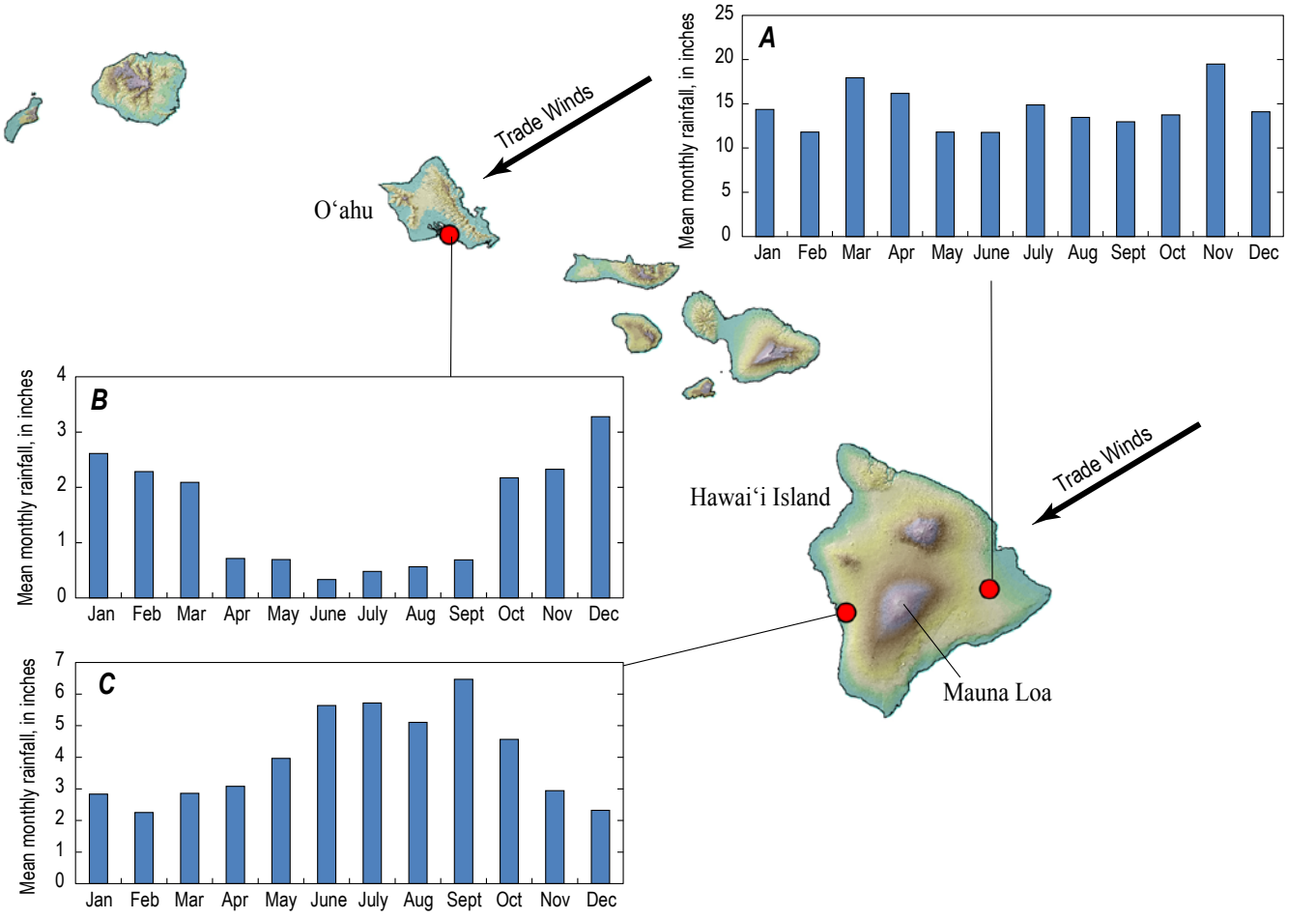

Figure 8. Graphs of mean monthly rainfall showing differences in seasonal variability at rain gages in various climate settings in Hawai‘i. (*A*) Rain gage on the northeast-facing (windward) slope of Hawai‘i Island, which receives abundant orographic rainfall from the prevailing trade winds. (*B*) Rain gage on the leeward coast of O‘ahu, where most rainfall comes from storms rather than the orographic effect. (*C*) Rain gage on the southwestern slope of Hawai‘i Island, which receives orographic rain from diurnal sea breezes and trade-wind flow wrapping around the south of Mauna Loa. Modified from Giambelluca and others (2013).

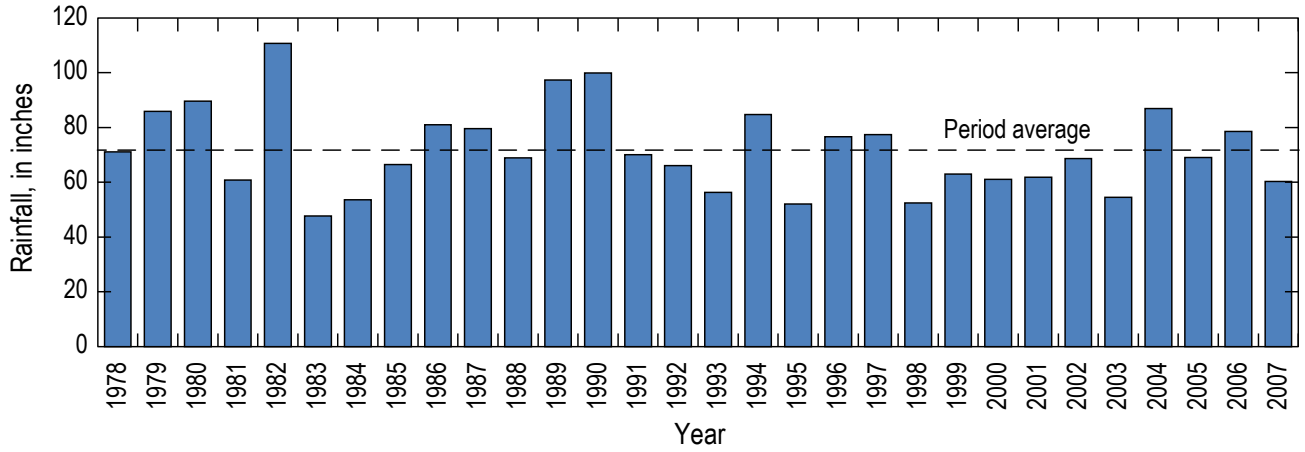

Figure 9. Graph of spatially averaged annual rainfall received on Kauaʻi, Oʻahu, Maui, and Hawaiʻi Island during 1978–2007, calculated from spatially gridded monthly rainfall data provided by Frazier and others (2016). The annual total for a given year was calculated by averaging rainfall totals for all grid cells in a given month, then summing the rainfall for all months in the year.

Precipitation data also indicate a long-term-average drying trend in Hawaiʻi's climate over the last century (Kruk and Levinson, 2008; Chu and others, 2010). Global temperature rises and climate change from anthropogenic greenhouse-gas emissions (Intergovernmental Panel on Climate Change, 2013) are likely to affect the future climate in Hawaiʻi. Recent statistical downscaling of the results from general circulation models (GCMs) indicates that by the end of the 21st century, the wet windward slopes of mountains are expected to become wetter or remain unchanged, whereas the dry leeward areas will become drier (Timm and others, 2015). However, climate predictions are currently in a state of flux and a subject of active research.

Hydrogeologic Overview

The shield volcanoes that form the islands of Hawaiʻi were built from the ocean floor by mid-plate hot-spot volcanism (Macdonald and others, 1983; Clague and Dalrymple, 1987; Clague and Sherrod, 2014). As a result of the northwestward motion of the Pacific lithospheric plate over the relatively stationary Hawaiʻi hot spot, the islands are successively younger toward the southeast of the chain. Basalt formations on Niʻihau and Kauaʻi at the northwestern end of the main island chain (fig. 1) date as far back as the Miocene, whereas volcanism is currently active on Hawaiʻi Island at the southeastern end of the chain (Langenheim and Clague, 1987; Sherrod and others, 2007). The shield volcanoes are enormous—estimates of the volume, including submarine and subaerial parts, of individual volcanoes in the four islands in this study range from one to several million cubic miles (Robinson and Eakins, 2006).

Eruptive Stages

Even before the advent of radiometric dating and the emergence of plate-tectonic theory, geologists recognized the age progression of islands in the Hawaiian archipelago and that the volcanoes are at different stages of development. On the basis of structural and stratigraphic relations and petrology observed during geologic mapping, Stearns (1946) described eight stages of development, from an initial submarine stage, through several subaerial stages, to a final atoll stage. The eruptive stages were redefined over the next few decades on the basis of geochemical characteristics and rates of lava production, which in turn were linked to changes in melting dynamics as a volcano passed over the hot spot (Wolfe and Morris, 1996). Four eruptive stages are currently recognized in Hawaiian volcanoes—in order of occurrence they are preshield, shield, postshield, and rejuvenated stages (Clague and Dalrymple, 1987; Clague and Sherrod, 2014). Major stratigraphic units generally correspond with eruptive stage, but not all stages are present or conspicuous on all of the shield volcanoes (table 2). Only the latter three of these stages (fig. 10) form aquifers containing freshwater resources presently used by humans.

Shield Stage

Rocks of the shield stage constitute, by far, the largest part of the volcanic aquifers in Hawaiʻi—90 percent or more of the subaerial part of each volcano is built during the shield stage, which probably lasts less than 1 million years (Clague and Dalrymple, 1987). The stage is characterized by voluminous eruptions of highly fluid lava having the chemical composition of tholeiitic basalt (Macdonald and Katsura, 1964; Macdonald, 1968; Macdonald and others, 1983). Most of the lava is erupted at the volcano's summit and from rift zones. Rift zones are corridors of concentrated activity that radiate from the summit (fig. 11). Most shield volcanoes in Hawaiʻi have two principal rift zones and some have a third minor rift zone, although some have no clearly discernable rift zones. Most shield volcanoes also have, or are presumed to have had, a summit caldera. The caldera is not a permanent feature—it can be alternately filled and reformed during the life of the shield volcano (Wolfe and Morris, 1996).

Table 2. Major stratigraphic units of Kaua‘i, O‘ahu, Maui, and Hawai‘i Island and their relation to the eruptive stages of Hawaiian volcanoes.

[Summarized from Sherrod and others, 2007. Volc., Volcanics; Mbr., Member]

Island	Volcano	Stratigraphic units	Eruptive stages
Hawai‘i	Kīlauea	Puna and Hilina Basalts	Preshield (submarine[1]) to shield
	Mauna Loa	Nīnole, Kahuku, and Ka‘u Basalts	Shield
	Hualālai	Hualālai Volc.	Shield (subsurface, submarine[1]) to postshield
	Mauna Kea	Laupāhoehoe Volc.	Postshield
		Hāmākua Volc.	Shield (subsurface[1, 2]) to postshield
	Kohala	Hāwī Volc.	Postshield
		Pololū Volc.	Shield
Maui	Haleakalā	Kula and Hāna Volc.	Postshield
		Honomanū Basalt	Late shield and transitional to postshield
	West Maui	Lahaina Volc.	Rejuvenated
		Honolua Volc.	Postshield
		Wailuku Basalt	Shield
O‘ahu	Ko‘olau	Honolulu Volc.	Rejuvenated
		Ko‘olau Basalt	Shield
	Wai‘anae	Pālehua and Kolekole Mbrs., Wai‘anae Volc.	Postshield
		Kamaile‘unu Mbr., Wai‘anae Volc.	Transitional shield to postshield
		Lualualei Mbr., Wai‘anae Volc.	Shield
Kaua‘i	Kaua‘i	Kōloa Volc.	Rejuvenated
		Waimea Canyon Basalt	Shield and postshield

[1]Submarine and subsurface occurrences are indicated only if confirmed by drilling or submarine samples.

[2]Some workers do not include the shield-stage rocks, which are known only from the subsurface, in the Hāmākua Volcanics.

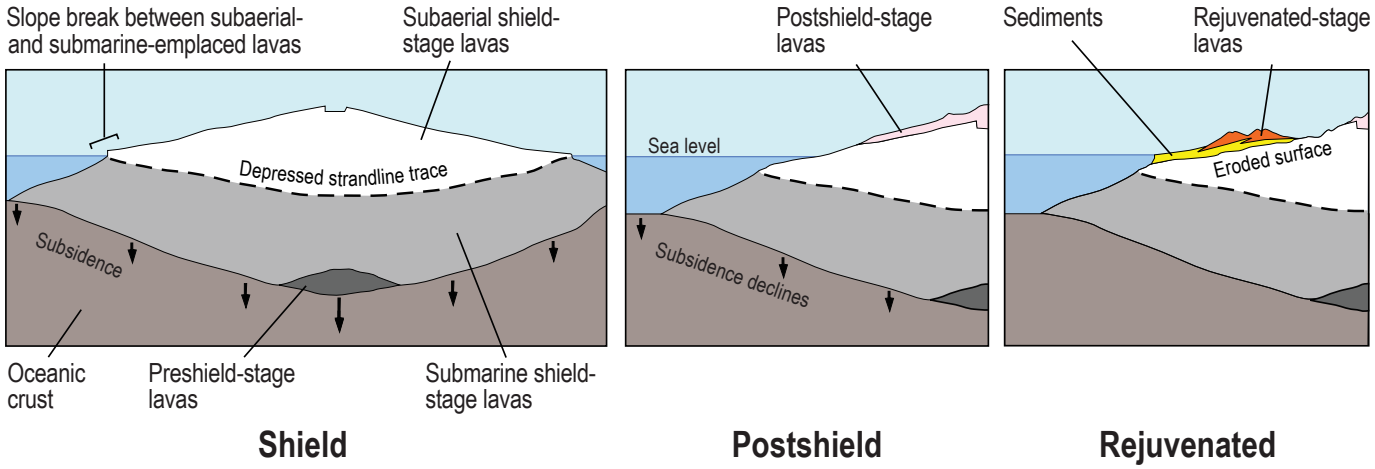

Figure 10. The last three eruptive stages of Hawaiian shield volcanoes. Modified from Clague and Sherrod, 2014.

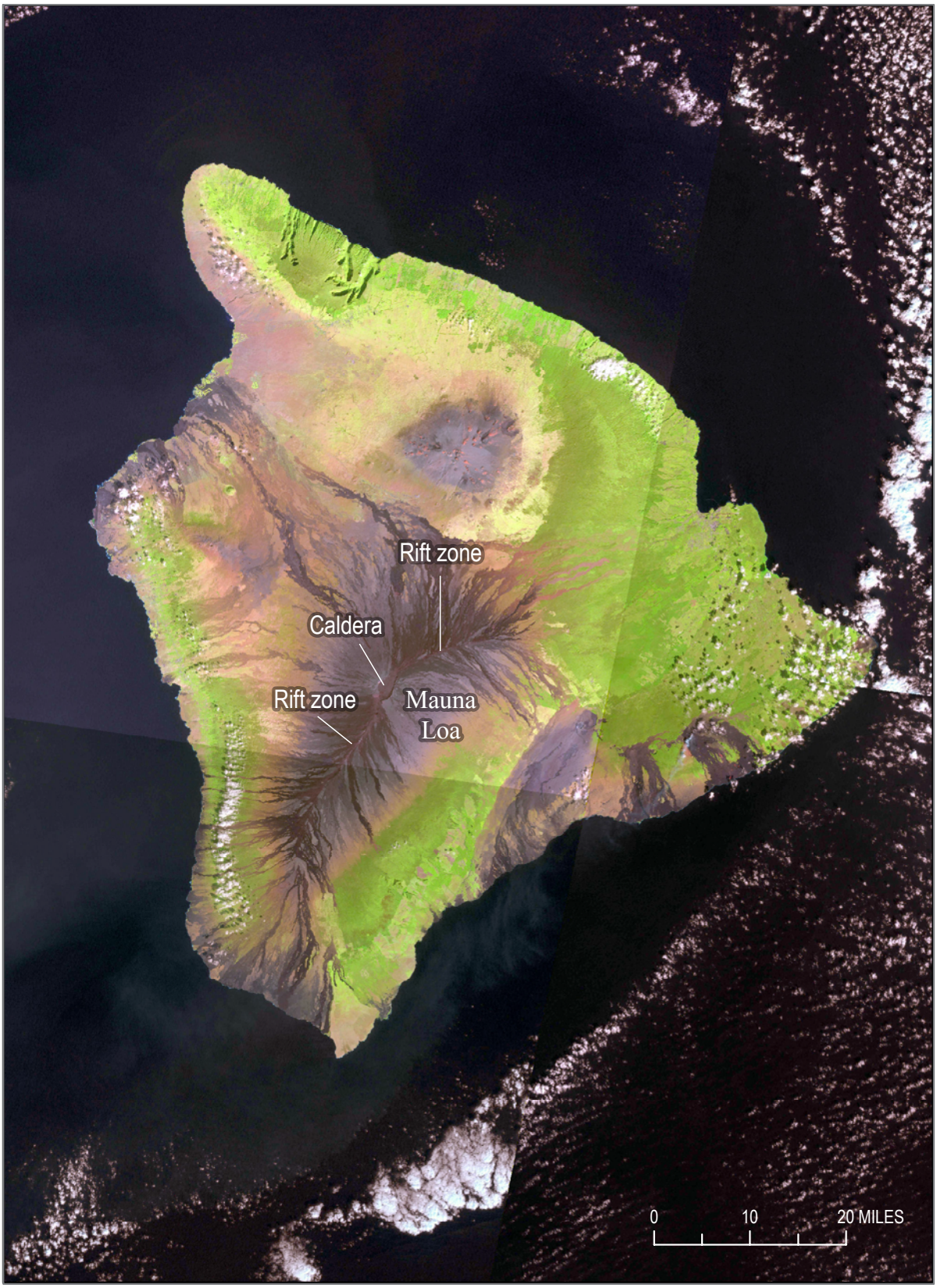

Figure 11. Mosaic of LANDSAT images of Hawai'i Island. Mauna Loa, one of the five volcanoes that form the island, is a typical shield-stage volcano. The dark streaks are lava flows. Images from U.S. Geological Survey (2012a).

Above sea level, the highly fluid shield-stage lava can flow for many miles down the sloped flanks of the volcano before congealing to form elongate, narrow tongues (fig. 11). Individual shield-stage lava flows are thin—the average thickness is about 15 ft (Macdonald and others, 1983)—but they accumulate to form the broad dome-shaped mountains that characterize these volcanoes (fig. 12*A*). Piles of thin, subaerially erupted lava flows can be seen where erosion has carved into the flanks of the shield volcano (fig. 12*B*).

Below sea level, eruptions build a steeper-sloped dome of pillow lavas topped by a thinner layer of volcaniclastic debris (Moore and Fiske, 1969; Mark and Moore, 1987) (fig. 10). However, the islands subside as they grow, and the submarine-emplaced pillow lavas and volcaniclastic debris, as well as part of the subaerially emplaced lava flows eventually sink thousands of feet below sea level. The slope change marking the edge of the subaerially emplaced lava flows can be recognized in bathymetric data from the seafloor surrounding all of the Hawaiian Islands (Moore and Fiske, 1969; Eakins and others, 2003) (fig. 13). As a result of subsidence, most of the fresh groundwater resources available for human use in Hawai‘i exists in the subaerially emplaced volcanic rock. Aquifers formed by the thin, high-permeability, subaerial flank lava flows of the shield stage are the most productive in Hawai‘i.

Eruptions in Hawaiian shield volcanoes are fed by dikes—fractures through which magma rises to the surface when the volcano is active. When magma cools in these fractures, it forms dense, near vertical sheet-like bodies of intrusive rock also known as dikes. Dikes cut across the pile of gently dipping lava flows that form most of the volcanoes (fig. 12*C*), and are particularly abundant beneath rift zones and the summit calderas.

Postshield Stage

Rocks from the postshield stage form a thin veneer capping some shield volcanoes in Hawai‘i (fig. 10). The veneer constitutes only about 1 percent of the volume of a shield volcano (Clague and Dalrymple, 1987). The postshield stage consists almost entirely of alkalic rocks such as alkalic basalt, hawaiite, mugearite, benmoreite, and trachyte (Macdonald, 1968; Sherrod and others, 2007). In many cases, the transition from shield to postshield stage is gradual, with interfingering lava flows of tholeiitic and alkalic basalts (Macdonald and Katsura, 1964; Clague and Sherrod, 2014).

Compared to the shield stage, the postshield stage is characterized by eruptions that are less frequent, lava that is more viscous, lava flows that are thicker and shorter, eruptions that are more violent, and more common occurrences of cinder cones and ash layers (Stearns, 1946, 1966; Macdonald and others, 1983). As a result, the postshield stage commonly forms a bumpy, steeper-sided cap on the shield volcano (fig. 14*A*,*B*). On some shield volcanoes, postshield vents follow the trend of preexisting rift zones, but on others they do not (Wolfe and Morris, 1996). Not all shield volcanoes have substantial postshield strata. Mauna Loa and Kīlauea on Hawai‘i Island do not have substantial postshield strata because they are still in the shield stage, but the Ko‘olau (on O‘ahu) and Kaua‘i volcanoes have passed into the subsequent rejuvenated stage without having a well-developed postshield stage (table 2).

Rocks from the postshield stage are important for groundwater resources on some islands. Postshield deposits, owing to the greater thickness of individual lava flows and low porosity of some lavas flows, have been generally regarded to have lower permeability than shield-stage lava flows. However, the very young postshield lava flows of Hualālai volcano on Hawai‘i Island are among the most permeable rocks in the Hawaiian Islands (Oki, 1999; Oki and others, 1999b).

Rejuvenated Stage

Of the ten shield volcanoes on the four islands considered in this report, only the Kaua‘i, Ko‘olau, and West Maui volcanoes have rocks of the rejuvenated stage (table 2). Rejuvenated-stage eruptions form small cones and lava flows that lie, commonly unconformably, on the surface of the much larger shield volcano (figs. 10 and 14*C*). Although the percentage varies among the volcanoes, even the most extensive deposits of rejuvenated-stage rocks constitute less than 1 percent of the volume of the shield volcano (Clague and Sherrod, 2014). Rejuvenated-stage volcanism is characterized by eruptions that are even less frequent and generally more alkalic than the postshield lavas (Stearns, 1946, 1966; Macdonald and others, 1983). Most of the lava is so high in alkalis and low in silica that feldspathoids form instead of plagioclase and the characteristic rocks are basanite and foidite, although other rocks also occur (Macdonald and others, 1983; Sherrod and others, 2007).

In early conceptualizations of the stages of Hawaiian shield-volcano evolution, rejuvenated volcanism was believed to occur hundreds of thousands to millions of years after the shield and postshield eruptions ceased. This long hiatus in eruptive activity was interpreted from the nearly ubiquitous erosional unconformity between the rejuvenated rocks and underlying shield and postshield rocks. Rocks that are now called the rejuvenated stage were in some cases referred to as posterosional (for example, Macdonald, 1968). Later, radiometric dating showed that the hiatus is 0.6 to about 2 million years on some volcanoes, but on Kaua‘i, the hiatus is almost nonexistent (Clague and Sherrod, 2014).

The rejuvenated-stage lava can be very fluid, but the violence of the eruptions can vary depending on whether or not the lava encounters water (Macdonald and others, 1983). As a result, the character of the volcanic rock ranges from thin lava flows to ash cones. The thickness of the lava flows can vary depending on whether they congealed as they flowed down a slope or accumulated in a preexisting depression. Rocks from the rejuvenated stage have accumulated to great thickness in eastern Kaua‘i, where they have been developed for groundwater resources. High drawdowns and low-yielding wells indicate that the thick, rejuvenated lava flows in the basin are much less

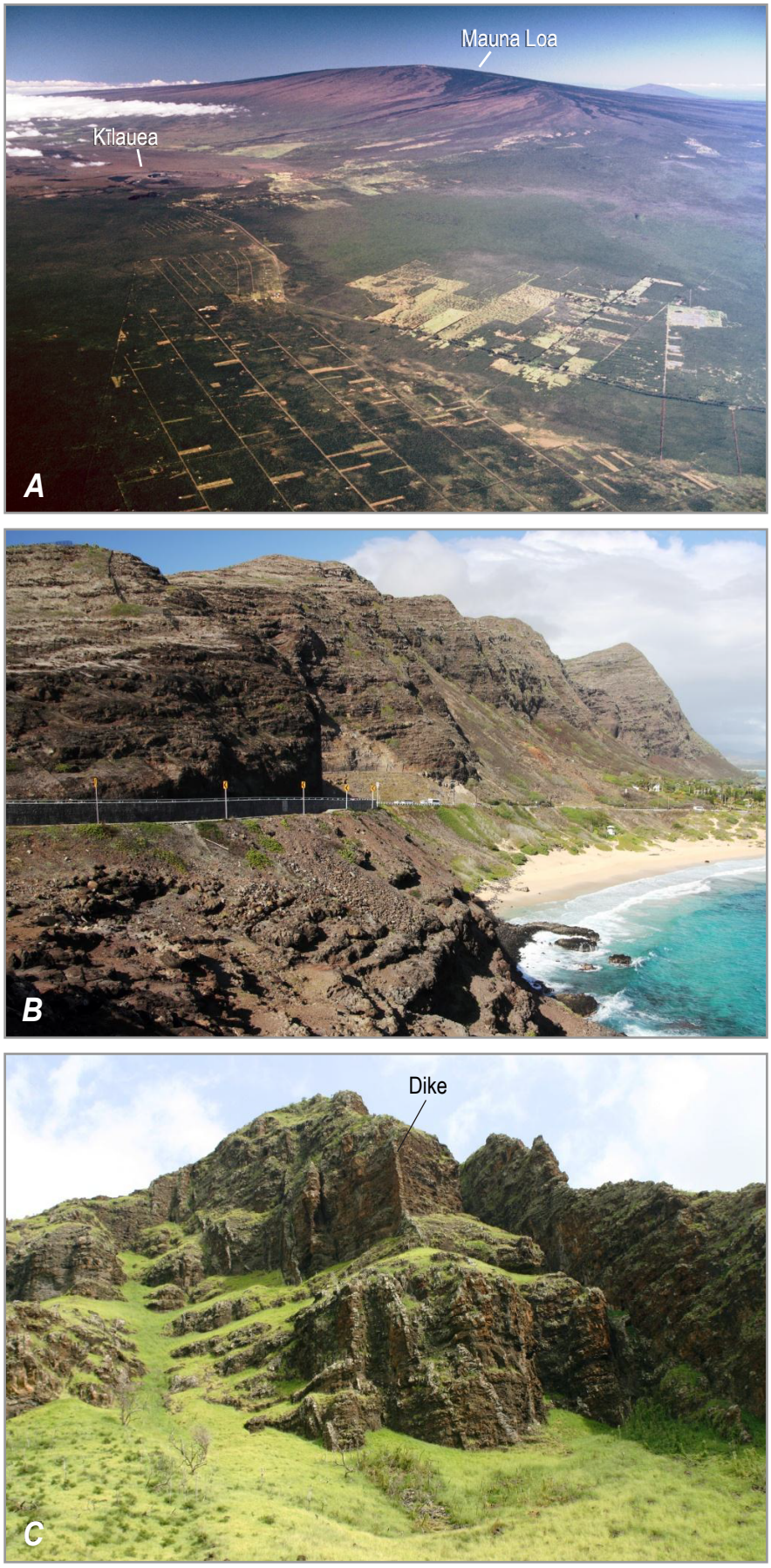

Figure 12. Features of the shield stage of Hawaiian shield volcanoes. (*A*) Mauna Loa, Hawai‘i Island, showing the smooth dome shape typical of volcanoes in the shield stage. (*B*) Thin shield-stage lava flows exposed in eroded cliffs of the Ko‘olau volcano, O‘ahu. (*C*) Dikes cutting across shield-stage lava flows exposed in an eroded cliff of the Wai‘anae volcano, O‘ahu. Photograph credits: (A) J.D. Griggs, courtesy of the USGS Hawaiian Volcano Observatory; (B) and (C) S.K. Izuka, USGS Pacific Islands Water Science Center.

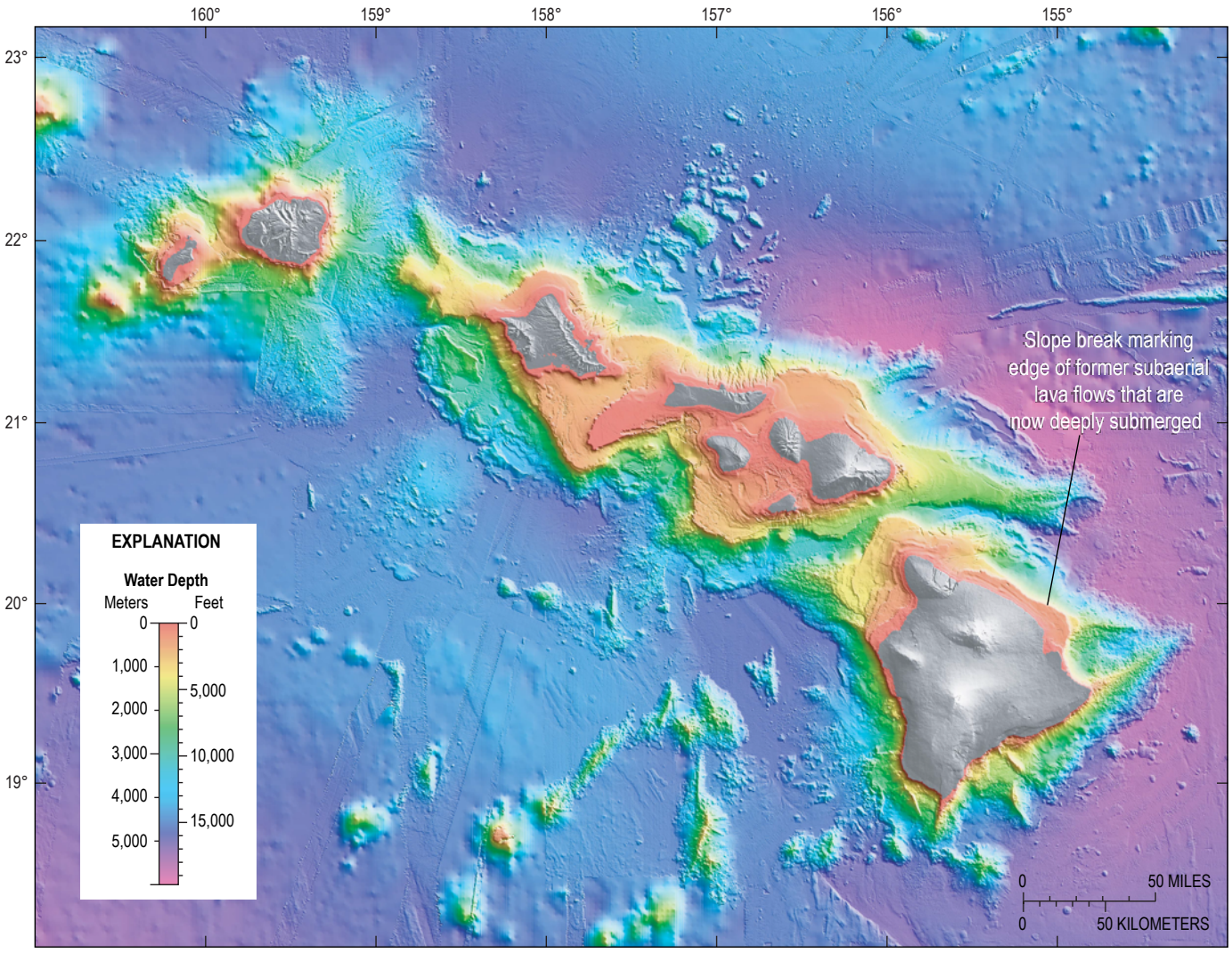

Figure 13. Image of the seafloor surrounding the main Hawaiian Islands. A submarine slope break marks the edge of lava flows that were formed above sea level, but are now submerged. Modified from Eakins and others, 2003.

Figure 14. Features of the postshield and rejuvenated stages of Hawaiian shield volcanoes. (*A*) Mauna Kea Volcano, Hawai‘i Island, showing the bumpy skyline (compare with fig. 12*A*) formed by a cap of postshield cinder cones and thick, short lava flows. (*B*) Cinder cones of the postshield stage of Mauna Kea, Hawai‘i Island. (*C*) Koko Crater, a rejuvenated-stage tuff (ash) cone on the southeastern coast of O‘ahu. Photographs by S.K. Izuka, USGS Pacific Islands Water Science Center.

permeable than dike-free rocks of the shield stage. On O‘ahu, rejuvenated-stage rocks interbedded with sediments form an extensive coastal plain. The deposits act as a semiconfining unit, locally known as caprock, that inhibits coastal groundwater discharge from the shield-stage lava-flow aquifer, thereby increasing groundwater storage. Rejuvenated-stage rocks also partly fill some valleys on O‘ahu, and rejuvenated-stage dikes may form barriers to horizontal groundwater flow.

Other Processes Affecting the Hydrogeologic Framework

Besides the constructive processes of volcanic eruptions, other processes work on the shield volcano throughout its existence. Processes such as faulting and slumping, subsidence, sea-level fluctuation, erosion, and sedimentation modify the hydrogeologic framework of the volcanic aquifers.

Faulting and Slumping

In some places, the lava flows of the shield volcano are cut by normal faults. In and near the summit and rift zones, faults form as a result of injection and withdrawal of magma (for example Duffield, 1975; Wolfe and Morris, 1996); these faults include those that bound calderas and pit craters as well as others that form groups of faults that approximately follow the rift-zone trends (fig. 15). Faults also result from large, gravity-driven slumping of the volcano’s flanks (Denlinger and Morgan, 2014). Some faults on the lower flanks of the volcanoes are the headward expressions of slumps that extend into the ocean and include submarine landslide debris (for example, Moore and others, 1989). Some very long slump-related fault systems on Kaua‘i cut completely across the island (Macdonald and others, 1960; Sherrod and others, 2015).

Whether they result from magma movement or slumping, faults on active volcanoes are commonly draped and eventually buried by younger lava flows. Although some faults have been mapped, many faults probably lie buried beneath the surface (Sherrod and others, 2007). Certain topographic features on some of the older islands have been interpreted as the eroded vestiges of fault scarps, even though the actual fault cannot be seen.

Faults can juxtapose rocks of contrasting hydraulic properties; for example, low-permeability caldera-fill lavas and high-permeability flank lava flows. Draping of faults by later lava flows has been suspected as possible low-permeability barriers resulting in anomalously high groundwater levels in Hualālai on Hawai‘i Island (Kauahikaua and others, 1998; Oki, 1999). However, the hydraulic properties of faults themselves are poorly known. The Koa‘e Fault System (fig. 15) is suspected to form one of the low-permeability barriers causing high groundwater levels in the summit area of Kīlauea on Hawai‘i Island, but the low-permeability may be the result of dike intrusion, rather than an intrinsic characteristic of the faults (Kauahikaua, 1993).

Island Subsidence and Sea-Level Fluctuation

Evidence that sea level has fluctuated relative to the height of the islands is widespread in Hawai‘i. Indicators of ancient sea levels, such as reefs, shallow-water fossils, shelves, slope breaks, and wave-cut benches, are now raised above or submerged below present sea level. The apparent fluctuation can result from vertical movement of either the island or ocean levels. Some evidence of sea-level fluctuation in Hawai‘i has been correlated with global sea-level fluctuations linked to continental glaciation (for example, Stearns, 1978), but some of the indicated fluctuations are too large to be attributed to glacial eustacy alone.

Multiple lines of evidence indicate that the islands in the Hawaiian chain subside as the lithosphere adjusts to the overburden of the volcano and due to cooling and thickening of the lithosphere as it moves away from the hot spot (Moore, 1987; Clague and Dalrymple, 1987). Subsidence is rapid initially—about 2.5 mm/yr or 0.008 ft/yr (Moore and Fornari, 1984; Moore, 1987; Ludwig and others, 1991; Webster and others, 2007)—but slows as an island is transported away from the hot spot. Moore (1987) estimated that most Hawaiian shield volcanoes have subsided 7,000–13,000 ft since reaching the sea surface. The slope change between the subaerial and submarine parts of the shield volcano becomes deeply submerged (Moore and Fiske, 1969; Eakins and others, 2003) (fig. 13). Data from two deep holes drilled in Hilo on Hawai‘i Island by the Hawai‘i Scientific Drilling Project (HSDP) indicate that even on this relatively young island, lavas originally erupted above sea level have already subsided to about 3,500 ft below sea level (Garcia and others, 2007). The hydrologic significance of subsidence is that in Hawai‘i, the principal volcanic freshwater aquifers both above and below sea level are made up of lava flows that originally formed above sea level; the pillow lavas that formed below sea level have subsided far below the reach of most present-day fresh groundwater resources.

Although the predominant trend for the islands is subsidence, mechanisms also exist for some uplift. The same overburden that causes the islands to sink creates a moat-like depression of the sea floor around the base of the volcanoes near the hot spot, and a more distal arch (Moore, 1970). Uplift can result as the island migrates out of the moat and onto the arch (Grigg and Jones, 1997). Local uplift can also result from forceful injection of magma when the shield volcano is active (Swanson and others, 1976).

Erosion and Sedimentation

Subaerial erosion processes—primarily stream erosion and mass wasting, but also wave erosion along the sea coast—begin to act on the shield volcano as soon as it is exposed above sea level. During the shield stage, however, evidence of stream erosion is minimal because the young lava flows on the surface are so permeable that rain water percolates into the ground rather than running off to form streams (Stearns, 1946, 1966). Also, the high rate of lava extrusion during the shield stage prevents the development of deep erosion features (Macdonald and others, 1983). In isolated cases, structural barriers such as fault scarps have prevented lava flows from reaching some parts of a shield

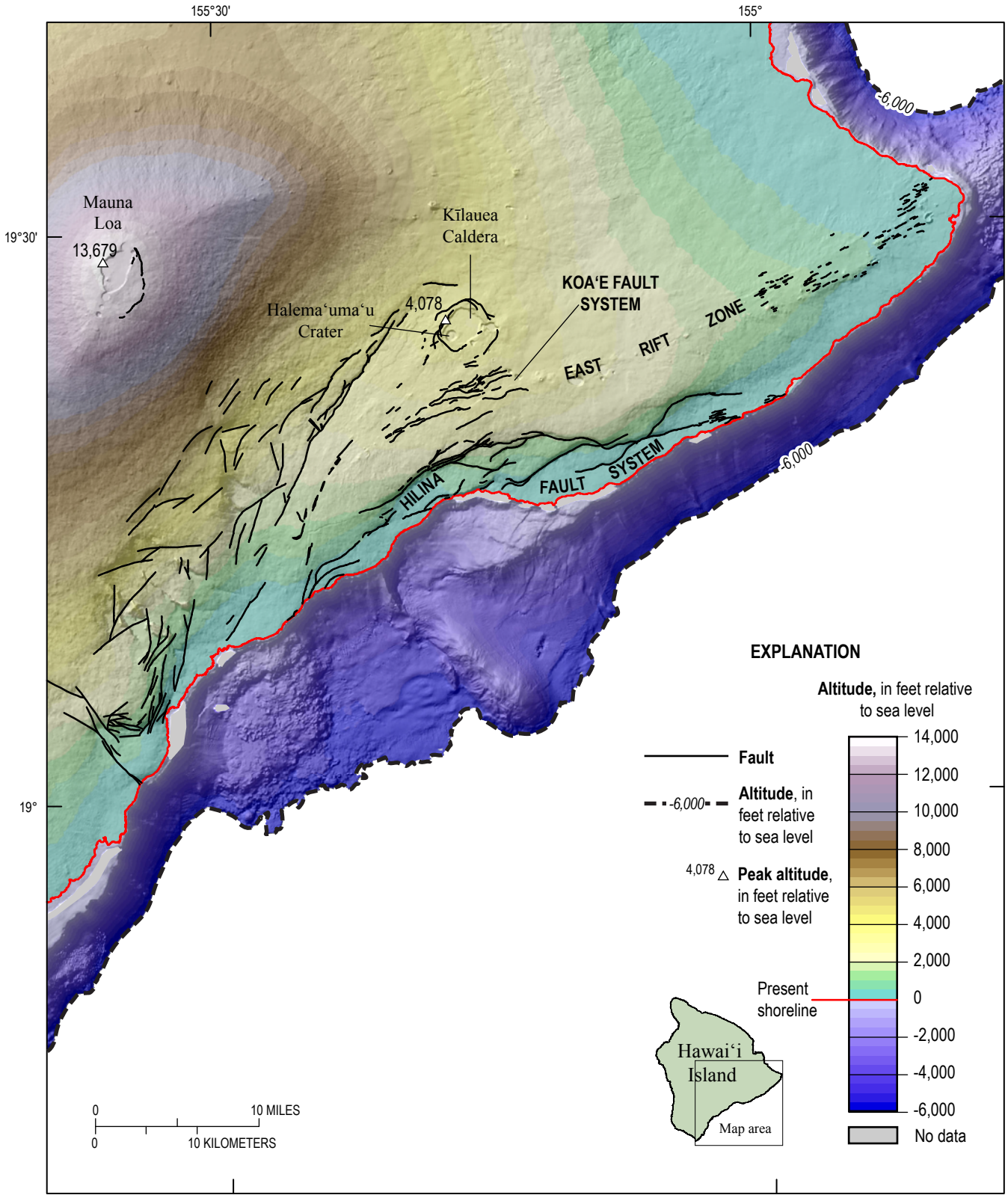

North American Datum 1983, Universal Transverse Mercator projection, zone 4N.

Figure 15. Map of faults on Kīlauea and part of the southeastern slope of Mauna Loa, Hawai'i Island. Faults from Sherrod and others (2007), base modified from University of Hawai'i (2011).

volcano’s flank, allowing deeper erosion during the shield stage. Most erosion of deep valleys, however, takes place after the major eruptive activity of the shield volcano has waned.

Downcutting by streams coupled with mass wasting produces valleys with v-shaped cross sections (Stearns and Vaksvik, 1935; Macdonald and others, 1983). Erosion patterns generally follow the radial dendritic drainage pattern of water running off a dome-shaped mountain (fig. 16), although structural features such as faults and dikes, as well as cones and lava flows of rejuvenated-stage eruptions have altered stream directions and erosion patterns in some areas. Incipient shallow, narrow gulches deepen and widen over time to form the amphitheater-headed valleys that are typically seen in the eroded remnants of older volcanoes such as those on Kaua‘i and O‘ahu (Jones, 1938; Stearns and Vaksvik, 1935; Macdonald and others, 1983). At an advanced stage, stream erosion can result in the coalescing of amphitheater-headed valleys, leaving only a scalloped cliff face, such as on the windward side of O‘ahu (Stearns and Vaksvik, 1935).

Most of the v-shaped valleys have only a very narrow ribbon of alluvium, although the valley walls may be weathered to various degrees depending on rainfall (Izuka, 1992, 2012). Larger valleys are partly filled with alluvium and, in some cases, rejuvenated-stage volcanic rocks; this partial filling forms a flattened valley floor (Stearns and Vaksvik, 1935). Global sea-level fluctuations coupled with island subsidence caused changes in stream base levels. The lower parts of some valleys were carved when sea level was lower than present and have been subsequently partly filled with sediment; as a result, the contact between alluvium and lava flows extends far below the present sea level (Palmer, 1927; Stearns, 1946; Macdonald and others, 1983). Some subaerial slopes have marine and terrigenous sedimentary deposits that formed when sea level was higher than it is today (Stearns and Vaksvik, 1935).

Sediment shed from the eroding volcano is deposited as alluvium in the valleys and along the coast. For reasons explained in the next section, alluvium in Hawai‘i, in most cases, is less permeable than the underlying lava-flow aquifer. On some islands, especially O‘ahu, terrigenous and marine sediments beneath the coastal plain form the caprock that resists groundwater discharge to the ocean. Alluvial deposits also partly fill valleys incised into the lava-flow aquifers; where the deposits extend below the water table, they can resist the horizontal flow of groundwater.

Rocks and Their Hydrologic Significance

Tholeiitic basalt is the most voluminous rock type on Hawaiian shield volcanoes, but alkalic basalt, hawaiite, mugearite, benmoreite, trachyte, basanite, foidite, and some other rocks also occur (Macdonald, 1968; Sherrod and others, 2007). The geochemical and petrologic classification on which these rock names are based do not connote any hydraulic properties. Any of these rocks can form lava flows, intrusive bodies, or tephra deposits, although some rock types have a propensity to take a certain form. Lava flows, intrusive bodies, and tephra each play a different role in the storage and movement of groundwater. Although volcanic aquifers are the subject of this study, weathered, metamorphic, and sedimentary rocks also warrant discussion because they affect groundwater occurrence and flow in some areas of Hawai‘i.

Lava Flows

Most of a shield volcano’s volume above sea level is formed by a thick accumulation of lava flows; thus, most groundwater in Hawai‘i is stored in lava-flow aquifers. Pāhoehoe lava flows form from relatively fluid lava; have a smooth, billowy, or ropy surface (fig. 17*A*); and can have within them lava tubes a few inches to several feet in diameter. ‘A‘ā lava flows form from more viscous lava, have a clinkery or rubbly surface, and a dense molten core (fig. 17*B*). In cross section, a stack of several ‘a‘ā lava flows has alternating layers of dense-rock cores and clinker (fig. 17*C*). Clinker layers are absent in a stack of pāhoehoe flows. Because most lava flows in Hawai‘i flow down the slopes of the shield volcano, they are much thinner than those of continental flood basalts, such as those of the Columbia Plateau in the northwestern United States (Macdonald and others, 1983). However, thick lava flows have formed in isolated areas in Hawai‘i where lava ponded in preexisting depressions such as calderas, grabens, and stream-eroded basins. Some highly viscous lavas such as trachyte can form thick individual lava flows, but these constitute a very small fraction of the volume of a shield volcano.

The porosity and permeability of lava flows come from vesicles, blisters, lava tubes, spaces between successive pāhoehoe lava flows (interflow zones), rubbly layers of ‘a‘ā clinker (which are especially permeable), and fractures (which also increases vertical connectivity) (fig. 17*C*) (Hunt, 1996). The permeability of a lava-flow aquifer is greater when the number of interflow zones or clinker layers is high—in other words, when the aquifer is formed by many thin lava flows rather than a few thick ones. The thin lava flows characteristic of Hawaiian shield volcanoes thus typically form highly permeable aquifers, with horizontal hydraulic conductivity (K_h) values of hundreds to tens of thousands of feet per day (for example, Soroos, 1973; Oki, 1999; Lau and Mink, 2006; Rotzoll and El-Kadi, 2008). Values of K_h can be orders of magnitude lower in the isolated cases where lava flows became thick by ponding in preexisting depressions (Izuka and Gingerich, 1998a, 2003). Thick individual lava flows of trachyte or other viscous lava are too small to form significant aquifers, but may locally resist groundwater flow.

Little direct information exists on the hydraulic anisotropy of lava-flow aquifers in Hawai‘i, but hydraulic conductivity is presumed to be much greater in the plane of the layers than it is in the direction perpendicular to the layers. Vertical hydraulic conductivity (K_v) has been estimated to be one to three orders of magnitude less than K_h (Souza and Voss, 1987). Additionally, lava-flow aquifers are assumed to be most conductive in the direction of elongation of the lava flows (in other words, the down-slope direction) (Nichols and others, 1996).

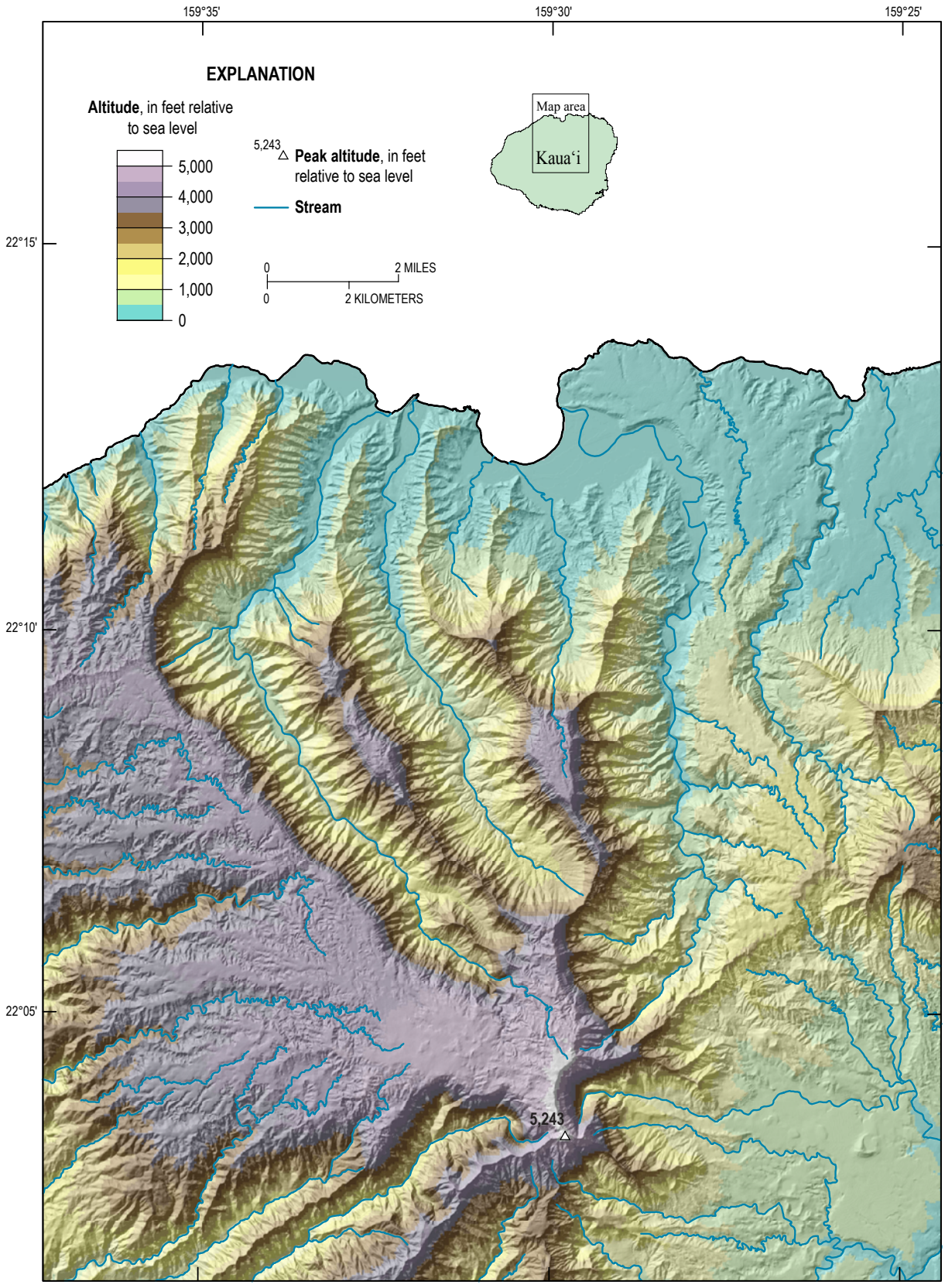

North American Datum 1983, Universal Transverse Mercator projection, zone 4N.

Figure 16. Map of deep stream valleys carved into the north flank of the Kaua'i shield volcano, Hawai'i. Topographic base modified from University of Hawai'i (2011), hydrography from U.S. Geological Survey (2012b).

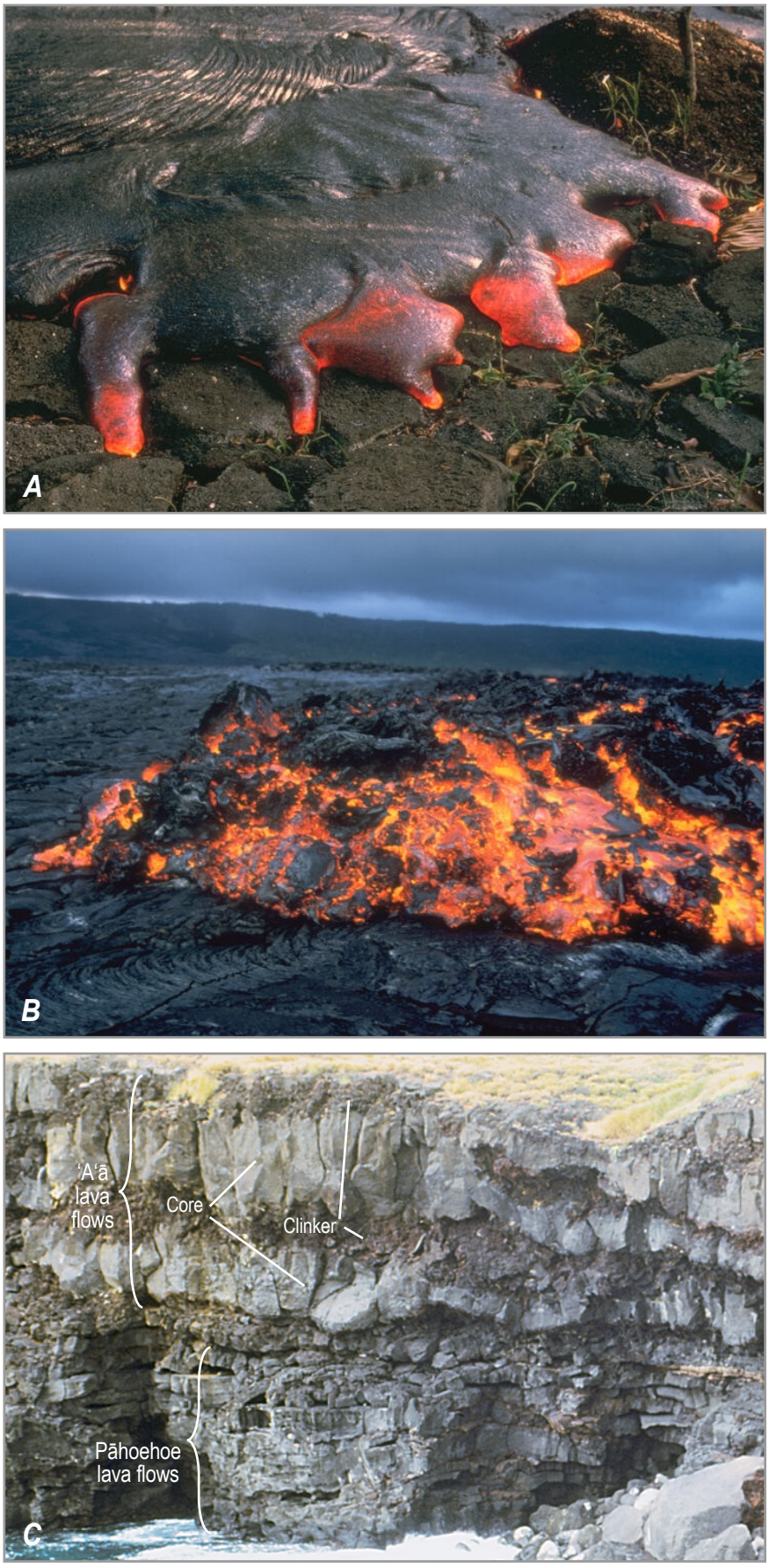

Figure 17. Examples of lava flows from Hawai‘i Island. (*A*) Active pāhoehoe lava flow at Kīlauea volcano. Photograph by J.D. Griggs, courtesy of the USGS Hawaiian Volcano Observatory. (*B*) Active ‘a‘ā lava flow at Kīlauea Volcano. Photograph courtesy of the USGS Hawaiian Volcano Observatory, photographer unknown. (*C*) Section of ‘a‘ā and pāhoehoe lava flows exposed in a fault scarp at the southern tip of the island. Photograph by S.K. Izuka, USGS, Pacific Islands Water Science Center.

Intrusive Bodies

Gravity data indicate that intrusive rocks constitute less than 30 percent of the volume of a shield volcano (Flinders and others, 2013), but these structures can substantially influence groundwater occurrence and flow in Hawai‘i’s volcanic aquifers. Dikes are the most common intrusive body in Hawaiian shield volcanoes (fig. 12*C*).

Studies of dikes exposed in the extensively eroded Ko‘olau shield volcano on O‘ahu (fig. 18) have contributed to the present knowledge of dike characteristics in Hawai‘i. Most of the dikes in the Ko‘olau volcano are less than 5 ft wide and inclined 65° to 85° relative to the horizontal (Walker, 1987). An individual dike can extend horizontally for more than a mile (Stearns and Vaksvik, 1935). Clusters of subparallel dikes form northwesterly trending linear complexes which have been interpreted as the location of rift zones of the Ko‘olau volcano, and dikes are abundant in an area believed to be the location of a caldera (Stearns and Vaksvik, 1935; Walker, 1987). Dikes are more abundant along the axis than at the margin of the dike complex. In the central part of the complex, dikes constitute 50 to 70 percent of the rock volume and average 100 to 200 dikes per horizontal mile transverse to the trend of the complex, whereas in the margins of the complex, dikes constitute less than 5 percent of the rock and abundances decline to about 10 to 100 per mile (Macdonald and others, 1983; Walker, 1987).

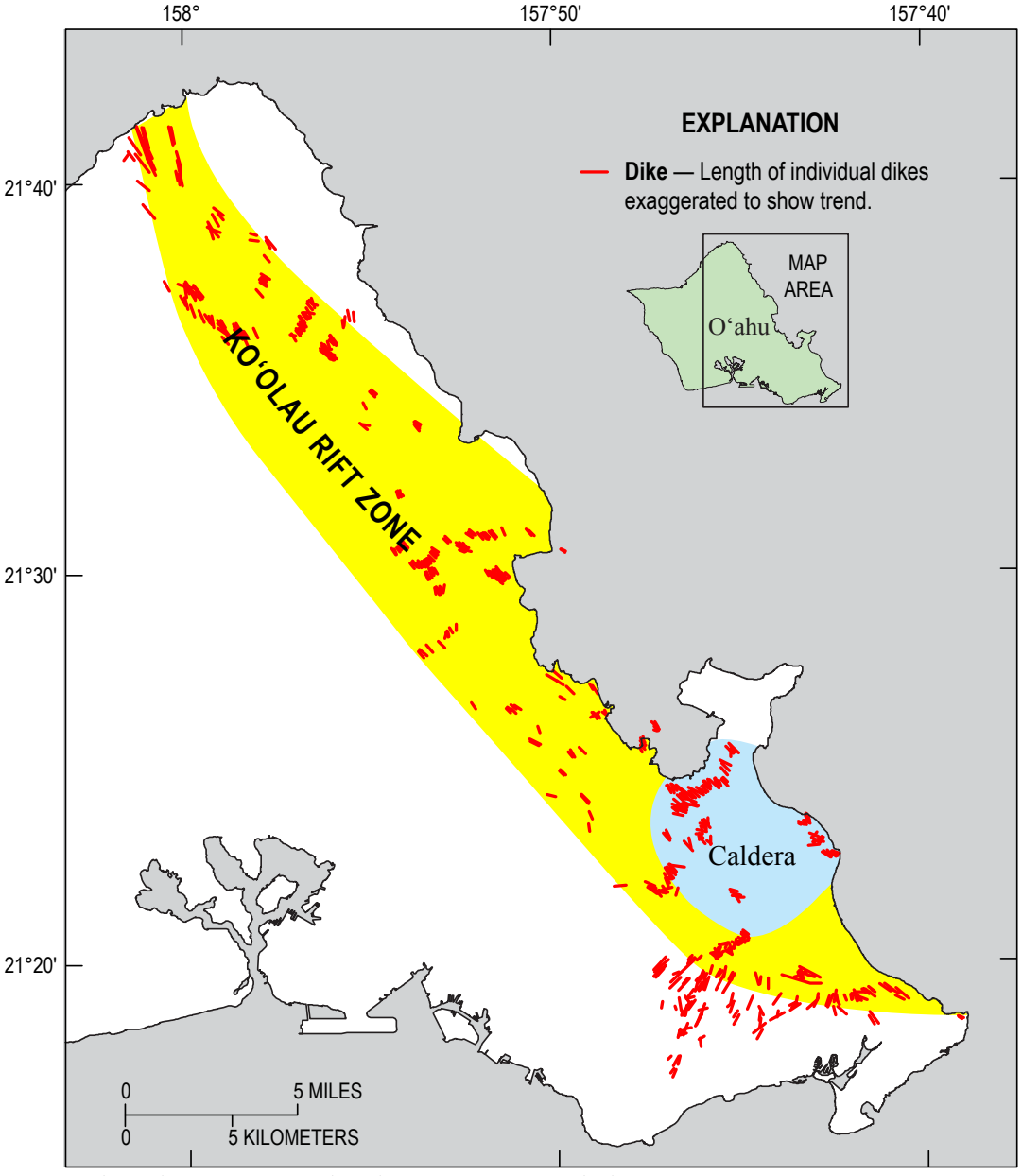

North American Datum 1983, Universal Transverse Mercator projection, zone 4N.

Figure 18. Map of dikes and interpreted locations of the rift zone and caldera of the Ko‘olau volcano, O‘ahu, Hawai‘i. Dikes and caldera outline modified from Sherrod and others, 2007; rift-zone trend modified from Hunt, 1996.

By analogy and by interpretation of geophysical data, dike complexes are presumed to exist beneath the rift zones and calderas of younger volcanoes in the Hawaiian archipelago, even though few dikes may have been exposed by erosion. The number of dikes and the width of the dike complexes increase with depth (Macdonald and others, 1983; Takasaki and Mink, 1985). Whereas a rift zone may be about 2 mi wide at the surface, it may be 7–10 mi wide at a depth of 2 mi (Fornari, 1987). On some volcanoes, for example Kaua‘i and West Maui, dikes exposed by erosion are not organized into clearly defined linear dike complexes or rift zones.

The rock that forms dikes is mostly massive with low effective porosity provided primarily by fractures (Hunt, 1996); thus, dikes have much lower permeability than typical lava-flow aquifers of Hawai‘i. Dikes impede horizontal groundwater flow and reduce the bulk permeability and storage of aquifers into which they intrude, especially if the dikes are numerous and closely spaced. However, a few dikes widely spaced in a large area of permeable lava-flow aquifer can impound groundwater and increase storage (fig. 2). Much of the present understanding of the relation between dikes and groundwater comes from O‘ahu, where the development of dike-impounded groundwater and its effects on spring flow, streamflow, and storage depletion have been well studied (for example Takasaki and others, 1969; Hirashima, 1971; Takasaki and Mink, 1985).

Other intrusive bodies such as stocks, plugs, sills, and laccoliths occur on some shield volcanoes, but are much less common than dikes (Macdonald and others, 1983) and are of minor hydrologic significance in Hawai‘i (Lau and Mink, 2006). No intrusive bodies attributed to ancient magma reservoirs are exposed in Hawai‘i. Seismic data indicate that a magma reservoir exists about 1 to 4 mi beneath the summit of Kīlauea (Ryan and others, 1981), but rocks formed in the magma chamber of older islands have probably subsided thousands of feet along with the rest of the island.

Tephra

Tephra deposits (also known as pyroclastic deposits) are accumulations of rock particles fragmented by the energy of an eruption. Two common types of tephra deposits in Hawaiian shield volcanoes are cinder and ash (fig. 19). The terms “cinder” and “ash” come from different classifications schemes—ash refers to tephra of a particular size (less than 0.5 cm or about 0.2 in.) whereas cinder refers to tephra that is scoriaceous (highly vesicular), regardless of size. Nevertheless, the terms “cinder” and “ash” are used in this report because they are widely used in reference to tephra in Hawai‘i. In this context, cinder refers to scoriaceous particles that are mostly larger than ash and commonly formed by fire-fountain eruptions, whereas ash consists of fine glassy particles commonly erupted more violently, such as in phreatomagmatic eruptions. Cinder and ash can be ejected from the same eruption and become sorted by the wind; both can form cones near the vents, but ash also can be carried by the wind and deposited in layers far from the eruption site (Macdonald and others, 1983).

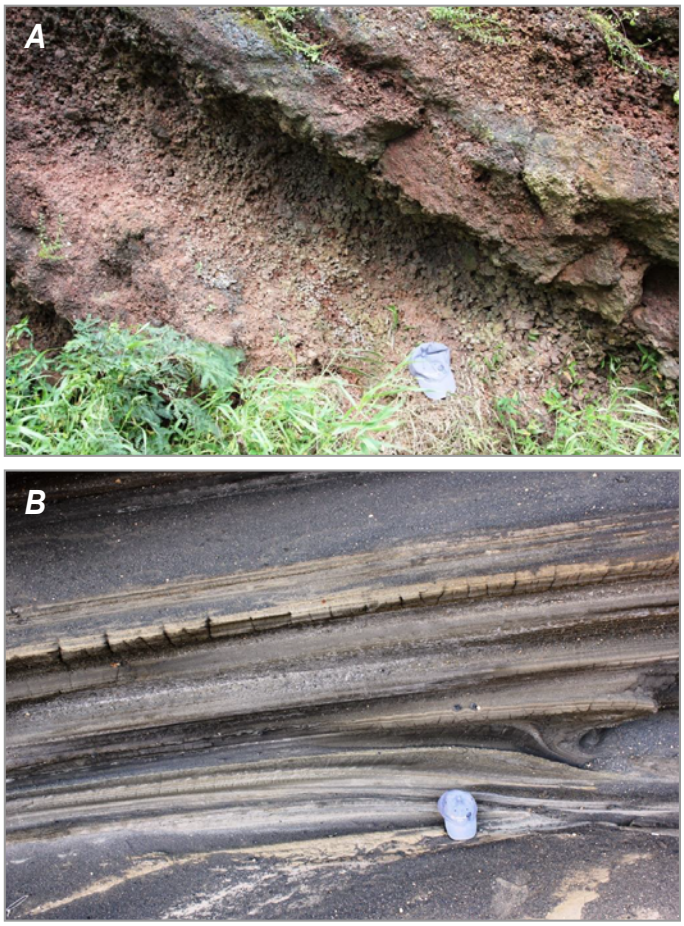

Figure 19. Tephra deposits of the Honolulu Volcanics on O‘ahu, Hawai‘i. (*A*) Cinder. (*B*) Consolidated ash (tuff). Photographs by S.K. Izuka, USGS Pacific Islands Water Science Center.

Tephra deposits constitute only a small fraction of a shield-volcano’s volume, but some deposits can have an important effect on groundwater flow. Like analogous clastic sedimentary rocks, the permeability of tephra varies with grain size. Coarse tephra deposits such as cinder tend to be more permeable than fine tephra deposits such as ash (fig. 19). Also, because ash is composed of fine particles and is commonly glassy, it weathers easily and becomes cemented relatively quickly. Tephra deposits are occasionally interlayered with the lava flows that form the shield volcano. Some important perched groundwater bodies (for example on Hawai‘i Island) have been attributed to extensive low-permeability ash layers embedded within lava-flow aquifers.

Weathered and Metamorphosed Volcanic Rock

The primitive basalts of Hawai‘i, being fine-grained and composed of minerals that formed at high temperature, are particularly susceptible to chemical weathering when exposed to water, oxygen, and relatively low temperatures at the earth’s surface (Macdonald and others, 1983). The original minerals in basalt are altered to oxides, hydroxides, and clays, and

soluble ions are mobilized by water. Weathering reduces rock porosity by formation of secondary minerals and volumetric increase of material caused by chemical alteration (Wentworth, 1928; Macdonald and others, 1983; Mink and Lau, 1980). Highly weathered basalt forms soft, red-brown soil. Soil thicknesses depend on climate, vegetation, slope, and time since the basalt became exposed to surface weathering agents. On the older islands such as O‘ahu, residual soil layers can be hundreds of feet thick (Stearns and Vaksvik, 1935). Ancient, low-permeability soil layers have been found buried within the lava flows of shield volcanoes. Some perched groundwater bodies have been attributed to such buried soils.

Low-grade metamorphism of volcanic rock occurs in isolated areas of Hawai‘i. For example, metamorphic rock that formed by hydrothermal alteration beneath the ancient caldera of the Ko‘olau volcano on O‘ahu (fig. 18) has been exposed by erosion. These rocks were originally tholeiitic basalt, but the mafic minerals have been altered and secondary minerals have been deposited in pores (Macdonald and others, 1983). Metamorphic rocks constitute only a small part of Hawai‘i’s geology and their permeability is generally too low to contain developable groundwater, but they may locally affect groundwater movement (Stearns and Vaksvik, 1935; Lau and Mink, 2006).

Sedimentary Rocks

Valley-filling alluvium consists mostly of consolidated to unconsolidated, poorly sorted gravel with clasts ranging from boulders to clay. The larger clasts are primarily lithic fragments and the finer clasts are clay. Quartz and potassium feldspar, common in continental clastic sediments, are rare in Hawai‘i because these minerals are not a primary component of basalt (Moberly and others, 1965; Macdonald and others, 1983). Most marine sediment consists of carbonate material precipitated by marine organisms; consolidation of carbonate sediment forms limestone.

The hydraulic properties of sediments vary widely (Hunt, 1996; Lau and Mink, 2006). As a whole, alluvium has hydraulic conductivities several orders of magnitude lower than that of lava-flow aquifers (Lau and Mink, 2006). The low permeability is likely due in part to continued weathering of the alluvium after deposition (Hunt, 1996). Indeed, the hydraulic properties of weathered alluvium are similar to that of deeply weathered basalt (Lau and Mink, 2006). On the other hand, the permeability of limestone can be as high as, or higher than, that of lava-flow aquifers (Lau and Mink, 2006). The high permeability results from primary porosity (from the reef framework itself) and from secondary porosity caused by limestone diagenesis.

Groundwater Occurrence and Flow

Hawai‘i’s fresh groundwater resources originate as precipitation (fig. 2). Most of this precipitation comes in the form of rain, but fog interception by forests and snow on the highest mountain tops also contribute to precipitation in some areas. A fraction of the water that falls as precipitation infiltrates the ground and contributes to groundwater recharge; the remainder is evaporated, transpired by plants, or runs off to the ocean by way of streams. In some areas, humans have diverted stream water back onto land to irrigate crops; this water is also subject to the same processes as precipitation and can enhance groundwater recharge. (Humans have also used groundwater for irrigation, but the amount of water withdrawn from the aquifer is always more than the aquifer receives back from irrigation return.) The rate of groundwater recharge is thus a function of climate, vegetation, soil properties, and human activity.

Much of Hawai‘i’s fresh groundwater resources exist in the dike-free lava flows of the shield volcanoes. In the dike-free lava flows, fresh groundwater forms a lens-shaped body that overlies denser saltwater from the ocean (fig. 2). The freshwater lens is dynamic—groundwater naturally flows from inland areas, where recharge occurs, toward the coast, where groundwater discharges to springs, streams, wetlands, and submarine seeps. At the bottom of the lens, the flowing freshwater mixes with the underlying saltwater to form a brackish mixing zone. The mixing zone is commonly referred to as the transition zone because salinity gradually transitions from fresh groundwater above to saltwater below (fig. 20). Water in the transition zone also flows toward discharge zones near the coast. The entrainment of saltwater into the flowing transition zone also sets up flow in the part of the aquifer occupied by saltwater (Cooper, 1964).

In the natural state, the overall thickness of the freshwater lens depends on aquifer permeability and the rate of groundwater flow through the lens—freshwater lenses are thinner where the hydraulic conductivity is high or flow rates are low. The Ghyben-Herzberg relation, which considers the density difference between seawater and freshwater, indicates that the freshwater-lens thickness below sea level is 40 times the water-table altitude above sea level. The relation has been used to estimate the freshwater-lens thickness, but it assumes that the boundary between the freshwater lens and underlying saltwater is sharp rather than a diffuse transition zone. The relation also assumes hydrostatic conditions that do not exist in the lens where freshwater is constantly flowing. The relation yields a reasonable approximation of the thickness of some parts of the freshwater lens, such as where flow is primarily horizontal, but is inaccurate in areas or parts of the lens where there are vertical head gradients (Izuka and Gingerich, 1998b). Data from deep monitoring wells indicate that where the freshwater lens is in a transient state, changes in the position of the transition zone lag behind changes in the water table (Rotzoll and others, 2010). Despite the inaccuracies, the Ghyben-Herzberg relation illustrates that the height of the water table above sea level and the thickness of the freshwater lens below sea level are linked.

The concept of the fresh groundwater lens is not unique to Hawai‘i or to volcanic aquifers—it is generic to coastal aquifers

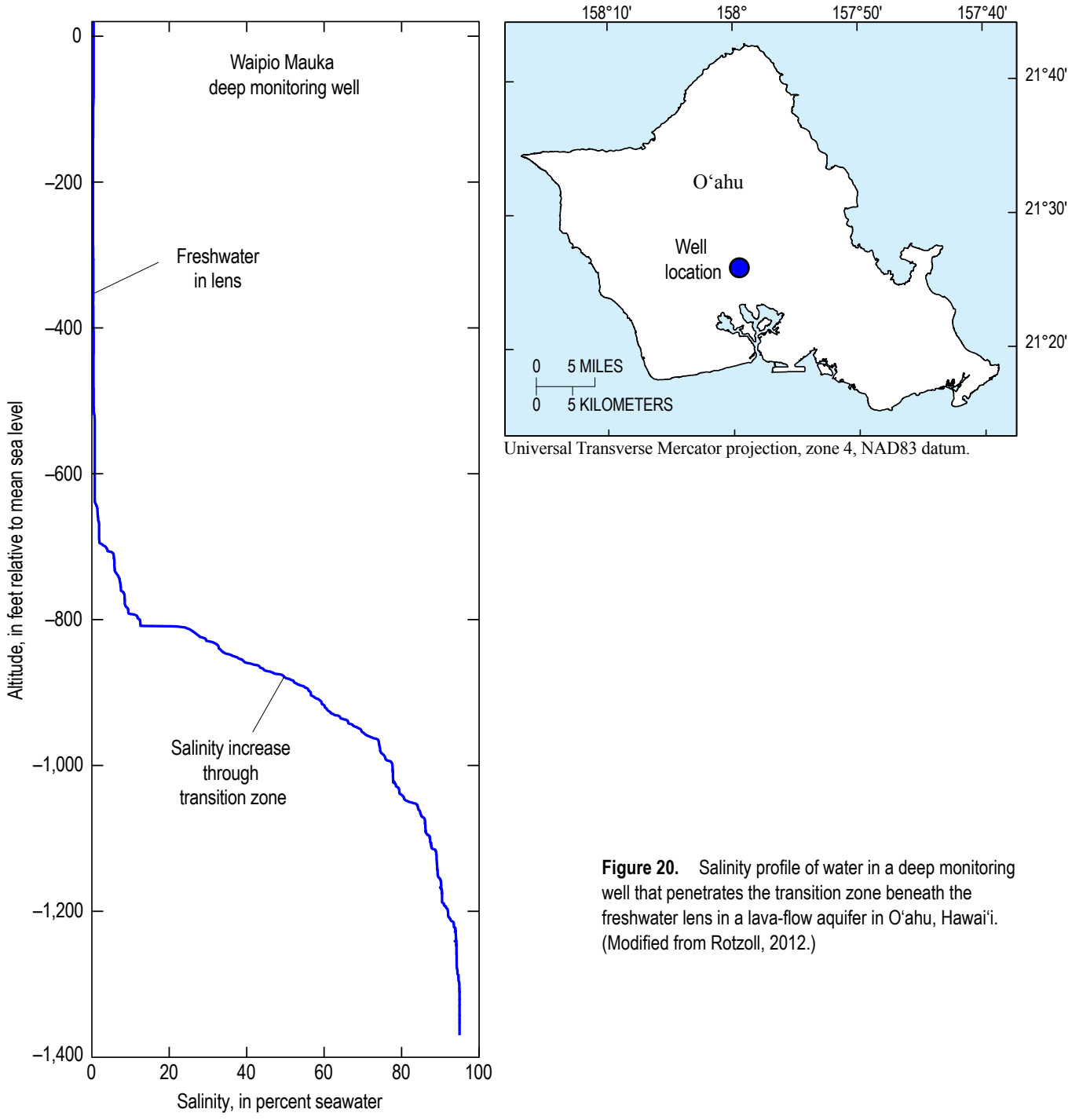

Figure 20. Salinity profile of water in a deep monitoring well that penetrates the transition zone beneath the freshwater lens in a lava-flow aquifer in O‘ahu, Hawai‘i. (Modified from Rotzoll, 2012.)

worldwide. However, Hawai‘i has a much steeper orographic rainfall gradient and higher aquifer permeability than most other coastal aquifers. Effects of dikes and other rocks and structures of volcanic and sedimentary origin add to the uniqueness of Hawai‘i’s groundwater setting. A general conceptual model for Hawai‘i, especially O‘ahu, emerged in the early to middle 20th century (for example Meinzer, 1923a, 1930; Stearns and Vaksvik, 1935; Stearns, 1940) (fig. 21). In this conceptual model, the freshwater lens was commonly referred to as “basal” groundwater. The dike-free lava flows were generally regarded as having high permeability, thus the basal water table sloped gently from a few tens of feet above sea level in inland areas to near sea level at the coast. Low-permeability coastal-plain sediments and rejuvenated-stage volcanics formed the semiconfining caprock that resisted groundwater discharge to the ocean and caused the freshwater lens to thicken, but even so, the basal water table in this conceptual model was nowhere more than about 50 ft above sea level. Higher groundwater occurrences—in some cases hundreds to thousands of feet above sea level—were referred to as “high-level” groundwater. High-level groundwater included water impounded by dikes and groundwater perched on buried low-permeability horizons formed by ash, soil, weathered rock, or unusually dense lava flows.

Variations from the general conceptual model were known even as it developed, but the general model provided the basis for groundwater exploration and management for many decades and is still applicable in many cases. However, as more information became available, particularly for islands other than O‘ahu, it became apparent that the general conceptual model could not explain all major groundwater occurrences in Hawai‘i. An updated review of aspects of Hawai‘i’s volcanic aquifer systems is presented in the *Hydrogeologic Framework of the Islands* and *Conceptual Models of Groundwater Occurrence and Movement* sections of this report.

Groundwater in Hawai‘i is developed by conventional vertical wells and by shafts and tunnels (fig. 21). Most wells are vertical, drilled into the semiconfined or unconfined parts of the freshwater lens. Shafts are large vertical or inclined borings excavated down to the water table, with one or more borings (galleries) parallel to the water table. The galleries are positioned to “skim” water off the top of the freshwater lens while minimizing drawdown. Shafts are the largest producing individual wells in Hawai‘i. Tunnels are large borings driven horizontally into dike-impounded groundwater.

Hydrogeologic Framework of the Islands

The hydrogeologic framework is the three-dimensional distribution of aquifer materials and their hydraulic properties. The general hydrogeologic aspects common to all four of the islands in the scope of this study were discussed above in the *Hydrogeologic Overview* section of this report. The more detailed discussion that follows describes the hydrogeologic-framework characteristics that are specific to each island.

Geologic and Hydrogeologic Units—The geologic units defined and described in the Division of Hydrography Bulletins (Stearns and Vaksvik, 1935; Stearns, 1939, 1940; Stearns and Macdonald, 1942, 1946; Macdonald and others, 1960), as well as subsequent revisions by Langenheim and Clague (1987) and Sherrod and others (2007), are based on lithology and

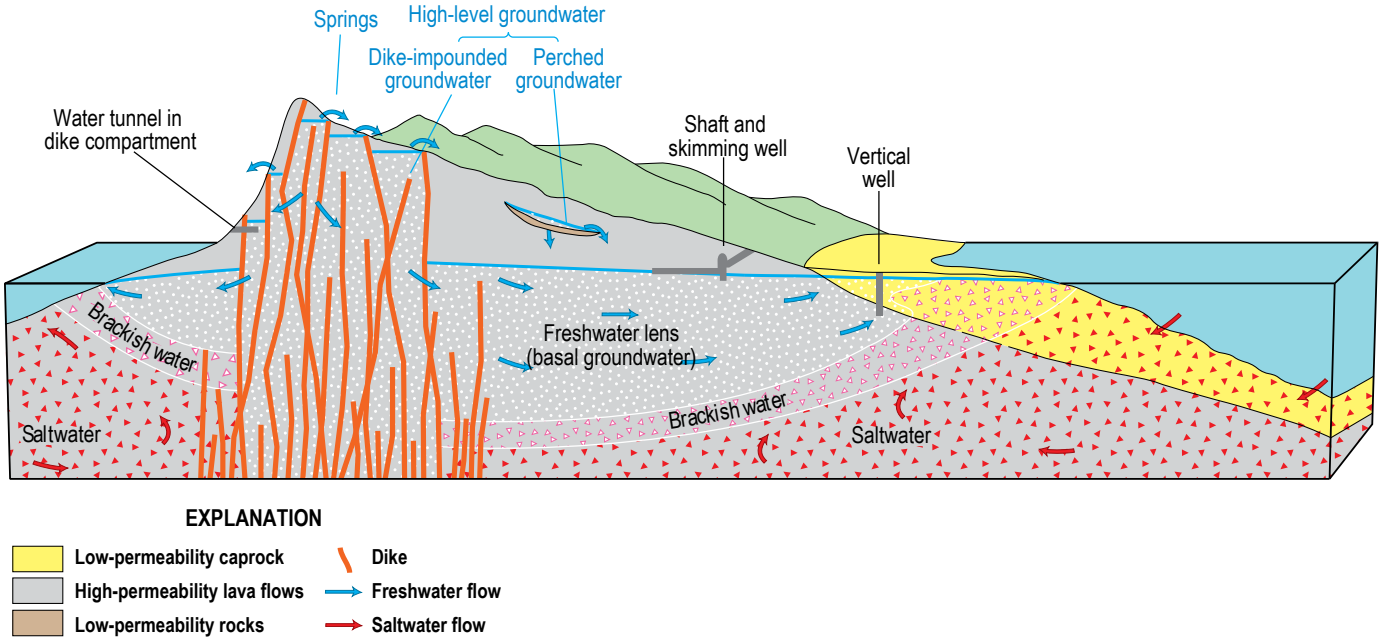

Figure 21. Conceptual model of groundwater occurrence and flow in Hawai‘i, developed by about the middle of the 20th century. Modified from Oki and others, 1999a.

stratigraphic relations. The Division of Hydrography Bulletins described the relative water-bearing properties of each geologic unit. In this report, information from hydrologic studies as well as data from unpublished sources, particularly the well files and databases of the Hawai‘i State Commission on Water Resource Management (CWRM) and the USGS-Pacific Islands Water Science Center (PIWSC) were used to define "hydrogeologic units" (HGUs)—mappable volumes of rock having characteristic hydraulic properties and distinct boundaries. "Characteristic" in this case does not necessarily mean "homogeneous"—some HGUs are characteristically heterogeneous. To a large extent, the hydrogeologic units conform to the mapped geologic units defined in previous literature. In some cases, a subunit is described within an HGU for an area that has distinctive hydraulic properties but whose boundaries are poorly known or gradational. For example, dikes reduce the overall permeability of the rocks into which they intrude (host rock), but the permeability-reduction depends on the number of dikes per unit volume of host rock, and dike abundances commonly diminish gradually from dike-intruded to dike-free areas. Dike-intruded areas are thus shown as subunits within the more clearly defined boundaries of some HGUs.

In some cases, geologic units that are stratigraphically adjacent and have similar characteristics were combined into one hydrogeologic unit. Also, geologic units that are volumetrically insignificant or contain little groundwater were combined with more voluminous stratigraphically adjacent geologic units.

Hydraulic Properties—Hydraulic-conductivity and storage-coefficient values from published literature and unpublished sources are summarized for each hydrogeologic unit in this report. Available hydraulic-conductivity and storage values are, however, limited in number and areal distribution. Values for the specific capacity of wells (discharge divided by drawdown measured during the testing) are more widely available over the study area. Specific capacity is an indicator of relative aquifer permeability (higher values indicate greater permeability) but is also affected by variables unrelated to permeability, such as well construction, testing length and conditions, and proximity to hydrologic boundaries. Even so, specific capacity is instructive for assessing the general distribution of aquifer permeability at the regional scale. Rotzoll and El-Kadi (2008) developed a regression relation between specific capacity and hydraulic conductivity for Maui, and used the relation to assess the regional distribution of hydraulic conductivity from specific-capacity data throughout most of the major Hawaiian Islands.

Structure and Thickness—Structure maps (maps that depict the above- and below-ground configuration of a surface, such as the top of a hydrogeologic unit) and thickness maps were created to help describe the distribution of hydrologic properties in the study area. Structure maps were created by analyzing data of the surface and subsurface geology, and subaerial and submarine topography. Surface geology was based on the State geologic map (Sherrod and others, 2007). Subsurface geology was determined from well-log and other data in published and unpublished sources, including the well files and databases of the USGS and CWRM. Subaerial and submarine topography was derived from a digital layer in which a 10-m subaerial digital elevation model (DEM) was merged with multibeam bathymetric data (University of Hawai‘i, 2011). Additional sources of information for the structure and thickness maps are cited in the descriptions of the hydrogeology of the individual islands, below.

Construction of the structure maps started with deriving topographic contours (lines of equal altitude, relative to sea level) at 200-ft intervals from the subaerial/submarine data layer using a geographic information system (GIS). Where a hydrogeologic unit crops out at the surface, the topographic contours represent the top of the unit. Where the top of the hydrogeologic unit lies beneath the ground surface, contours were modified manually to make them consistent with the subsurface geologic data. Because the State geologic map does not provide information offshore, submarine geology was interpreted by projecting slopes derived from the geologic map and subsurface data (fig. 22). The thickness maps were created by generating raster maps from the 200-ft structure contour maps, and subtracting the elevations in one raster map (representing the top of an underlying unit) from another (representing the top of the overlying unit).

Water-table maps—Generalized water-table maps are provided for each island. The shape of the water table reflects the distribution of aquifer properties and the flow of groundwater. The groundwater table generally slopes downward in the direction of groundwater flow. The steepness (gradient) of the water table is a function of aquifer permeability and groundwater-flow rate. Other factors being equal, the water-table gradient will be steeper where aquifer permeability is lower or the flow rate is higher.

Ideally, water-table maps would be based on groundwater levels measured at about the same time (synoptically) to isolate spatial variations from temporal variations caused by changes in climate or withdrawal rates from wells. In the study area, however, available water-level data for any given instant in time were not distributed widely enough in space to create synoptic water-table maps at island-wide scales. Inasmuch as the magnitude of temporal water-level variations in Hawai‘i is generally smaller than the magnitude of spatial water-level variations resulting from contrasts in permeability and recharge from one location to the next, water levels measured at different times can be used to provide enough spatial coverage to allow creation of generalized water-table maps for Kaua‘i, O‘ahu, and Maui. Because of the limitations of using data from different times, the resolution of these maps is coarse, but the maps are sufficient to show gross differences in water-table elevation resulting from contrasts in hydraulic properties.

The water-table maps in this section were constructed on the basis of water levels measured at wells, supplemented by information on springs and wetlands, which are surface expressions of the water table. The water-level data from wells are stored in the USGS National Water Information System (NWIS, http://dx.doi.org/10.5066/F7P55KJN or http://waterdata.usgs.gov/nwis). Water-level data used in this report include data that were already in NWIS as well as data added to the NWIS database during the course of this study. Most of the data added during this study were acquired from CWRM and verified by cross checking with written documentation in physical well files at the USGS and CWRM. The water-table maps reflect the earliest reported

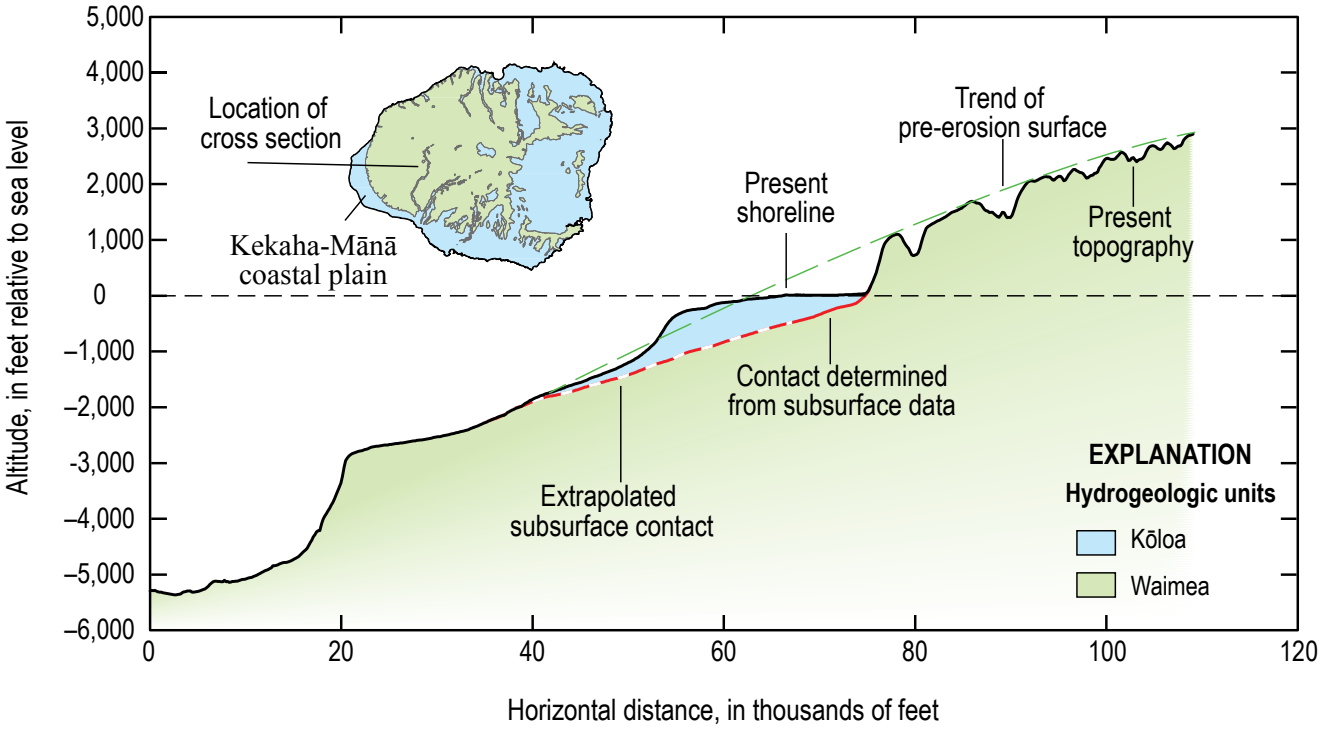

Figure 22. Topographic profile and interpretations of the geology beneath the Kekaha-Mānā coastal plain, Kauaʻi, Hawaiʻi.

water-level measurement, relative to sea level, as well as locations of springs and wetlands from the U.S. Geological Survey (2012b) National Hydrography Dataset, and their altitudes from a DEM (University of Hawaiʻi, 2011). A GIS was used to create rough contour lines using simple triangulation. The rough contours were manually adjusted in the GIS to ensure that the water table was consistent with the water-level data and was not higher than ground surface. Small areas of slightly elevated groundwater levels in small alluvial deposits and minor occurrences of perched water indicated by small isolated springs or anomalous high water levels in wells were not included.

Kauaʻi

Kauaʻi lies near the northwest end of the main islands of Hawaiʻi (fig. 1). With a land area of 552 mi^2, it is the fourth largest island in the Hawaiian archipelago and constitutes 8.6 percent of the total land area in the main islands (table 1). The highest point is 5,243 ft, near the island's center (fig. 23). Most of the population of 66,921 (about 5 percent of the population of the State of Hawaiʻi) lives in the eastern part of the island.

Geology

The geology of Kauaʻi has been presented comprehensively in Division of Hydrography Bulletin 13 by Macdonald and others (1960), the Hawaiʻi State geologic map by Sherrod and others (2007), and other publications by Stearns (1946) and Macdonald and others (1983). The synopsis presented here is largely based on these sources, with additional specific information as cited.

Kauaʻi is geologically the oldest of the four islands in this study. Radiometric dating indicates that most of the part of Kauaʻi above sea level was formed between about 5.5 and 4 million years ago, but eruptions occurred as recently as 0.15 million years ago. The prevailing view in current geologic literature is that the bulk of Kauaʻi was built by a single shield volcano. A central summit caldera—the Olokele Caldera—was identified on the basis of outcrops of nearly horizontal, thickly bedded lava flows and associated breccia interpreted as caldera fill, and high-angle bounding faults exposed in deeply cut stream valleys and canyons (fig. 24). With a diameter of 6–8 mi, the Olokele Caldera is larger than any other caldera in Hawaiʻi.

Stream erosion carved a generally radial pattern of valleys in the original shield surface of Kauaʻi, but large-scale faulting and collapse during and after the shield stage also modified the topography, altered erosion patterns, and influenced the deposition of younger rock units. Large-scale faulting produced the Makaweli graben, which was partly filled by later shield and postshield lavas, and rerouted the radial drainage pattern to cause the erosion of Waimea Canyon (figs. 23 and 24). Another large depression—the Līhuʻe basin in eastern Kauaʻi—was partly filled by rejuvenated-stage lavas.

Sediments also contributed to filling the depressions, and to the formation of a coastal plain. Alluvium primarily consists of clasts and clays derived from the volcanic rock

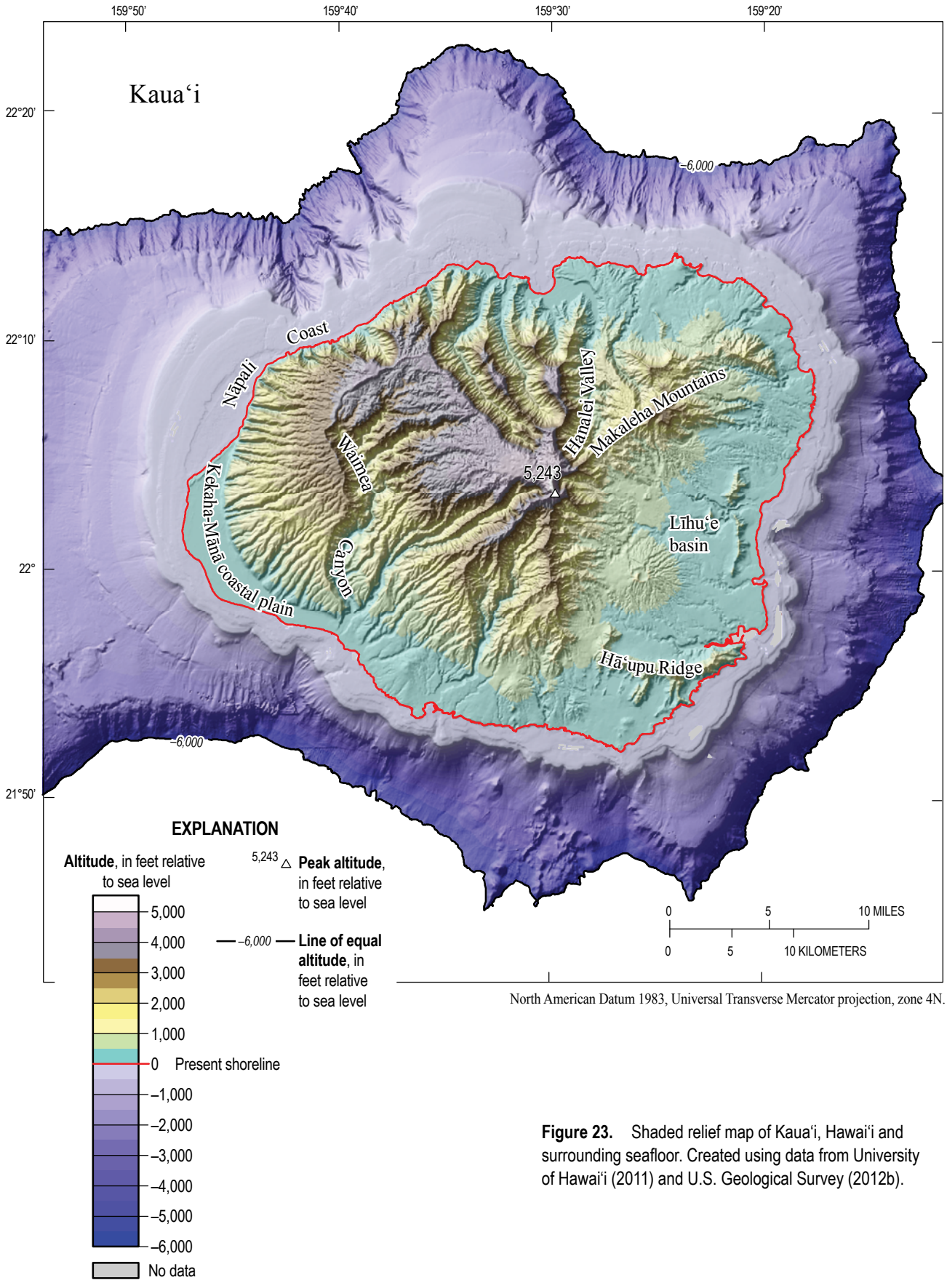

Figure 23. Shaded relief map of Kaua‘i, Hawai‘i and surrounding seafloor. Created using data from University of Hawai‘i (2011) and U.S. Geological Survey (2012b).

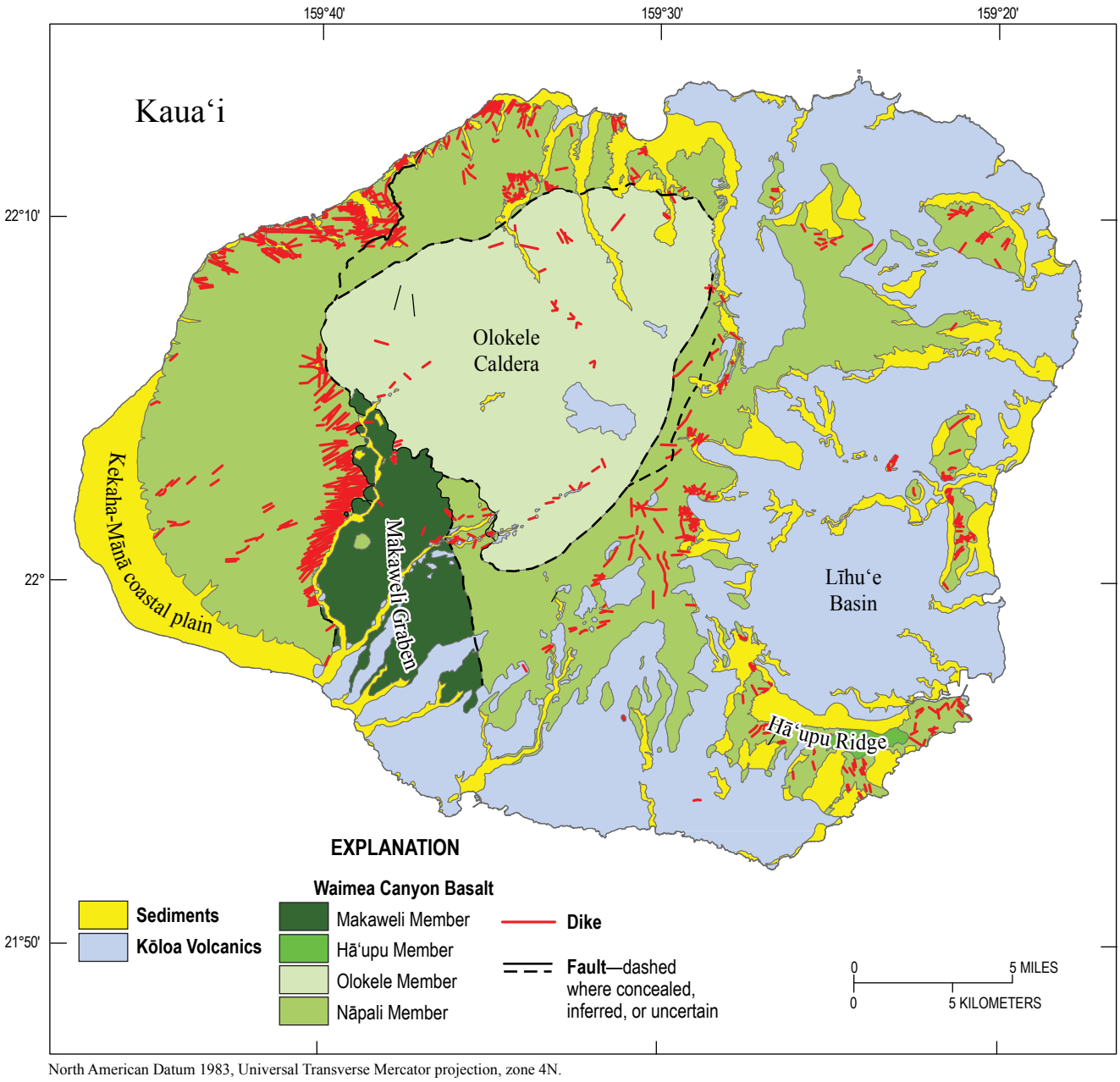

Figure 24. Simplified geologic map of Kauaʻi, Hawaiʻi. Modified from Sherrod and others (2007).

of the island, and may be consolidated or unconsolidated. Carbonate and mixed carbonate-silicate sediments include consolidated and unconsolidated calcareous sand dunes, poorly consolidated lagoon deposits, and consolidated to unconsolidated beach deposits. Reef and lagoon deposits have also been encountered in drill holes (Izuka and Resig, 2008). The most extensive sedimentary outcrop on Kaua‘i is the Kekaha-Mānā coastal-plain deposit on the southwest coast of the island (fig. 24).

The igneous rocks of Kaua‘i are divided into two formations—the Waimea Canyon Basalt and the Kōloa Volcanics—that are separated by an erosional unconformity (Macdonald and others, 1960; Langenheim and Clague, 1987; Sherrod and others, 2007) (table 2, fig. 24). The Waimea Canyon Basalt includes all of the rocks formed during Kaua‘i’s shield stage and forms the bulk of the island. The formation is divided into the Nāpali, Olokele, Makaweli, and Hā‘upu Members. The most voluminous of these is the Nāpali Member, which chiefly consists of a thick pile of thin lava flows of tholeiitic-basalt composition. The dike-free parts of the Nāpali Member include some of the most productive aquifers on Kaua‘i (Izuka, 2006). The Olokele Member is formed by the thick-bedded basalts and associated breccia that accumulated in the Olokele caldera. The Makaweli Member is composed of the thick-bedded basalts that accumulated in the Makaweli graben, but parts of the Makaweli Member, especially in the east of the graben, are thin bedded like the Nāpali Member. The Olokele and Makaweli Members include a few flows of postshield-stage lavas; these deposits are too small to warrant mapping as a separate unit. The Hā‘upu Member is composed of thick-bedded tholeiitic lava flows and breccia interpreted as the fill of a small satellite caldera on the flank of the Kaua‘i shield, south of the Līhu‘e basin; this member is volumetrically much smaller than the other members of the Waimea Canyon Basalt.

Overlying the Waimea Canyon Basalt is the Kōloa Volcanics, which consists mostly of alkalic rejuvenated-stage volcanic rocks (Macdonald and others, 1960; Langenheim and Clague, 1987; Sherrod and others, 2007) (table 2, fig. 24). The Kōloa Volcanics is important to Kaua‘i because most of the wells in the Līhu‘e area, the island’s center of population and industry, develop water from the formation. The Kōloa Volcanics is the most extensive rejuvenated-stage formation in Hawai‘i, covering more than a third of Kaua‘i’s surface and having an estimated volume of 58 km^3 (Garcia and others, 2010). In some places, such as in the Līhu‘e basin, the Kōloa Volcanics filled depressions in the shield surface and accumulated to thicknesses of more than 1,000 ft (Macdonald and others, 1960; Gingerich and Izuka, 1997; Izuka and Gingerich, 1997a–d; Reiners and others, 1999; Gandy, 2006). Lava-flow thicknesses vary substantially depending on whether the flows descended a slope or ponded in a depression; ponded lava flows can reach thicknesses of more than 500 ft. Lava flows of the Kōloa Volcanics are interlayered with ash and cinder deposits and layers of terrigenous and marine sediments (Macdonald and others, 1960; Izuka and Resig, 2008). Macdonald and others (1960) considered the sedimentary units within the Kōloa Volcanics substantial enough to warrant a formal stratigraphic name; the most recent revisions of Kaua‘i’s stratigraphic nomenclature (Langenheim and Clague, 1987) refer to this unit as the Palikea Breccia Member. Other sedimentary rocks on Kaua‘i have not been formally named.

Geologic Enigmas—Macdonald and others (1960) recognized that Kaua‘i is the most geologically complex island in Hawai‘i. Indeed, data from subsequent studies have challenged the interpretations of Stearns (1946) and Macdonald and others (1960). A positive gravity anomaly (similar to those associated with the dense rocks beneath the summit calderas of Hawai‘i shield volcanoes) lying east of, not over, the outline of the Olokele Caldera proposed by Macdonald and others (1960) (fig. 24) has led researchers to question the postulated location of the ancient caldera (Krivoy and others, 1965; Flinders and others 2010, 2013). Isotopic differences between lavas in western and eastern Kaua‘i led Holcomb and others (1997) to suggest that Kaua‘i was built of two sequential shield volcanoes, and that the thick-bedded lavas of the Olokele Member formed as lava from the younger eastern volcano ponded against an escarpment on the collapsed flank of the older western volcano. The controversies raised by these alternative hypotheses have not yet been resolved.

The origin of the large, semicircular Līhu‘e basin (fig. 23) is also unresolved. Stearns (1946) attributed the basin’s formation to advanced stream erosion. Macdonald and others (1960) described the basin as a flank caldera (in contrast to the summit caldera they interpreted from the Olokele Member), citing the nearly circular shape of the basin. Other theories also invoke some mechanism of collapse, faulting, or landsliding (Holcomb and others, 1997; Reiners and others, 1999; Sherrod and others, 2007; Sherrod and others, 2015). No specific mechanism or combination of mechanisms has been widely accepted, however, and the formation of the Līhu‘e basin has remained one of the most evasive enigmas in Hawai‘i geology.

Other complexities that set Kaua‘i apart from the rest of the main islands in Hawai‘i include the lack of well-defined rift zones. Although many dikes have been exposed by erosion on Kaua‘i (fig. 24), they are not organized in easily defined linear zones as are the dikes on O‘ahu (Macdonald and others 1960). Macdonald and others (1960) suggested, on the basis of dike trends and submarine contours, possible rift zones extending northeastward and west-southwestward from the island’s center. Fiske and Jackson (1972) proposed rift zones that are virtually perpendicular to those suggested by Macdonald and others (1960), but suggest that there was little tendency for well-defined rift zones to form in the nearly symmetrical stress field in which Kaua‘i grew.

Hydrogeologic Units

Macdonald and others (1960) described the water-bearing properties of each of the mapped geologic units on Kaua‘i. At the time of their study, all but one of the wells in the Waimea Canyon Basalt were in the highly productive Nāpali Member. Numerous wells also tapped the less-productive Kōloa Volcanics because this formation covers much of eastern Kaua‘i, where most of the population and industry was located. Wells were completely absent in the Olokele and Hā‘upu Members of the Waimea Canyon Basalt, and only one well (a water tunnel) developed

water from the Makaweli Member, so Macdonald and others (1960) used geologic characteristics observed in the field—such as the thickness of beds, proportion of clinker, and presence of dikes—to infer what the water-bearing properties of these geologic units would be.

Macdonald and others (1960) wrote that the thin-bedded Nāpali Member, where unaltered and free of dikes, was highly permeable and freely yielded water to wells. Because the Olokele and Hā‘upu Members had thicker-bedded lavas than the Nāpali Member, they were described as having lower permeability. The Makaweli Member was described as having intermediate permeability, but the permeability probably varies widely because some parts are thickly bedded and other parts are thinly bedded. The Kōloa Volcanics was described as poorly to moderately permeable, having average and maximum lava flow thicknesses that are "distinctly greater" than those of the Nāpali Member. Intrusion by dikes can substantially reduce the regional permeability of all of the volcanic units. Sediments, including the Palikea Breccia Member of the Kōloa Volcanics as well as other alluvium and marine sediments, were described as having relatively low permeability.

On the basis of the water-bearing properties of the rocks described by Macdonald and others (1960), in this study, the rocks of Kaua‘i are divided into two principal hydrogeologic units (HGUs): the Kōloa and Waimea (fig. 25). The Kōloa HGU includes the lava flows of the Kōloa Volcanics, intercalated sedimentary layers of the Palikea Breccia Member, and younger surficial sediments; all of these components have been described as having relatively low permeability. The Waimea HGU includes all of the members of the Waimea Canyon Basalt, and thus has a wide range of hydraulic properties.

Kōloa Hydrogeologic Unit

The thickness map of the Kōloa HGU shows extensive deposits in eastern Kaua‘i corresponding with the Kōloa Volcanics (fig. 26). The lava flows of the Kōloa Volcanics that constitute a large fraction of the volume of the Kōloa HGU filling the on-shore depressions such as the Līhu‘e basin and Hanalei Valley probably also extend offshore and contribute substantially to the thickness of this hydrogeologic unit off the northeastern, eastern, and southern coasts. The thicknesses of the Kōloa HGU in these areas are generally consistent with the thickness of the Kōloa Volcanics computed by Gandy (2006). However, the maximum thickness of the Kōloa HGU computed in this study (about 1,600 ft) is notably less than the "greatest exposed thickness" of 2,100 ft reported by Macdonald and others (1960) for the Kōloa Volcanics in Hanalei Valley. Macdonald and others (1960) may have been referring to the difference in elevation between the lowest exposure (at the coast near the mouth of the valley) and highest exposures (at a peak about three-fourths up the valley) of Kōloa Volcanics, not to an actual vertical thickness. In the west, the Kōloa HGU is formed by the sediments beneath the Kekaha-Mānā coastal plain. Sediment probably also forms the Kōloa HGU off the northwest coast.

Izuka and Gingerich (1998a), citing aquifer-test analyses archived by the USGS, indicated that K_h of the Kōloa HGU ranges from less than 0.05 ft/d to greater than 100 ft/d, but the regional K_h is "probably less than 1ft/d." Gingerich (1999a) estimated K_h of 0.042 to 5.5 ft/d by analyzing aquifer-test data from wells in the Kōloa HGU in the Līhu‘e basin. In numerical-model simulations, K_h values between 0.275 and 1.10 ft/d and K_v values between 5.5×10^{-4} and 2.2×10^{-3} ft/d have been used for the dike-free part of the Kōloa HGU to match groundwater-level and stream base-flow data from the Līhu‘e basin (Izuka and Gingerich, 1998a; Izuka and Oki, 2002; Izuka, 2006). Izuka (2006) used K_h values of 0.220 to 0.275 ft/d and K_v values of 0.9×10^{-3} to 1.1×10^{-3} ft/d for the dike-intruded part of the Kōloa HGU in a numerical model. Burt (1979) estimated a K_h value of 0.12 ft/d for sediments beneath the Kekaha-Mānā coastal plain. Estimates of specific storage (S_s) for the Kōloa HGU from aquifer tests and numerical modeling range from 10^{-6} 1/ft to 10^{-4} 1/ft (Gingerich, 1999a; Izuka and Oki, 2002; Izuka, 2006).

The Kōloa HGU has heterogeneous aquifer properties, probably related to the presence or absence of dikes or sediments, or to variations in the thickness, degree of alteration, or secondary mineralization of lava flows. The analysis of Rotzoll and El-Kadi (2008, their fig. 5) indicates that much of eastern Kaua‘i has low permeability. Although they attributed the low permeability to dike intrusion, most of eastern Kauai is covered by hundreds of feet of dike-free Kōloa Volcanics (fig. 26). It is likely, therefore, that most of the wells analyzed by Rotzoll and El Kadi (2008) are in dike-free parts of the Kōloa Volcanics, and that the low-permeability values are representative of the Kōloa HGU. This interpretation is consistent with the interpretation that the Kōloa Volcanics has a low overall permeability because it consists of thickly bedded lava flows that formed by ponding in depressions (Macdonald and others, 1960). It is also consistent with K_h values from aquifer-test analyses and numerical modeling in the Līhu‘e basin discussed above. A few wells in eastern Kaua‘i indicate higher permeabilities, but these areas of high permeability are limited in extent (Izuka and Gingerich, 1998a).

The analysis of Rotzoll and El-Kadi (2008) indicates that some parts of the Kōloa HGU in southern Kaua‘i have relatively high permeability. In addition, the water table in the Kōloa HGU has a gentler gradient in southern Kaua‘i than in eastern Kaua‘i (fig. 27). The gentler gradient is consistent with the higher permeability, but it could also reflect a lower groundwater-flow rate, which is also plausible in the drier southern coast. If the permeability of the Kōloa HGU is higher in the south than it is in the east, the reason for the difference is not known, but perhaps ponding of the Kōloa HGU was not as extensive in southern Kaua‘i as it was in eastern Kaua‘i.

Macdonald and others (1960) described the sediments beneath the Kekaha-Mānā coastal plain as a confining unit that retards groundwater flow from the Nāpali Member toward the sea. Geologic maps of Kaua‘i (Macdonald and others, 1960; Sherrod and others, 2007) show a few dikes in the Kōloa HGU that probably reduce permeability locally (Izuka, 2006).

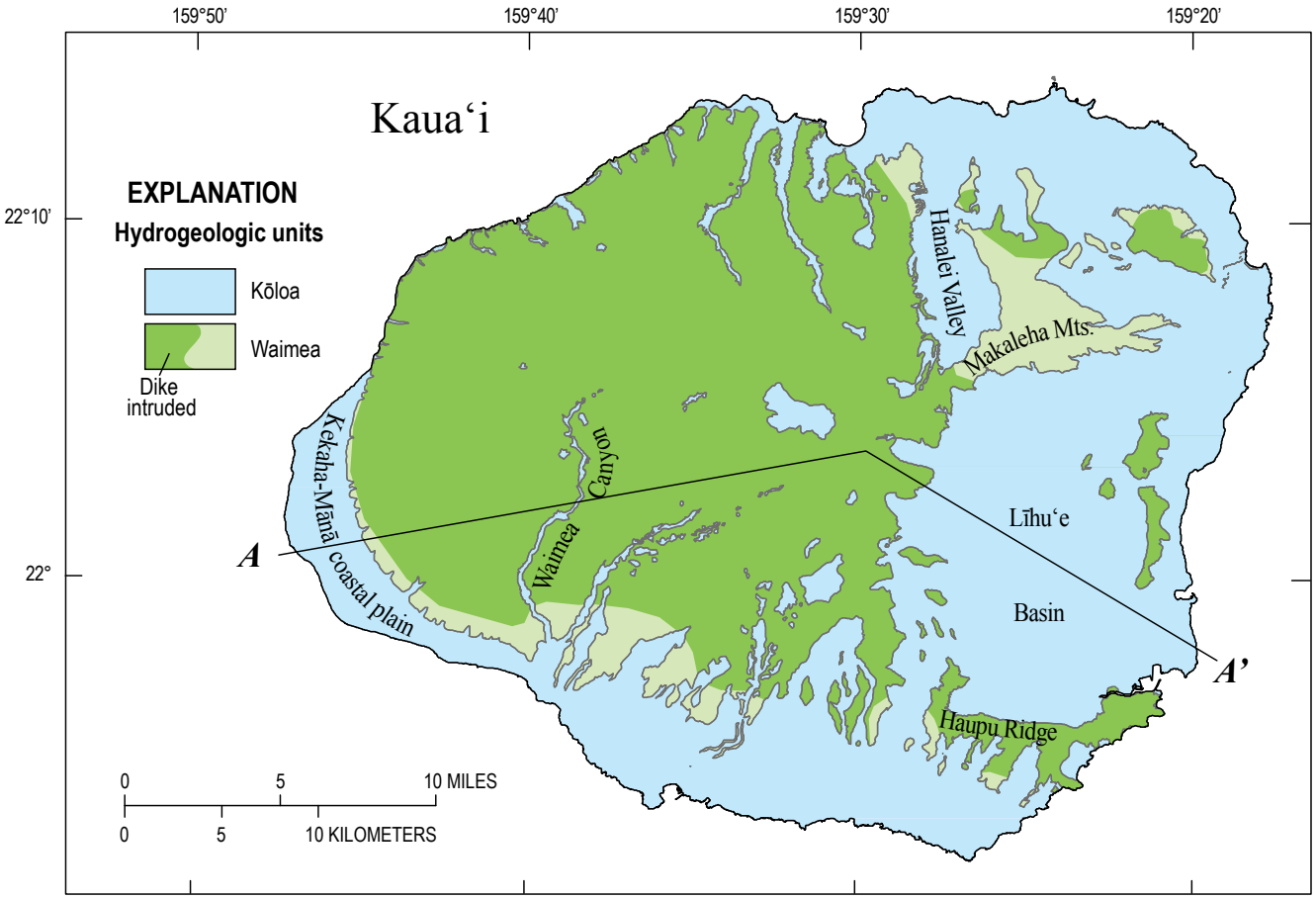

North American Datum 1983, Universal Transverse Mercator projection, zone 4N.

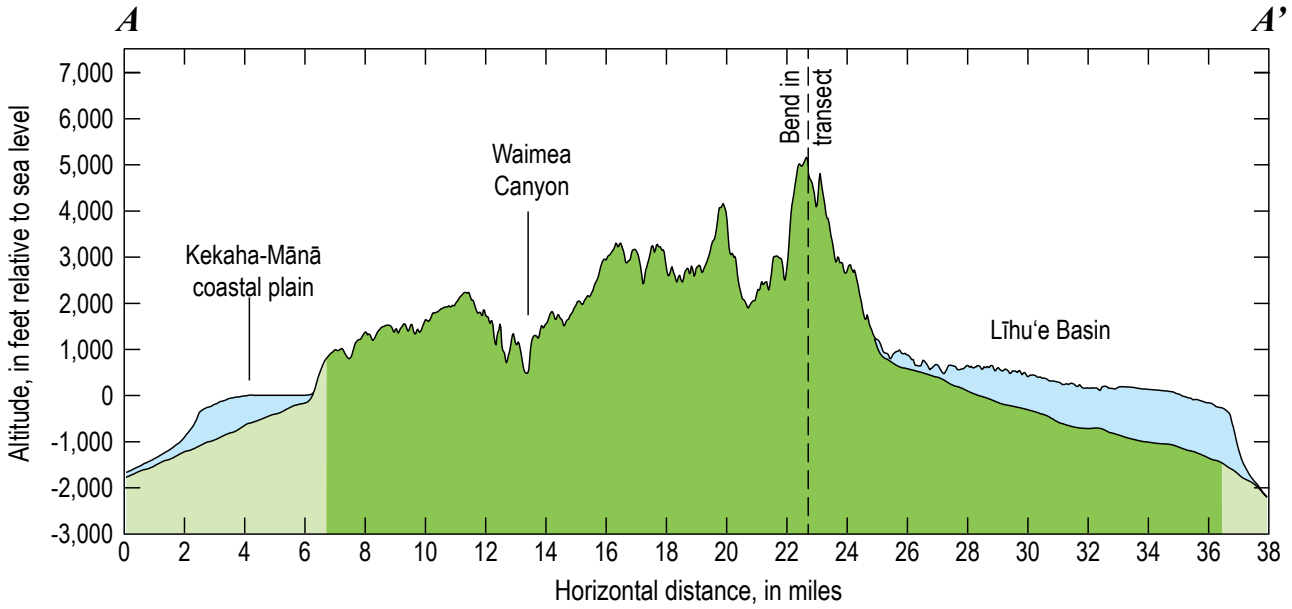

Figure 25. Map of the hydrogeologic units on Kaua‘i, Hawai‘i. Hydrogeologic-unit outlines modified from geologic map of Sherrod and others (2007). Map-view extent of dike-intruded area interpreted from mapped dikes shown by Sherrod and others (2007) and water-level data in the National Water Inventory System database; cross-section depiction of dike intrusion is speculative.

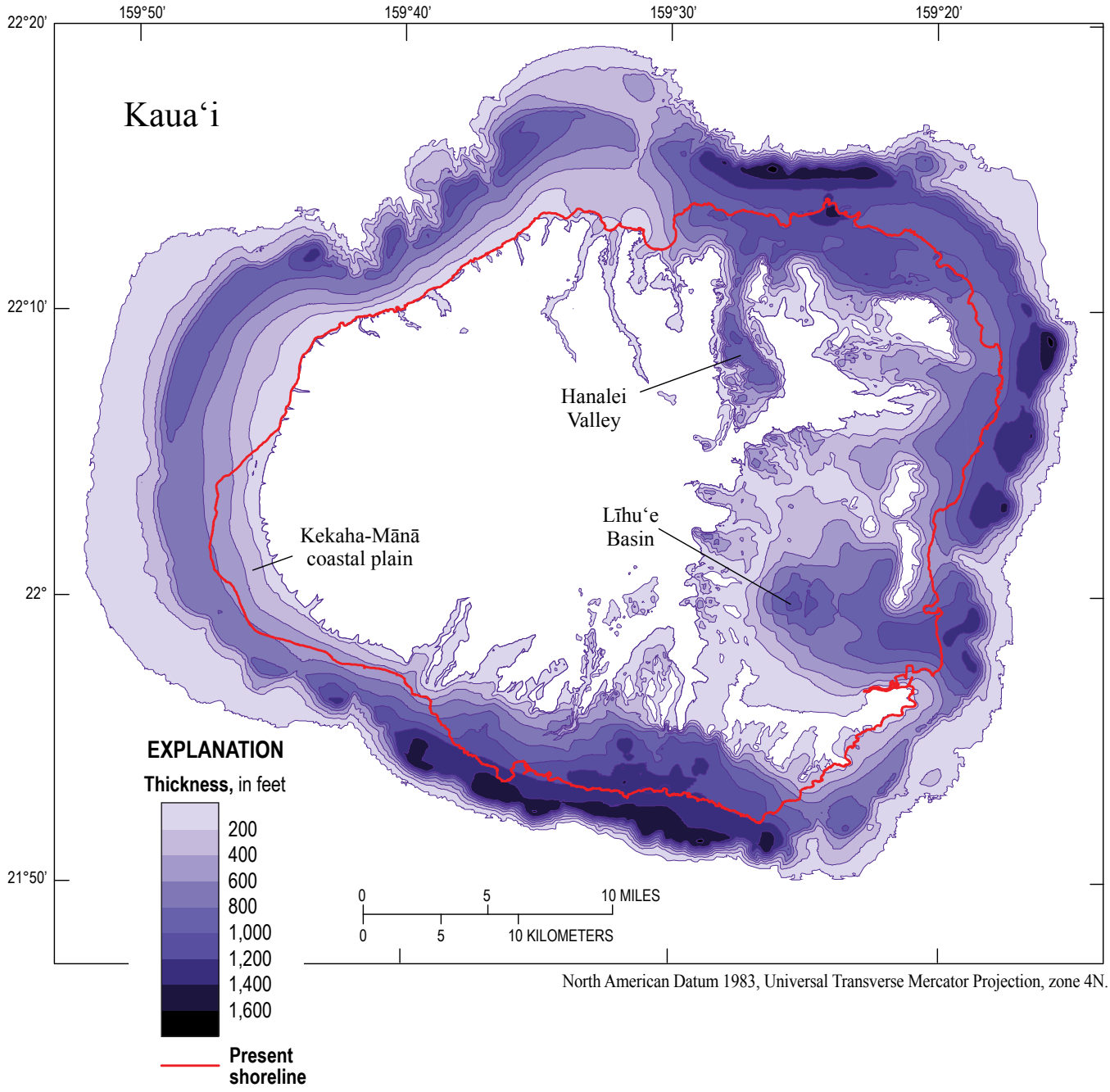

Figure 26. Map of the thickness of the Kōloa hydrogeologic unit, Kaua‘i, Hawai‘i.

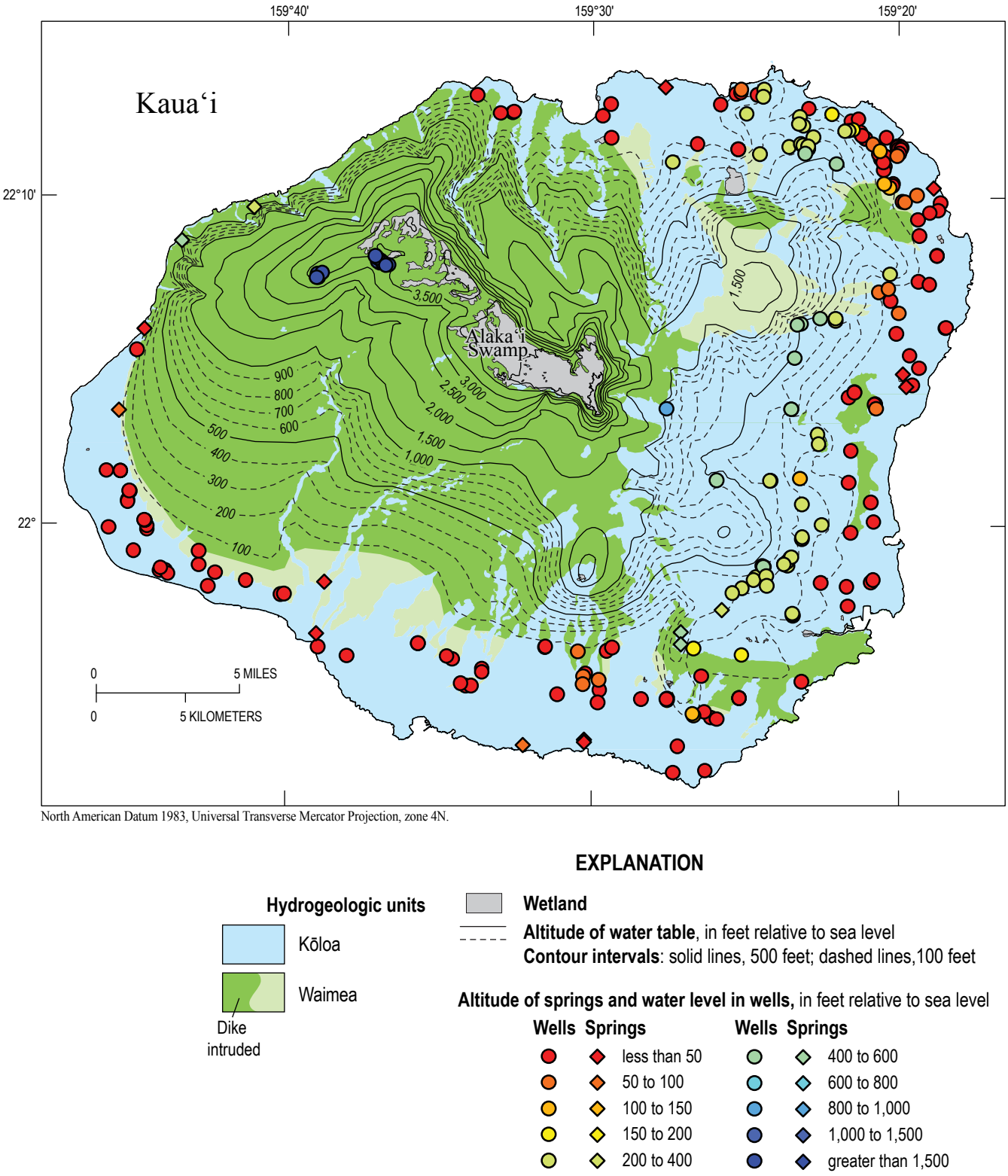

Figure 27. Map of generalized water-table altitude on Kaua‘i, Hawai‘i. Some water levels may be from wells in sedimentary rock rather than volcanic rock. Hydrogeologic units shown for reference.

Waimea Hydrogeologic Unit

The Waimea HGU encompasses the same rocks as the Waimea Canyon Basalt mapped by Macdonald and others (1960) (figs. 24 and 25), but also includes submarine extensions of the formation. Although the Nāpali, Makaweli, Olokele, and Hā‘upu Members of the Waimea Canyon Basalt have different hydraulic properties, the members are not defined as separate hydrogeologic units in this study because boundaries between members are gradational or indistinct in some places. Also, the precise location of some other boundaries is unknown due to the unresolved geologic enigmas discussed above.

Highly productive wells indicate high permeability in the thin-bedded part of the Waimea HGU in southern and southwestern Kaua‘i. Most of the high-production wells in the Waimea HGU in southern Kaua‘i are in the Nāpali Member, but one is in the thin-bedded eastern margin of the Makaweli Member. The geologic map shows fewer dikes in this part of Kaua‘i, although there are some dikes in the Waimea HGU inland from the Kekaha-Mānā coastal plain (fig. 24). No wells have been drilled into the thickly bedded western part of the Makaweli Member, but it probably has low permeability similar to the thick-bedded Olokele Member. The east-to-west transition from high to low permeability in the Makaweli Member is probably gradual.

The caldera and dike-intruded areas of the Waimea HGU are delineated as a subunit in figure 25. The extent of the subunit, approximated by the distribution of dikes and caldera rocks mapped by geologists (Macdonald and others, 1960; Sherrod and others, 2007), covers most of the exposed part of the Waimea HGU (fig. 24). Most mapped dikes are in the walls of canyons and valleys because these were accessible to field observation, but the presence of dikes in adjacent areas can be inferred. Numerous dikes have been mapped in the west wall of the Waimea Canyon; it is likely that dikes also intrude the lava flows that form the west flank of the island, although the frequency appears to diminish toward the coast. Dikes likely also intrude the Nāpali Member beneath the rocks of the Makaweli Member east of the Waimea Canyon. Dike exposures in the ridges surrounding the Līhu‘e basin suggest that dikes are also present in the Waimea HGU buried beneath the Kōloa HGU (Izuka and Gingerich, 1998a); these dikes probably contribute to the relatively low yields of wells in the Waimea HGU in and surrounding the Līhu‘e basin (Izuka and Gingerich, 1998a; Izuka, 2006; Rotzoll and El-Kadi, 2008).

Gingerich (1999a) estimated K_h values of 17 to 25 ft/d for the Waimea HGU using aquifer-test data from a well in the dike-intruded part of the thin-bedded lava flows underlying the southern margin of the Līhu‘e basin near Hā‘upu Ridge (fig. 24); however, the bulk K_h in the ridge is likely to be lower because some dikes known to exist in the ridge probably were not detected during the short period of the aquifer test (Izuka and Gingerich, 1998a). Values of K_h are also likely to be lower where dikes are more abundant, such as near Waimea Canyon. In contrast, thin-bedded, dike-free areas of the Waimea HGU likely have hydraulic conductivities higher than that indicated by Gingerich (1999a) for Hā‘upu Ridge. In numerical-model simulations of the Līhu‘e basin, K_h and K_v values of 200 and 1.0 ft/d, respectively, have been used for the thin-bedded dike-free part of the Waimea HGU (Izuka and Gingerich, 1998a; Izuka and Oki, 2002; Izuka, 2006). Rotzoll and El-Kadi (2008) estimated a mean K_h value of 794 ft/d for dike-free lavas on Kaua‘i, but they did not distinguish between wells in the Kōloa Volcanics and wells in the Waimea Canyon Basalt. There are only a few wells in the thick-bedded parts of the Waimea HGU. Specific capacities of wells drilled into the Olokele Member indicate low permeability (Rotzoll and El-Kadi, 2008), which is consistent with the low permeability described for this geologic unit by Macdonald and others (1960). In numerical groundwater modeling of the Līhu‘e basin, values of S_s between 10^{-6} 1/ft and 10^{-4} 1/ft have been used for both the Waimea and Kōloa HGUs (Izuka and Gingerich, 1998a; Izuka and Oki, 2002; Izuka, 2006).

The water table in the Waimea HGU rises steeply toward the center of the island, where it intersects with the extensive Alaka‘i Swamp at the island’s summit (fig. 27). High groundwater recharge in the center of the island (see *Groundwater Recharge* section below) probably contributes to the steep water-table gradient, but so does the steep topography and the low permeability of the caldera and dike-intruded rocks.

The structure map of the top of the Waimea HGU shows the distribution of this unit with the overlying Kōloa HGU stripped away (fig. 28). In western Kaua‘i, the surface of the Waimea HGU retains a semblance of a shield-volcano slope, even though faulting has modified the surface and influenced erosion (notably the formation of the Waimea Canyon, fig. 23). In contrast, the Waimea HGU in eastern Kaua‘i is pitted with large depressions, including the prominent Līhu‘e basin. In northeastern and southern Kaua‘i, the steep surfaces of the Waimea HGU just inland from where it descends below sea level have been interpreted as former sea cliffs that were subsequently buried by the Kōloa HGU (Macdonald and others, 1960). Offshore, the Waimea HGU extends more than 6,000 ft below sea level, except in the west, where the lavas of Kaua‘i overlie the older lavas of the adjacent island of Ni‘ihau (Flinders and others, 2010).

Hydrologic Implications of Geologic Enigmas

The enigmatic origin of the Olokele Member has hydrologic implications. If the Olokele Member was formed in a caldera as proposed by Macdonald and others (1960), the low-permeability character of this unit, as well as the dense intrusive and metamorphic rocks that typically underlie the summit caldera, would extend through the freshwater resource to great depths (fig. 29*A*). On the other hand, if the Olokele Member formed as flank lava flows from the east ponded against an escarpment (Holcomb and others, 1997), the low-permeability character may not extend to great depths and the unit may be more permeable away from the ponding (fig. 29*B*).

The enigmatic origin of the Līhu‘e basin also has hydrologic implications. If a large volcanic intrusion underlies the Līhu‘e basin as indicated by gravity data (Krivoy and others, 1965; Flinders and others, 2010, 2013), closely spaced dikes and caldera-filling rocks above the intrusion may cause the Waimea HGU in the basin to have an even lower permeability than the overlying Kōloa HGU (fig. 29*B*).

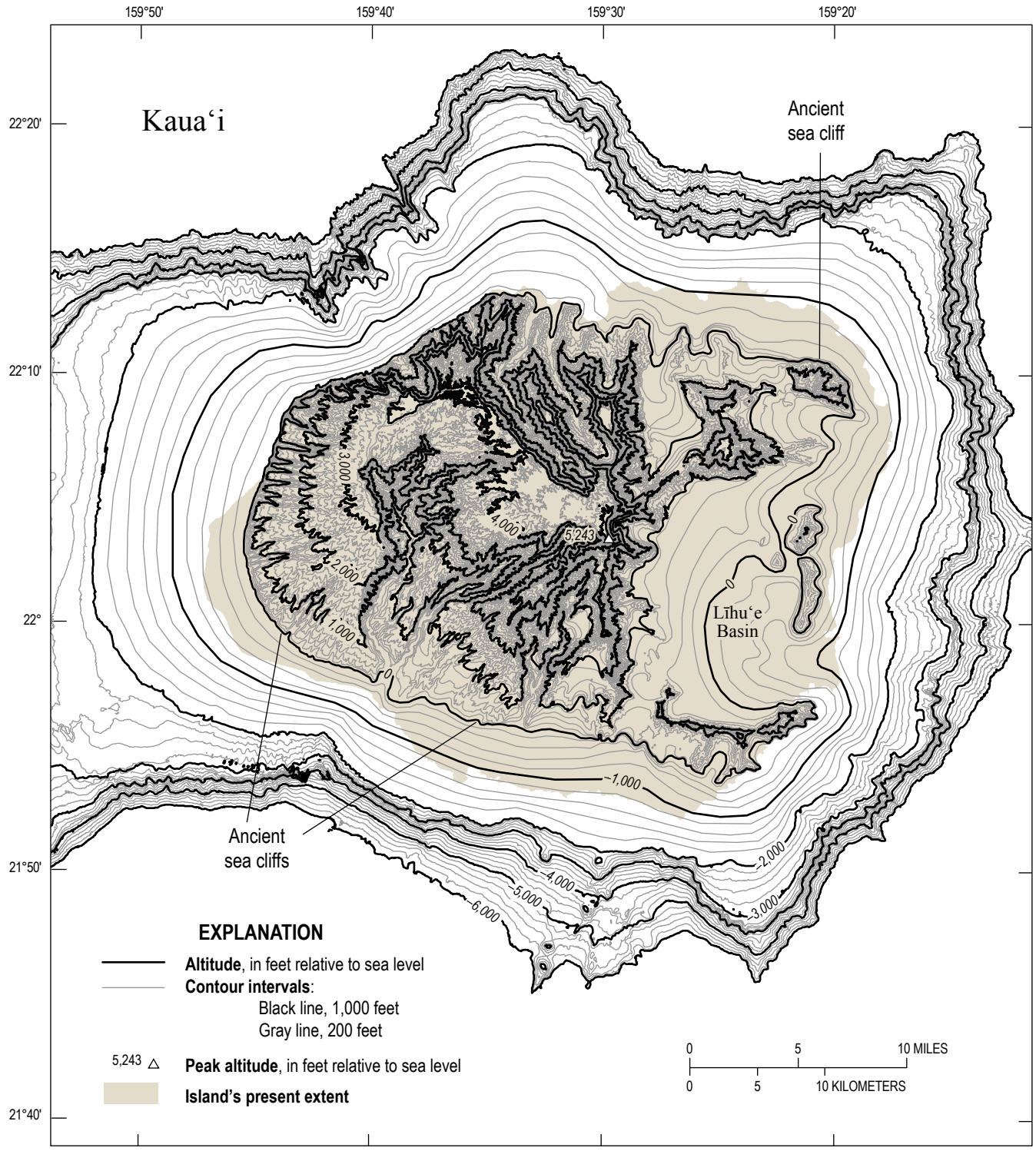

North American Datum 1983, Universal Transverse Mercator projection, zone 4N.

Figure 28. Structure map of the altitude of the top of the Waimea hydrogeologic unit, Kaua‘i, Hawai‘i.

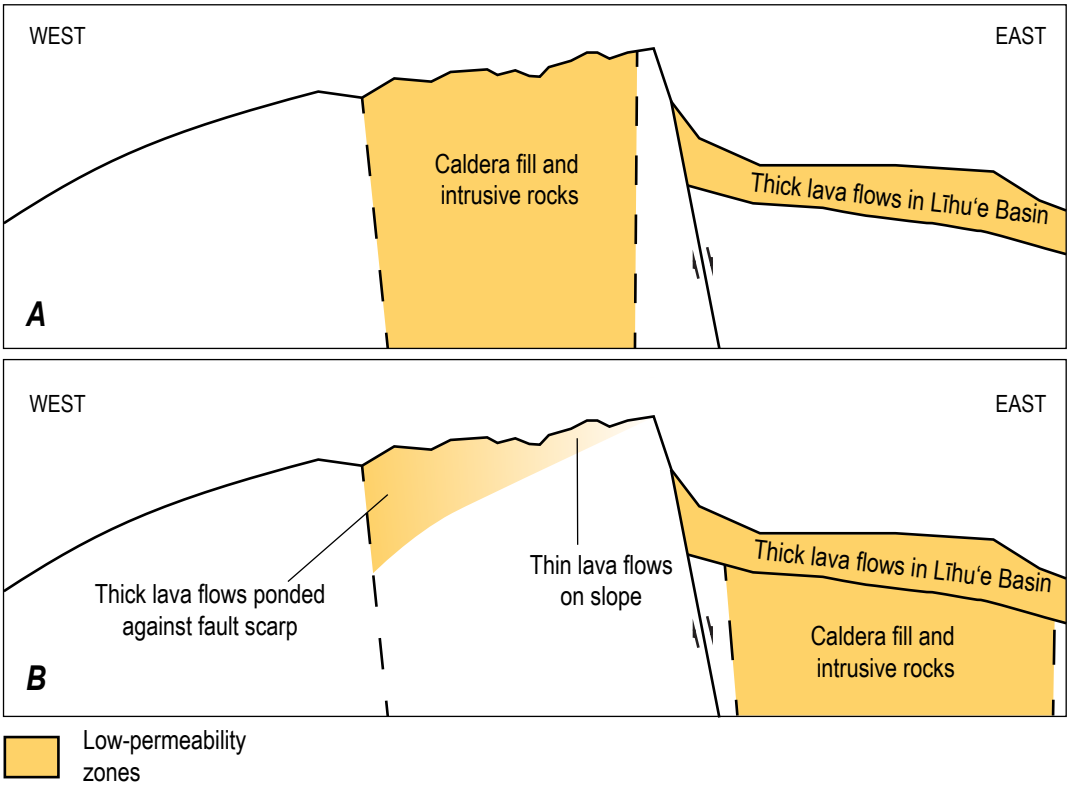

Figure 29. Alternative hypotheses for the structure beneath central Kaua'i, Hawai'i.

O'ahu

O'ahu lies in the northwestern part of the main Hawaiian Islands (fig. 1). With an area of 597 mi^2 and population of about 953,000 (U.S. Census Bureau, 2011), it is by far the most densely populated of the Hawaiian Islands (table 1). It is also the site of the state's capital city, Honolulu, most of the state's U.S. military presence, and the center of the state's industry and commerce. The island has two prominent mountain ranges, the Wai'anae and Ko'olau Ranges (fig. 30). The Wai'anae Range reaches an altitude of 4,025 ft, and the Ko'olau Range reaches an altitude of 3,105 ft. Between the two mountain ranges is an elevated saddle known as the Schofield Plateau. A coastal plain surrounds much of O'ahu.

O'ahu has extensive fresh groundwater resources that are more readily accessible to humans than on any other island in the state. These resources are the result of a set of geologic circumstances that are either lacking or not as fully developed on other islands as they are on O'ahu.

Geology

The geology of O'ahu was described comprehensively by Stearns and Vaksvik (1935) and Stearns (1939, 1940, 1985). Commonly cited overviews were also provided by Wentworth (1938, 1951) and Macdonald and others (1983). Langenheim and Clague (1987) updated the stratigraphic nomenclature of the main Hawaiian Islands and Sherrod and others (2007) updated the geologic maps of the state with more recent information, including a summary of radiometric ages collected over decades of studies. This section summarizes information from these references. Additional specific information and concepts from other sources are cited.

The Wai'anae and Ko'olau Ranges (fig. 30) are the erosional remnants of the two shield volcanoes that built the subaerial part of O'ahu. The Wai'anae volcano is older than the Ko'olau volcano. A third volcano, even older than the Wai'anae volcano, has been described recently, but this volcano is thousands of feet below sea level and much of it

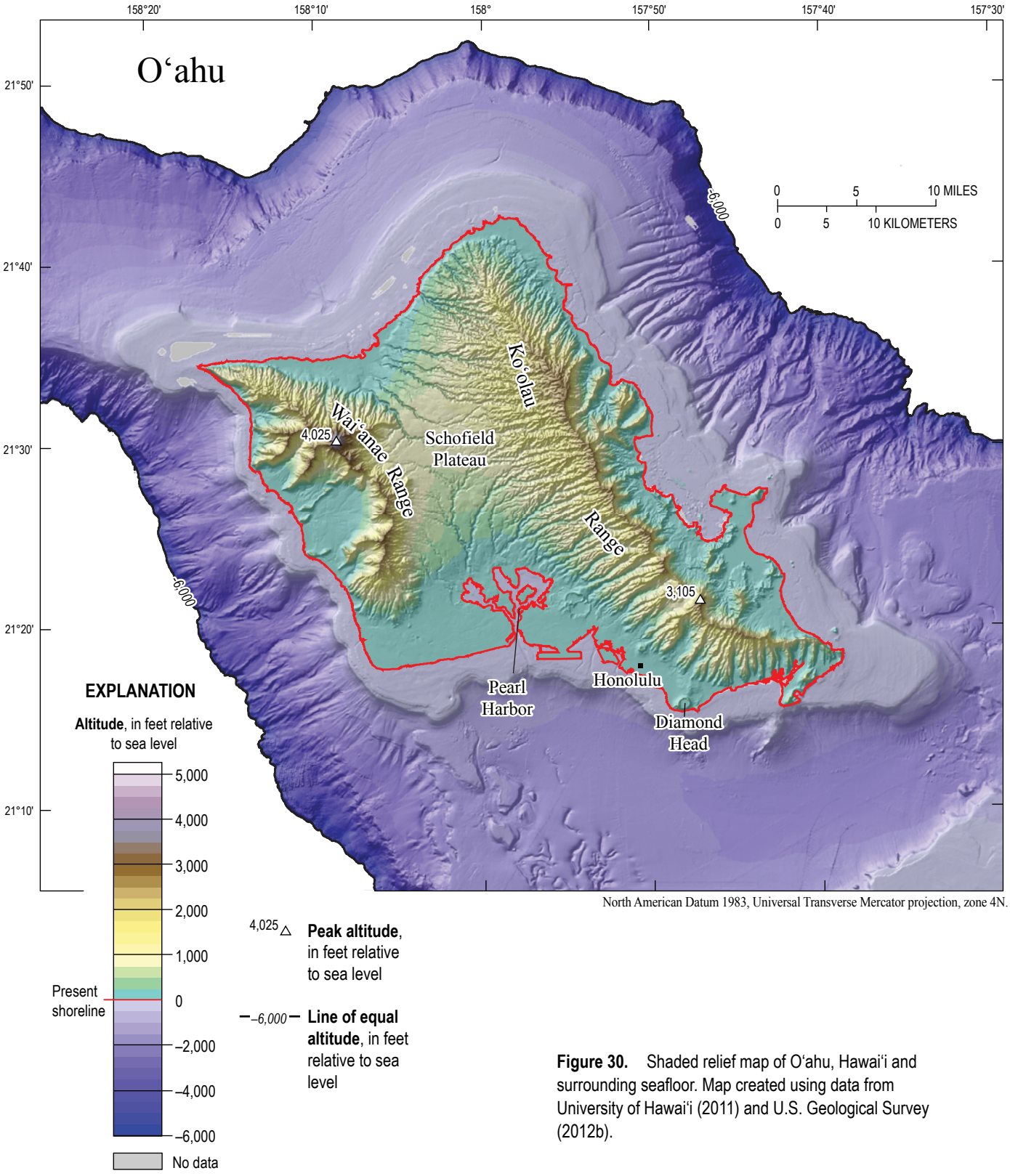

Figure 30. Shaded relief map of O‘ahu, Hawai‘i and surrounding seafloor. Map created using data from University of Hawai‘i (2011) and U.S. Geological Survey (2012b).

is buried by the Waiʻanae volcano (Sinton and others, 2014); therefore, it probably does not affect fresh groundwater resources on Oʻahu. Strata from the southwest flank of the younger Koʻolau volcano lap onto the eroded northeast flank of the older Waiʻanae volcano beneath the Schofield Plateau. Soil, weathered basalt, and alluvium separate the Koʻolau and Waiʻanae rocks in some places. Eruptions of the Koʻolau volcano were partly contemporaneous with that of the Waiʻanae volcano, but interfingering of flows beneath the Schofield Plateau has not been observed in drill holes or outcrops (Hunt, 1996).

Waiʻanae—All igneous rocks of the Waiʻanae volcano are included in the formation known as the Waiʻanae Volcanics (table 2, fig. 31). Radiometric dating of subaerial rocks from the Waiʻanae volcano indicates ages between 4.0 and 2.9 million years. The thin, tholeiitic shield-stage lava flows that constitute most of the volume of the volcano are assigned to the lower two members—the Lualualei and Kamaileʻunu (Sinton, 1987). The Lualualei Member crops out at the surface only over a small area, but as with analogous shield-stage formations on other volcanoes, the Lualualei Member probably forms most of the volume of the Waiʻanae volcano. The Kamaileʻunu Member consists of thick-bedded lava and breccia that filled the ancient caldera and contemporaneous thinner-bedded lava that flowed down the flank of the Waiʻanae volcano. The member has tholeiitic basalt, but also includes transitional alkalic basalt, hawaiite, and some ankaramite. The Kamaileʻunu Member also includes a lava flow of rhyodacite, the most silicic lava rock known from Hawaiʻi (Sherrod, 2007). Thin layers of ash occur sparingly within the lava-flow pile and a soil layer separates the two members in some places.

The shield-stage lavas were erupted from the summit caldera and rift zones that extended to the northwest and south (fig. 31). The location of the rift zones was interpreted from dike abundances and orientations. Stearns and Vaksvik (1935) and Stearns (1939) differentiated a dike complex that was "injected with numerous dikes a few inches to 15 feet wide and few sills" from other dike-intruded areas where the dikes were "not so close together." Some authors show a minor rift zone extending from the caldera towards the northeast (for example, Macdonald, 1972). The location of the ancient caldera of the Waiʻanae volcano was interpreted from the distribution of breccia and thick ponded lavas of the Kamaileʻunu Member (Stearns and Vaksvik, 1935; Sinton, 1987). Gravity anomalies are consistent with the presence of high-density magma-chamber rock beneath the postulated caldera site (Flinders and others, 2013).

Overlying the shield-stage and transitional rocks of the Lualualei and Kamaileʻunu Members are the rocks of the Pālehua and Kolekole Members of the Waiʻanae Volcanics (Sinton, 1987; Presley and others, 1997) (table 2, fig. 31). The members include hawaiite, mugearite, and alkalic basalt that were erupted as relatively short, massive lava flows and cinder cones. Although the two members are separated by an erosional unconformity, they are both considered to be part of the postshield stage on the basis of geochemistry and radiometric ages (Presley and others, 1997). Waiʻanae volcano does not have rejuvenated-stage rocks.

A large landslide is thought to have removed most of the southwestern part of the Waiʻanae shield volcano and contributed to the extensive submarine landslide deposit known as the Waiʻanae slump (Moore and others, 1989). The Waiʻanae shield volcano has also been deeply eroded by streams (fig. 30). Southwest of the crest of the Waiʻanae Range are large valleys with broad floors flattened by sediments; the valley fill is continuous with coastal-plain deposits (fig. 31). Another large valley lies northeast of the crest near the Schofield Plateau; the floor of this valley has been partly filled with alluvium and lava flows from the Koʻolau shield volcano.

Koʻolau—The Koʻolau volcano is unique among the shield volcanoes of Hawaiʻi in having shield-stage and rejuvenated-stage rocks but no postshield-stage rocks (Mauna Loa and Kīlauea on Hawaiʻi Island lack both postshield- and rejuvenated-stage rocks) (table 2). Some slightly alkalic cobbles have been found in alluvium in a few streams in the Koʻolau Range, but no outcrops indicative of postshield-stage volcanism have been found (Macdonald and others, 1983). Radiometric ages of rocks from the Koʻolau volcano, including shield- and rejuvenated-stage rocks, range from about 3.0 to 0.04 million years.

The shield-stage rocks of the Koʻolau volcano are assigned to the Koʻolau Basalt (table 2, fig. 31). The formation constitutes all but a small fraction of the volume of the volcano, and consists of a pile of thousands of thin tholeiitic lava flows (fig. 12*B*) with a few intercalated ash beds. The location of the volcano's caldera was interpreted on the basis of dikes, thick caldera-filling lavas, and low-grade metamorphism; these rocks constitute the Kailua Member of the Koʻolau Basalt. Gravity anomalies are consistent with this interpretation (Flinders and others, 2013). Two principal rift zones of the Koʻolau volcano have been interpreted from patterns and orientation of dike intrusion, dips of lava flows, and the overall northwest elongation of the Koʻolau Range. The more prominent of the two rift zones extends northwest of the caldera for about three-fourths of the length of the Koʻolau Range; a shorter rift zone extends to the southeast. A less distinct rift zone extending south-southwest of the caldera has also been noted in some literature (for example, Stearns and Vaksvik, 1935; Macdonald, 1972; Takasaki and Mink, 1985). Dike frequency is greatest along the center of the rift zones—geologists and hydrologists have referred to the zone where dikes constitute more than 10 percent of the rock volume as the "dike complex," and the zones at the periphery where dikes are less abundant as the "marginal dike zones." Many details of the Koʻolau rift zones have already been presented in the *Hydrogeologic Overview* section above because the well-exposed, intensively studied dikes in the Koʻolau volcano constitute the basis for much of the general understanding of rift zones and dikes in Hawaiʻi.

Rejuvenated-stage rocks of the Koʻolau volcano are assigned to a formation known as the Honolulu Volcanics (table 2, fig. 31). Rocks of the Honolulu Volcanics occur only in the southern part of the Koʻolau volcano, where they lie unconformably on the Koʻolau Basalt. Some vents of the Honolulu Volcanics appear to be aligned along trends that are transverse to the principal rift zones of the Koʻolau shield volcano. The Honolulu Volcanics includes alkalic basalt,

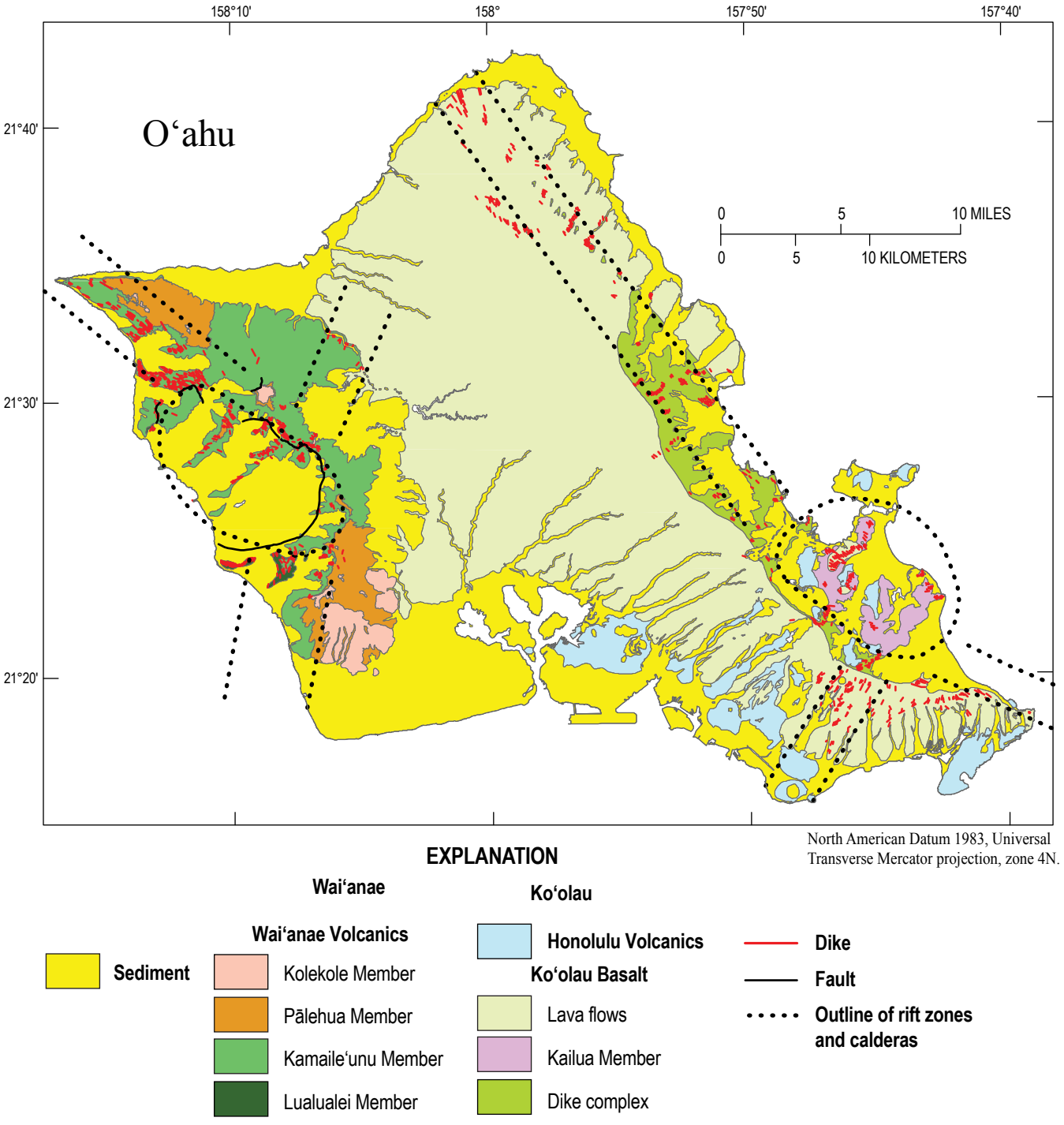

Figure 31. Simplified geologic map of O‘ahu, Hawai‘i. Modified from Sherrod and others (2007). Rift zone and caldera traces modified from Macdonald (1972) and Hunt (1996).

basanite, nephelinite, and nephelinite-melilitite (Macdonald and others, 1983; Clague and Dalrymple, 1987). Volcanic edifices vary from small shield volcanoes composed of thin pāhoehoe lava flows to cones built of spatter, cinder, or ash, and include some of the most famous landmarks in Hawai‘i, such as Diamond Head. Thick lava flows of the Honolulu Volcanics partly fill stream valleys in the Ko‘olau Range. Rocks of the Honolulu Volcanics also are interbedded with sediments that form O‘ahu’s coastal plain.

The morphology of the Ko‘olau Range, lava-flow dips, and interpreted locations of rift zones and caldera indicate that much of the northeastern part of the Ko‘olau shield has been removed (figs. 30 and 31). Erosional and structural processes have contributed to this removal. Part of the removal below sea level has been attributed to large submarine landslides that contributed to the submarine deposit known as the Nu‘uanu debris avalanche mapped on the ocean floor northeast of the windward flank of O‘ahu (Moore and others, 1989). Removal of the flank above sea level has been attributed primarily to extensive stream erosion on the wet windward side of O‘ahu (Stearns and Vaksvik, 1935; Sherrod and others, 2007). Enlarging stream-eroded valleys coalesced to form the scalloped northeast-facing cliffs (*pali*) of the present Ko‘olau Range, although structures and the susceptibility or resistance of the various rocks probably influenced the erosion pattern (Sherrod and others, 2007).

The remaining southwest flank of the Ko‘olau shield volcano also has been carved by stream erosion, although to a lesser extent than the northeast flank (fig. 30). Most of the stream valleys on the southeast flank are long and narrow, but the valleys in and near Honolulu are somewhat larger and partly filled with sediment and rejuvenated-stage volcanic rocks (figs. 30 and 31). As a result of island subsidence and fluctuating sea level and stream base levels, the sedimentary valley fill extends both below and above sea level, and is continuous with coastal-plain deposits.

Coastal-Plain Deposits—O‘ahu has extensive coastal-plain deposits that partly overlie the lava flows of the shield volcanoes and almost completely encircle the island (fig. 31). Coastal-plain deposits also are present on Kaua‘i and Maui, but they are not as wide or thick, and do not encircle those islands as completely as they do on O‘ahu. The significance of the coastal-plain deposits on O‘ahu was expressed by Stearns and Vaksvik (1935, p. 35): “It is this coastal plain that has made Oahu the commercial center of the Hawaiian Islands, because it has provided excellent harbors and extensive areas of splendid agricultural land, has made highways far less costly, [and] has given to Oahu its great artesian basins.” For groundwater resources, the primary importance of the coastal-plain deposits is not as an aquifer, but as the semiconfining caprock that resists natural groundwater discharge from O‘ahu’s high-permeability volcanic aquifers, thus allowing large volumes of groundwater to accumulate.

The O‘ahu caprock consists predominantly of marine calcareous and noncalcareous sediments, but also includes terrigenous sediments shed from the Ko‘olau and Wai‘anae shield volcanoes as well as rejuvenated-stage rocks of the Honolulu Volcanics (fig. 31). The contact between the caprock and underlying Ko‘olau Basalt has a maximum altitude of about 80 ft; the caprock extends offshore, in some places for miles. The altitudes, multiple terrace levels, fossil-reef horizons, and unconformities of the strata in the caprock indicate that it formed during several episodes of sea transgressions and regressions.

Hydrogeologic Units

Stearns and Vaksvik (1935) described the water-bearing properties of each of O‘ahu’s mapped geologic units. The hydraulic characteristics were updated in several subsequent studies and summarized by Takasaki and Mink (1982) and Hunt (1996). In general, the thin shield-stage lava flows of the Wai‘anae (the Lualualei and Kamaile‘unu Members of the Wai‘anae Volcanics) and Ko‘olau (the Ko‘olau Basalt) volcanoes are described as very permeable to extremely permeable. The permeability of the dike complexes (greater than 50 percent dike material by volume) and caldera rocks are considered to be low to moderate, whereas that of the marginal dike zone is considered to be moderate to high. Most of the postshield-stage rocks of the Wai‘anae volcano do not contain groundwater, but Stearns and Vaksvik (1935, p. 76) write that the “upper basalt unit” (equivalent to the units later ascribed to postshield volcanism) “yields water abundantly” in the southeastern and eastern sides of the Wai‘anae Range. The Honolulu Volcanics, with a variety of rock types and structures, is described as having permeabilities ranging from very low to very high, depending in part on whether the unit consists of ash, cinder, or lava flows, and whether the rocks are cemented or altered by weathering. The permeability of sedimentary rocks also varies widely—carbonate rocks can have moderate to very high permeabilities, whereas consolidated and weathered terrigenous clastic rocks can have low to very low permeabilities. The coastal-plain sediments and rejuvenated-stage volcanic rocks on O‘ahu have been referred to as “caprock” because they act as a semiconfining unit over parts of the high-permeability lava-flow aquifers. On the basis of descriptions of the rock and water-bearing properties described in the cited literature, this study divides the rocks of O‘ahu into two principal HGUs: (1) the Caprock HGU, and (2) the Wai‘anae-Ko‘olau HGU (fig. 32).

Caprock Hydrogeologic Unit

The Caprock HGU includes all sedimentary units and the rocks of the Honolulu Volcanics shown in the geologic map of O‘ahu by Sherrod and others (2007). This HGU forms the extensive coastal plain that overlies parts of the Wai‘anae-Ko‘olau HGU (fig. 32). The HGU is thickest along the southern coast of O‘ahu (fig. 33), where it is more than 1,000 ft thick beneath the present coastline and more than 1,600 ft thick farther offshore. The Caprock HGU also includes sedimentary rocks and rejuvenated-stage volcanics that partly fill valleys; although these deposits are not often referred to as “caprock” in other literature, the valley-fill deposits share the same low-permeability character and are continuous with the sediments of the coastal plain. On the southeast flank of the Ko‘olau Range, the valley-fill deposits attain thicknesses of hundreds of feet.

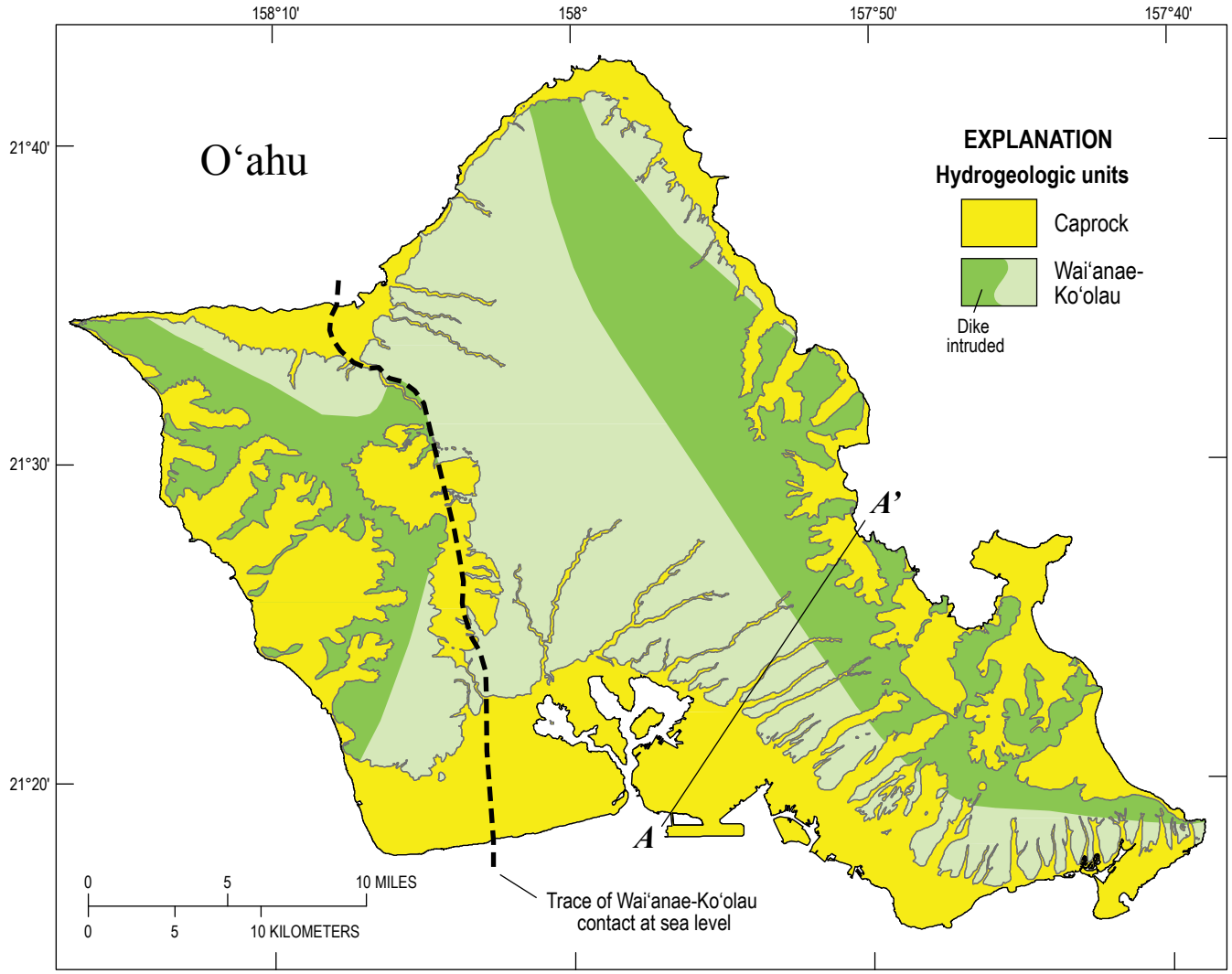

Figure 32. Map of the hydrogeologic units on O‘ahu, Hawai‘i. Hydrogeologic-unit outlines modified from the geologic map of Sherrod and others (2007). Trace of Wai‘anae-Ko‘olau contact from D.S. Oki, USGS written commun., 2014. Map-view extent of dike-intruded area based on Takasaki and Mink (1985) and Hunt (1996), with additional interpretation of data from Stearns (1939), Sherrod and others (2007), Flinders and others (2013), and the National Water Information System database; cross sectional depiction of dike intrusion is speculative.

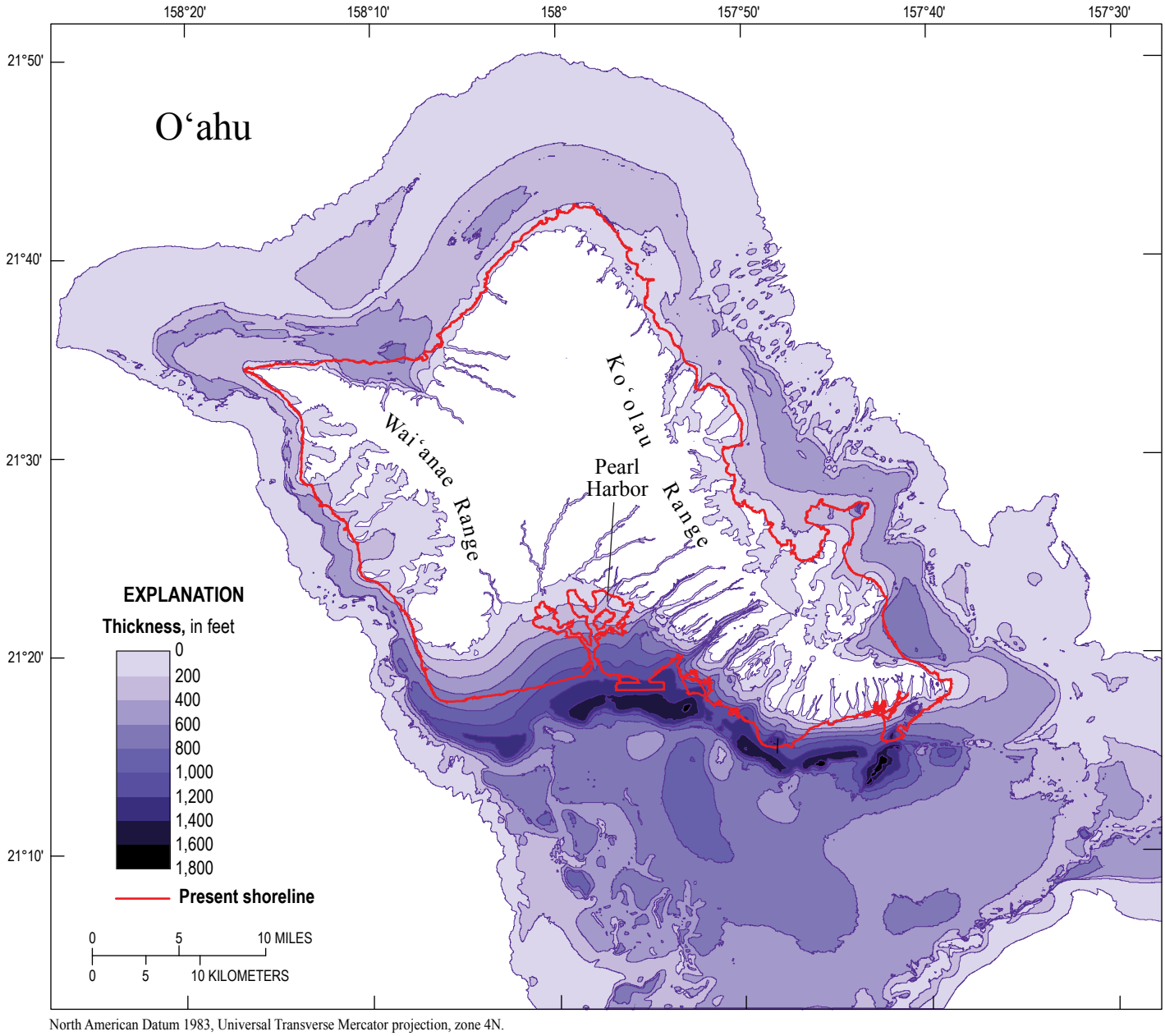

Figure 33. Map of the thickness of the Caprock hydrogeologic unit, O‘ahu, Hawai‘i.

A typical sequence beneath the coastal plain consists, from bottom to top, of (1) unweathered basalt of the lava-flow aquifer, (2) weathered basalt, (3) terrigenous clastic sediment (alluvium), and (4) limestone (Mink and Lau, 1980). Because low-permeability weathered basalt and alluvium lie at its base, the Caprock HGU acts as a semiconfining unit where it overlies the lava-flow aquifer, even though part of the sediment beneath the coastal plain, such as limestone, may be highly permeable.

Oki and others (1996) and Oki (2005) cited previous studies that estimated hydraulic conductivity (direction unspecified) from laboratory experiments and field aquifer tests; these estimates ranged from 0.0028 to 283 ft/d (mostly 0.1 ft/d or less) for weathered basalt, 0.1 to 1.0 ft/d for alluvium, and 2 to 33,000 ft/d for limestone on O‘ahu. Rotzoll and Fletcher (2013) estimated a K_h value of 1,300 ft/d from tidal analyses for the upper-limestone unit in Honolulu. In an overview of O‘ahu hydrogeology, Hunt (1996) listed general K_h values of 100 to 20,000 ft/d for limestone; 1 to 1,000 ft/d for sand; less than 1 to 500 ft/d for lagoon sand and mud; and less than 1 to 500 ft/d for alluvium.

Souza and Voss (1987) estimated values of 0.15 ft/d for K_h, 1:200 for K_v:K_h, and 0.04 for the specific yield of the sedimentary confining unit at the coast (they did not simulate high- and low-permeability layers separately) by matching a vertical cross-sectional numerical model of the Pearl Harbor groundwater area to observed data. Values for K_h of other aquifer materials in the Caprock HGU used in previous numerical models of O‘ahu include 0.06 ft/d for alluvium (Oki, 2005; Rotzoll and El-Kadi, 2007); 2,500 ft/d for limestone (Oki, 2005); and 0.001 to 1.0 ft/d for nonlimestone units in the caprock. Specific-yield values in numerical models have ranged between 0.04 and 0.2 (Voss and Souza, 1987; Camp Dresser & McKee, 1993; Oki and others, 1998; Gingerich and Voss, 2005; Oki, 2005; Rotzoll and El-Kadi, 2007; Rotzoll, 2012).

Wai‘anae-Ko‘olau Hydrogeologic Unit

The Wai‘anae-Ko‘olau HGU includes all of the rocks in the Wai‘anae Volcanics and Ko‘olau Basalt (fig. 32). A low-permeability unit of weathered rock and soil separates the underlying Wai‘anae Volcanics from the overlying Ko‘olau Basalt, and water levels on either side of the low-permeability unit differ (Hunt, 1996; Oki, 1998). Much of the Wai‘anae-Ko‘olau HGU is composed of high-permeability dike-free lava flows, but parts of the HGU are intruded by low-permeability dikes. As discussed above, the overall permeability of dike-intruded areas depends on the number of dikes per unit area, but in general, the permeability of dike-intruded areas is much less than that of dike-free areas. Part of the Wai‘anae-Ko‘olau HGU is formed by low-permeability metamorphic rocks of the Kailua Member of the Ko‘olau Basalt. The region of metamorphic rocks has very low permeability (Stearns and Vaksvik, 1935), but it occupies a small area (fig. 31).

Where the Wai‘anae Volcanics and the Ko‘olau Basalt meet, water levels in the two units may differ by a few to more than 10 ft. The difference has been attributed to the low permeability of the soil, weathered basalt, and alluvium that separate and resist groundwater flow between the high permeability rocks of the two shield volcanoes (for example, Stearns and Vaksvik, 1935). The shape and location of the buried low-permeability layer is not well known, but previous investigators have estimated its trace where it would intersect the freshwater table on the basis of groundwater data and by extrapolating the eastern slope of the Wai‘anae Range (fig. 32; Visher and Mink, 1964; Dale, 1978; Hunt, 1996; Oki, 1998).

A low-permeability dike-intruded subunit is delineated within the Waianae-Ko‘olau HGU (fig. 32) on the basis of mapped dikes (Stearns, 1939; Sherrod and others, 2007), dike-zone delineations in previous studies (Takasaki and Mink, 1985; Hunt, 1996), recent gravity data (Flinders and others, 2013), and water levels in wells. The subunit also includes areas that have been interpreted as calderas. The extent of the subunit is better understood on O‘ahu than it is on Kaua‘i because the dikes of the Ko‘olau and Wai‘anae shield volcanoes are more clearly organized into linear rift zones. Even so, the boundary of the dike-intruded subunit is not truly sharp, but gradational. How the unit appears at depth (section *A-A’* of figure 32) is speculative. In previous literature, cross sectional depictions of O‘ahu dike complexes (for example, Stearns, 1939; Walker, 1987) show complexes that are wider at depth than they are at the surface, but the depictions are highly generalized.

Most estimates of K_h for dike-free lava-flow aquifers on O‘ahu range between 500 and 5,000 ft/d (Hunt, 1996). Analysis of aquifer tests yielded K_h values of 26 to 5,000 ft/d, with the majority of the results between 200 and 1,500 ft/d (Wentworth, 1938; Visher and Mink, 1964; Takasaki and others, 1969; Rosenau and others, 1971; Todd and Meyer, 1971; Soroos, 1973; Williams and Soroos, 1973; Dale, 1978; Mink, 1980; Eyre, 1983; Eyre and others, 1986). Estimates of K_h based on analysis of specific capacities range from 3 to 8,000 ft/d, with a geometric mean and median about 550 ft/d (Rotzoll and El-Kadi, 2008); although these estimates spanned over three orders of magnitude, the interval spanned by the standard deviation (138 to 2,261 ft/d) is smaller than that of estimates for the other islands of Hawai‘i. Values of K_h used in numerical models to match observed groundwater data range from about 100 to 7,500 ft/d (Eyre and others, 1986; Voss and Souza, 1987; Oki, 1997, 1998; Oki and others, 1998; Gingerich and Voss, 2005; Whittier and others, 2004; Rotzoll and El-Kadi, 2007). Oki (2005) used 4,500 ft/d and Rotzoll (2012) used 1,350 ft/d for K_h along the general lava-flow direction for dike-free volcanic rock in the Pearl Harbor area. Regional values of specific yield used in numerical modeling range between 0.03 and 0.1 (Eyre and others, 1986; Souza and Voss, 1987; Oki and others, 1996; Oki, 1997, 1998; Gingerich and Voss, 2005; Oki, 2005; Rotzoll and El-Kadi, 2007; Whittier and others, 2010; Rotzoll, 2012).

Meyer and Souza (1995) used an analytical solution to scale down the results of a numerical model and estimated K_h for dike rock to be about 10^{-3} to 10^{-2} ft/d. Most other estimates of hydraulic conductivity related to dikes are for regions of lava-flow aquifers intruded by dikes, not for the dike rock itself. These estimates probably mostly reflect the conductivity parallel to the general dike trend (Takasaki and Mink, 1985). Takasaki and others (1969) and Williams and Soroos (1973) analyzed aquifer-test data and found K_h in the dike-intruded lava flows on O‘ahu to be a few tens of feet per day. Rotzoll and El-Kadi (2008) used specific-capacity data and estimated K_h values for the “dike-zone complex” of O‘ahu to range from 0.2 to 4,300 ft/d, with a median K_h of 30 ft/d. In a summary of hydrogeology of O‘ahu for the RASA study, Hunt (1996) reported that estimates of K_h in dike-intruded lava-flow aquifers ranged between 1 and 500 ft/d within the dike complex, and between 100 and 1,000 ft/d in the marginal dike zone. Values of K_h ranging between 0.1 to 1.6 ft/d for the dike complex and between 3 and 800 ft/d in the marginal dike zone have been used in numerical-modeling studies (Meyer and Souza, 1995; Whittier and others, 2004; Rotzoll and El-Kadi, 2007). Direct estimates of the specific yield of dike-intruded lava flows are lacking, but a value of 0.05 has been used in numerical models (Whittier and others, 2004; Rotzoll and El-Kadi, 2007).

The water-table map (fig. 34) is consistent with the distribution of dikes (fig. 31). Where dikes are absent or sparse in the Wai‘anae-Ko‘olau HGU, the water table is less than about 50 ft above sea level, whereas in the dike-intruded regions, water levels can be more than 1,000 ft above sea level. An exception is the area of high water levels in the saddle between the Wai‘anae and Ko‘olau volcanoes; this enigmatically high water table, known as the Schofield high-level groundwater, is discussed in the *Conceptual Models* section, below.

The structure map of the top of the Wai‘anae-Ko‘olau HGU shows the distribution of this unit (fig. 35). The HGU dips beneath the coastal plain that surrounds most of the island. Erosion features evident at the surface, such as stream-eroded valleys, continue beneath the cover of sedimentary rock and rejuvenated-stage volcanics. Offshore, the steep southwest flank of the Wai‘anae volcano and northeast flank of the Ko‘olau volcano result from the large landslides previously discussed. In contrast, structure contours on the northwestern and southern sides of O‘ahu are suggestive of the relatively intact slopes of the saddle between the shield volcanoes. In this study, the slope break at about –2,000 ft relative to sea level is presumed to be the submerged boundary between subaerial and submarine lavas of the shield stage (Eakins and others, 2003).

Maui

Maui lies near the southeastern end of the Hawaiian archipelago, west of Hawai‘i Island and east of Kaua‘i and O‘ahu (fig. 1). It is the second largest island in Hawai‘i, with a land area of 727 mi^2 or 11 percent of the total land area in the main islands (table 1). The population of Maui is 144,444 (U.S. Census Bureau, 2011), which constitutes about 11 percent of the population of the State of Hawai‘i. The island has two large shield volcanoes that are connected by a lowland isthmus of sedimentary deposits (fig. 36) (Stearns and Macdonald, 1942; Macdonald and others, 1983; Sherrod and others, 2007). West Maui volcano, the older of the two volcanoes, reaches an altitude of 6,788 ft. To the east lies the younger and larger Haleakalā, which is also referred to as East Maui volcano in some literature. Haleakalā reaches an altitude of 10,023 ft, making it the third tallest shield volcano in Hawai‘i.

Geology

Division of Hydrography Bulletin 7 on the geology and groundwater resources of Maui by Stearns and Macdonald (1942), the Hawai‘i State geologic map by Sherrod and others (2007), as well as publications by Stearns (1946, 1966) and Macdonald and others (1983) contain extensive and comprehensive descriptions of Maui’s geology. The stratigraphy for West Maui volcano originally described by Stearns and Macdonald (1942) in Bulletin 7 was recast to conform with the 1983 North American Stratigraphic Code by Langenheim and Clague (1987). This section presents a synopsis largely derived from these sources, with additional specific information from other sources as cited.

West Maui—Thin pāhoehoe and ‘a‘ā lava flows from the shield stage form most of the volume of the West Maui volcano and the base on which younger rocks lie; these rocks are known as the Wailuku Basalt (table 2, fig. 37). Stearns and Macdonald (1942) remarked that the Wailuku Basalt had a “loose” and “vesicular slaggy, tubular, clinkery” character. Overlying some parts of the shield-stage lavas is a 50- to 500-ft thick mantle of postshield-stage lavas known as the Honolua Volcanics. Individual lava flows of the Honolua Volcanics are generally thicker than those of the shield-stage Wailuku Basalt. Some particularly viscous postshield-stage lavas of trachyte formed thick, short flows and domes. A layer of soil several inches thick commonly separates the Wailuku Basalt and Honolua Volcanics.

Most of the shield- and postshield-stage rocks were erupted from the summit and rift zones (fig. 37). The location of the former summit caldera was identified in the head of ‘Īao Valley by the presence of breccia, dense horizontal caldera-filling lavas, intrusive structures, hydrothermal alteration, and other features indicative of shield-volcano calderas. Two major rift zones, marked by lines of postshield cones extending to the northwest and southeast of the caldera, have contributed to the elongation of the shield in those directions. Available radiometric ages span from about 2 to 1.3 million years for the shield stage and 1.3 to 1.1 million years for the postshield stage.

Stearns and Macdonald (1942) mapped hundreds of dikes exposed in the eroded valleys of West Maui volcano (fig. 37) and postulated that thousands more exist. Unlike the dikes of the Ko‘olau volcano on O‘ahu, which are oriented parallel to the rift zones and are clustered in linear dike zones, most dikes on West Maui volcano are oriented radially from the summit. The dikes in West Maui volcano are thicker than most known dikes in the other islands of Hawai‘i, and the volcano has more large intrusive

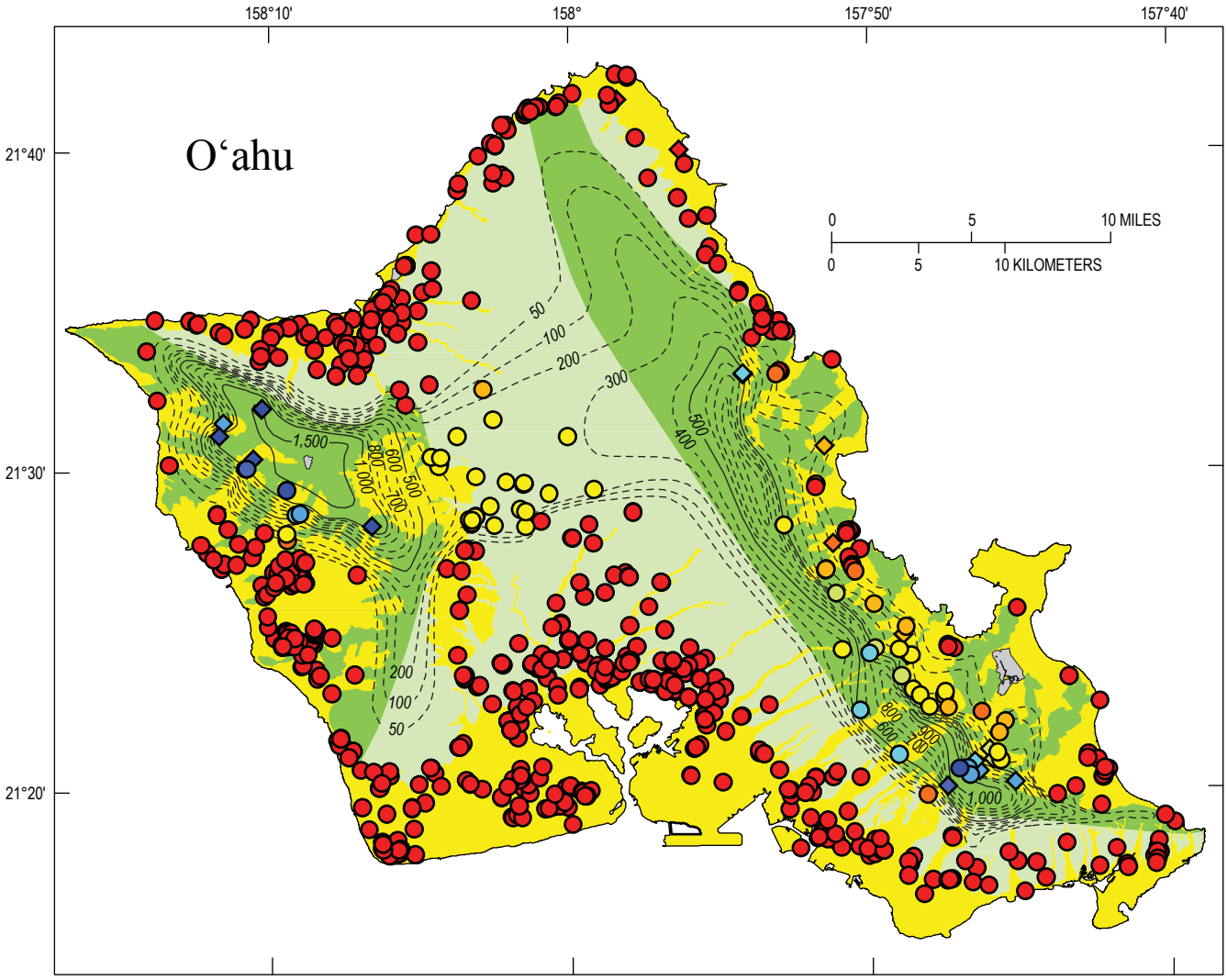

Figure 34. Map of the generalized water-table altitude on O‘ahu, Hawai‘i. Some water levels may be from wells in sedimentary rock rather than volcanic rock. Hydrogeologic units shown for reference.

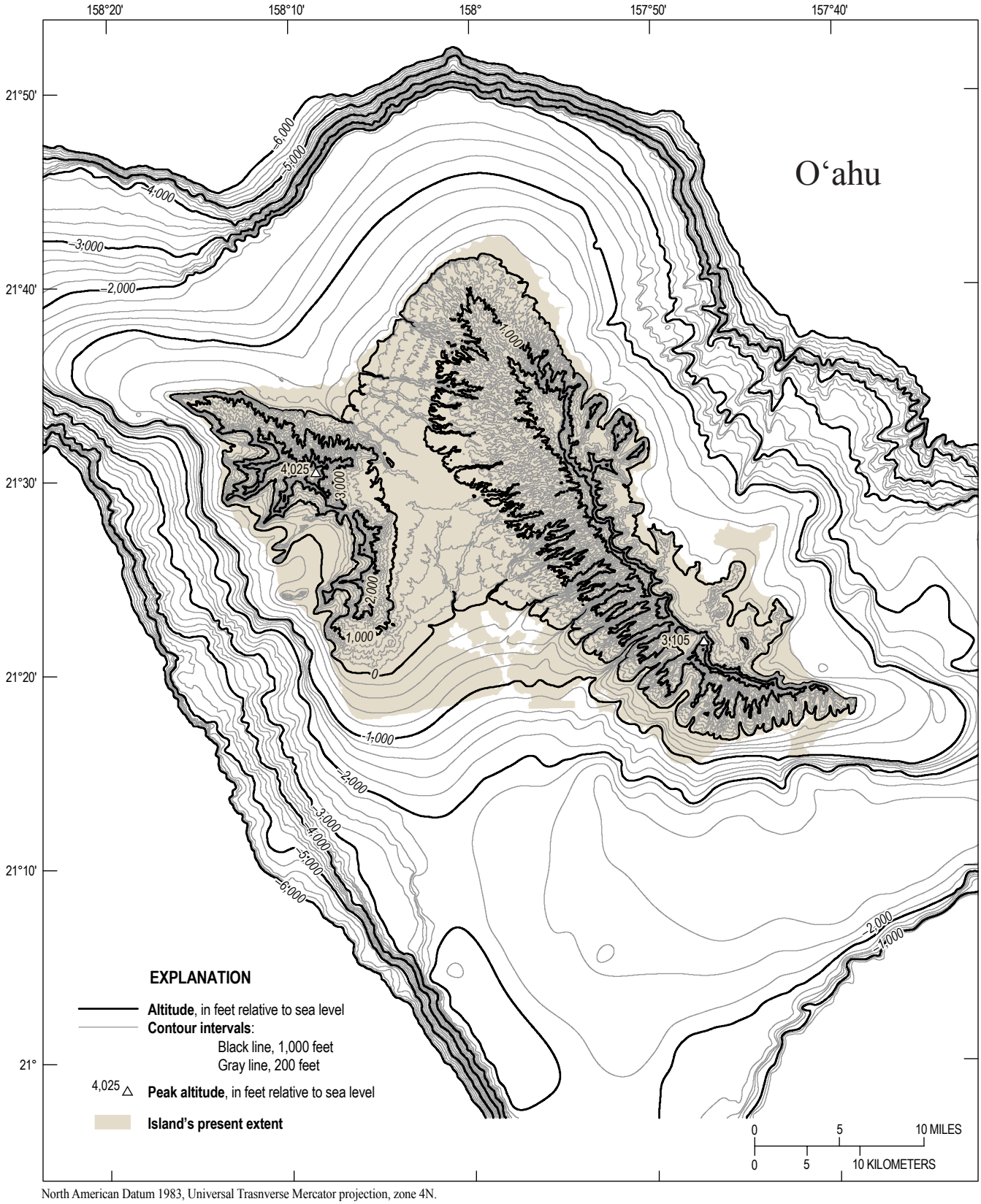

Figure 35. Structure map of the altitude of the top of the Waiʻanae-Koʻolau hydrogeologic unit, Oʻahu, Hawaiʻi. Modified from Palmer (1946), Wentworth (1951), Visher and Mink (1964), Zohdy and Jackson (1969), Tenorio and others (1970), Andrews and Bainbridge (1972), Coulbourn and others (1974), Dale (1978), Gregory (1980), Hawaii Marine Research (1980), Hunt and De Carlo (2000), Oki (2005), Oki and others (2006), and Rotzoll and El-Kadi (2007).

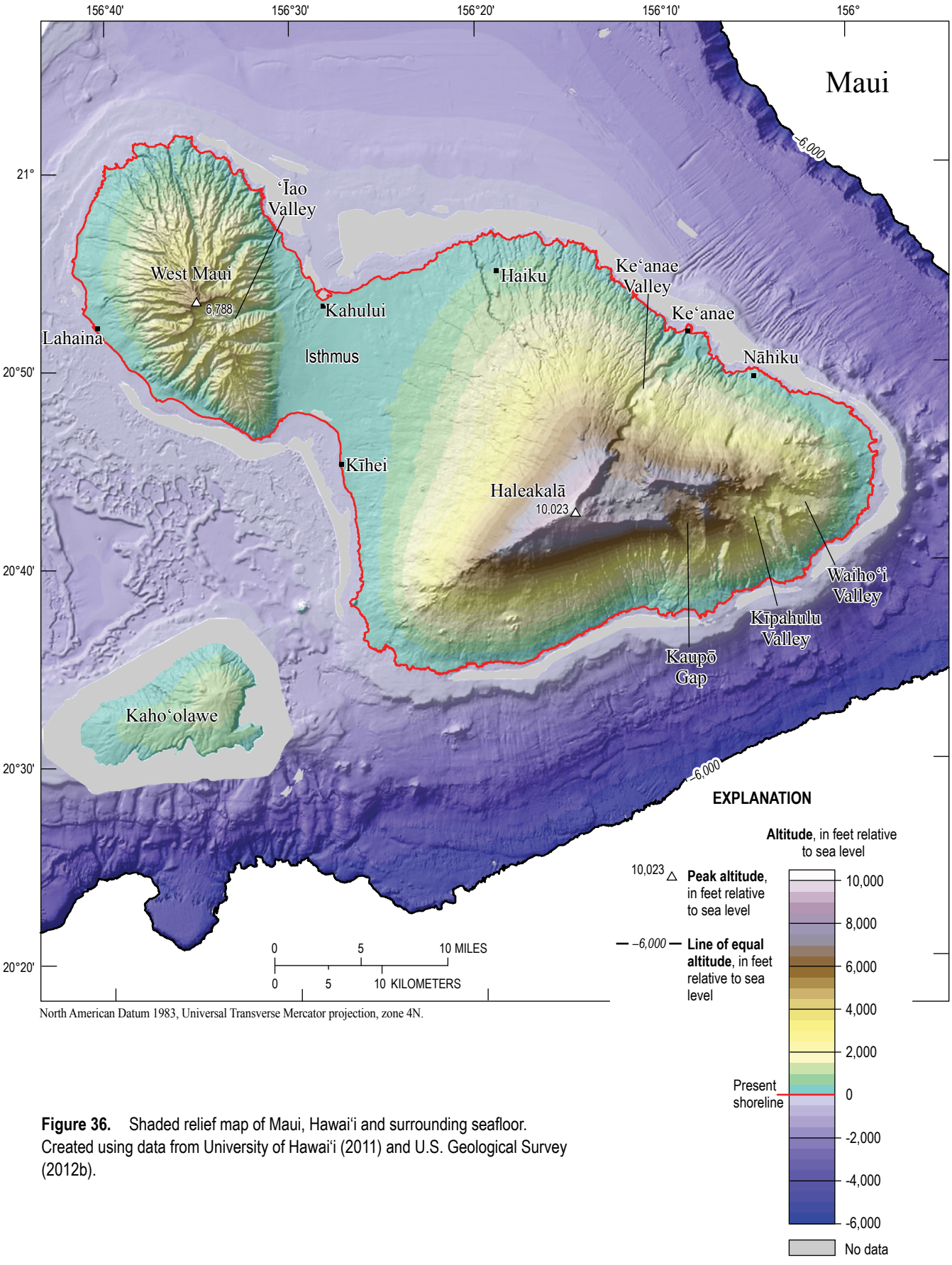

Figure 36. Shaded relief map of Maui, Hawai‘i and surrounding seafloor. Created using data from University of Hawai‘i (2011) and U.S. Geological Survey (2012b).

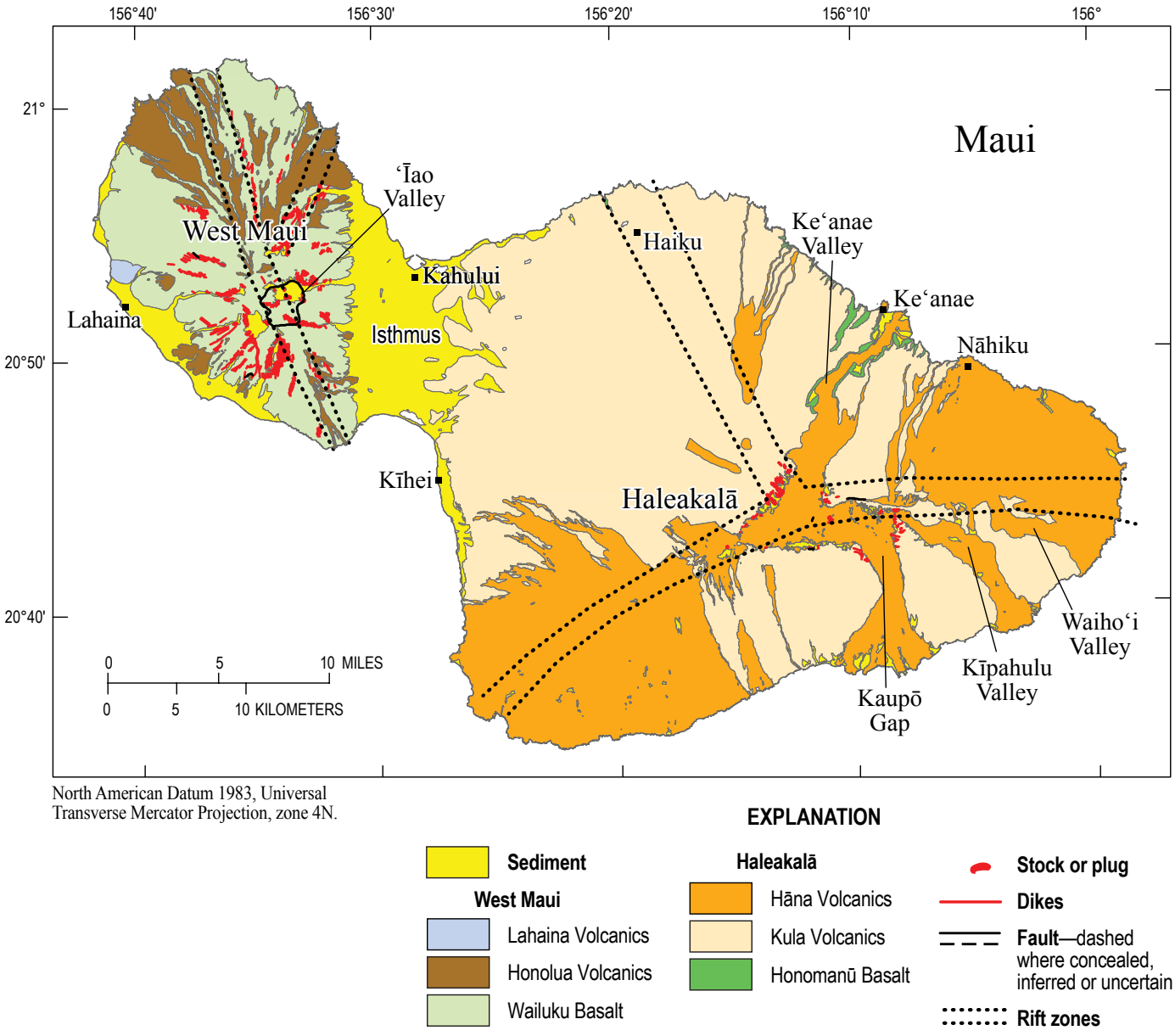

Figure 37. Simplified geologic map of Maui, Hawai'i. Modified from Sherrod and others (2007). Approximate rift-zone traces are based on a small-scale illustration by Stearns and Macdonald (1942).

bodies, such as stocks, plugs, and sills, than other shield volcanoes in Hawai‘i. Gravity surveys show an anomaly consistent with the presence of intrusive rocks in the central region of the volcano (Kinoshita and Okamura, 1965; Flinders and others, 2013). The upland topography of West Maui volcano is dotted by small hills of cinder and trachyte from the postshield stage.

The original form of West Maui volcano has been deeply carved by streams radiating from the summit (fig. 36); the largest valleys and canyons are thousands of feet deep. Some of the material eroded from the valleys form large alluvial fans that skirt the volcano, particularly along its margin with the isthmus and along the southwestern coast near Lahaina (fig. 37). Alluvium also partly fills some valleys. The location of coastal sedimentation and erosion changed with sea-level fluctuations during the Pleistocene, removing soil and cutting sea cliffs at some times and locations, and causing the deposition of marine sediments, calcareous sand dunes (now consolidated), and gravel terraces at other times and locations.

Rejuvenated-stage rocks of West Maui volcano are known as the Lahaina Volcanics (table 2, fig. 37). Rejuvenated-stage eruptions formed small cones and lava flows along the southwestern part of West Maui volcano about 0.6 to 0.3 million years ago. Rocks from these eruptions are partly interbedded with the alluvial fans. The volume of rocks formed by the rejuvenated-stage volcanism on West Maui volcano is much less than analogous formations on Kaua‘i and O‘ahu.

Haleakalā—Haleakalā is one of the largest shield volcanoes in Hawai‘i. As in other Hawaiian volcanoes, thousands of thin shield-stage lava flows form the base of Haleakalā volcano and constitute most of its volume; these shield-stage rocks are known as the Honomanū Basalt (table 2). On the geologic map, however, the shield-stage rocks are almost completely covered by younger rocks (fig. 37). The only outcrops of the shield-stage rocks above sea level are along the sea cliffs and some valleys on the northern flank of the volcano, where they primarily consist of pāhoehoe and have geochemical and petrologic characteristics indicative of the latter part of the shield stage or a transition to the postshield stage. Even so, shield-stage rocks constitute most of the volcano’s volume, both above and below sea level. Radiometric ages for the shield-stage outcrops range from 1.1 to 0.97 million years.

Extensive postshield-stage rocks overlie the shield-stage rocks of Haleakalā. The postshield rocks are divided into two formations—the older Kula Volcanics and the younger Hāna Volcanics (table 2, fig. 37). Stearns and Macdonald (1942) described the Hāna Volcanics as all the volcanic rocks laid down above the “great erosional unconformity,” that is, after Ke‘anae, Waiho‘i, Kīpahulu, Kaupō Gap and other large valleys had been carved. In this respect, the Hāna Volcanics was thought to be analogous to “posterosional” formations such as the Honolulu Volcanics on O‘ahu and the Kōloa Volcanics on Kaua‘i, both of which constitute the rejuvenated stages of their respective volcanoes. The term “rejuvenated-stage volcanics” as it pertains to eruptive stages of Hawaiian shield volcanoes had not yet been adopted at the time Stearns and Macdonald (1942) mapped Maui’s geology, but the label was attached to the Hāna Volcanics by later workers (for example, Clague and Dalrymple, 1987; Langenheim and Clague, 1987). More recently, the Hāna Volcanics has been assigned to the postshield stage because the formation is geochemically similar to the upper part of the Kula Volcanics, the vents of the Hāna and Kula Volcanics are on the same trends, and only a short period (0.03 million years) separates the known ages of the two formations (Sherrod and others, 2003). Soil separates the shield- and postshield-stage lavas in some places and there is a marked erosional unconformity between shield and postshield rocks on the northern coast near Nāhiku, but in many places there is no distinct marker at the contact and the transition from shield- to postshield-stage lavas is gradual. The total thickness of the postshield strata of Haleakalā is more than 3,000 ft at the summit but decreases toward the coast to about 50–200 ft. Individual lava flows are generally thicker than those of the underlying shield stage. The oldest radiometric date for postshield rocks on Haleakalā is 0.93 million years; the most recent lavas erupted sometime between A.D. 1499 and 1633 (Sherrod and others, 2006).

The difference in topography between Haleakalā and its older neighbor West Maui volcano is striking. Whereas West Maui volcano has been deeply carved by stream valleys, most of the surface of Haleakalā is incised only by shallow narrow gulches (fig. 36). The exceptions are four large valleys—Ke‘anae, Waiho‘i, Kīpahulu, and Kaupō Gap—on the eastern part of the volcano. Erosion of Ke‘anae Valley and Kaupō Gap advanced to the summit and the heads of the valleys coalesced to form the depression known as Haleakalā Crater. The valleys and the summit depression were partly filled with younger postshield-stage volcanic rocks as well as sedimentary rocks (fig. 37).

Three rift zones on Haleakalā are marked by the distribution of vents of the postshield stage (fig. 37); it is likely that these rift zones were also eruptive sites during the shield stage. Dikes exposed by erosion near the summit roughly parallel the rift zones. No caldera has been identified in Haleakalā volcano, but if one existed, it may now be buried beneath the postshield-stage lavas. Gravity data indicate that high-density rocks lie beneath an area close to the summit of Haleakalā, which is consistent with the presence of intrusive rocks beneath a caldera (Kinoshita and Okamura, 1965; Flinders and others, 2013).

Maui Nui—The two volcanoes that form Maui are part of a group of closely positioned shield volcanoes including those of Maui, Moloka‘i, Lāna‘i, and Kaho‘olawe (figs. 1 and 13). When sea level was lower during periods in the Pleistocene, these volcanoes emerged as a single large island—referred to as Maui Nui in recent literature—that had an area greater than that of present-day Hawai‘i Island (Stearns and Macdonald, 1942; Price and Elliot-Fisk, 2004). Because the shield volcanoes forming Maui, Moloka‘i, Lāna‘i, and Kaho‘olawe are so close to each other, the lava flows of one volcano likely overlap or are interlayered with those of the adjacent volcano.

Hydrogeologic Units

Stearns and Macdonald (1942) described the water-bearing properties of each of the mapped geologic units on Maui. They described the shield-stage formations as extremely permeable, and even suggested that the Wailuku Basalt, because of its loose character and thin beds, may be more permeable than the highly

productive Koʻolau Basalt on Oʻahu. The postshield-stage Honolua Volcanics was described as having lower permeability because it consisted of massive lava flows; the postshield-stage Kula Volcanics was also described as having lower permeability because it had massive lava flows interstratified with soil and ash layers. On the other hand, Stearns and Macdonald (1942) described the postshield-stage lava flows of the Hāna Volcanics as highly permeable, citing the observation that streams are unable to flow far over the unit except during heavy rain and that the unit generally lacks interstratified low-permeability layers. Meyer (2000) noted, however, that some streams flowing over the Hāna Volcanics are perennial at altitudes as high as 2,100 ft. Stearns and Macdonald (1942) reported that the few small deposits of the rejuvenated-stage Lahaina Volcanics contained only brackish or insignificant amounts of fresh water.

Stearns and Macdonald (1942) described the existence of high-level water in the dike-intruded center of West Maui volcano and its relation to stream base flow and tunnel yields. At the time of their study, no wells or tunnels had yet developed water from the rift zones of Haleakalā (Gingerich, 1999c), but the authors anticipated that dikes in the rift zones of Haleakalā volcano would affect the movement and storage of groundwater (fig. 38).

Stearns and Macdonald's (1942) descriptions of the permeability of sediments ranged from "virtually impermeable" to "exceedingly permeable" depending on sediment composition, coarseness and sorting, and degree of consolidation. The permeability of siliceous sediments could be high—approaching that of the underlying shield lavas—where coarse, well sorted, unweathered, and unconsolidated, but very low where fine and weathered or consolidated. Calcareous sediments, even if consolidated, may be highly permeable, but on Maui, they mostly form small deposits or are above the zone of groundwater saturation. On the basis of the permeability and water-bearing properties of rocks described by Stearns and Macdonald (1942) and subsequent studies (as cited below), three principal HGUs are defined for Maui in this study: (1) Sedimentary, (2) Haleakalā, and (3) West Maui (fig. 39).

Sedimentary Hydrogeologic Unit

All sedimentary rocks are combined with the rejuvenated-stage rocks of the Lahaina Volcanics into the Sedimentary HGU. Most of this HGU consists of sediments; the volumetrically small Lahaina Volcanics has little hydrologic significance at the scale of this study. The Sedimentary HGU occurs primarily as surficial deposits and has low permeability, although some calcareous sedimentary units can be highly permeable locally (Stearns and Macdonald, 1942). The Sedimentary HGU covers most of the isthmus and extends into valleys, especially those of West Maui volcano (figs. 39 and 40). Sediments also form an apron around the southwestern coast of West Maui volcano.

Rotzoll and others (2007) calculated a geometric mean of 164 ft/d, a median of 98 ft/d, and a standard deviation of 262 ft/d for K_h from analysis of aquifer-test data from 16 wells in sediments on Maui. In numerical models of groundwater flow in Maui, values of K_h from 6.9 to 190 ft/d and values of K_v from 0.38 to 3.8 ft/d have been used for sedimentary units to match measured hydrologic data (Gingerich, 2008; Gingerich and Engott, 2012).

Haleakalā Hydrogeologic Unit

All of the shield-stage and postshield-stage volcanic rocks of Haleakalā volcano are grouped into the Haleakalā HGU in this study (fig. 39). This grouping is consistent with the numerical-model units of Gingerich (2008). By far, most of the Haleakalā HGU is composed of the shield-stage Honomanū Basalt. The mantle of postshield-stage Kula and Hāna Volcanics constitutes only about 0.4 percent of the volcano's total (submarine and subaerial) volume (Eakins and Robinson, 2006). The Honomanū Basalt and Hāna Volcanics are described as highly permeable by Stearns and Macdonald (1942). The Kula Volcanics has lower permeability than the Hāna Volcanics or Honomanū Basalt, but as noted by Stearns and Macdonald (1942, p. 85), it is "very permeable compared with most other rocks in the earth." Thus, the three formations can be grouped into one HGU having relatively high permeability. Local variations in hydraulic properties result from interstratification with low-permeability layers such as soil and ash, and variations in lava-flow thicknesses due to viscosity and erosional unconformities.

A dike-intruded subunit has been designated within the Haleakalā HGU in this study on the premise that dikes underlie the rift zones of all shield volcanoes in Hawaiʻi (fig. 39). Because few dikes are exposed on the surface of Haleakalā volcano, the extent of the dike intrusion is largely unknown; therefore, the extent of the Haleakalā dike intrusion shown in figure 39 is speculative—dike intrusion may affect a larger or smaller area than shown in the map and cross-section views. Some dikes must reach the surface to feed the most recent eruptions along the rift zones and summit, but whether these dikes have a substantial affect on hydraulic properties or groundwater occurrence is not known. As discussed previously, the area of dike intrusion is probably wider at depth than indicated by the surface trace of the rift zones, but the actual subsurface shape of the dike-intruded subunit is unknown.

The structure map of the top of the Haleakalā HGU shows submarine terraces off the eastern coast (fig. 41). In this study, the terrace is interpreted as the break in slope between subaerial and submarine lavas that is now submerged due to island subsidence (Moore and others, 1990; Eakins and others, 2003) (see discussion in *Study Area*, above); the terrace is not a submerged analog of the sedimentary coastal plain on Oʻahu. The western end of the Haleakalā HGU dips under the sediment of the isthmus but overlaps the eastern slope of the West Maui volcano (fig. 39), which is consistent with published radiometric ages for the West Maui and Haleakalā volcanoes. Parts of the Haleakalā HGU beneath the isthmus are above sea level. To the southwest, strata of the Haleakalā HGU probably extend to the submarine saddle between Maui and the older Kahoʻolawe volcano.

Most of what is known about the hydraulic properties of the Haleakalā HGU comes from the numerous wells on the west flank of Haleakalā volcano. Published estimates of hydraulic conductivity are consistent with the description of Stearns and Macdonald (1942) in that the dike-free areas of Haleakalā volcano

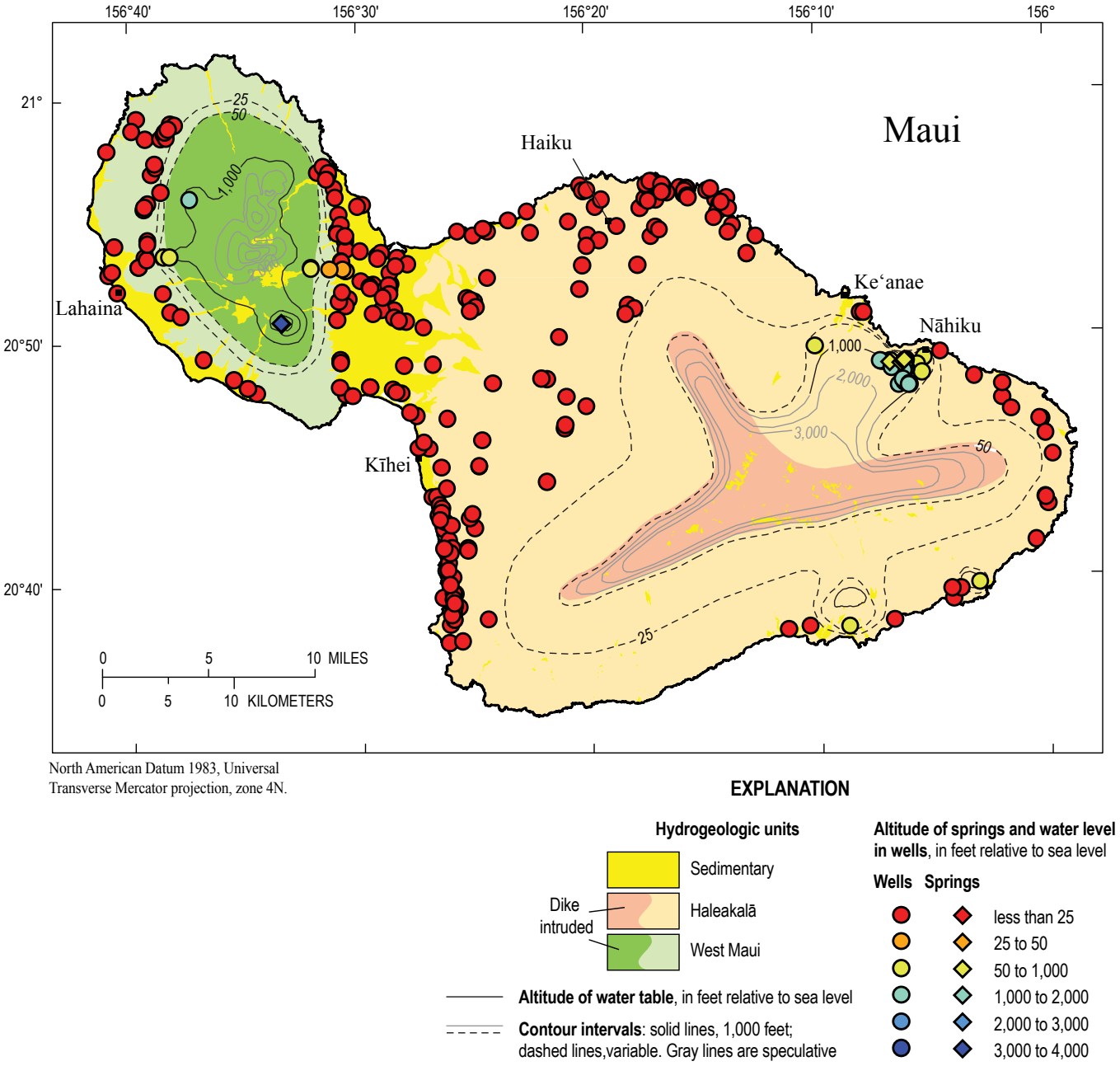

Figure 38. Map of the generalized water-table altitude and the areas of presumed dike-impounded groundwater on Maui, Hawai‘i. Some water levels may be from wells in sedimentary rock rather than volcanic rock. Hydrogeologic units shown for reference.

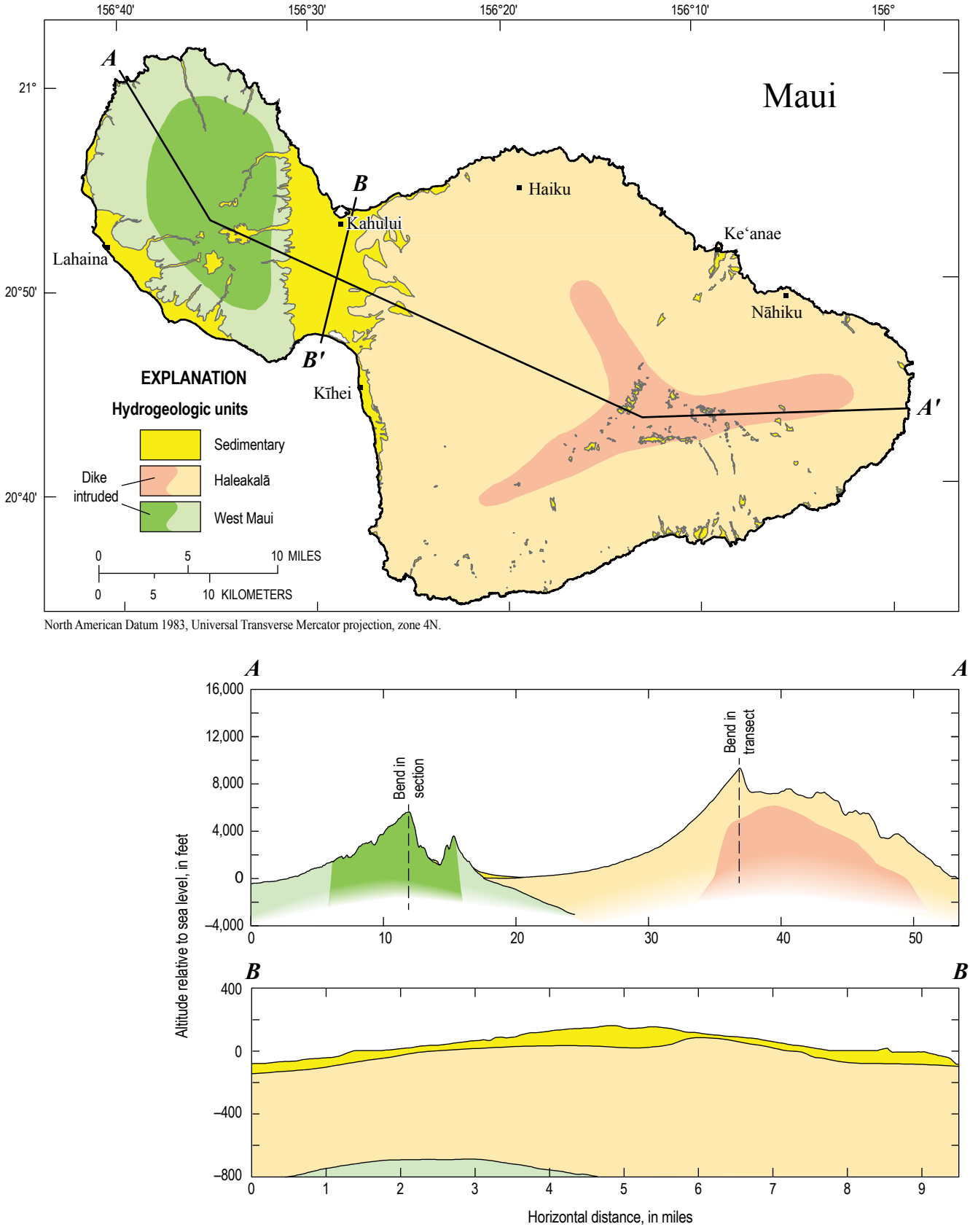

Figure 39. Map of the hydrogeologic units on Maui, Hawai'i. Hydrogeologic-unit outlines modified from geologic map of Sherrod and others (2007). Map-view extent of dike-intruded area based on Stearns and Macdonald (1942), Yamanaga and Huxel (1969, 1970), Gingerich (2008), and Gingerich and Engott (2012); cross sectional depiction of dike-intrusion extent is speculative.

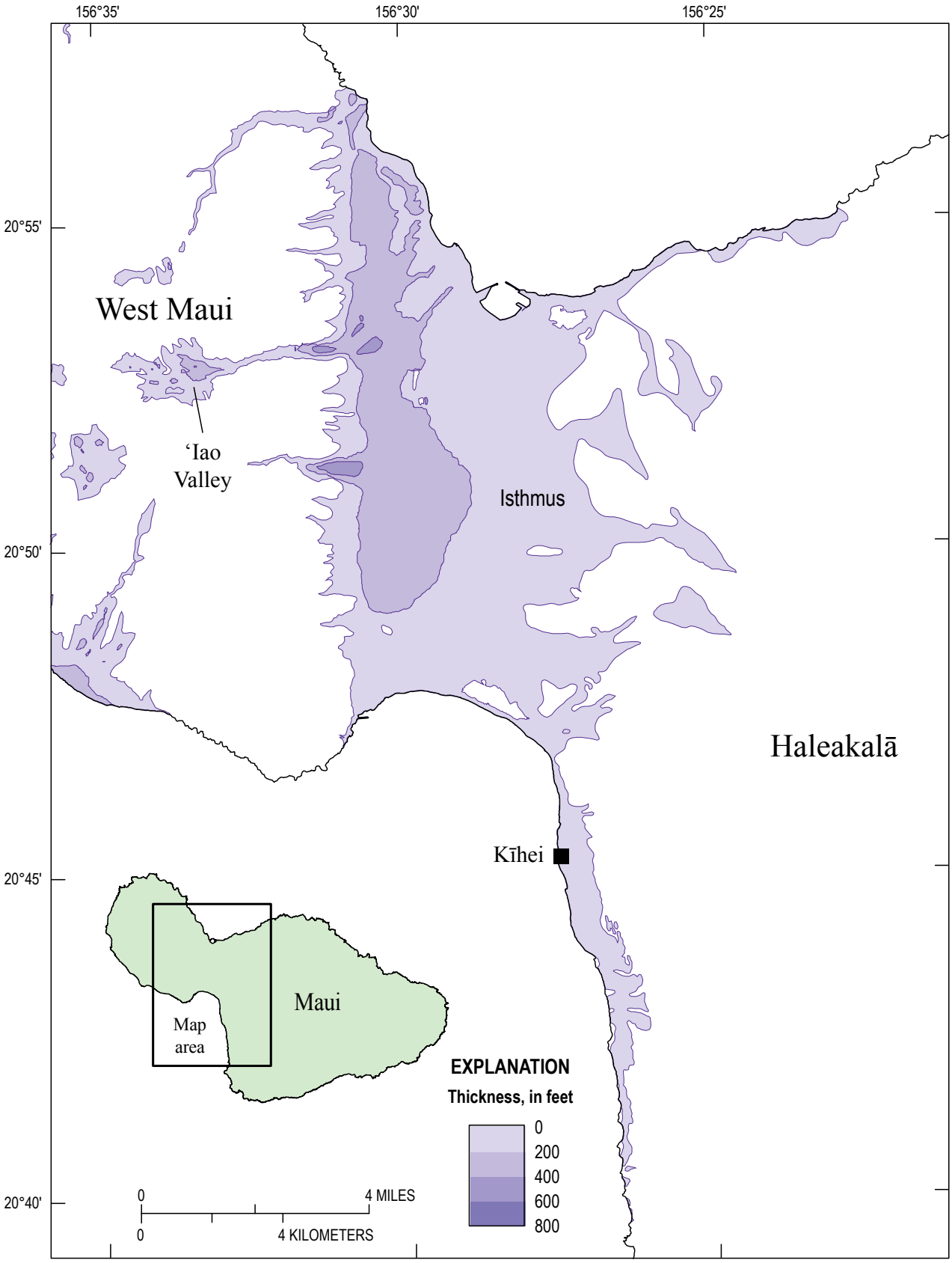

North American Datum 1983, Universal Transverse Mercator projection, zone 4N.

Figure 40. Map of the thickness of the Sedimentary hydrogeologic unit in central Maui, Hawai'i. Offshore thickness not shown.

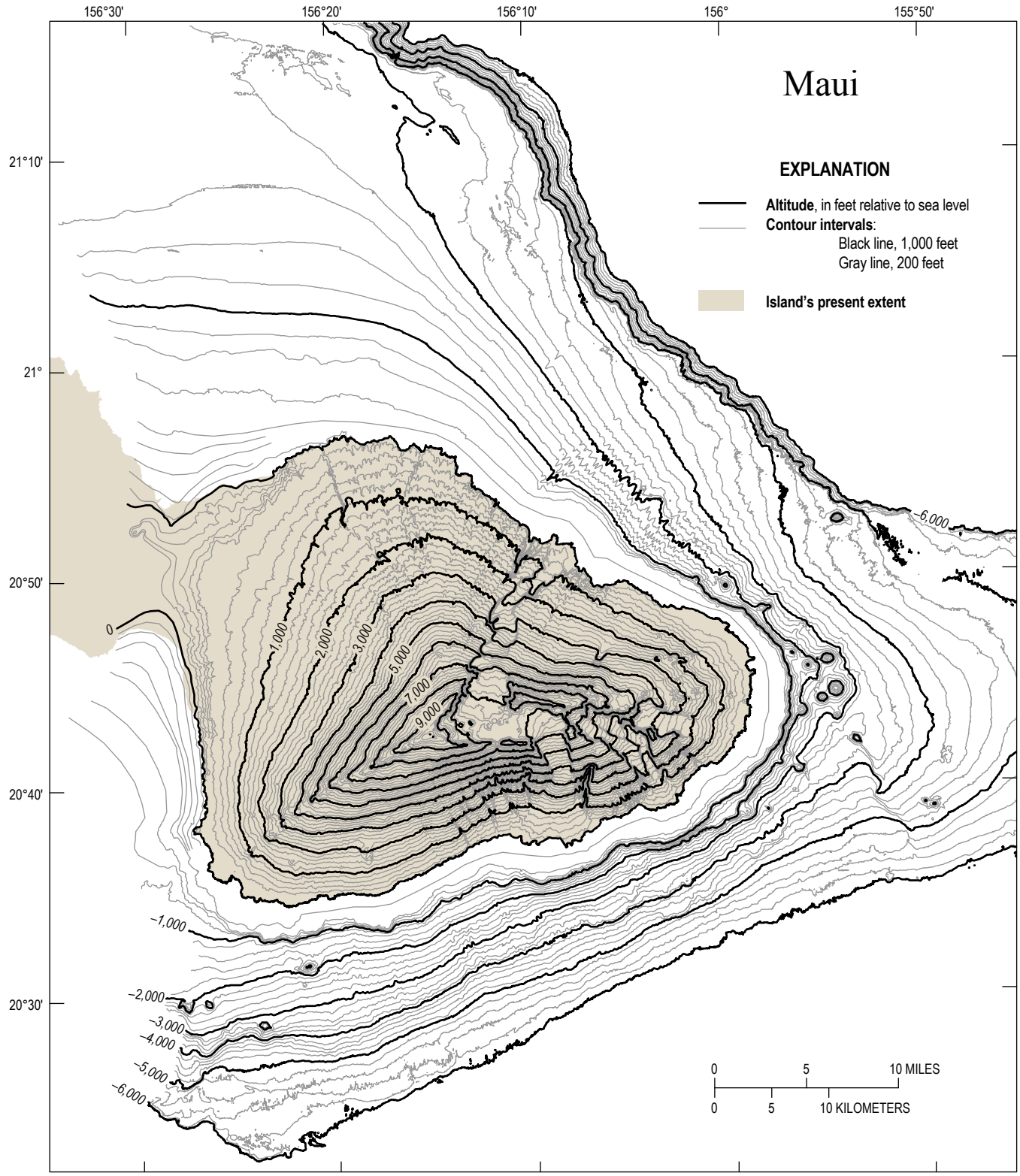

Figure 41. Structure map showing the altitude of the top of the Haleakalā hydrogeologic unit, Maui, Hawai'i.

have high aquifer permeability. Burnham and others (1977) estimated a value of 3,456 ft/d for K_h using data from a test hole in strata of the Haleakalā HGU near Kahului. Gingerich (1999b) used an analytical solution to estimate K_h values of 3,300 to 4,400 ft/d for the Honomanū Basalt. Hunt (2007) used a value of 9,800 ft/d for K_h in a numerical model to match water-table and salinity data near Kīhei. Rotzoll and others (2007) calculated a geometric mean of 1,017 ft/d, a median of 1,214 ft/d, and a standard deviation of 1,969 ft/d for K_h on the basis of analysis of aquifer-test data from 151 wells in the Honomanū Basalt and Kula Volcanics. Gingerich (2008) used K_h values of 3,694 to 11,083 ft/d and a K_v value of 13.85 ft/d for the dike-free part of the Honomanū Basalt and Kula Volcanics in numerical-model simulations to match groundwater and stream base-flow data. The high permeability of the western part of the HGU is also evident in the low, gentle water-table gradients in the area (fig. 38). Wells as far as 8 mi from the coast have water levels that are less than 50 ft above sea level.

Aquifer permeability in localized areas of the Haleakalā HGU may be considerably lower, even where dike intrusion is not suspected. On the north coast between Ke‘anae and Nāhiku, large springs and water levels in wells less than two miles from the coast are hundreds of feet above sea level, indicating a water-table gradient much steeper than would be possible in a high-permeability aquifer (fig. 38). The anomalously high water levels were originally attributed to a perched water body (Stearns and Macdonald, 1942; Takasaki and Yamanaga, 1970), but subsequent drilling and analyses indicate that the high water levels are part of a groundwater system that is saturated down to sea level (Gingerich, 1999c; Meyer, 2000). A fully saturated system implies that a steep water-table gradient exists, which in turn indicates that a local low-permeability zone exists in this part of the Haleakalā HGU. Low permeability of rocks in the Ke‘anae-Nāhiku area is also indicated by a K_h value of 0.83 ft/d determined by an analysis of aquifer-test data (Gingerich, 1999b; Meyer, 2000). The cause of the low permeability is not known, but the area is a complex of eroded surfaces subsequently filled by younger lavas and sediment (Stearns and Macdonald, 1942). A similar occurrence of high water levels in lava flows and sediments filling Kaupō Gap and Kīpahulu Valley along the southeastern coast suggests that this area may also have a thickly saturated low-permeability groundwater system. Not all high-level water bodies along the northern coast of Haleakalā volcano are part of fully saturated systems. Gingerich (1999b,c) provided evidence that a high-level groundwater body near Ha‘ikū is perched (perched groundwater is not included in the water-table map shown in figure 38).

The hydraulic properties and water-table altitude for most of the interior of Haleakalā volcano is uncertain because of a lack of well data (fig. 38). High-permeability dike-free lava flows probably extend farther inland than the wells, but dikes likely intrude the lava flows beneath the rift zones. Dike-impounded groundwater probably exists along the rift zones (Stearns and Macdonald, 1942), but as discussed above, the extent of dike intrusion is uncertain. No data are available that confirm whether the low bulk permeability and elevated groundwater levels typically associated with dike-impounded groundwater exist in the Haleakalā HGU.

West Maui Hydrogeologic Unit

The West Maui HGU encompasses all of the shield- and postshield-stage rocks of West Maui volcano (fig. 39). It is approximately equivalent to the combination of the Wailuku Basalt and Honolua Volcanics (Stearns and Macdonald, 1942; Langenheim and Clague, 1987) except that it includes all igneous intrusions in the shield-stage lava flows of West Maui volcano, regardless of whether they were emplaced during the shield, postshield, or rejuvenated stages. Although Stearns and Macdonald (1942) described the Honolua Volcanics as having a lower permeability than the Wailuku Basalt, the two geologic units are combined in one HGU because the Honolua Volcanics is volumetrically small and contains relatively little groundwater. The vast majority of the volume of the HGU consists of thin, shield-stage lava flows of the Wailuku Basalt.

Stearns and Macdonald (1942) delineated an area of dike-impounded groundwater in West Maui volcano, but the area has been modified as more information became available (Yamanaga and Huxel, 1969, 1970; Gingerich, 2008; Gingerich and Engott, 2012). Superimposing the latest version of the area on the map of the generalized water-table altitude (fig. 38) shows the effect of contrasting hydraulic properties within the West Maui HGU. Within the area where low-permeability dikes intrude and reduce the overall permeability of the aquifer, the water table rises steeply toward the center of the volcano. The water table in this area, like the ground surface, is lower in the deep stream valleys of West Maui; as a result, water-table contours in the dike zone are crenulated. In contrast, where the shield-stage lava flows are free of dikes, aquifer permeability is high and the water table is mostly less than 50 ft above sea level and slopes gently toward the coast.

The dike-intruded area of West Maui HGU is delineated as a hydrogeologic subunit in this study (fig. 39). Numerous dikes have been mapped in the deeply eroded West Maui shield (fig. 37), and high water levels indicated by wells and springs (fig. 38) are consistent with dike-impounded groundwater. Like the boundaries of similar subunits in other shield volcanoes, however, the boundary of the dike-intruded subunit in West Maui is gradational, not distinct. The extent of the dike-intruded area of West Maui volcano was outlined in a page-size illustration by Stearns and Macdonald (1942), but the extent was later revised by Yamanaga and Huxel (1969, 1970), Gingerich (2008), and Gingerich and Engott (2012) as additional hydrologic data became available. The subsurface extent of the dike intrusion shown in the cross section of figure 39 is speculative; like other areas of dike intrusion discussed above, it is probably wider at depth than it is at the surface, but the actual subsurface shape of the dike-intruded subunit is unknown.

The structure map in figure 42 shows the top of the West Maui HGU with all of the overlying HGUs removed. The position of the top of the HGU as it extends west and southwest is not clearly known because the contact between the West Maui volcano and the volcanoes of neighboring islands (Moloka‘i, Lāna‘i, and Kaho‘olawe, figs. 1 and 13) is under water. The spans of known radiometric ages of the strata of these volcanoes overlap considerably between 1 and 2 million years (Clague and Dalrymple, 1987; Langenheim and Clague, 1987; Sherrod and

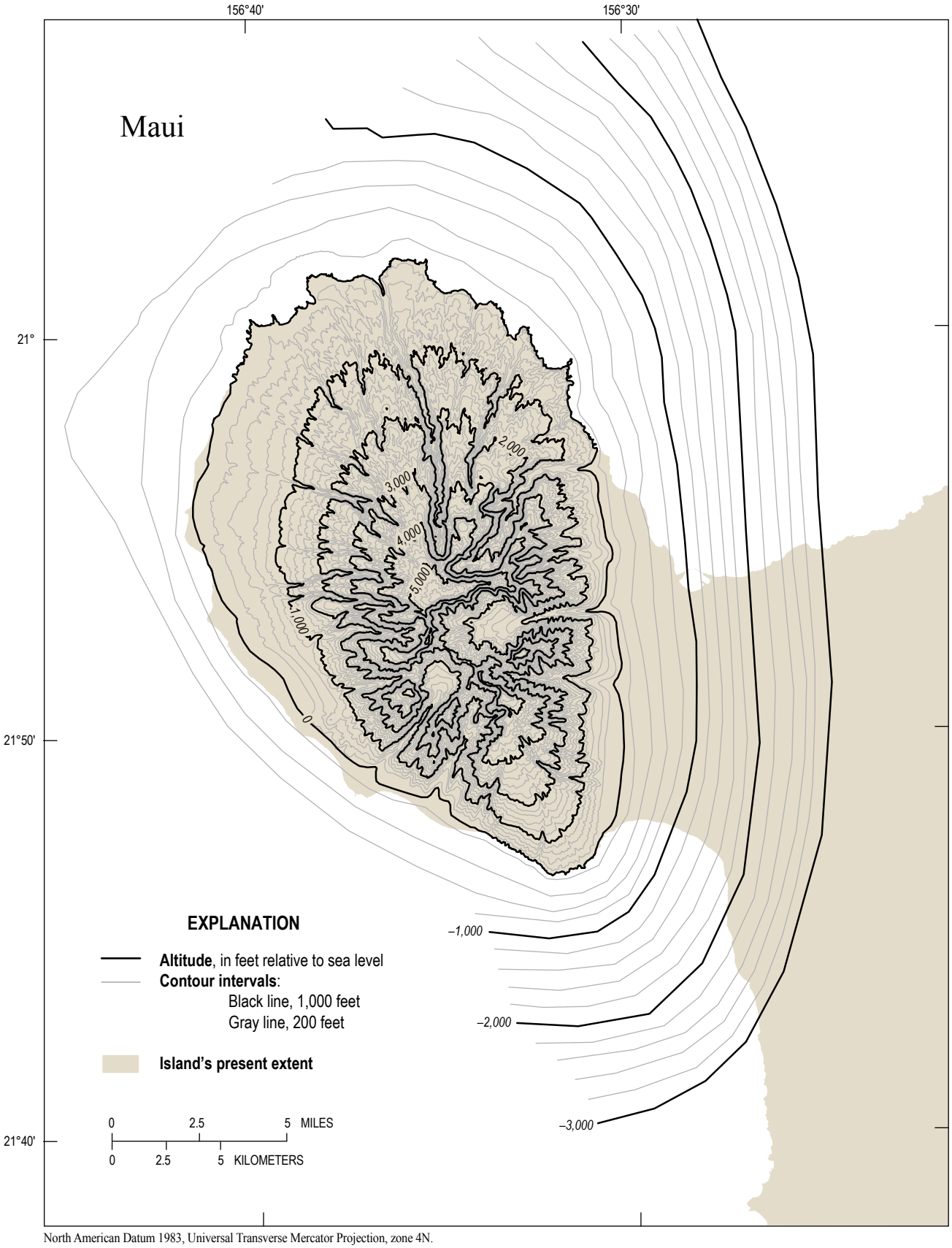

North American Datum 1983, Universal Transverse Mercator Projection, zone 4N.

Figure 42. Structure map showing the altitude of the top of the West Maui hydrogeologic unit, Maui, Hawai'i.

others, 2007); therefore, it is possible that at depth, strata from one volcano are complexly interlayered with those of its neighbor. Contacts between West Maui volcano and the volcanoes of Moloka‘i, Lāna‘i, and Kaho‘olawe probably exist along axes of the intervening saddles.

On the other hand, most radiometric ages for Haleakalā are younger (less than 1.2 million years) than the adjacent West Maui and Kaho‘olawe volcanoes (Sherrod and others, 2007), which indicates that most of the upper strata of Haleakalā volcano overlie those of the older volcanoes. The surface of the West Maui HGU thus dips below the younger hydrogeologic units to the east, including the Sedimentary HGU in the isthmus and the Haleakalā HGU (fig. 39, *A–A'*). Sedimentary deposits between the West Maui and Haleakalā HGUs have been detected in drilled wells (Meyer and Presley, 2000). Although these sediments are too thin to show at the scale of cross section *A–A'* in figure 39, they likely form a low-permeability structure that resists flow between the two HGUs.

In an analysis of aquifer-test data from 167 wells, Rotzoll and others (2007) calculated a geometric mean of 820 ft/d, a median of 1,214 ft/d, and a standard deviation of 1,214 ft/d for K_h in the dike-free areas of the Wailuku Basalt. Gingerich (2008) and Gingerich and Engott (2012) estimated K_h values between 200 and 7,778 ft/d and K_v values between 0.38 and 10 ft/d for the dike-free part of the Wailuku Basalt by adjusting K_h and K_v values in numerical-model simulations to match groundwater and stream base-flow data. Gingerich and Engott (2012) used K_h values of 60 to 180 ft/d and a K_v value of 12 ft/d to match water levels in an area transitioning between the dike and dike-free zones of the Wailuku Basalt. Rotzoll and others (2007) calculated a K_h value of 20 ft/d using aquifer-test data from a well in the dike zone of West Maui volcano. Gingerich (2008) and Gingerich and Engott (2012) simulated the Honolua Volcanics as a confining unit in numerical models, and used values of K_h ranging from 0.08 to 3.8 ft/d and K_v ranging from 0.08 to 190 ft/d to match measured water levels.

Other Hydrogeologic Data for Maui

Some studies have presented measured or estimated hydraulic properties for Maui without specifying values for individual hydrogeologic units. Rotzoll and El-Kadi (2008) used a regression between specific capacity and hydraulic conductivity to estimate a geometric mean K_h of 1,388 ft/d for all of Maui, but their standard deviation spanned a wide range—397 to 4,866 ft/d. Rotzoll and others (2007) estimated a specific-storage value of 2.1×10^{-5} 1/ft and a specific-yield value of 0.073 using aquifer-test data from the Haleakala HGU beneath the isthmus. Effective-porosity values of 0.04 to 0.15 have been used in transient-mode numerical models of Maui to match data on historical movement of the transition zone (Gingerich, 2008; Gingerich and Engott, 2012) and groundwater ages (Hunt, 2007).

Hawai‘i Island

Hawai‘i Island, at the southeastern end of the Hawaiian archipelago (fig. 1), is the youngest, largest, and tallest of the Hawaiian Islands (table 1). Paleomagnetic data and radiometric dating indicate that the entire surface of Hawai‘i Island is less than 1 million years old (Sherrod and others, 2007). Mauna Kea is the highest point at 13,796 ft (fig. 43). The island has a land area of 4,028 mi^2—more than the land area of all of the other Hawaiian Islands combined—but it has only 13.6 percent of the population of the State of Hawai‘i and the lowest population density among the four islands in this study.

The subaerial part of Hawai‘i Island is made of five shield volcanoes—Kohala, Mauna Kea, Hualālai, Mauna Loa, and Kīlauea (table 1, fig. 43). Stream erosion is not as advanced on this relatively young island as it is on the older islands in the archipelago. The most extensive erosion features are the large valleys on the windward northeast slope of Kohala volcano, but even there, much of the original form of the shield volcano is still preserved. Streams have dissected numerous youthful gulches in the wet northeast slope of Mauna Kea and the southeast slope of Mauna Loa, but their incision is relatively shallow. Stream erosion is even less distinct in drier areas, such as the leeward, west side of the island and the arid peaks of Mauna Loa and Mauna Kea, and where erosion competes with the emplacement of new lava flows erupted from the active Kīlauea, Mauna Loa, and Hualālai volcanoes. Weathering and soil development are shallower and less extensive on Hawai‘i Island than on the older islands in the archipelago. Much of the land surface is bare rock, particularly on active parts of volcanoes and where the climate is arid (Sato and others, 1973). Sedimentary rocks are rare compared to the older islands in the archipelago. As discussed earlier in this report, Hawai‘i Island is subsiding relatively rapidly (about 2–3 mm/yr) as the lithosphere is depressed to adjust to the overburden of the island's growing volcanoes (Moore, 1987).

Geology

The geology of Hawai‘i Island has been the subject of many studies since the late 19th century. Much of the intensive geologic interest is related to the active volcanoes on the island. Geologists at the Hawaiian Volcano Observatory have monitored the activity of Kīlauea and Mauna Loa since 1912, and the work of scientists worldwide has greatly advanced knowledge of the internal structure of Hawaiian shield volcanoes. This knowledge is relevant to understanding the storage and flow of groundwater in all of the major islands in the Hawaiian archipelago. Although numerous summaries of Hawai‘i Island geology exist, the following discussion is largely derived from descriptions in Stearns and Macdonald (1946), Macdonald and others (1983), Peterson and Moore (1987), Moore and Clague (1992), Wolfe and Morris (1996), and Sherrod and others (2007). Specific citations are given where descriptions or interpretations in these references differ, or where information or concepts originate from other sources.

Based on the time elapsed since the last eruptive activity, Kohala is the oldest of the shield volcanoes on Hawai‘i Island, followed by Mauna Kea. Hualālai last erupted in 1801, Mauna Loa erupted as recently as 1984, and Kīlauea has been erupting continuously since 1983 (U.S. Geological Survey, 2013). Kohala, Mauna Kea, and Hualālai have reached the postshield stage.

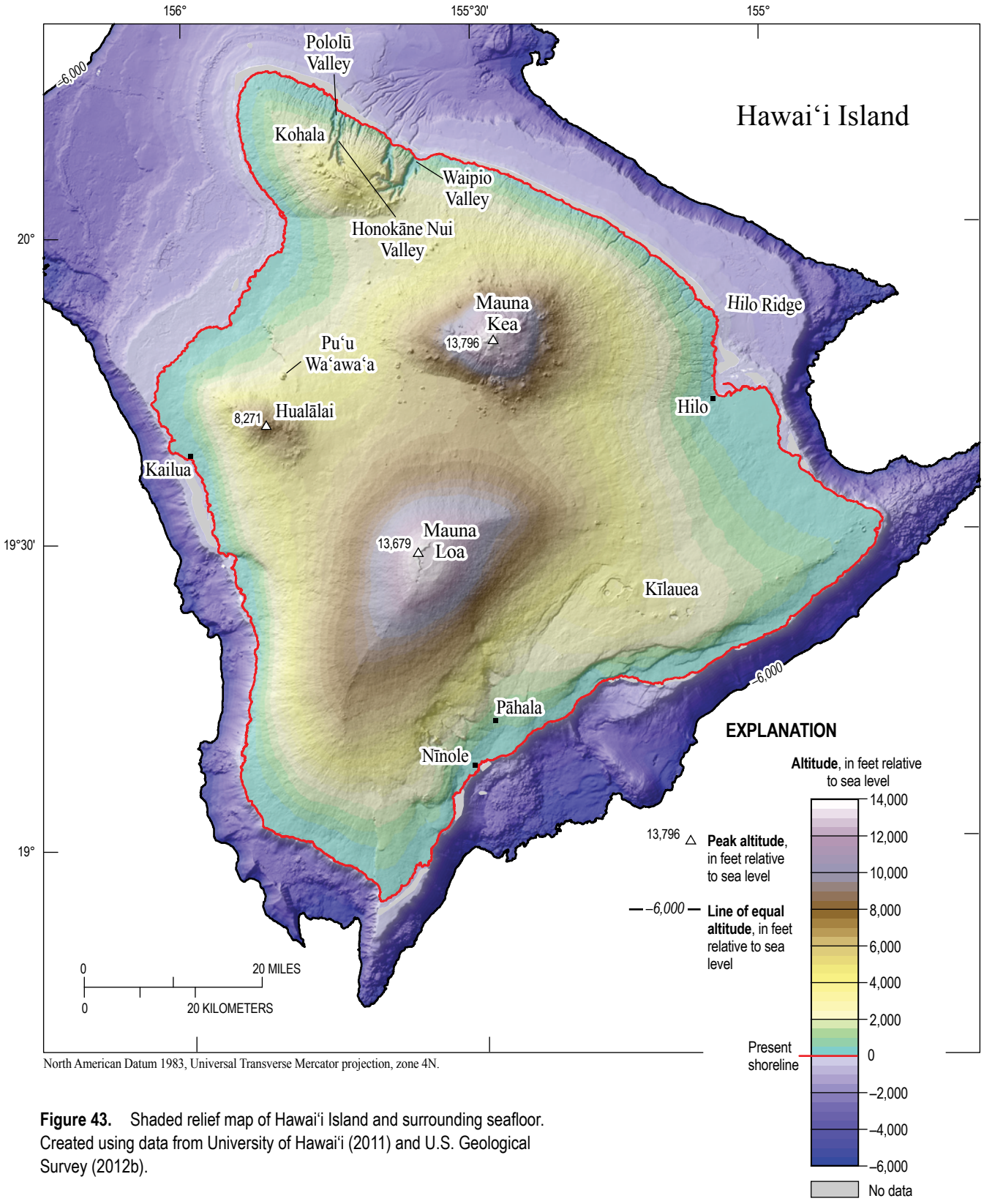

Figure 43. Shaded relief map of Hawai‘i Island and surrounding seafloor. Created using data from University of Hawai‘i (2011) and U.S. Geological Survey (2012b).

Mauna Loa and Kīlauea are in the shield stage. None of the volcanoes on Hawai‘i Island has rocks from the rejuvenated stage.

Each volcano was formed at least partly contemporaneously with the ones before and after it, therefore strata of one volcano are probably complexly interbedded with that of its neighbors (Wolfe and Morris, 1996; Wolfe and others, 1997). No interbedding, however, was indicated in the stratigraphic sections of the two Hawai‘i Scientific Drilling Project (HSDP) deep scientific borings (HSDP1, 3,465-ft [1,056 m] deep and HSDP2, 10,164 ft [3,098 m] deep; fig. 44) drilled near the coast in the saddle between Mauna Kea and Mauna Loa (Rhodes, 1996; Garcia and others, 2007). On the other hand, Stearns and Macdonald (1946, p. 139) write that the lavas of Hualālai “definitely interfinger” with Mauna Loa lavas, and Wolfe and others (1997) described field evidence of interlayering of strata from Mauna Loa, Mauna Kea, and Hualālai in the saddle formed by the juncture of these volcanoes.

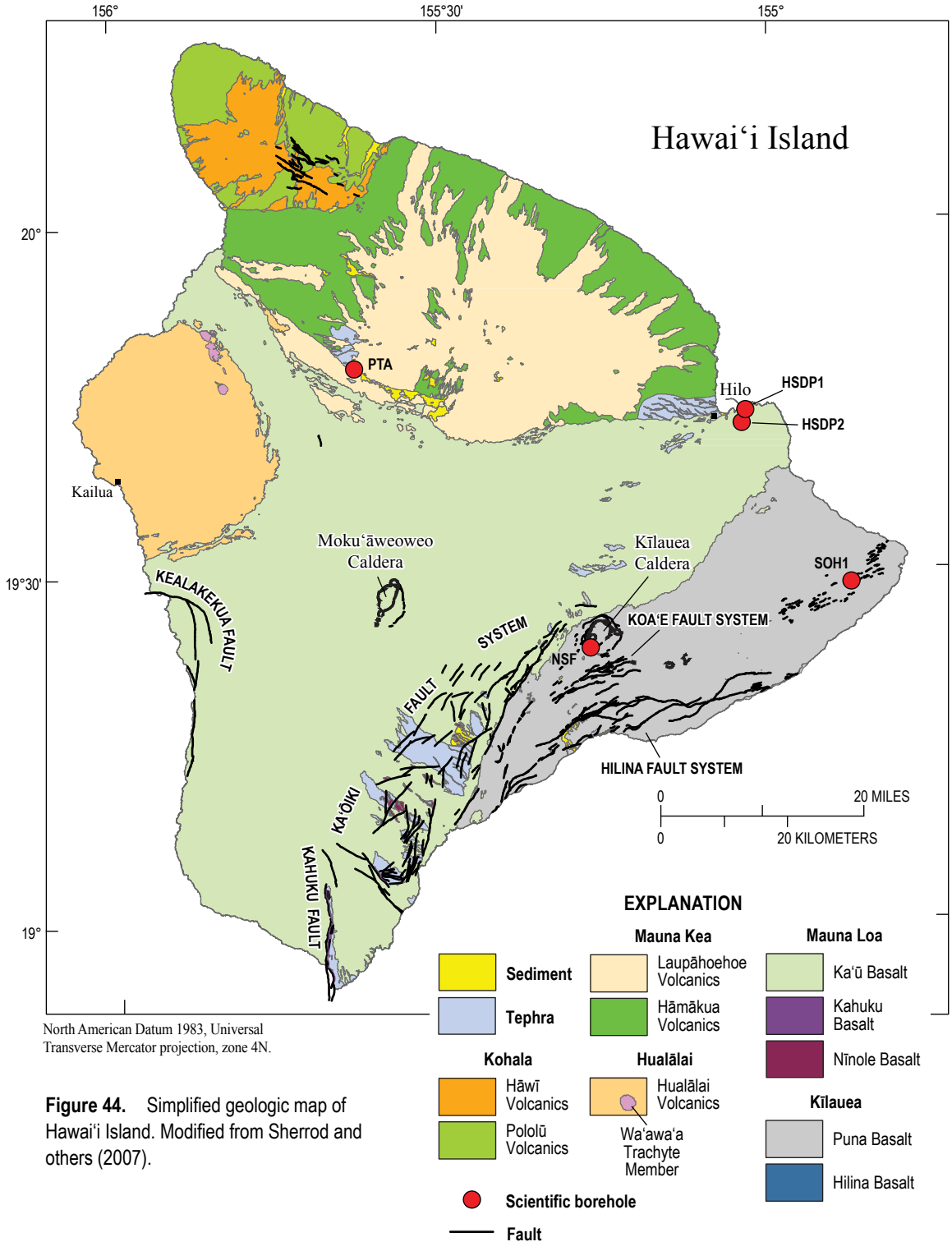

Figure 44. Simplified geologic map of Hawai‘i Island. Modified from Sherrod and others (2007).

Pāhala Ash—Before discussing the geology of each shield volcano in Hawai‘i Island, it is helpful to introduce the Pāhala Ash, a unit of weathered primary and reworked ash that is widespread on Hawai‘i Island and used in many places as a stratigraphic marker. Near its namesake town of Pāhala on the southeast slope of Mauna Loa (fig. 43), the unit consists of a single 55-ft thick layer, but elsewhere the unit is thinner or consists of several thin layers. Stearns and Macdonald (1946) recognized that the ash came from different sources and accumulated over a long period, but considered the bulk of the deposit to have formed relatively contemporaneously and used the unit as a stratigraphic marker separating formations on Mauna Kea, Mauna Loa, and Kīlauea. Later radiometric dating showed the age of the Pāhala Ash to range widely from 3,000 to 39,000 years (Beeson and others, 1996). Recent definitions of the Pāhala Ash have been more restrictive than that of Stearns and Macdonald (1946). For example, Langenheim and Clague (1987) and Wolfe and Morris (1996) limited the name Pāhala Ash to specific ash horizons on Mauna Loa and Kīlauea. It is also noteworthy that not all ash layers on Hawai‘i Island were included in the Pāhala Ash, even by Stearns and Macdonald (1946). Whether or not a given ash layer is assigned to the Pāhala Ash does not change its hydraulic properties. Sherrod and others (2007) referred to ash outcrops large enough to be shown at the 1:250,000 scale of their geologic map simply as “tephra” (fig. 44).

Kohala Volcano—The bulk of Kohala volcano is formed by thin shield-stage basalt lava flows of the Pololū Volcanics (table 2, fig. 44). The lava flows were erupted from two prominent rift zones extending to the northwest and southeast (fig. 45), and possibly from a summit caldera. Stearns and Macdonald (1946) described a third smaller rift zone extending to the southwest, but it was not shown in their illustration (their figure 6) nor in subsequent publications (for example, Fiske and Jackson, 1972; Macdonald and others, 1983; Fornari, 1987; Sherrod and others, 2007). Stearns and Macdonald (1946) and Macdonald and others (1983), citing a slight curvature of faults near the summit, suggested that Kohala volcano once had a caldera that is now covered by younger rocks. Gravity data show that Kohala volcano has positive anomalies that are consistent with the presence of dense magma-chamber cumulates and zones of dike intrusion associated with calderas (Kinoshita, 1965; Clague and Dalrymple, 1987; Kauahikaua and others, 2000; Flinders and others, 2013). Swarms of dikes (not shown on fig. 44) are also exposed in the heads of the large valleys eroded into the northeast flank of the volcano. Subparallel faults formed a southeast-trending graben along the crest of Kohala volcano. Other subparallel faults occur near to and northeast of the graben. On the basis of growth rates of shield-stage volcanoes and radiometric dating of submarine outcrops, Sherrod and others (2007) estimated that the shield stage of Kohala volcano may have started about 1 million years ago and lasted to about 0.25 million years ago. The uppermost part of the Pololū Volcanics has some hawaiite and mugearite that indicate a transition to alkalic rocks of the postshield stage (Feigenson and others, 1983; Sherrod and others, 2007).

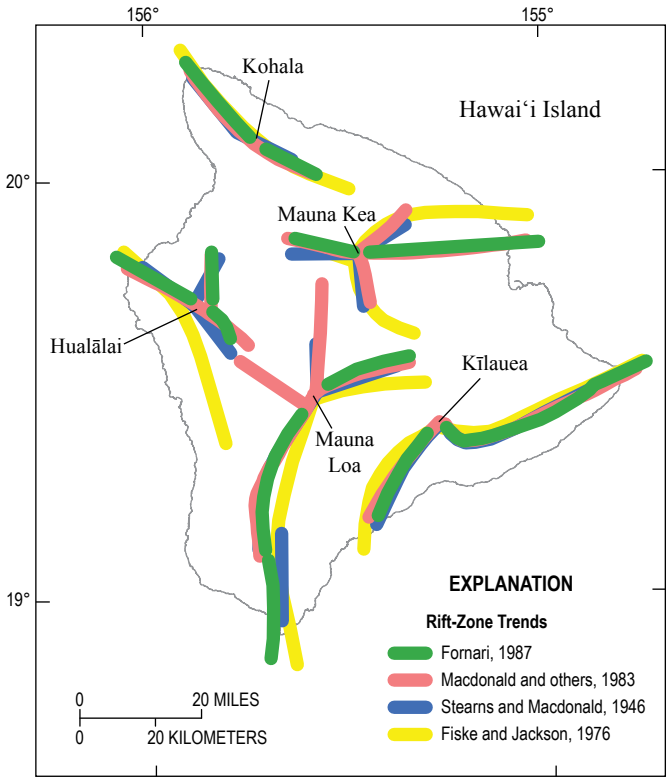

North American Datum 1983, Universal Transverse Mercator projection, zone 4N.

Figure 45. Interpretations of rift-zone trends on Hawai‘i Island.

Overlying the Pololū Volcanics is the Hāwī Volcanics, which consists of postshield alkalic rocks ranging from basanite to trachyte (table 2, fig. 44). The postshield stage produced thicker lava flows and tephra cones that partly covered the Pololū Volcanics. Stearns and Macdonald (1946) estimated that the Hāwī Volcanics probably attain a total maximum thickness of only a few hundred feet. Vents of the postshield stage are aligned approximately along the same northwest and southeast trends of the shield-stage rift zones (fig. 45). Postshield-stage lava flows originating from the northwest rift spread over a large area of the shield surface. On the other hand, postshield flows from the southeast rift filled the graben at the crest of the Kohala volcano, and the faults bounding the graben in turn restricted the spread of the postshield lava flows in this part of the volcano. Radiometric dating indicates that the postshield stage eruptions occurred between about 0.26 and 0.12 million years ago.

The northeast flank of Kohala volcano between Pololū and Waipio Valleys is more deeply eroded than the rest of the island (fig. 43). Large valleys have been carved into the shield-stage lavas and the lower parts of the valleys have been partly filled with sediments. The subparallel faults at the crest of the volcano caused the headward erosion of the valleys to bend away from the typical radial pattern on shield volcanoes. The coastline along this section is also indented and sea cliffs are substantially higher than elsewhere along the Kohala coastline. Jagger (1920) postulated that the high sea cliffs and indented coastline marked a fault line and that the seaward downthrown block was now entirely below sea level. Stearns and Macdonald (1946) and Stearns (1946)

attributed the distinctive topography in this section to differential erosion—because the summit graben (fig. 44) restricted the spread of more resistant postshield-stage lavas, stream and wave erosion were able to cut more deeply into the less resistant shield-stage lavas. Moore and others (1989) revived the idea of a fault origin, suggesting that the distinctive topography is part of a slope-failure system that extends from slumping at the head above sea level to submarine landslides at the bottom. In this hypothesis, the graben and associated subparallel faults at the crest of the mountain are pull-apart basins formed by the northeastward movement of the slope-failure system.

As originally described, the Pololū Volcanics and the Hāwī Volcanics are separated by an erosional unconformity that formed during a hiatus in volcanism. Stearns and Macdonald (1946) mapped postshield-stage lavas that descended into the large valleys on the northeast flank of the Kohala shield, but additional mapping, geochemical and petrologic analysis, and radiometric dating done after Stearns and Macdonald (1946) indicate that there was no significant hiatus (Spengler and Garcia, 1988).

Mauna Kea—The Mauna Kea shield volcano forms the north-central part of Hawai'i Island (fig. 43). Like the other Hawaiian shield volcanoes, the bulk of Mauna Kea was probably built during the shield stage, but above sea level, the shield-stage rocks are almost entirely covered by postshield-stage rocks. The boundary between shield-stage and postshield-stage strata on Mauna Kea is gradational and not clearly defined. Rocks recovered from the deep scientific boreholes HSDP1 and HSDP2 near Hilo (fig. 44) indicate that tholeiitic shield-stage strata lie at depth (Rhodes, 1996; Rhodes and Vollinger, 2004). Both holes penetrated Mauna Kea strata, the upper 200 to 350 ft of which consisted of interlayered transitional tholeiitic and alkalic basalt analogous to outcrops that have been interpreted as postshield-stage lavas (Wolfe and Morris, 1996; Wolfe and others, 1997; Sherrod and others, 2007). The rest of the strata to the bottom of the holes were all tholeiitic basalt indicative of the shield stage (Rhodes, 1996; Rhodes and Vollinger, 2004).

The lowermost volcanic rocks exposed above sea level on Mauna Kea are known as the Hāmākua Volcanics (Stearns and Macdonald, 1946; Langenheim and Clague, 1987) (table 2, fig. 44). Whether the tholeiitic shield-stage rocks found in the HSDP1 and HSDP2 deep drill holes should also be considered part of the Hāmākua Volcanics is a matter of debate. Stearns and Macdonald (1946, p. 153) listed the total thickness of the formation as "12,000+" feet, which indicates that they intended the Hāmākua Volcanics to include the bulk of the shield volcano, not just the lower part of the postshield cap. Langenheim and Clague (1987) also include shield- and postshield-stage rocks in their definition of the Hāmākua Volcanics. In contrast, Wolfe and others (1997) and Sherrod and others (2007) restricted their definitions of the Hāmākua Volcanics to only the basalts of postshield origin. The debate primarily revolves around geochemistry and has little bearing on hydrology. For the purposes of this report, the name Hāmākua Volcanics is used in the broader sense, inclusive of both shield- and postshield-stage basalts.

The younger volcanic rocks of Mauna Kea are more readily recognized as postshield stage in terms of their chemistry, petrology, lava-flow thickness, and geomorphology. These rocks are grouped in a formation known as the Laupāhoehoe Volcanics (table 2, fig. 44). In the original descriptions of this unit, Stearns and Macdonald (1946) described the Laupāhoehoe Volcanics as a veneer on the flanks of the volcano, probably less than a few hundred feet thick and in many places being only a few tens of feet thick. They described an unconformity separating the Laupāhoehoe Volcanics from the underlying Hāmākua Volcanics at the type section, but they wrote that elsewhere the separation is indistinct or is marked only by an ash layer. In a revised stratigraphy, Wolfe and others (1997) placed all of the hawaiite, mugearite, and benmoreite lavas in the Laupāhoehoe Volcanics, and all basaltic lavas in the Hāmākua Volcanics. Lava flows of the Laupāhoehoe Volcanics are generally thicker than those of the Hāmākua Volcanics, and some form small hills or domes, which is consistent with the more viscous nature of postshield-stage lava. Most lava flows stop short of reaching the coast and cinder cones are numerous. As a result, the youngest postshield-stage strata form a steeper cap with a bumpy skyline when Mauna Kea is viewed from a distance (fig. 14). Discontinuous layers of ash and soil occur on top of the lava flows as well as interbedded between some lava flows. A somewhat extensive outcrop of ash near Hilo was described as Pāhala Ash by Stearns and Macdonald (1946) and mapped by Wolfe and Morris (1996).

The oldest radiometric age obtained for surface outcrops of volcanic rocks on Mauna Kea is about 300,000 years. The age of the oldest Mauna Kea rocks in the 3,465-ft deep HSDP1 hole is estimated to be about 400,000 years (Sharp and others, 1996; Stolper and others, 1996), and the age of the oldest Mauna Kea rocks in the 10,165-ft deep HSDP2 hole is estimated to be about 683,000 years (Sharp and Renne, 2005). The youngest radiometric age for volcanic rocks on Mauna Kea is about 4,600 years.

Mauna Kea does not have clearly defined rift zones. Cinder cones on Mauna Kea are not arranged in distinctly linear trends (fig. 43), although Stearns and Macdonald (1946) used cinder cones to describe three rift zones (fig. 45). Fiske and Jackson (1972) delineated rift-zone trends that differ significantly from those of Stearns and Macdonald (1946). Fiske and Jackson (1972) delineated their rift zones on the basis of gravity data and the hypothesis that rift-zone formation on Mauna Kea was governed by the stresses that developed as Mauna Kea grew against the preexisting masses of Kohala volcano and Hualālai. Subsequent radiometric dating, however, indicates that Mauna Kea is mostly older than Hualālai (Moore and others, 1987; Moore and Clague, 1992; Sherrod and others, 2007). Macdonald and others (1983) described, on the basis of cinder-cone locations and subaerial and submarine topography, a long east-west rift extending from the east flank of the volcano through the summit and to a submarine feature known as the Hilo Ridge, and two shorter rift zones extending from the summit to the northeast and south-southeast. Later studies, however, suggest that the Hilo Ridge is an extension of Kohala volcano, not Mauna Kea (Holcomb and others, 2000; Kauahikaua and others, 2000; Sherrod and others, 2007). Wolfe and others (1997) suggest that the distribution of postshield-stage

vents on Mauna Kea may be unrelated to rift-zone structure. Subsequent interpretations of gravity data (Kauahikaua and others, 2000; Flinders and others, 2013) do not appear to favor any one postulated rift-zone trend over the others.

Stearns and Macdonald (1946) and Macdonald and others (1983) suggest that Mauna Kea probably had a caldera that is now completely covered by postshield-stage rocks. If so, the postshield-stage rocks beneath Mauna Kea's summit must be thousands of feet thick. Whether or not a caldera existed in the past, positive gravity anomalies indicate the presence of dense magma-chamber cumulates and intrusive rocks centered directly beneath the summit of Mauna Kea (Kauahikaua and others, 2000; Flinders and others, 2013).

Mauna Kea, being very young, does not have extensive sedimentary deposits, although mappable deposits of sand and gravel form alluvial fans on the southern slope and smaller deposits elsewhere (fig. 44). Between about 280,000 and 9,080 years ago, multiple cycles of glaciation on Mauna Kea affected the land forms, types of eruptive products, and sediment deposition at the summit (Porter, 1979a,b). No glaciers exist today on Mauna Kea, but a small patch of permafrost was reported at the summit in 1969 (Woodcock, 1974). Also near the summit is a small perched alpine lake (Lake Waiau) that fluctuates in size with precipitation and has been rapidly shrinking in recent years (Patrick and Delparte, 2014).

Hualālai—Hualālai lies on the central west coast of Hawai'i Island (fig. 43). Hualālai's subaerial surface is completely covered by postshield-stage rocks including pāhoehoe and 'a'ā flows of mostly alkalic basalt, with minor hawaiite and trachyte as well as tephra cones (Moore and others, 1987). All of these rocks are grouped into a single formation called the Hualālai Volcanics (table 2, fig. 44). The Wa'awa'a Trachyte Member of the Hualālai Volcanics consists of the trachyte pumice cone known as Pu'u Wa'awa'a and its associated thick lava flows; although volumetrically small, this member warrants mention in this report because it has hydrologic properties that are distinct from those of the rest of the formation (see *Hydraulic Properties* section below). Occurrences of trachyte in drill holes and as xenoliths erupted from some vents, as well as gravity and aeromagnetic data, indicate that trachyte is more widespread beneath younger rocks (Moore and others, 1987).

Shield-stage lavas have been reported from submarine outcrops and from water wells, indicating that the postshield-stage rocks form a relatively thin veneer over a thick accumulation of shield-stage lava flows (Moore and others, 1987). The shield stage ended about 130,000 to 105,000 years ago (Moore and Clague, 1992); the postshield stage is ongoing.

Hualālai is surrounded on the north, east, and south by lava flows from Mauna Loa (fig. 44). Postshield-stage lavas from Hualālai are interbedded with the Mauna Loa lava flows (Moore and others, 1987). Offshore to the west, a slope failure removed a large part of Hualālai's submarine flank and created a steep submarine scarp (fig. 43); this failure probably took place during the shield stage (Moore and others, 1989; Moore and Clague, 1992).

Numerous postshield-stage vents are scattered in the higher altitudes of Hualālai (fig. 43). Northwest of the summit, they delineate a rift zone from which both postshield- and probably shield-stage lava erupted (fig. 45). East of the summit, the cones initially trend east-southeast then curve to a more southerly trend, and another group of vents extends north of the summit. Previous authors have interpreted various rift-zone trends from these vents (for example, Stearns and Macdonald, 1946; Macdonald and others, 1983; Fornari, 1987). Fiske and Jackson (1972), basing their interpretation on gravity data, suggested a rift zone that has a more north-south trend and does not align with the summit or surface vents.

No caldera is evident on Hualālai. It is possible that a caldera once existed, but was later buried by postshield-stage rocks. A gravity anomaly is present beneath Hualālai, but it does not indicate rock densities consistent with magma-chamber cumulates typically found beneath summit calderas (Flinders and others, 2013). Hualālai's gravity data are also unusual in that the highest anomaly is centered not beneath the summit, as it is in Kohala, Mauna Kea, Mauna Loa, and Kīlauea, but several miles to the southwest (Kauahikaua and others, 2000).

The youthful surface of Hualālai has been affected very little by stream erosion. Most of the volcano has no mapped streams (U.S. Geological Survey, 2012b) and there is only a small area of mapped sediments near Pu'u Wa'awa'a.

Mauna Loa—Mauna Loa is the largest of the five shield volcanoes forming Hawai'i Island (fig. 43). It has held the reputation as the largest volcano on Earth, but Sager and others (2013) recently suggest that the submarine Tamu Massif in the northwest Pacific Ocean is a larger volcano. Mauna Loa is an active volcano, having last erupted in 1984. It is currently in the shield stage. Alkalic lavas were found on two small submarine vents on the western flank of Mauna Loa, but they are not considered to be an indication that the volcano has entered the postshield stage (Wanless and others, 2006). By far, the bulk of the volcano consists of thin shield-stage lava flows of tholeiitic basalt.

The oldest subaerial outcrop on Mauna Loa is the Nīnole Basalt (table 2, fig. 44). The unit primarily consists of thin lava flows but includes at least one bed of weathered ash. The formation is exposed in the hills near Nīnole and Pāhala on the southeast-facing flank of the volcano (figs. 43 and 44). The hills are somewhat enigmatic because their strata are discordant with younger Mauna Loa strata. Deep valleys had been carved into the strata of the Nīnole Basalt before they were almost completely buried—except for the hills—by younger Mauna Loa lavas. Before the availability of radiometric dating, Stearns and Macdonald (1946) reasoned that the erosion evident in the hills near Nīnole must have required a long hiatus in eruptive activity and placed the formation of the Nīnole Basalt in the Pliocene. Radiometric dating, however, indicates that the Nīnole Basalt is only about 0.1 to 0.2 million years old (Lipman and others, 1990)—similar to ages of the oldest Mauna Loa rocks in the two deep borings of the HSDP (Sharp and others, 1996; Sharp and Renne, 2005). Some workers (for example Stearns and Clark, 1930; Macdonald and others, 1983) proposed that the Nīnole Basalt is part of an older shield volcano separate from Mauna Loa,

but this hypothesis was later challenged by the radiometric dates as well as geochemical, gravity, and submarine data (Lipman and others, 1990).

Stratigraphically above the Nīnole Basalt is the Kahuku Basalt, which consists primarily of thin shield-stage lava flows with minor tephra (table 2, fig. 44). The Kahuku Basalt is almost completely covered by younger rocks. Surficial outcrops of the formation are limited to fault scarps and sea cliffs near the southernmost point of the volcano (the outcrops are difficult to see in fig. 44). The formation is topped in almost all places by the Pāhala Ash (described above), which separates it from the overlying younger formation, the Ka‘ū Basalt. The Ka‘ū Basalt is similar lithologically to the underlying Kahuku Basalt, but is defined as the lava flows and minor tephra layers that were formed after the Pāhala Ash. The Ka‘ū Basalt covers nearly the entire surface of Mauna Loa, but it is only a thin veneer.

Except for the valleys in the hills near Nīnole and Pāhala, the current youthful surface of Mauna Loa shows little stream dissection (fig. 43). Gulches have been mapped on the southeast flank of the volcano (U.S. Geological Survey, 2012b) but their incision is shallow. Sediments include small deposits of loose gravelly alluvium in the streams, unconsolidated dunes of beach sand, and some landslide deposits.

At the summit of Mauna Loa is Moku‘āweoweo Caldera (figs. 11 and 44). The caldera is about 3.8 mi long and 1.6 mi wide and is floored by thick, massive, columnar-jointed lavas. Prominent rift zones marked by vents, pit craters, and a slight cresting of the otherwise dome-like topography, extend to the northeast and southwest (figs. 11 and 45). Stearns and Macdonald (1946) and Macdonald and others (1983) showed additional subordinate rift zones extending north and northwest from the summit caldera. Few dikes are exposed on Mauna Loa because the volcano has been little dissected by erosion, but high concentrations of dikes are presumed to exist beneath the rift zones. A gravity anomaly centered beneath the summit is consistent with the concept that a dense body of magma-chamber cumulates and dike swarms exist beneath Mauna Loa (Flinders and others, 2013).

Numerous faults have been mapped on Mauna Loa. The most prominent of these are arcuate faults and subparallel fault systems on the volcano’s flank, such as the Kealakekua Fault on the west and the Ka‘ōiki Fault System on the east (fig. 44). Another prominent fault, the Kahuku Fault at the southern tip of Mauna Loa, was originally thought to be a rift-zone fault (Stearns and Macdonald, 1946, p. 97), but later studies have categorized it with the flank faults and even proposed that it has a buried connection with the Kealakekua Fault (Lipman and others, 1990). All of these flank faults dip seaward and the seaward blocks have been displaced downward from a few feet to more than a thousand feet. Some faults have been covered by younger lavas. In some cases, younger lavas drape over fault scarps, but the fault traces are still evident in the topography. Stearns and Macdonald (1946) recognized that the flank faults are outlines of the large landslide blocks. Later studies of detailed bathymetric data connected these fault traces to submarine landslide debris (for example, Moore and others, 1989). The faults and submarine landslide debris on Mauna Loa indicate that large-scale slope failure is a common occurrence during the shield stage and that more unknown faults may lie buried beneath the surface.

Kīlauea—Kīlauea, on the southeast of Hawai‘i Island, is an active shield volcano (fig. 43). Its latest eruption has been going on almost continuously since 1983 (U.S. Geological Survey, 2013). Like Mauna Loa, Kīlauea is currently in the shield stage of volcanism and its volume consists largely of thin shield-stage tholeiitic basalt lava flows with some tephra. Scientific drilling in Kīlauea’s lower east rift zone indicated that rocks are entirely tholeiitic to a depth of at least several thousand feet (Quane and others, 2000). Rocks having compositions indicative of alkalic preshield-stage lavas have been reported from submarine outcrops, but these were recovered from about 9,000 ft below sea level (Lipman and others, 2000). Estimates of the start of tholeiitic volcanism on Kīlauea range from about 225,000 years ago (Sherrod and others, 2007) to 450,000 years ago (Quane and others, 2000).

The lowermost stratigraphic formation on Kīlauea is the Hilina Basalt (table 2). It is almost completely covered by younger rocks and only crops out in fault scarps (fig. 44), but it constitutes most of Kīlauea’s volume. The Hilina Basalt includes all of the volcanic rocks erupted from Kīlauea before the formation of the Pāhala Ash. Overlying the Hilina Basalt and Pāhala Ash are the rocks of the Puna Basalt. The Puna Basalt consists of the volcanic rock erupted after the Pāhala Ash was laid down, including the rocks formed during recent and current eruptions. The Hilina Basalt and Puna Basalt are both composed primarily of thin shield-stage ‘a‘ā and pāhoehoe lava flows with minor ash beds.

Kīlauea has an oval summit caldera that is about 3 mi long and 2 mi wide (fig. 44). A crater about 0.6 mi in diameter, Halema‘uma‘u, lies near the southwest edge of the caldera (fig. 15). Another smaller crater (about 450 ft across) formed within Halema‘uma‘u in 2008 and has been mostly active since then (Tilling and others, 2010; U.S. Geological Survey, 2013). The caldera is surrounded by faults and probably floored by thick, massive, columnar-jointed lavas. Rift zones extending to the southwest and east of the caldera are marked by volcanic activity, vents, pit craters, and faults (figs. 44 and 45). Modeling of seismic data indicates that a large magma-reservoir complex exists about 1 to 4 mi beneath the summit; the magma chamber feeds eruptions and dike intrusions at both the summit and rift zones (Ryan and others, 1981). Gravity data show anomalies centered beneath the caldera and extending beneath the east rift zone (Flinders and others, 2013), which is consistent with the seismic model. Structural support from Mauna Loa apparently has had an effect on the location of Kīlauea’s rift zones. Whereas Kīlauea’s north flank is buttressed against Mauna Loa, the south flank is unsupported; as a result, the south flank and rift zones have migrated southward in response to dike intrusion (Swanson and others, 1976; Denlinger and Morgan, 2014)

In addition to the faults associated with the caldera and rift zones, two major groups of faults occur on the south flank of Kīlauea. About 3 mi south of the summit caldera is the Koa‘e Fault System, a group of faults trending northeast with fault scarps facing north (fig. 44). The Koa‘e Fault System has been interpreted

as a tear-away zone as the south flank is pushed southward by dike intrusion into the east and southwest rifts (Duffield, 1975). Farther downslope is the Hilina Fault System, another group of large faults trending east-northeast with scarps facing southward toward the ocean. The Hilina Fault System is still active, but in many places the scarps in the system are draped by lava flows from the highly productive east rift zone. Fault planes in the Hilina system are believed to penetrate through most of the thickness of the south flank of Kīlauea, dipping steeply at the surface, and then becoming more horizontal where they approach the ocean crust at depths of 4–5 mi below sea level (Lipman and others, 1985). Conceptual models of buttressed volcanoes like Kīlauea have tied faults and large-scale slumping to a cycle of upward rift-zone growth during magma buildup, punctuated by periodic displacement of the seaward flank of the volcano (Denlinger and Morgan, 2014).

The young surface of Kīlauea shows little stream erosion or alluvial sedimentation (figs. 43 and 44). Stearns and Macdonald (1946) briefly mentioned sedimentary deposits of volcanic sand on Kīlauea, but did not show them on their 1:125,000-scale geologic map. Wolfe and Morris (1996) mapped a small deposit of alluvium and colluvium in the Hilina Fault System.

Hydraulic Properties

The hydrogeologic framework of Hawai‘i Island is not known as well as that of the other islands described in this report. The island is large, the number of wells per unit area is small, and the wells are clustered rather than uniformly spaced. Although a few exploratory and scientific wells and some geophysical studies provide subsurface information in other areas, much of the island—especially the high-altitude interior—has little or no subsurface hydrologic data. Also, because Hawai‘i Island is in a youthful stage of erosion, the relation between groundwater occurrence and geologic structures remains more obscured than it is on other islands. To some degree, these relations can be presumed by analogy with the other islands, but Hawai‘i Island has some settings—such as active volcanoes and areas where geologic structures allow fresh groundwater bodies to extend under saltwater—that have no analog on the other islands. Researchers attempting to quantitatively analyze the hydrogeology of Hawai‘i Island on an island-wide basis (for example, Mink and Lau, 1993; Whittier and others, 2004) have acknowledged that there are limitations due to a lack of data.

For these reasons, this section on the hydrogeology of Hawai‘i Island departs from the format used to discuss the hydrogeology of other islands in this report. Available water levels are shown on a map, but the number and distribution of wells is inadequate for contouring of an island-wide water-table map. The hydraulic properties of the rocks are summarized for areas where information is available, but the information is not complete enough to allow definition of hydrogeologic units. Instead, the following presentation of available information on hydraulic properties for Hawai‘i Island is organized into subsections corresponding to three principal groundwater settings: (1) dike-free lava flows, (2) dike complexes, and (3) sediments and tephra. Enigmatic groundwater occurrences that do not fit in one of these principal settings will be discussed later, in the section *Conceptual Models of Groundwater Occurrence and Movement*.

Dike-Free Lava Flows

Formations consisting almost entirely of shield-stage lava flows, including those of the Nīnole, Kahuku, and Ka‘ū Basalts of Mauna Loa, and the Hilina and Puna Basalts of Kīlauea (fig. 44), were described by Stearns and Macdonald (1946) as highly or extremely permeable. The predominantly shield-stage Pololū Volcanics of Kohala volcano was also described as having high permeability, even though the upper part of the formation has postshield-stage rocks. Similarly, most of the shield- and postshield-stage lava flows of the Hualālai Volcanics (with the exception of the Wa‘awa‘a Trachyte Member) were described as having high permeability. Descriptions varied for the permeability of formations consisting entirely of postshield-stage lava flows. The Hāmākua Volcanics of Mauna Kea, whose upper part consists of postshield-stage rocks, was described as being moderately to highly permeable. Postshield-stage lava flows of the Hāwī Volcanics on Kohala were described as having high-permeability clinker zones, but low-permeability ‘a‘ā cores. Thick trachyte lava flows and domes constituting the Wa‘awa‘a Trachyte Member of Hualālai and parts of the postshield Hāwī Volcanics on Kohala and the Laupāhoehoe Volcanics on Mauna Kea, were described as having low to moderate permeability.

Groundwater levels are consistent with a high-permeability, dike-free coastal aquifer. Most wells along the coast and some wells as far as 6 mi inland also have water levels that are less than 25 ft above sea level (fig. 46). Mauna Loa and Kīlauea are in the shield stage, thus wells in the flanks of these volcanoes are clearly in shield-stage lava flows. On Kohala, Hualālai, and Mauna Kea, postshield-stage lavas are at the surface, but production wells may have been drilled past the postshield veneer and into the more productive shield-stage or transitional lava flows. Definitive determinations of the stratigraphic units penetrated by wells are rare.

Estimates of hydraulic conductivity for dike-free lavas are consistent with the descriptions of Stearns and Macdonald (1946). Takasaki (1993), using estimated flow rates and the slope of the water table, estimated K_h to be 2,885–6,670 ft/d for dike-free lava flows in Kīlauea. Underwood and others (1995) estimated a K_h of 610–6,400 ft/d, with a median of 1,100 ft/d and arithmetic average of 2,300 ft/d, from aquifer tests of five wells in the dike-free lavas of Kohala volcano. Oki (1999) cited previous studies that estimated K_h from ocean tidal signals in wells and estimations of groundwater flow rates and head gradient; these estimates ranged from 500 to 34,000 ft/d for the dike-free lava-flow aquifers on the west coast of Hawai‘i Island. The specific-capacity/hydraulic-conductivity regression analysis of Rotzoll and El-Kadi (2008) yielded a geometric mean of 1,102 ft/d and the standard deviation spanned a range of 269 to 4,502 ft/d for K_h in dike-free lavas on Hawai‘i Island.

Several studies have yielded estimates of hydraulic properties by adjusting model input values to obtain a match between measured and simulated water levels or

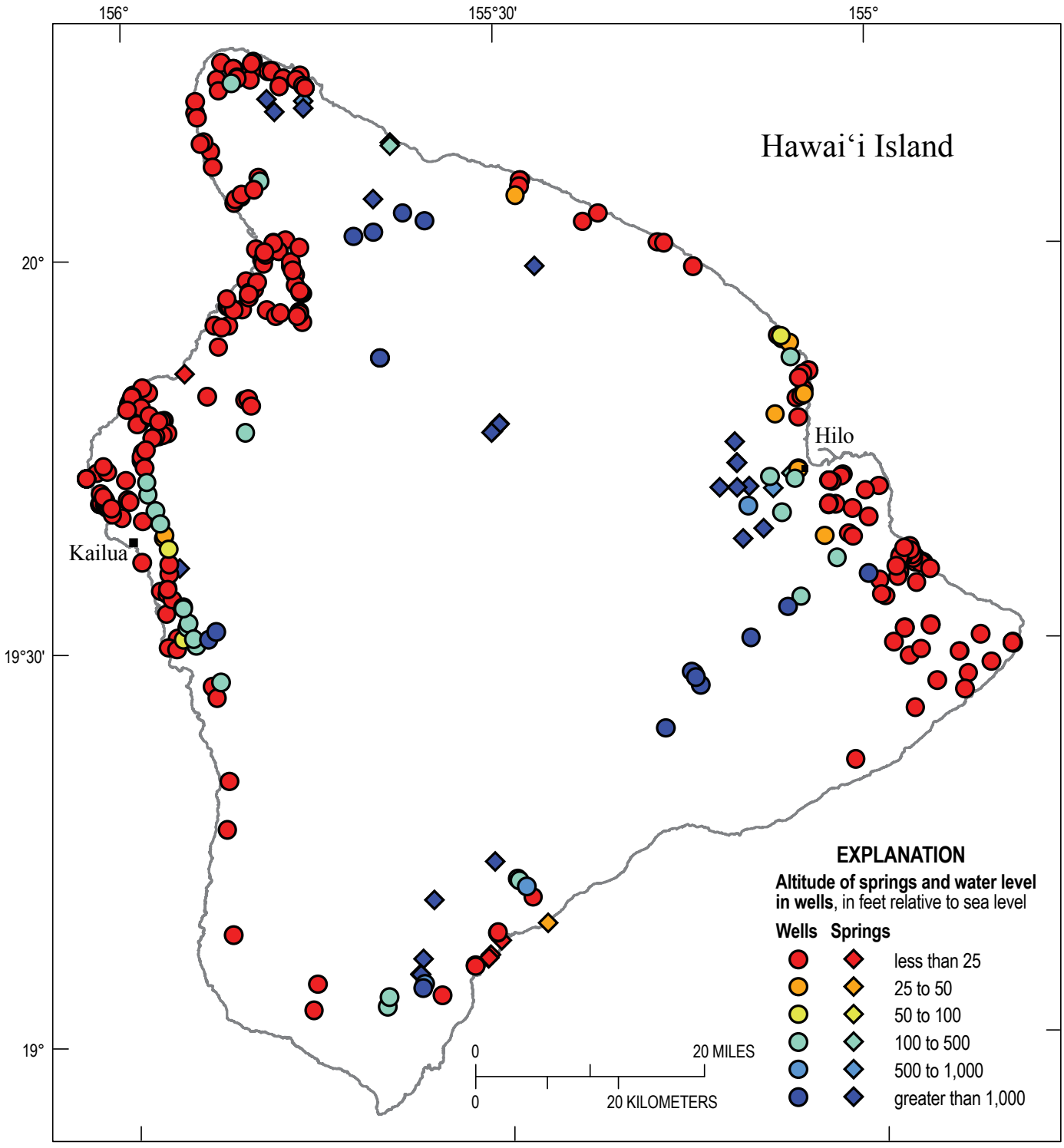

Figure 46. Map of initial groundwater levels for selected wells on Hawai‘i Island.

tidal efficiencies in numerical models. Gingerich (1995) estimated K_h values of 3,000 to 20,000 ft/d for dike-free lavas on Kīlauea. Using recharge estimated by Shade (1995), Underwood and others (1995) determined that K_h values between 650 and 5,000 ft/d for dike-free lavas and ocean-floor leakance values of 0.01 to 0.1 ft/d/ft resulted in the best match between measured and model-simulated water levels in the northeast flank of Kohala volcano. Oki (2002) later revised recharge estimates and the numerical model for the same study area of Kohala and used K_h values of 300 to 3,000 ft/d for dike-free lavas, and ocean-floor leakance values of 0.005 to 0.1 ft/d/ft. Oki (1999) and Oki and others (1999b) used a value of 7,500 ft/d and an ocean-floor leakance of 0.5 ft/d/ft in a numerical model of western Hawai‘i Island.

For dike-free lavas in three separate numerical models of different sectors of Hawai‘i Island, Whittier and others (2004) used K_h values of 39 to 656 ft/d for Kohala volcano, 918 to 3,116 ft/d for Mauna Kea, 2,460 ft/d for Hualālai, 2,460 to 8,200 ft/d for Mauna Loa, and 3,050 to 6,560 ft/d for Kīlauea. Izuka (2011) used values of 0.055 for specific yield, 8×10^{-6} 1/ft for specific storage, and 0.1 for porosity in a numerical model to match observed data on time needed for an infiltration pulse to travel from the surface to the water table in dike-free lavas of Hualālai.

Dike Complexes

Stearns and Macdonald (1946) described dikes and other intrusive bodies as having very low permeability and noted that high-level groundwater occurred where dikes intruded permeable lava flows. The association between dike complexes and high-level groundwater is evident in the deep valleys on the northeastern slope of Kohala volcano, where erosion into the rift zone has resulted in springs fed by dike-impounded groundwater. One tunnel at the head of Honokāne Nui Valley (fig. 43) reportedly penetrates several dikes and develops groundwater from the dike zone. Stearns and Macdonald (1946) postulated that dike-impounded groundwater occurs in the rift zones of other shield volcanoes on Hawai‘i Island, but concluded that the resource was too deep to be economically developed. Since their report, no new tunnels were constructed that definitively develop dike-impounded water on Hawai‘i Island. A few wells and springs inland from the coast have water levels that are more than 1,000 ft above sea level and may represent groundwater impounded by dikes. A scientific well drilled more than 4,000 ft deep near the summit of Kīlauea in the 1970s (NSF borehole in fig. 44) had an initial water level more than about 2,000 ft above sea level; subsequent geophysical data indicated that the water level in this well is part of a high water table that extends into the rift zones, which is consistent with anticipated dike-impoundment of groundwater (Kauahikaua, 1993; Ingebritsen and Scholl, 1993; Takasaki, 1993). The high water levels do not extend the entire length of the rift zones, however. Water levels in the Kīlauea east rift zone where it meets the coast are low, similar to those in the adjacent dike-free lavas. The contrasting water levels indicate that permeability of the rift zone is lower near the summit and higher near the coast (Imada, 1984). Gingerich (1995) noted that tidal efficiencies in wells indicate a similar permeability contrast between inland and coastal parts of the rift zone. The change in water levels and permeability has been attributed to a seaward decrease in the number of dikes shallow enough to affect fresh groundwater flow (Imada, 1984; Takasaki, 1993).

Characterizing the hydraulic properties of dike complexes on Hawai‘i Island is difficult because data are scant and uncertainty about the location of rift zones of some volcanoes makes it difficult to identify definitively which wells are in dike complexes. Also, because the numbers of dikes and degree of thermal alteration vary spatially within an area identified as a rift zone, hydraulic properties vary widely (Ingebritsen and Scholl, 1993). Further complicating the characterization of hydraulic properties is geothermal heat, which can affect viscosity-dependent indicators of permeability, such as hydraulic conductivity (Imada, 1984).

Takasaki (1993) estimated bulk K_h to be less than 33 ft/d in Kīlauea rift zones near the summit, where dikes impede groundwater flow, but as high as 7,100 ft/d in the coastal part of the rift zone where dikes did not affect fresh groundwater movement. In a review of literature on the hydrology of Kīlauea, Ingebritsen and Scholl (1993) suggested that a greater number of dike intrusions and greater alteration at depths of several hundred feet in the Kīlauea rift zones cause permeabilities to be many orders of magnitude lower than they are at the surface. To match low tidal efficiencies measured in wells in Kīlauea, Gingerich (1995) found that model-simulated K_h values in the rift zone must be at least two orders of magnitude lower than that of the dike-free areas. Oki (1999) and Oki and others (1999b) used K_h values of 0.1 ft/d for the dike complex and 0.5 to 10 ft/d for the marginal dike zone of Hualālai to match groundwater levels in numerical models of west Hawai‘i Island. To match water levels in their numerical models, Whittier and others (2004) used K_h values of 0.7 to 1.6 ft/d for the Kohala dike complex, 0.03 to 3.3 ft/d for the Mauna Kea dike complex, 0.16 ft/d to 0.50 ft/d for the dike complexes of Hualālai and Mauna Loa, and 0.16 ft/d to 7,100 ft/d for the Kīlauea dike complex (on the basis of Takasaki, 1993). For the marginal dike complexes of Mauna Kea and Hualālai, Whittier and others (2004) used 196–328 ft/d and 1.1–49 ft/d, respectively.

Sediments and Tephra

Although the origins of tephra and sediments are different, their hydraulic properties are related to grain size and weathering. Also, tephra and sedimentary deposits in Hawai‘i Island are volumetrically minor compared to the great accumulations of lava flows. Accumulations of coarse tephra such as cinder are highly permeable, but most contain little or no water (Stearns and Macdonald, 1946). Layers of weathered fine tephra such as ash can, however, affect groundwater resources because they have low permeability and form widespread perching units within otherwise permeable lava-flow aquifers. Stearns and Macdonald (1946) attributed some of the perched water bodies on the windward sides of both Kohala volcano and Mauna Kea to low-permeability ash layers. By the time they wrote Bulletin 9, numerous water tunnels had been constructed to exploit these perched groundwater

bodies. There are no measured or estimated quantitative values for hydraulic properties of ash on Hawai‘i Island.

Stearns and Macdonald (1946) described sedimentary rocks of Hawai‘i Island as having low to moderate permeability, regardless of whether they are consolidated or unconsolidated. Most sediments on Hawai‘i Island occur as small deposits of poorly sorted gravel, sand, and silt deposited by fluvial, glacial, and landslide processes. Some perched groundwater bodies have been attributed to buried soil or sediments, but there is little quantitative information on hydraulic properties for these thin layers specifically for Hawai‘i Island. The largest sedimentary deposits are in the valleys on the northeast flank of Kohala and those forming the alluvial fans on Mauna Kea (fig. 44). Whittier and others (2004) used a K_h value of 65 ft/d for the valley-filling sediments of the Kohala volcano in their numerical model.

Because of its youthful geology, Hawai‘i Island does not have extensive sedimentary deposits analogous to those forming the thick coastal-plain deposits of O‘ahu and Kaua‘i or the isthmus deposits of Maui. Marine sedimentary deposits such as reefs exist, but their hydraulic properties are usually lumped together with K_h in the offshore-leakance parameter in numerical models (for example, Oki, 1999).

Fresh Groundwater-Flow Budget

A fresh groundwater-flow budget is an accounting of all of the freshwater entering, leaving, and stored in the aquifer. Groundwater budgets typically have three components: (1) inflows, (2) outflows, and (3) change in storage (fig. 3). Under steady-state conditions inflows equal outflows, and there is no change in storage. Under transient-state conditions, outflows equal the sum of inflows minus change in storage (see discussion in the *Introduction*).

Considering an island as a unit that is isolated from other islands by seawater, freshwater inflow comes almost solely through the surface from groundwater recharge. The source of most of the water for recharge is precipitation, but some water comes from artificial sources such as irrigation. Water-system leaks and waste-water injection are additional, but small, sources of inflow. Outflows include withdrawals from wells and natural groundwater discharge to springs, streams, wetlands, and submarine groundwater discharge (in some areas, phreatophytes may also remove water from the aquifer [see, for example, Shade and Nichols, 1996]). In this study, inflows to the groundwater budget are quantified by an analysis of groundwater recharge; outflows from wells are quantified in an analysis of water use by humans. If the groundwater flow in an island is assumed to be in steady state, then natural groundwater discharge can be computed from the difference between recharge and withdrawals from wells (eq. 3).

Groundwater Recharge

Groundwater recharge is water that flows into the aquifer from the ground surface or near it. Most of this water comes from precipitation (mostly rainfall but also fog interception), but in some places irrigation can contribute substantially to recharge. Other sources of water entering from near the surface include septic-system leaching and leaks from water systems, sewers, and cesspools.

In this study, the effects of human activity and climate variations on groundwater recharge were studied by calculating recharge for various scenarios representing historical conditions. Recharge distributions were calculated for recent and predevelopment scenarios. For Kaua‘i, O‘ahu, and Maui, the recent scenario was calculated using the groundwater recharge model described in appendix 1, climate conditions for the 1978–2007 period from Frazier and others (2016) and Giambelluca and others (2013, 2014), and anthropogenic factors (such as land cover and irrigation) from 2010. This scenario represents what would happen if the precipitation and evapotranspiration (ET) patterns of the last 30 years continued to persist while land use and agriculture remained at today’s condition. It includes effects from multi-year climatic cycles in precipitation, such as those associated with the El-Niño-Southern Oscillation (ENSO), that are likely to recur. Results from Engott (2011) were used for the recent scenario for Hawai‘i Island. Methods and data used by Engott (2011) are mostly similar to those in this study. The calculated recharge results of Engott (2011) are considered comparable to the results of this study. A synopsis of the differences and their relevance to comparing the results among the islands is discussed in appendix 1. Geospatial datasets of recent recharge on each island can be accessed online using their digital object identifiers (DOIs): doi:10.5066/F7571931 (Kaua‘i), doi:10.5066/F7XP72ZX (O‘ahu), doi:10.5066/F7K64H14 (Maui), and doi:10.5066/F7668B89 (Hawai‘i Island).

Predevelopment recharge was calculated for Kaua‘i, O‘ahu, and Maui using the methods in appendix 1. The predevelopment scenario uses the same climate input as the recent scenario, but uses land-cover spatial data representative of 1870 (Samuel Gon, III, The Nature Conservancy, and Jim Jacobi, USGS Pacific Islands Ecosystems Research Center, written commun., 2014), before the first modern well was drilled in 1879. Although large-scale groundwater withdrawals had not yet occurred in 1870, humans had already affected land cover substantially—particularly as a result of agriculture and deforestation. These changes would have altered plant transpiration rates, and in turn affected groundwater recharge. Predevelopment recharge for Hawai‘i Island was also computed using a map of 1870 land cover, but using an earlier version of the recharge model, as described in Engott (2011). Soil properties also can affect recharge (appendix 1). Because soil data for 1870 were not available for this study, the 2006 soil-distribution maps (U.S. Department of Agriculture, 2006a,b,c) were used in the predevelopment scenario. A few areas shown as artificial fill on the 2006 soil maps may not have been present in 1870, but these areas are small and their effects are negligible. Geospatial datasets of predevelopment recharge on each island can be accessed online using their DOI numbers: doi:10.5066/F71G0JBV (Kaua‘i), doi:10.5066/F7SX6B9H (O‘ahu), doi:10.5066/F7DR2SKT (Maui), and doi:10.5066/F7XP730S (Hawai‘i Island).

Supplemental recharge computations that may be useful for future studies were also computed in this study. These computations include annual recharge and irrigation demand

for Kauaʻi, Oʻahu, and Maui for the period 2001–2010. The results of these computations are not discussed in the following sections, but are provided in appendix 2. Geospatial datasets of 2001–2010 recharge on each island can be accessed online using their DOI numbers: doi:10.5066/F79021VS (Kauaʻi), doi:10.5066/F72F7KH4 (Oʻahu), and doi:10.5066/F7P8490T (Maui).

Recent

Estimated volumetric recharge rates, averaged for each island from the recent scenarios, were 875 Mgal/d for Kauaʻi, 660 Mgal/d for Oʻahu, 1,308 Mgal/d for Maui, and 6,595 Mgal/d for Hawaiʻi Island (table 3). As expected, the largest islands—Maui and Hawaiʻi—have the greatest volumetric recharge rate because they have the largest amount of surface area, but Kauaʻi has greater recharge than Oʻahu, even though Kauaʻi is smaller. Island-wide recharge expressed as depth (inches per year) allows comparison irrespective of land area. In this case, recharge is greatest on Maui (37.7 in/yr), followed by Hawaiʻi Island (34.4 in/yr), Kauaʻi (33.2 in/yr), and Oʻahu (23.3 in/yr).

The spatial distribution of recent recharge (figs. 47–50) generally mimics the rainfall-distribution pattern (fig. 7). Recharge is high on windward slopes and mountain tops below the top of the trade-wind inversion. The mountains of Kauaʻi, the Koʻolau Range (Oʻahu), West Maui, and Kohala (Hawaiʻi Island) are all below the top of the trade-wind inversion, thus the areas of high recharge—as much as several hundred inches per year—on these mountains are at or near the summits. The summit of the Waiʻanae Range also is an area of locally high recharge, although the recharge is not as high or areally extensive as that on the Koʻolau Range. The peaks of Haleakalā on Maui, and Mauna Kea and Mauna Loa on Hawaiʻi Island, rise into the arid subalpine climates above the top of the trade-wind inversion; therefore, the areas with high recharge (hundreds of inches of recharge per year) are on the windward slopes at lower altitudes. The windward slopes of Mauna Kea, Mauna Loa, and Kīlauea on Hawaiʻi Island form a zone in which rainfall and recharge are particularly high. The lower middle altitudes of leeward Mauna Loa and southwestern Hualālai have somewhat elevated recharge because of the slightly higher orographic rainfall generated by diurnal sea breezes (Giambelluca and others, 1986, 2013).

Recharge is generally lower on the leeward sides of mountains and islands, particularly on the low-lying coastal areas, which is consistent with the rainfall in these areas (figs. 47–50). The distribution pattern of recent recharge departs from that of rainfall where other sources of water contribute to recharge. Local patches of higher recharge in areas of otherwise low recharge result from irrigation (for example, golf courses, residential developments, and agricultural land). Areas covered by standing water that continuously seeps into the aquifer, such as reservoirs and taro fields, also appear as patches of high recharge in contrast to surrounding areas of low recharge.

Table 3. Mean annual components determined in the analysis of groundwater recharge.

[Septic, septic-system leachate; Total ET, total evapotranspiration, which is actual ET plus canopy evaporation; Net precipitation, rainfall plus fog for most areas, rainfall plus fog minus canopy interception for forest areas; Direct recharge, leakage from water mains and cesspools and seepage beneath land covers that are typically saturated, including taro, water bodies, and reservoirs; Predevelopment scenario used 1978–2007 rainfall and 1870 land cover; recent scenario used 1978–2007 rainfall and 2010 land cover. Componenets may not balance because of rounding and direct recharge. The land areas of Oʻahu and Hawaiʻi Island are slightly different in the predevelopment and recent senarios, resulting in different annual rainfall rates]

Island	Scenario	Rainfall	Fog	Irrigation	Septic	Direct recharge	Runoff	Canopy evaporation	Actual ET	Total ET	Net precipitation	Storm-drain capture	Recharge
						Million gallons per day							
Kauaʻi	Predevelopment	2,220.97	107.42	69.78	0.00	0.00	556.47	276.33	697.78	974.13	2,052.06	0.00	870.56
	Recent	2,220.97	105.68	47.51	1.94	55.53	555.76	277.52	725.64	1,003.15	2,049.13	3.07	875.28
Oʻahu[1]	Predevelopment	1,820.09	11.68	97.11	0.00	0.00	265.68	269.81	727.86	997.68	1,561.92	0.00	675.44
	Recent	1,821.35	10.63	114.75	1.32	20.71	264.77	237.90	777.55	1,015.44	1,594.07	39.96	660.21
Maui	Predevelopment	2,806.02	250.85	28.78	0.00	0.00	854.60	297.90	656.40	954.29	2,758.98	0.00	1,279.37
	Recent	2,806.02	179.93	288.85	3.75	54.58	854.23	232.45	939.59	1,172.01	2,753.53	3.60	1,307.77
Hawaiʻi	Predevelopment	13,376.04	1,011.04	15.33	0.00	0.00	1,684.93	3,009.98	4,398.53	7,408.51	11,376.98	0.00	5,291.33
	Recent	13,378.71	1,022.94	43.90	0.00	12.94	1,685.96	1,874.21	4,301.27	6,175.48	12,527.40	0.00	6,594.50
						Inches per year							
Kauaʻi	Predevelopment	84.20	4.07	2.65	0.00	0.00	21.10	10.48	26.45	36.93	77.80	0.00	33.00
	Recent	84.20	4.01	1.80	0.07	2.11	21.07	10.52	27.51	38.03	77.69	0.12	33.18
Oʻahu[1]	Predevelopment	64.28	0.41	3.43	0.00	0.00	9.38	9.53	25.71	35.24	55.16	0.00	23.85
	Recent	64.20	0.37	4.04	0.05	0.73	9.33	8.39	27.41	35.79	56.19	1.41	23.27
Maui	Predevelopment	80.96	7.24	0.83	0.00	0.00	24.66	8.60	18.94	27.53	79.60	0.00	36.91
	Recent	80.96	5.19	8.33	0.11	1.57	24.65	6.71	27.11	33.82	79.45	0.10	37.73
Hawaiʻi	Predevelopment	69.77	5.27	0.08	0.00	0.00	8.79	15.70	22.94	38.64	59.34	0.00	27.60
	Recent	69.78	5.34	0.23	0.00	0.07	8.79	9.78	22.43	32.21	65.34	0.00	34.40

[1]Excludes Sand Island and Ford Island.

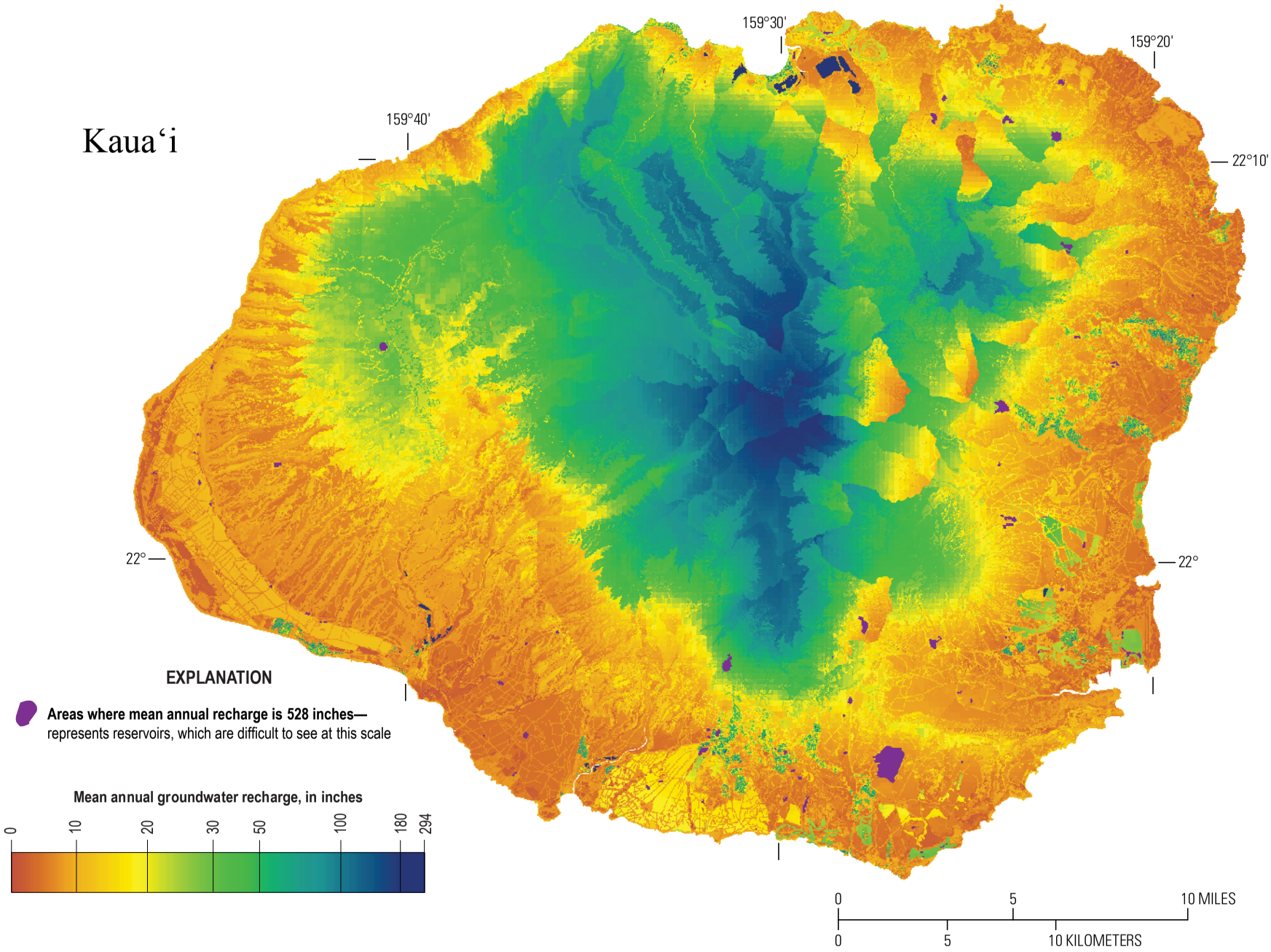

Figure 47. Map of estimated mean annual recharge for recent conditions (2010 land cover, 1978–2007 rainfall) on Kaua'i, Hawai'i.

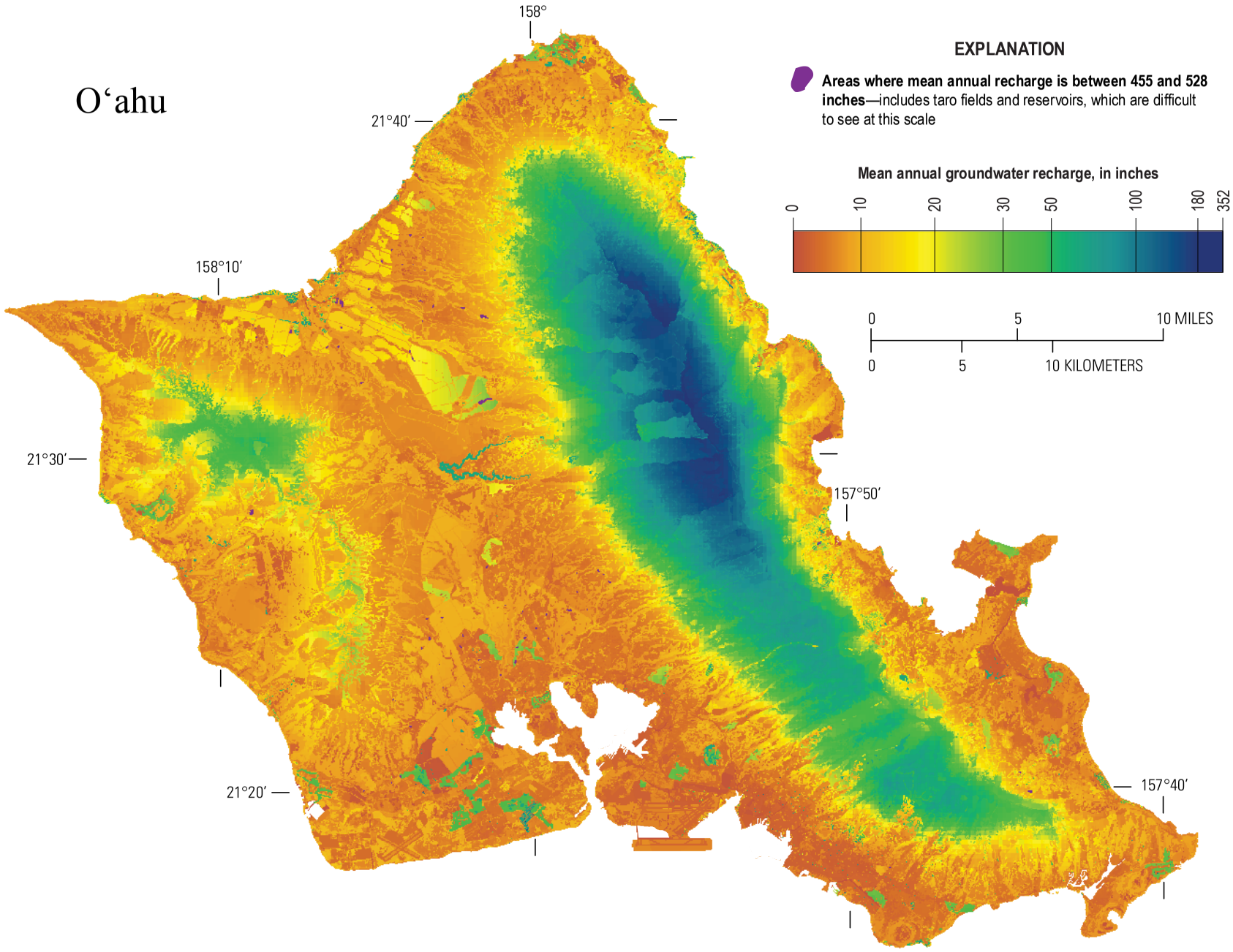

Figure 48. Map of estimated mean annual recharge for recent conditions (2010 land cover, 1978–2007 rainfall) on O‘ahu, Hawai‘i.

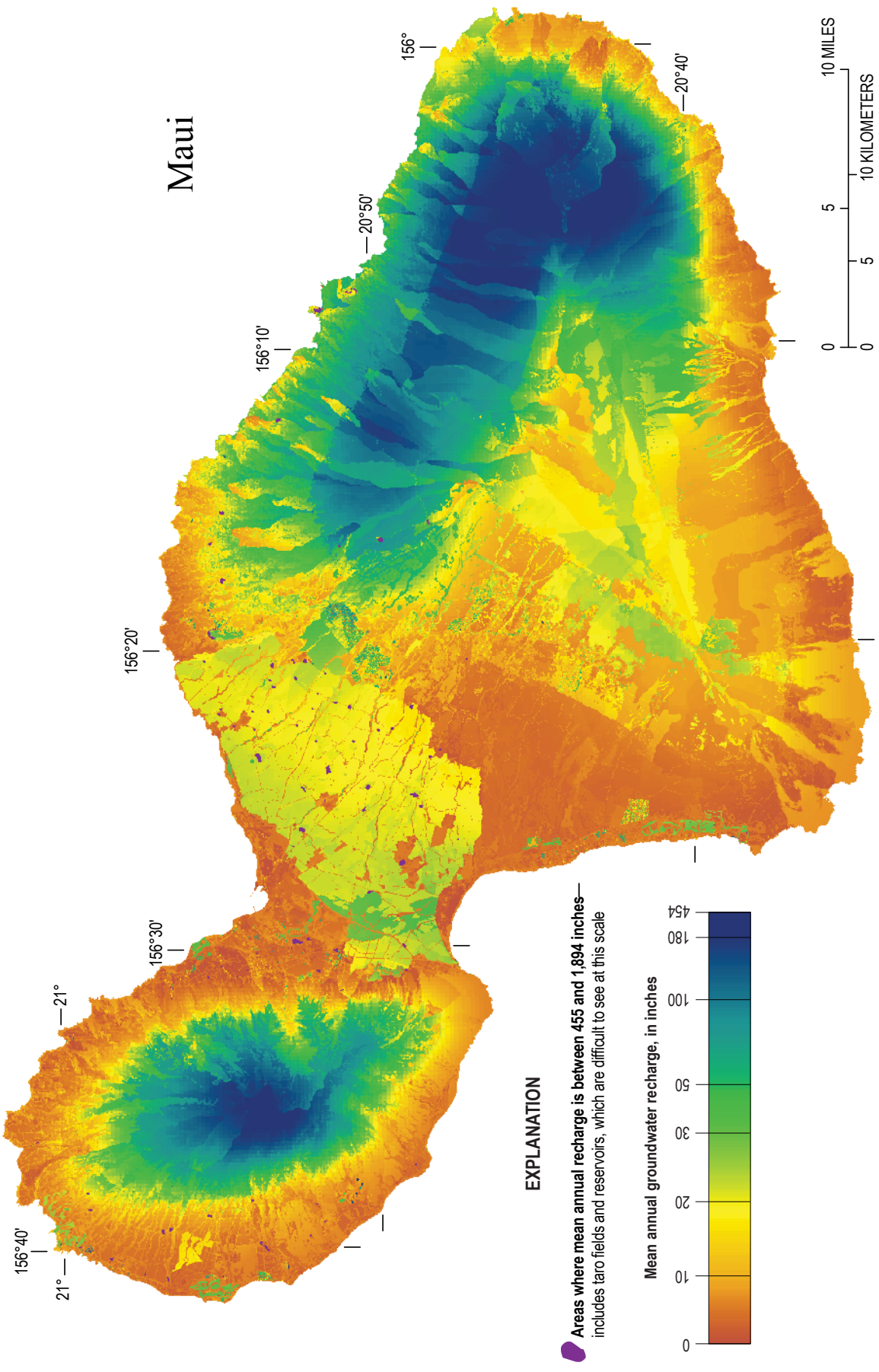

Figure 49. Map of estimated mean annual recharge for recent conditions (2010 land cover, 1978–2007 rainfall) on Maui, Hawai'i.

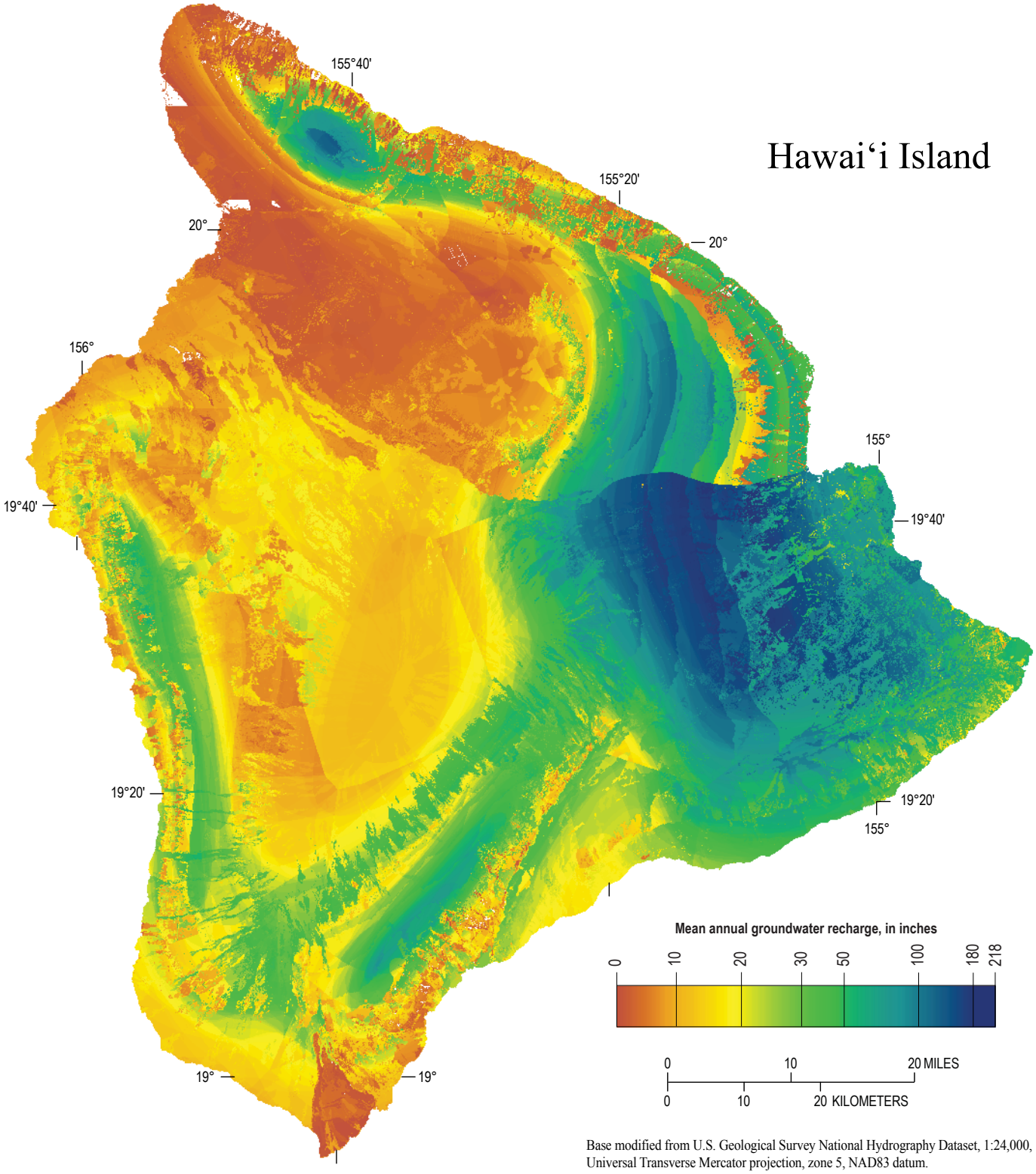

Base modified from U.S. Geological Survey National Hydrography Dataset, 1:24,000, Universal Transverse Mercator projection, zone 5, NAD83 datum.

Figure 50. Map of estimated mean annual recharge for recent conditions (2008 land cover, 1916–1983 rainfall) on Hawai'i Island. Modified from Engott (2011).

Predevelopment

For predevelopment conditions, estimated mean annual groundwater recharge was 871 Mgal/d for Kaua‘i, 675 Mgal/d for O‘ahu, 1,279 Mgal/d for Maui, and 5,291 Mgal/d for Hawai‘i Island (table 3). On a depth basis, Maui (36.9 in/yr) had the highest rate of recharge, followed by Kaua‘i (33.0 in/yr), Hawai‘i Island (27.6 in/yr), and O‘ahu (23.9 in/yr). On O‘ahu, Kaua‘i, and Maui, the difference between estimated recharge for predevelopment and recent conditions is only a few percent. In contrast, estimated recharge for predevelopment on Hawai‘i Island is 19.8 percent lower than estimated recharge for recent conditions; much of this difference is attributable to canopy evaporation, which occurs in forested land covers. The area of forested land cover on Hawai‘i Island is 41 percent greater and canopy evaporation was 61 percent greater for predevelopment (1870) than for recent (2008) conditions. However, the recharge model used in this study does not directly account for the differences in runoff conditions that may exist between forested and nonforested areas. This limitation to the model is discussed further in the *Study Limitations* section.

The spatial distribution of predevelopment recharge is similar to that of recent recharge, except that the areas of relatively higher recharge owing to modern human activities—large-scale agriculture, golf courses, and areas subject to leakage from water mains and cesspools—are absent in the predevelopment distribution (figures 51–54). Because of this absence, high recharge rates in taro-growing areas are more readily apparent in the predevelopment distribution.

Water Use

Water use by humans includes both groundwater and surface-water withdrawals. Fresh groundwater withdrawals are an outflow component of the fresh groundwater budget (fig. 3). Quantification of historical well withdrawals and examination of trends is an important part of assessing groundwater availability. Groundwater withdrawals include freshwater, brackish water, and saltwater, but because this study concerns only freshwater resources, saltwater and brackish water are excluded from consideration.

Freshwater withdrawals from surface-water sources are relevant to the groundwater budget when the water is used for irrigation. Irrigating with stream water that would normally run off to the ocean adds to the amount of water contributing to groundwater recharge. Contributions to groundwater from irrigation using surface water is accounted for in the recharge estimates (see *Groundwater Recharg*e section, above), but it is helpful to discuss the historical trends in surface-water use together with trends in groundwater use to show how the two sources have been used to meet the freshwater needs of humans in Hawai‘i.

Water use in Hawai‘i historically has been dominated by irrigation, beginning with irrigation for subsistence farming by Polynesians (Takeguchi and others, 1999) and ultimately developing into the extensive irrigation networks used by large, single-crop plantations beginning in the mid-1800s (Wilcox, 1996). By 1920, an average of 800 Mgal/d of surface water and 400 Mgal/d of groundwater was being withdrawn by the sugarcane industry in Hawai‘i (Wilcox, 1996). The plantations used water for irrigation, power production, and processing. The plantations also supported staff to operate and maintain irrigation systems and record diversion and withdrawal amounts. The closure of many large plantations across the state in the late 20th century (see *Study Area* section, above) affected water use, water-use reporting, and the operation and maintenance of irrigation systems (State of Hawai‘i, 2012b).

The Hawaii Water Authority (1959) completed a comprehensive compilation and evaluation of water resources in the Territory of Hawai‘i to inform legislators and the general public of the status of water resources. The report summarized water use in 1957 and described the occurrence of groundwater and surface-water resources, changing conditions, adequacy of water resources, water rights and water law, and conservation and management of water resources. The gross water use for Hawai‘i in 1957 was about 1.92 billion gallons per day of which about 60 percent came from surface-water supplies and 40 percent from groundwater sources. About 74 percent of the total water used in 1957 was for irrigation, 19 percent for industrial purposes, 5 percent for municipal supply, and 1 percent for other purposes.

In 1987, the State Water Code (State of Hawai‘i, 2008a) was enacted. As part of the code, water users were required to file a declaration of water use with the Hawai‘i State Commission on Water Resource Management (CWRM), the state agency legally mandated to collect and maintain water-use records. By 1990, about 1,550 users of wells, streams, and water systems were identified. Most (1,300) were classified as small users, which included “domestic supplies, water systems involving small water capacities (pump motors less than five horsepower, or gravity-fed pipes less than two inches in diameter), and agricultural irrigation of fewer than three acres,” (State of Hawai‘i, 2008b). The remaining 250 declarants had medium-to-large uses. In 1992, CWRM adopted a policy that exempted “individual water systems where the quantity of use averaged over a one-year period does not exceed 50,000 gallons per month” from the requirements for measuring and reporting monthly water use unless a specific need was determined (State of Hawai‘i, 2008b).

The USGS National Water-Use Information Program (U.S. Geological Survey, 2014) has compiled and published national and state water-use data every five years since 1950. These compilations are a not an average of water-use data over a 5-year period, but a snapshot of water use every fifth year. Data in the USGS National Water-Use Information Program database were used in this study, but the data were supplemented as described below.

Water-Use Estimates

The water-use discussion in this report spans the period 1980–2010, to approximate the recent period (1978–2007) in the recharge analysis (see *Groundwater Recharge* section, above). The fifth-year estimates for 1980–2010 in the USGS’s National Water-Use Information Program show water-use trends over a 30-year period that included substantial changes in water use related to agriculture, particularly the closure of sugarcane plantations. Although the average of estimates made every fifth year is not precisely equivalent to an average of all years between 1980 and 2010, it is probably close and in the absence of annual data, is used in this report to indicate the 30-year average.

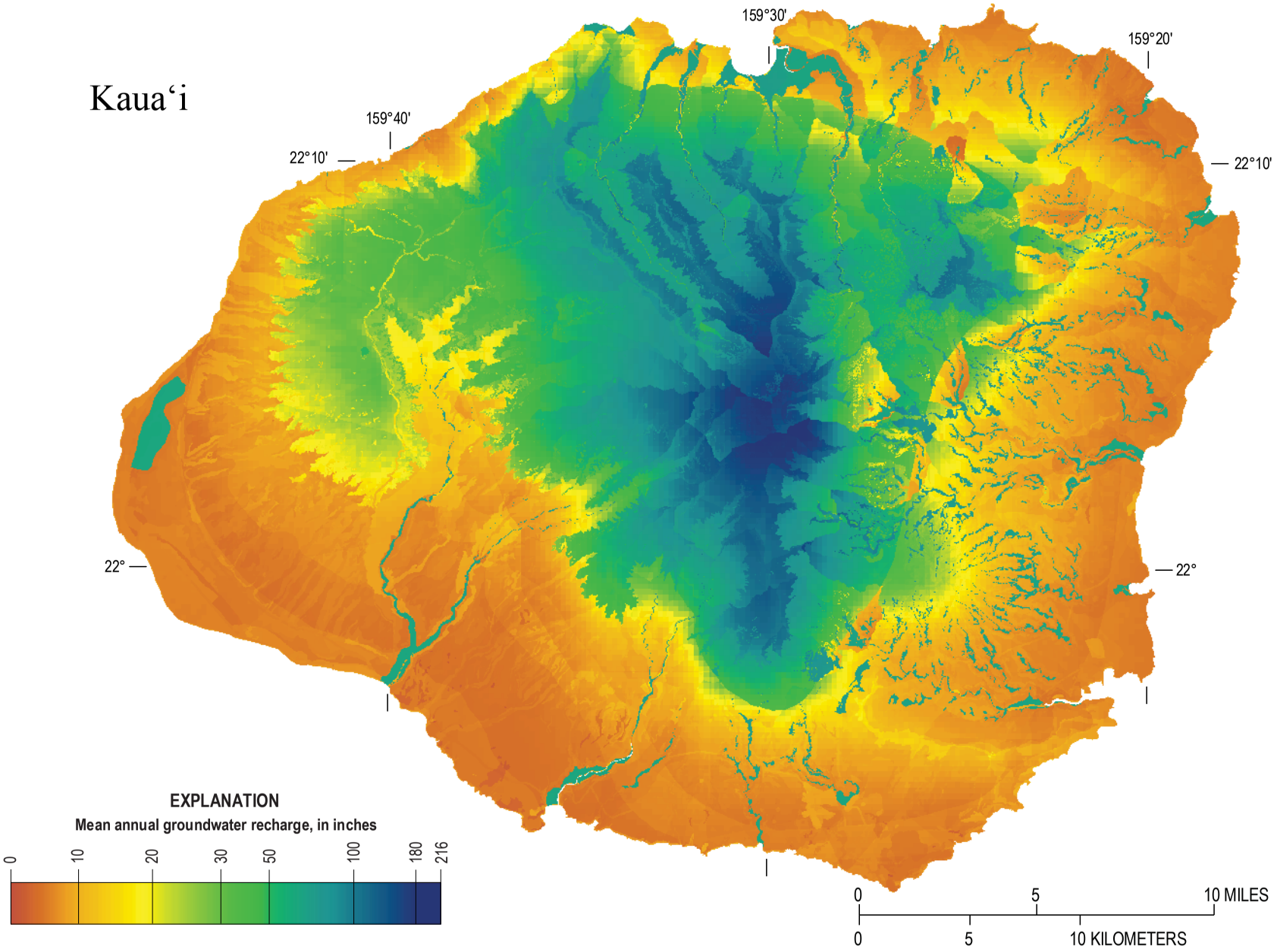

Figure 51. Map of estimated mean annual recharge for predevelopment conditions (1870 land cover, 1978–2007 rainfall) on Kaua‘i, Hawai‘i.

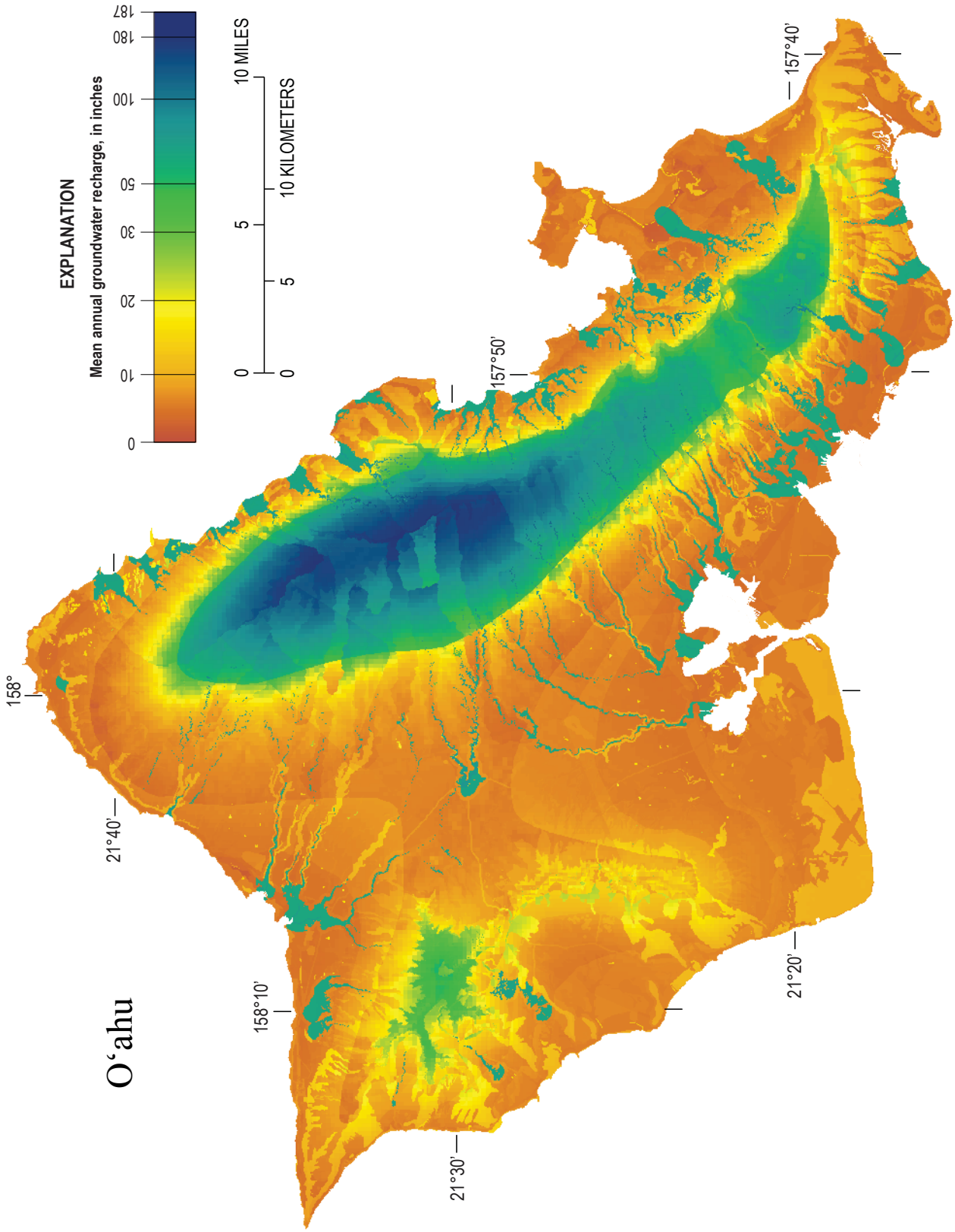

Figure 52. Map of estimated mean annual recharge for predevelopment conditions (1870 land cover, 1978–2007 rainfall) on O‘ahu, Hawai‘i.

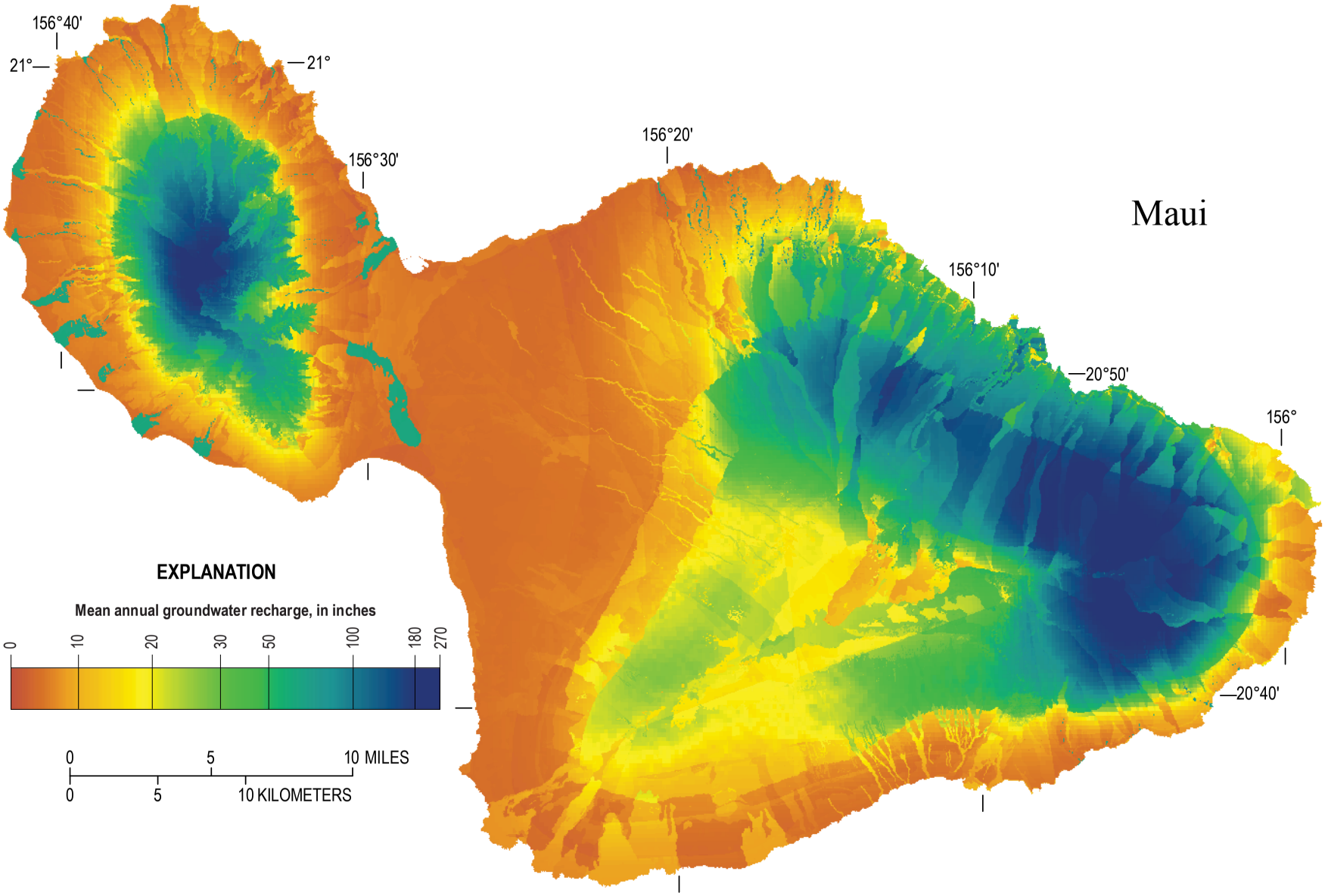

Figure 53. Map of estimated mean annual recharge for predevelopment conditions (1870 land cover, 1978–2007 rainfall) on Maui, Hawai'i.

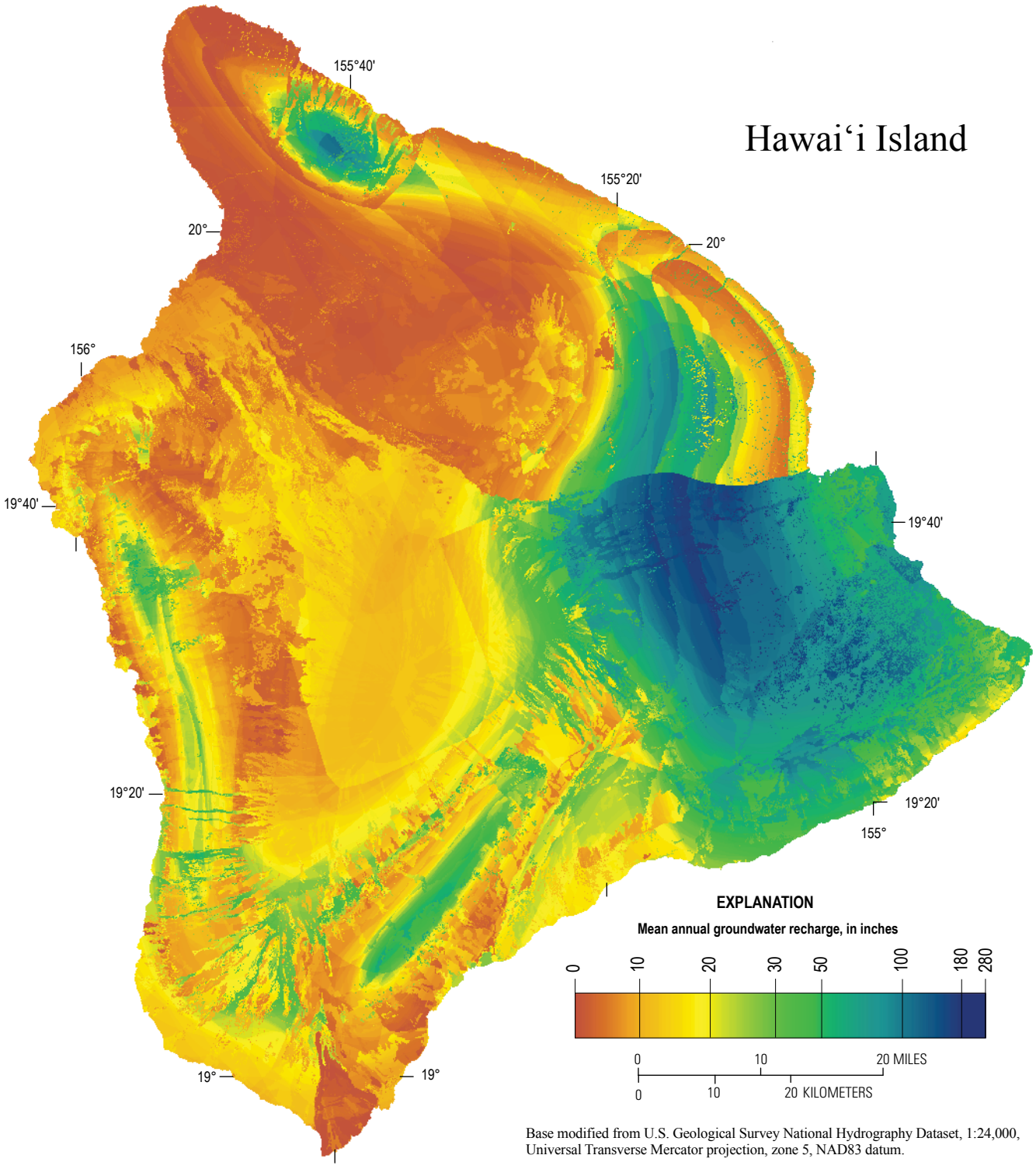

Figure 54. Map of estimated mean annual recharge for predevelopment conditions (1870 land cover, 1916–1983 rainfall) on Hawai‘i Island.

After the enactment of the State Water Code in 1987, CWRM's database of user-reported withdrawals has been the source of much of the water-use data for the USGS National Water-Use Information Program. The available data are not complete, however, because of underreporting or lack of reporting, especially for surface water. Water-use records probably were more complete prior to 2000 because the large sugar plantations had the resources to measure their withdrawals. For the purposes of this report, withdrawals prior to 2000 in the USGS database were assumed to be accurate, although anomalous values are noted in the discussions below.

For the period after 2000, the USGS worked closely with CWRM to ensure that the most current data were analyzed for this study. Withdrawal values for wells with data, along with well-construction information, were compiled from CWRM's database. Excluded from analysis were (1) wells classified as abandoned or unused with no reported withdrawal values, (2) wells with casings less than or equal to 1-in. in diameter, (3) monitor and observation wells, unless withdrawals were reported, and (4) wells identified as test holes or drill holes. The remaining 676 wells (92 on Kaua‘i, 260 on O‘ahu, 142 on Maui, and 182 on Hawai‘i Island) were used in the analysis.

Data were checked for outliers, missing or duplicate information, and other likely errors. The USGS worked with CWRM to resolve apparent errors if possible. Other sources were used to supplement CWRM's reported groundwater-withdrawal data, including documents such as the State of Hawai‘i Agricultural Water Use and Development Plans, County Water Use and Development Plans, Water Use Protection Plans, and various consultant reports, as well as direct communication with water users, the State of Hawai‘i Department of Agriculture, and County water departments. The updated values were used to compute annual values for each well and island for the 2001–2010 period. The annual values were used to revise the USGS National Water-Use Information Program's database.

CWRM's priority has been to acquire information from medium-to-large groundwater users; thus, many surface-water withdrawals and withdrawals by small groundwater users were not included in CWRM's database as of 2010 (State of Hawai‘i, 2008b, 2014b). The lack of small-user groundwater data was assumed to have a negligible effect on the estimates in this study—CWRM estimated that wells of small capacity (equal to or less than 25 gallons per minute) had a total statewide withdrawal rate of about 2 Mgal/d (State of Hawai‘i, 2008b), which constitutes less than one percent of the total groundwater withdrawal in Hawai‘i. Reporting from medium-to-large groundwater users is also incomplete, however (State of Hawai‘i, 2008b). For example, Gingerich (USGS, written commun., 2014) estimated that groundwater withdrawals on Maui were underreported by about 5 Mgal/d in CWRM's database. At the time of this study, the completeness of the water-use data varied from island to island and from year to year.

Even though hundreds of stream diversions have been registered in the state, very few surface-water users reported withdrawal values to CWRM as of 2010 because most surface-water users were exempted from reporting requirements (State of Hawai‘i, 2008b). Nearly all surface-water withdrawals in Hawai‘i are for agricultural use, and the primary agricultural water use is irrigation. For the purposes of this study, surface-water withdrawals for irrigation were determined on the basis of agricultural demand, calculated as part of the groundwater recharge analysis for 2001–2010 (see appendix 1 for a description of the method), and added to the reported nonirrigation use. Part of the irrigation demand was met by groundwater and reclaimed water; therefore, surface-water use for irrigation in this study was determined by subtracting the amount of groundwater withdrawn for irrigation and the amount of reclaimed water used for irrigation from the calculated irrigation demand. Calculation of recharge for the year 2000 was not within the scope of this study, thus, the irrigation demand from the 2001 recharge analysis (appendix 2) was used as a surrogate to estimate surface-water use for irrigation in 2000; both 2000 and 2001 are within an extended drought period that affected Hawai‘i from 1998–2003.

Distinguishing Freshwater from Brackish Water and Saltwater—To meet the freshwater-assessment objectives of this study, freshwater withdrawals were distinguished from brackish-water and saltwater withdrawals. Because most irrigation requires freshwater, all surface-water withdrawals estimated on the basis of irrigation demand in this study were assumed to be freshwater. On the other hand, groundwater withdrawals may be fresh, brackish, or saline. In this study, fresh-groundwater withdrawals were distinguished from brackish-water and saltwater withdrawals on the basis of reported measurements of total-dissolved-solids or chloride concentrations. Water with total-dissolved-solids concentrations of less than 1,500 mg/L was included in the freshwater budget of this study. Withdrawals from wells with no information on dissolved-solids or chloride concentrations were assumed to be freshwater, because most of these wells supplied water for domestic, municipal, or irrigation use.

Kaua‘i

Water use on Kaua‘i constitutes one of the smaller fractions of the total water used on the four islands in this study. Between 1980 and 2010, Kauai's total freshwater withdrawal (groundwater and surface water) averaged about 193 Mgal/d (table 4), or about 19 percent of the total for the four islands in this study.

Most of the freshwater used on Kaua‘i comes from surface-water sources (fig. 55), and most of the surface water withdrawn has been used for irrigation (table 4, fig. 56). On average between 1980 and 2010, 153 Mgal/d or 79 percent of the total freshwater withdrawn came from surface water. Surface-water-use estimates show a sharp decline between 1990 and 2010. The timing of these declines corresponds with the closure of large sugarcane plantations on Kaua‘i—a major sugar plantation in eastern Kaua‘i closed in 2000 (Izuka and Oki, 2002), and the last of the large sugarcane plantations on Kaua‘i closed in 2010 (Leone, 2009). Changes in agricultural practices such as using more efficient irrigation application techniques and replacing high water-use crops with lower water-use crops also may have contributed to the lowering of agricultural water use over time (Shade, 1995). Corn, coffee, and diversified crops were being grown on some of the old sugarcane plantation lands in 2010, but much of the land was

Table 4. Freshwater-use estimates for Kaua‘i, O‘ahu, Maui, and Hawai‘i Island, 1980–2010.

[From U.S. Geological Survey National Water-Use Information Program and Hawaii State Commission on Water Resource Management, modified as described in this report. Mgal/d, million gallons per day; NA, not available]

Island	Year	Groundwater (Mgal/d)				Surface water (Mgal/d)				Total surface water and groundwater (Mgal/d)
		Public supply	Irrigation	Other	Total	Public supply	Irrigation	Other	Total	
Kaua‘i	1980	5.44	45.49	27.73	78.66	0.46	240.52	17.40	258.39	337.05
	1985	10.48	48.28	2.86	61.62	0.33	160.68	2.70	163.71	225.33
	1990	12.54	19.22	15.11	46.87	0.32	224.17	6.47	230.96	277.83
	1995	13.62	20.99	7.31	41.92	0.00	201.90	0.00	201.90	243.82
	2000	14.94	10.62	1.29	26.85	0.00	89.16[a]	0.00	89.16	116.01
	2005	14.40	0.58	2.08	17.06	0.75	85.99	0.00	86.74	103.80
	2010	12.50	0.02	1.05	13.57	2.02	34.93	0.00	36.95	50.52
	Mean				40.94				152.54	193.48
O‘ahu	1980	172.81	192.10	28.03	392.95	NA	44.13	0.00	44.13	437.08
	1985	130.40	144.47	83.27	358.14	0.00	43.42	0.00	43.42	401.56
	1990	157.72	118.11	57.85	333.68	1.42	37.27	0.00	38.69	372.37
	1995	141.59	46.26	54.66	242.51	0.00	36.38	0.00	36.38	278.89
	2000	164.81	31.10	18.25	214.16	0.00	30.45[a]	0.49	30.94	245.10
	2005	179.84	16.56	5.46	201.86	0.00	22.93	0.98	23.91	225.77
	2010	166.32	36.43	7.28	210.03	0.00	19.97	0.87	20.84	230.87
	Mean				279.05				34.04	313.09
Maui	1980	10.46	129.23	7.68	147.38	9.56	352.81	7.95	370.33	517.70
	1985	14.78	134.89	0.75	150.42	22.02	309.26	1.25	332.53	482.95
	1990	22.65	41.36	4.08	68.09	12.20	316.10	1.45	329.75	397.84
	1995	18.80	88.06	6.53	113.39	11.30	235.47	0.41	247.18	360.57
	2000	17.02	96.40	2.74	116.16	5.10	193.74[a]	0.33	199.17	315.33
	2005	30.88	48.53	4.31	83.73	10.68	196.66	0.59	207.93	291.66
	2010	31.28	80.20	1.03	112.50	10.96	204.50	0.16	215.62	328.13
	Mean				113.10				271.79	384.88
Hawai‘i	1980	6.23	4.70	77.16	88.09	0.27	9.92	11.23	21.42	109.51
	1985	15.19	2.61	58.31	76.11	9.00	52.14	0.00	61.14	137.25
	1990	23.87	9.31	63.74	96.92	3.00	9.70	20.83	33.53	130.45
	1995	23.42	12.63	72.78	108.83	2.60	0.50	3.88	6.98	115.81
	2000	31.16	13.35	56.11	100.62	2.50	8.61[a]	9.68	20.79	121.41
	2005	39.33	10.66	54.09	104.08	0.00	11.47	11.07	22.54	126.62
	2010	39.08	11.24	54.95	105.27	2.82	10.90	8.85	22.57	127.84
	Mean				97.13				27.00	124.13
All four islands	1980	194.95	371.53	140.60	707.08	10.30	647.38	36.58	694.26	1401.34
	1985	170.85	330.25	145.19	646.29	31.35	565.50	3.95	600.80	1247.09
	1990	216.78	188.00	140.78	545.56	16.94	587.24	28.75	632.93	1178.49
	1995	197.43	167.94	141.28	506.65	13.90	474.25	4.29	492.44	999.09
	2000	227.93	151.47	78.39	457.79	7.60	321.96[a]	10.50	340.06	797.85
	2005	264.45	76.33	65.94	406.73	11.43	317.05	12.64	341.12	747.85
	2010	249.18	127.88	64.31	441.37	15.80	270.31	9.88	295.99	737.36
	Mean				530.21				485.37	1015.58

[a]Demand-based estimates of surface-water irrigation values for 2001 used as surrogate for 2000.

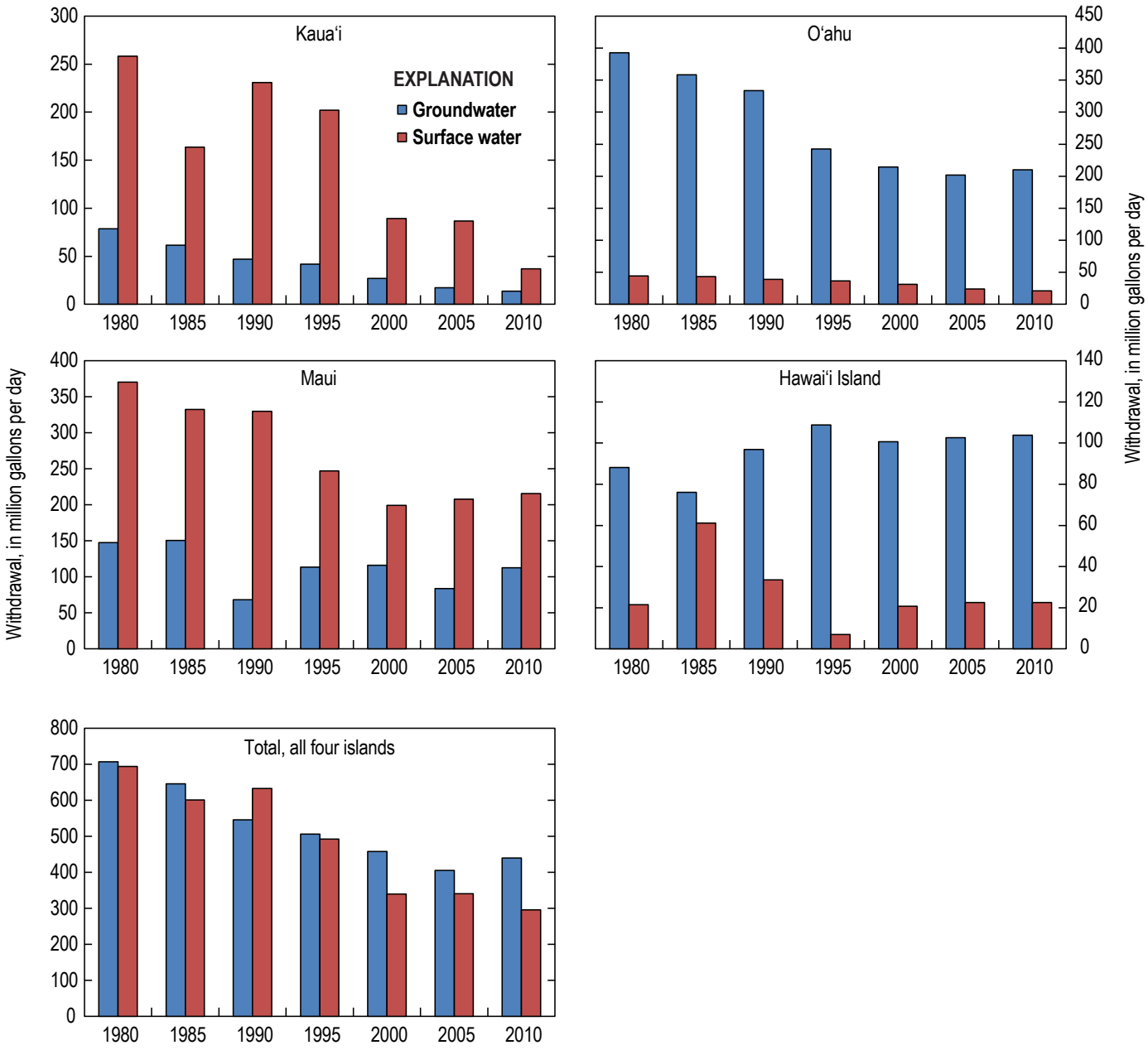

Figure 55. Graphs of freshwater withdrawals in 1980–2010 for Kaua'i, O'ahu, Maui, and Hawai'i Island.

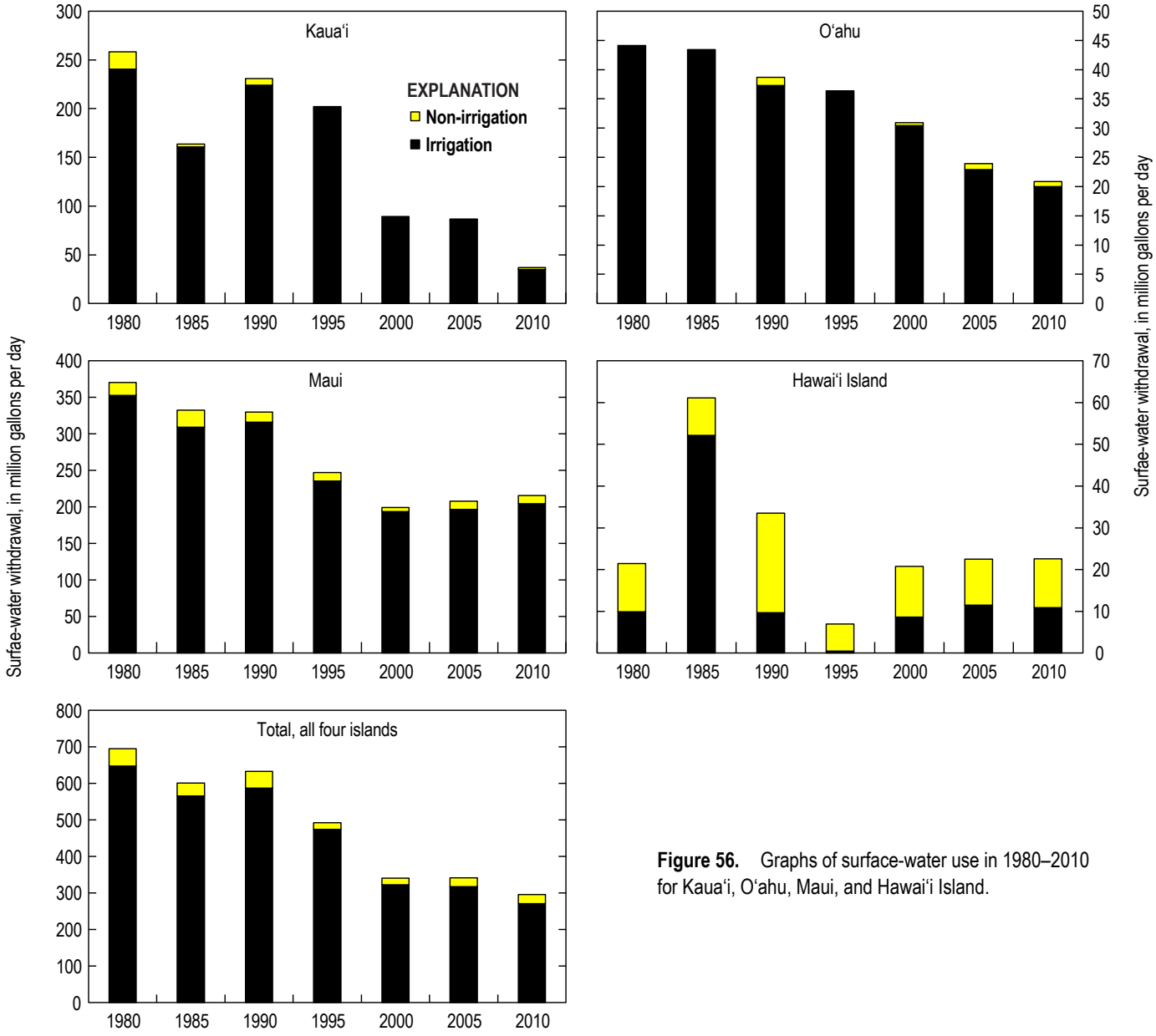

Figure 56. Graphs of surface-water use in 1980–2010 for Kaua‘i, O‘ahu, Maui, and Hawai‘i Island.

left unplanted (fig. 6). The reduction of surface-water irrigation accompanying the demise of sugarcane agriculture affected recharge and groundwater levels on some parts of the island (Izuka and others, 2005).

Groundwater withdrawals on Kaua‘i averaged 41 Mgal/d and decreased between 1980 and 2010 (table 4, fig. 57). Much of this decline can be accounted for by a decline in groundwater used for irrigation, which is consistent with the history of sugarcane-plantation closures. Part of the decline may, however, be due to a decrease in groundwater-use reporting.

O‘ahu

Water use on O‘ahu accounts for one of the larger fractions of the total water used on the four islands in this study. Between 1980 and 2010, O‘ahu’s total groundwater- and surface-water-withdrawal averaged about 313 Mgal/d or about 31 percent of the combined average for the four islands. Unlike on Kaua‘i, most of the freshwater used on O‘ahu comes from groundwater (fig. 55). On average between 1980 and 2010, 279 Mgal/d, or about 89 percent, of the total estimated freshwater withdrawn on O‘ahu came from groundwater, and after 1990, most of this water was used for public supply (table 4, fig. 57). The high reliance on groundwater stems from the extensive and relatively easily exploited groundwater resources on O‘ahu. Also, O‘ahu has 70 percent of the population in the State of Hawai’i (table 1), and groundwater provides almost all of the drinking water. Groundwater withdrawals on O‘ahu decreased from 1980 to 2000 (fig. 57). Most of the decrease can be attributed to a decline in groundwater used for irrigation, consistent with the demise of sugarcane plantations on the island. The last sugar plantations on O‘ahu closed in the mid-1990s (Wilcox, 1996; Dorrance and Morgan, 2000). Some of the land formerly used for

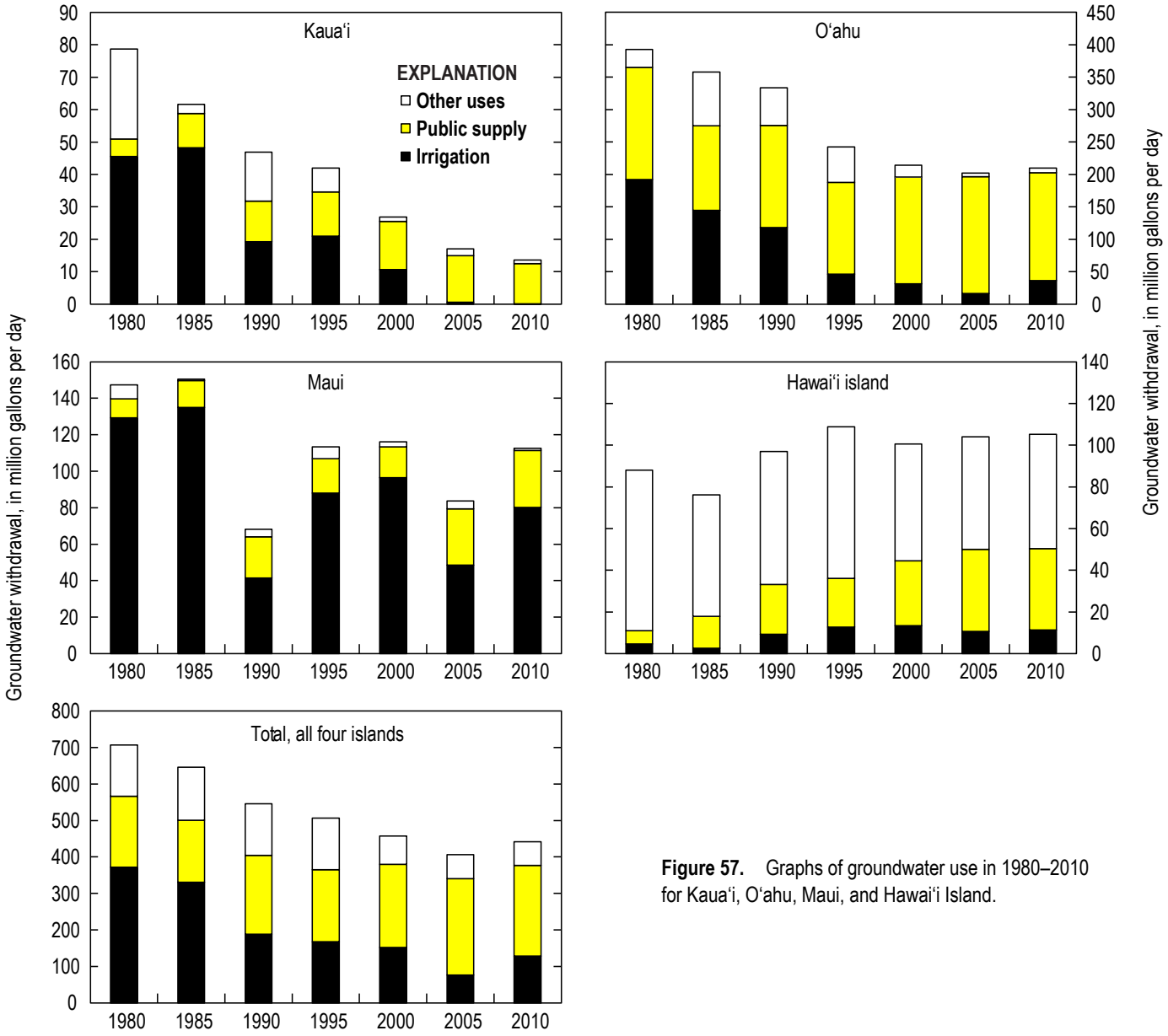

Figure 57. Graphs of groundwater use in 1980–2010 for Kaua'i, O'ahu, Maui, and Hawai'i Island.

growing sugarcane has been converted to diversified agriculture or agricultural-research uses, but much of the land is currently covered by grass and shrub or has been converted to urban use.

Surface-water withdrawals on O'ahu averaged 34 Mgal/d or about 11 percent of the total freshwater used on O'ahu between 1980 and 2010 (table 4). Surface-water-use decreased during this period (fig. 56), which is generally consistent with the concurrent decrease in agriculture.

Maui

Maui has the highest freshwater use of the islands in this study, exceeding even that of heavily populated O'ahu. The fifth-year estimates (table 4) indicate an average combined groundwater-and-surface-water withdrawal of 385 Mgal/d or about 38 percent of the total for the four islands in this study. Unlike on O'ahu, however, most of the water withdrawn on Maui is used for irrigation—Maui was the only island in Hawai'i on which sugarcane was still being grown at the time of this study.

Most of the water used on Maui comes from surface-water sources (fig. 55). In the period from 1980 to 2010, 272 Mgal/d or about 71 percent of the total freshwater used came from surface water, and nearly all of this water was used for irrigation (table 4, fig. 56). A sharp decline in surface-water use between 1990 and 2000 corresponds with the closure of two large sugar plantations—one in 1988 and the other in 1999 (Dorrance and Morgan, 2000). Some of the land used for sugarcane cultivation was converted to other forms of agriculture, including pasture, pineapple, and macadamia nuts, which demand less water than sugarcane (Engott and Vana, 2007). Changes in agricultural irrigation have affected the amount and distribution of groundwater recharge on Maui (Engott and Vana, 2007) and possible future changes can affect groundwater levels and salinity (Gingerich, 2008).

Groundwater use on Maui averaged 113 Mgal/d between 1980 and 2010 but varied widely (fig. 57) mainly due to variations in irrigation. Groundwater withdrawals for uses other than irrigation are mostly for public supply (table 4, fig. 57), which has increased with population growth—the population of Maui County grew from about 71,000 in 1980 to 155,000 in 2010 (State of Hawai‘i, 2014c).

Hawai‘i Island

Hawai‘i Island has the lowest freshwater use of the four islands in this study. The 1980–2010 fifth-year water-use estimates (table 4) indicate an average combined groundwater-and-surface-water withdrawal of about 124 Mgal/d or about 12 percent of the total for the islands in this study.

Most of the freshwater used on Hawai‘i Island comes from groundwater sources (fig. 55). Between 1980 and 2010, an average of 97 Mgal/d or about 78 percent of the total freshwater withdrawal on the island came from groundwater. Unlike on other islands in this study, most of the fresh groundwater withdrawn on Hawai‘i Island was used for purposes other than public supply or irrigation—a large amount of groundwater is used by power plants for cooling (power plants on other islands mostly use saltwater for this purpose), but the used water is injected back into the groundwater system. Groundwater use generally increased from 1980 to 1995 (figs. 55 and 57). Groundwater used for public supply increased throughout the 1980–2010 period, which is consistent with population growth. From 2000 to 2010, the population of Hawai‘i Island increased by 24.5 percent, the highest population growth rate in the state for that period (State of Hawai‘i, 2014c). Unlike on other islands, groundwater use for irrigation on Hawai‘i Island did not decrease between 1980 and 2010.

Surface-water use on Hawai‘i Island averaged 27 Mgal/d (table 4). This average includes a value for irrigation water use in 1985 that is much higher than other years (fig. 56). The singularly high value for 1985 is not consistent with the history of sugar plantations on Hawai‘i Island. Many sugar plantations had closed before 1985 and the closures continued with the last two plantations in 1994 and 1996 (Dorrance and Morgan, 2000). Crops that replaced sugarcane—macadamia nuts, coffee, eucalyptus, and products of diversified agriculture—require less water; and much of the former sugarcane lands were unused and therefore not irrigated. Given the history of agriculture, the reported high irrigation water use in 1985 is anomalous. If the 1985 value is omitted from analysis, total surface-water use on Hawai‘i Island averaged 21 Mgal/d. In any case, the average surface-water use on Hawai‘i Island is lowest of the four islands in this study.

Groundwater-Storage Depletion

Groundwater storage depletion (not to be confused with “change in storage” in eq. 2, which is a component only of transient groundwater budgets) is the volumetric difference in storage between two different moments in an aquifer’s history. Storage depletion is a result of groundwater withdrawal, and therefore is a potential limitation to groundwater availability. In regional groundwater studies, storage depletion is sometimes calculated by multiplying measured changes in groundwater levels in wells by an estimate of the specific yield (for unconfined aquifers) or storage coefficient (for confined aquifers) (for example Konikow, 2013). On oceanic islands and in coastal areas, however, lowering of the water table accounts for only a fraction of the storage depletion of a freshwater lens—a much larger fraction of the storage depletion results from a rise of the bottom of the freshwater lens, that is, a rise in the transition zone (fig. 4). Well water-level data are widely available for some aquifers in Hawai‘i, but few monitoring wells are deep enough to allow tracking of the transition zone; thus, insufficient monitoring data exist to measure groundwater storage depletion directly. The Ghyben-Herzberg relation cannot be used to estimate the rise in the transition zone from water-level data because the vertical flow fields that form around partly penetrating pumped wells invalidate the relation’s assumptions of hydrostatic conditions. In addition, transition-zone rise in response to well withdrawal may lag behind water-table decline (Gingerich and Voss, 2005; Rotzoll and others, 2010).

Because of these difficulties, quantification of groundwater storage depletion in Hawai‘i requires a tool, such as a numerical model, that can comprehensively assess freshwater-over-saltwater aquifer systems in Hawai‘i’s volcanic aquifers. Although quantification by numerical modeling is beyond the scope of this report, examination of water-level data and review of previous studies provides a means to qualitatively discuss storage depletion.

Figure 58 shows manually measured water-level data from the NWIS database for selected wells in Hawai‘i’s volcanic aquifers. Although measurements flagged in the database as having been taken while the wells were pumping have been eliminated from the graphs, some of the data still show high variability, likely due to pumping effects from nearby wells. Even so, a general long-term decline in water levels is evident in many graphs, and indicates an overall reduction in storage for most areas where groundwater has been developed.

Water-level declines in Hawai‘i’s most heavily developed aquifers have been documented in various studies (see for example Oki, 2005). Konikow (2013) used water-level declines and estimates of specific yield to determine that groundwater storage on O‘ahu deceased by about 0.08 mi^3 between 1900 and 2008, but did not differentiate between freshwater and saltwater, and therefore did not consider the rise of the interface and the associated additional freshwater storage depletion from below. Data from deep monitoring wells have shown a general rise in the transition zone and diminishing fresh groundwater storage since monitoring began in the late 1960s (Oki, 2005; Rotzoll and others, 2010). Numerical-model simulations of the heavily developed Pearl Harbor aquifer on O‘ahu indicate that the transition zone in some areas has risen by hundreds of feet since groundwater development began in the 1880s (Gingerich and Voss, 2005).

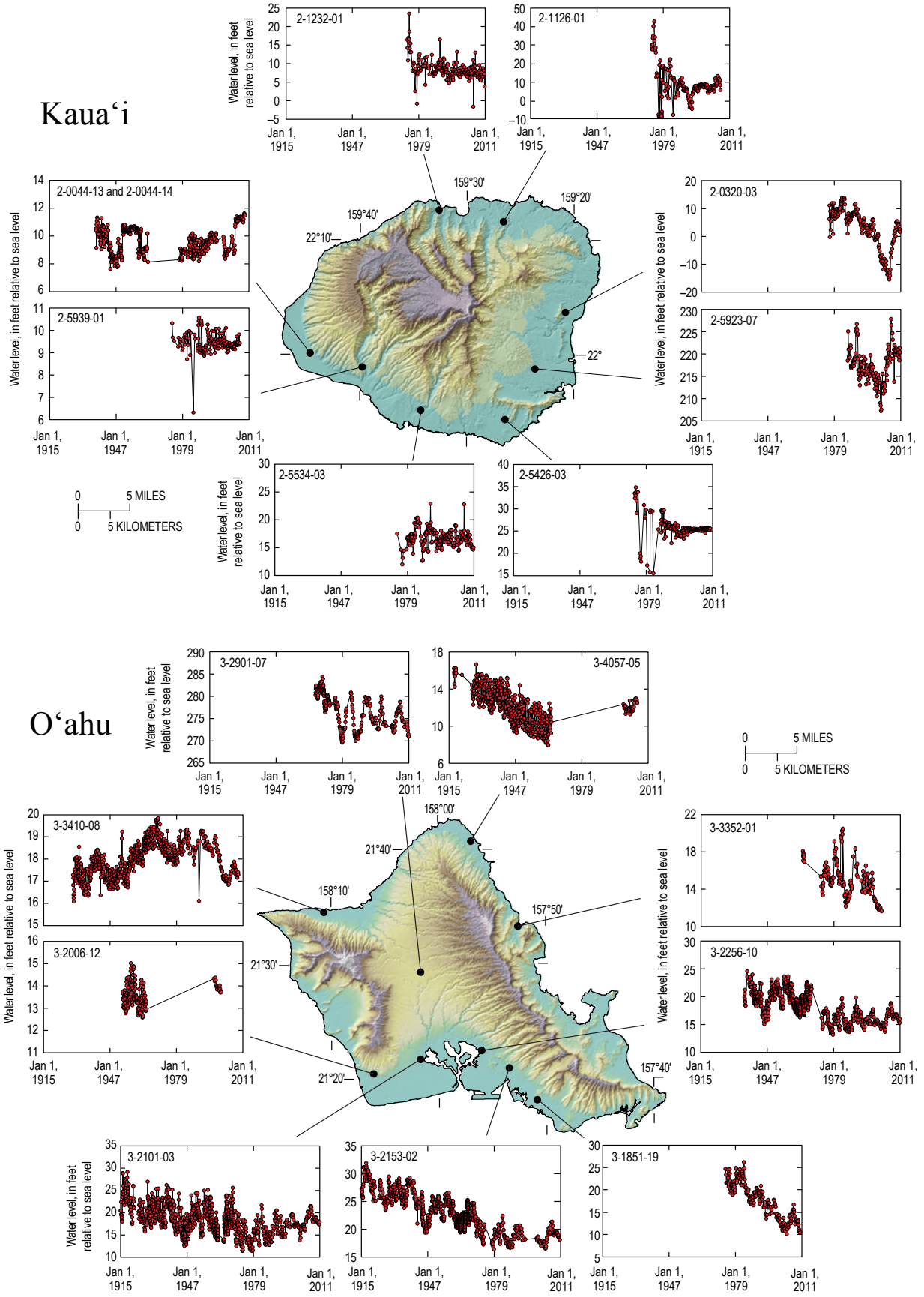

North American Datum 1983, Universal Transverse Mercator projection, zone 4N.

Figure 58. Graphs of water levels in selected representative wells in Hawai‘i.

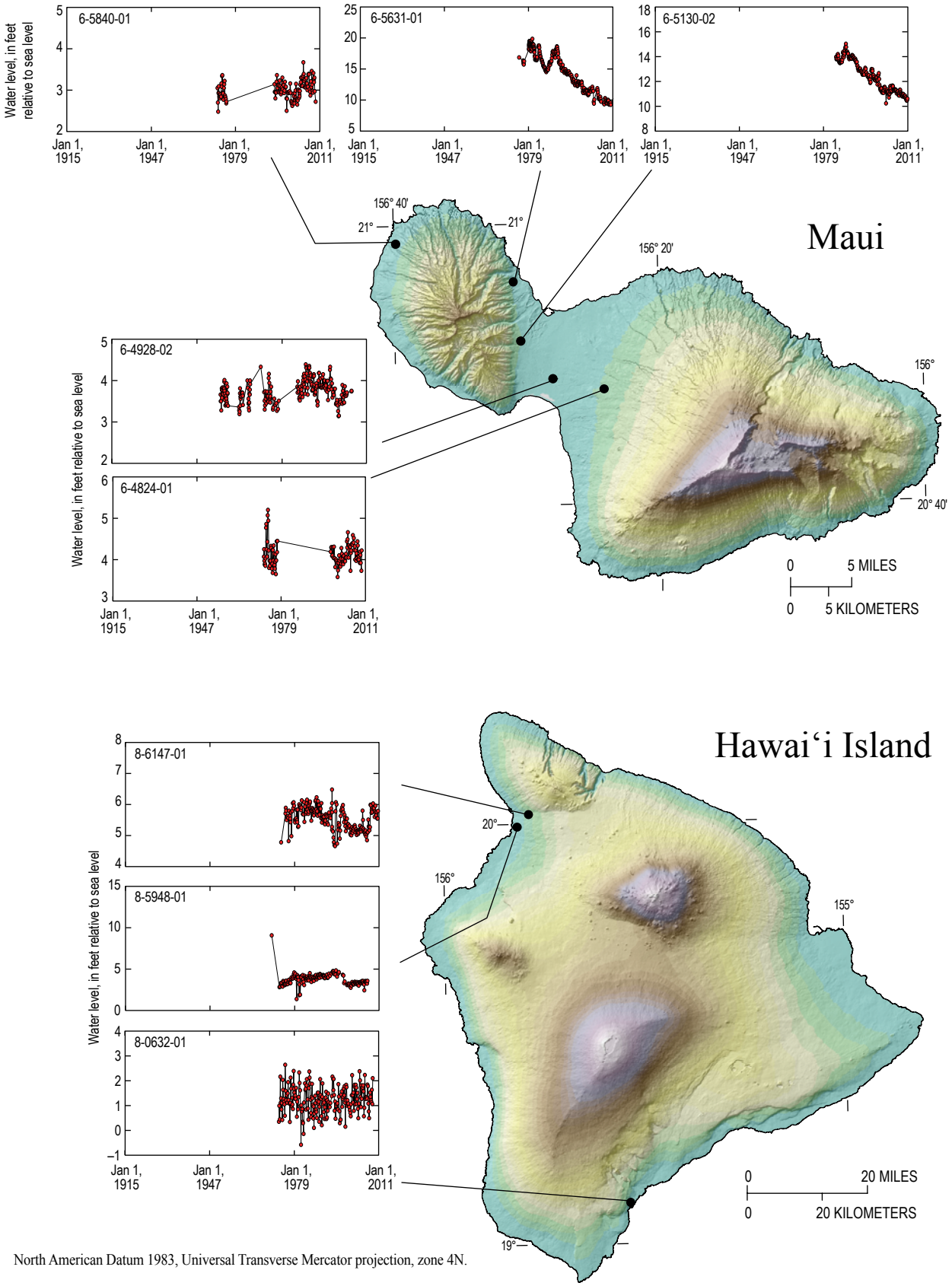

Figure 58. Graphs of water levels in selected representative wells in Hawai‘i.—Continued

Declining groundwater storage is also evident in diminished streamflow. Oki (2004a) and Bassiouni and Oki (2013) analyzed data from nine long-term stream gages on Kauaʻi, Oʻahu, Molokaʻi and Maui; eight of the gages showed statistically significant downward trends in base flow in analysis of data from 1913 to 2008. The downward trends indicate declines in base flow of 20 to 70 percent in 100 years and coincide with downward trends in rainfall measured in Hawaiʻi.

Steady-State Groundwater Budgets

The recharge and withdrawal estimates can be used with the mass balance shown in equation 3 to estimate natural groundwater discharge to springs, streams, wetlands, and submarine seeps, assuming the groundwater flow systems are in steady state. It is not known if the aquifers on Kauaʻi, Oʻahu, Maui, and Hawaiʻi Island are in steady state. However, equation 3 can be used to indicate what natural discharge would be if a given set of groundwater-recharge and well-withdrawal values was maintained until steady state could be achieved. Comparing steady-state groundwater budgets for predevelopment and recent conditions provides an indication of how humans have affected groundwater resources on each of the islands in this study.

The groundwater-budget components for predevelopment and recent conditions are shown diagrammatically by the blue arrows in figures 59 and 60. Groundwater withdrawal for predevelopment conditions was assumed to be zero. Groundwater withdrawals for recent conditions were approximated by averaging the groundwater-withdrawal values from the fifth-year water-use estimates for 2000, 2005, and 2010 (table 4); this period represents the water use after most of the sugarcane plantations had closed, eliminating some high withdrawals that no longer exist. For reference, components used in the calculation of groundwater recharge such as precipitation, ET, and runoff are also shown in figures 59 and 60 (white arrows).

The only groundwater withdrawal at the time represented by the predevelopment scenario was from dug wells, which is considered negligible. Variations in precipitation may have resulted in short-term imbalances, but on average, inflow from recharge equaled natural outflow. Agriculture and other human activities that affected recharge during the predevelopment period probably also resulted in short-term water-budget imbalances, but the imbalances were probably small compared to the total predevelopment groundwater flux through the aquifers. Also, because the impact of withdrawals developed over centuries of human activity, the aquifers had some time to adjust. Assuming steady-state conditions, predevelopment natural groundwater discharge probably was equal or close to recharge: 871 Mgal/d for Kauaʻi, 675 Mgal/d for Oʻahu, 1,279 Mgal/d for Maui, and 5,291 Mgal/d for Hawaiʻi Island (fig. 59). Predevelopment natural groundwater discharge rates for the four islands total 8,116 Mgal/d.

Recharge estimates for recent conditions (fig. 60) are generally within a few percent of predevelopment estimates except for Hawaiʻi Island; differences are attributable to human activities and differences in precipitation (see *Groundwater Recharge* section, above). In the groundwater budget for recent conditions, groundwater withdrawals constitute an outflow component in addition to natural discharge. The total recent withdrawal for the four islands in this study is 435 Mgal/d, or about 5 percent of recent recharge (9,438 Mgal/d). If these recharge and withdrawal values are allowed to reach steady state, natural groundwater discharge will be 9,003 Mgal/d, or about 95 percent of recharge.

The relatively small ratio of withdrawal to recharge for Hawaiʻi's aquifers can be misleading because the withdrawal is not distributed the same way as recharge. Nearly half of the total withdrawal for the four islands comes from Oʻahu, yet Oʻahu's recharge constitutes only 7 percent of the total recharge for the four islands. Oʻahu's withdrawal (209 Mgal/d) constitutes 32 percent of the island's estimated recent recharge (660 Mgal/d). In contrast, groundwater withdrawals on Kauaʻi, Maui, and Hawaiʻi Island are each only 2 to 8 percent of their respective recharge values. If these rates of recharge and groundwater withdrawal are allowed to achieve steady state, the groundwater withdrawals would cause an equal reduction of natural groundwater discharge. Thus, Oʻahu's natural groundwater discharge to springs, streams, wetlands, and submarine seeps under recent conditions would be 451 Mgal/d, or only about 68 percent of what it was in predevelopment time. The simple island-wide water budgets show that Oʻahu currently bears the brunt of the impact of human groundwater use in Hawaiʻi. Because there is no freshwater flow between islands, effects of high withdrawals on Oʻahu cannot be mitigated by the lower withdrawals on other islands.

Even within an island, high withdrawals from one area cannot be completely mitigated by groundwater flow from adjacent areas. For example, most of Oʻahu's groundwater withdrawal comes from aquifers in the central and southern parts of the island. Much of the groundwater withdrawal on Maui comes from the aquifers beneath and adjacent to the Isthmus. Likewise, the impacts are focused in the areas close to the withdrawal. Assessing the impacts of unevenly distributed groundwater withdrawal requires consideration of the actual well locations and withdrawal rates, spatial distribution of recharge, aquifer properties, and nearby aquifer boundaries. The best tool currently available for comprehensive analysis of such spatially distributed factors is numerical groundwater modeling.

The natural discharge component (ND) in the water budgets depicted in figures 59 and 60 includes groundwater discharge above sea level (spring flow and stream base flow), as well as below sea level (submarine groundwater discharge). Whether groundwater withdrawals affect mostly subaerial or submarine groundwater discharge can be important to groundwater availability assessments in some cases. For example, if streamflow depletion is a concern, then groundwater availability will be limited where withdrawals affect subaerial groundwater discharge. However, quantifying each of these subcomponents of natural groundwater discharge separately is beyond the scope of this study. Base-flow-separation analysis has been used to quantify groundwater discharge to streams in basins having long-term stream gages, but not all streams in Hawaiʻi are gaged and no reliable method presently exists to quantitatively extrapolate base-flow data from gaged streams to ungaged streams in

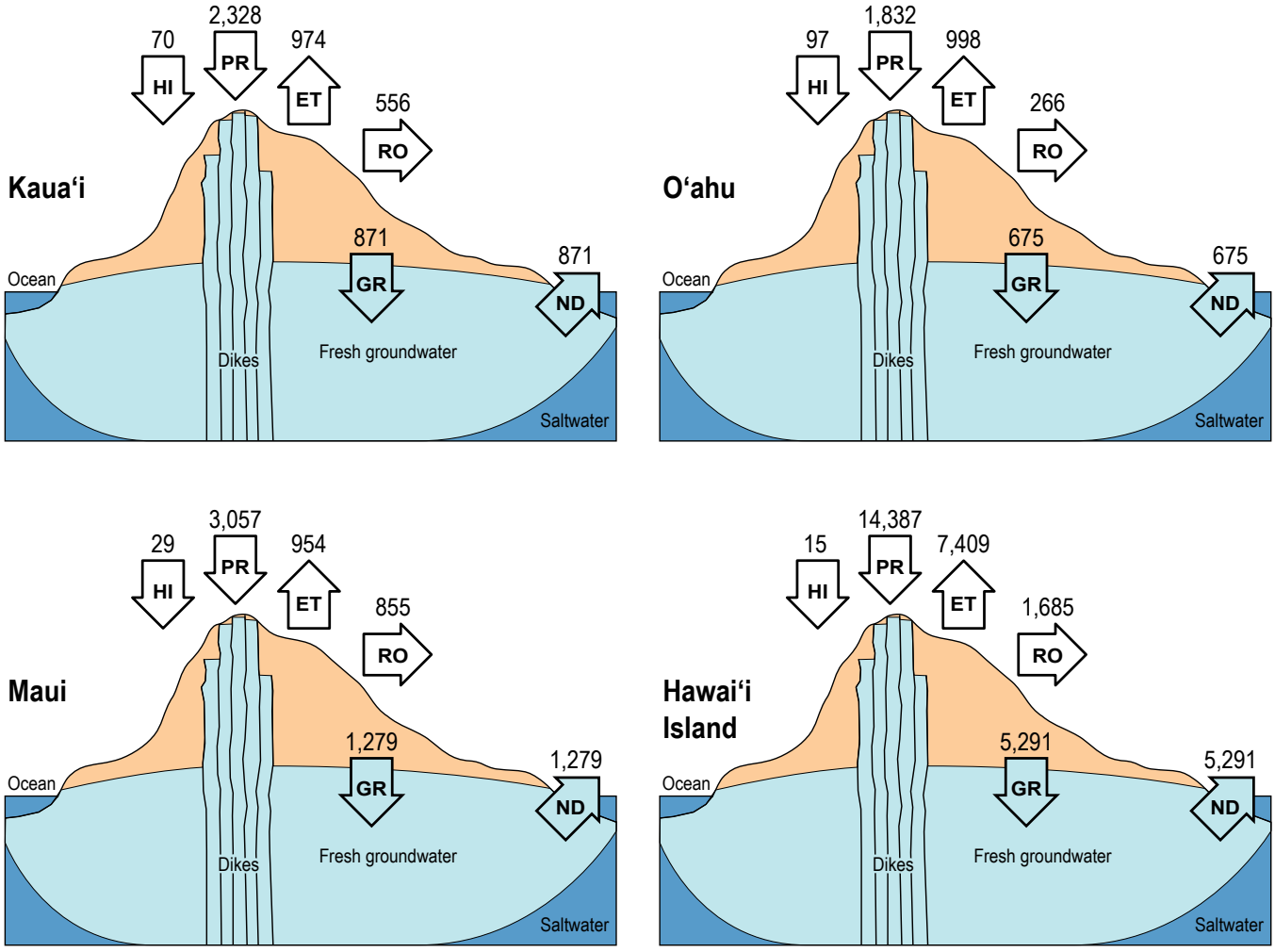

EXPLANATION

(All values in million gallons per day)

PR, Precipitation, including rain and fog

HI, Input from human activities, including irrigation and leaks from water-supply, septic, and sewer systems

ET, Evapotranspiration

RO, Runoff, including runoff from natural surfaces as well as runoff from paved surfaces flowing into storm drains

GR, Groundwater recharge

ND, Natural discharge, such as spring flow, stream base flow, and submarine groundwater discharge

Figure 59. Steady-state fresh groundwater budget for predevelopment conditions on Kaua‘i, O‘ahu, Maui, and Hawai‘i Island.

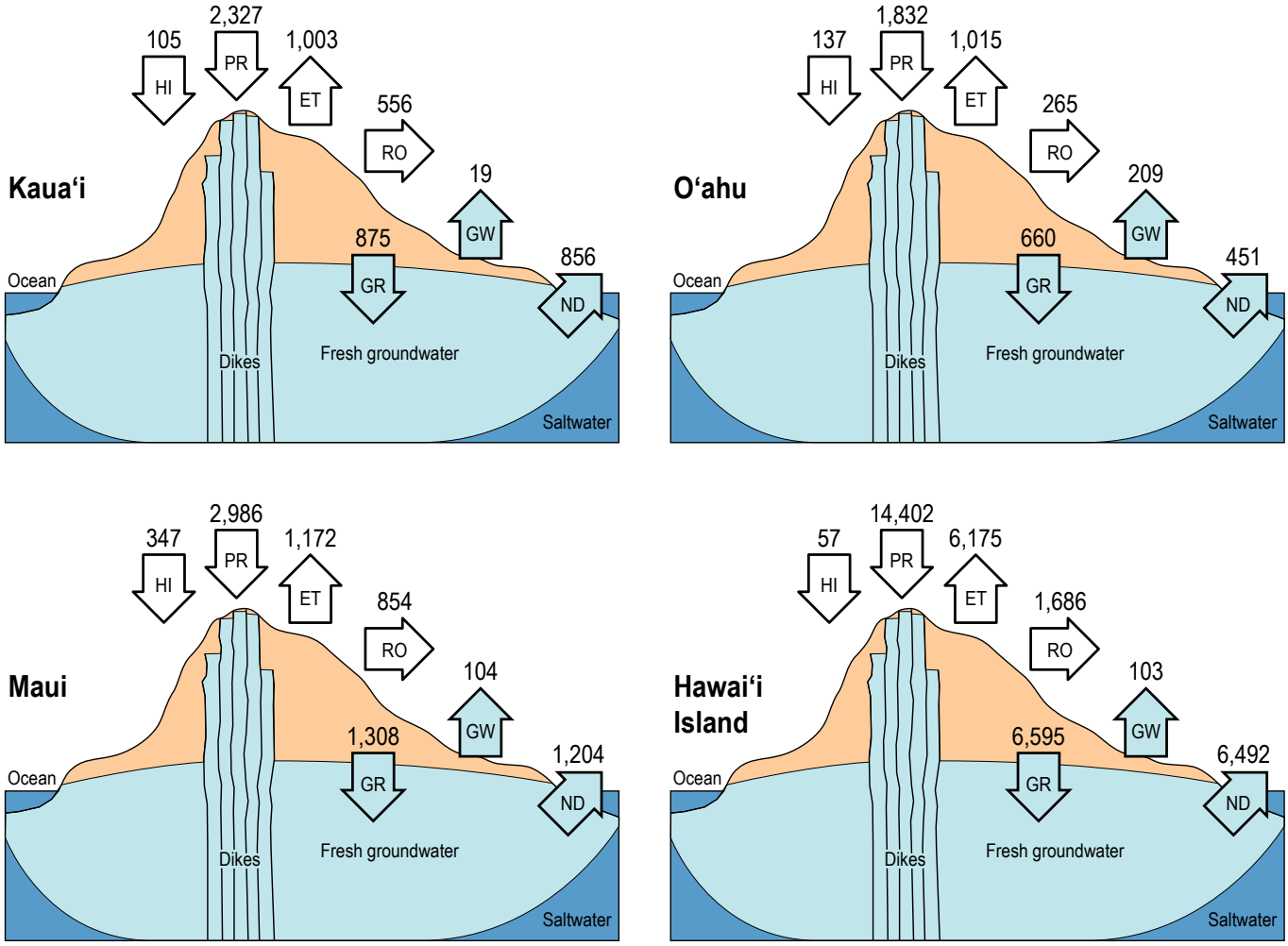

EXPLANATION

(All values in million gallons per day)

PR, Precipitation, including rain and fog

HI, Input from human activities, including irrigation and leaks from water-supply, septic, and sewer systems

ET, Evapotranspiration

RO, Runoff, including runoff from natural surfaces as well as runoff from paved surfaces flowing into storm drains

GR, Groundwater recharge

ND, Natural discharge, such as spring flow, stream base flow, and submarine groundwater discharge

Figure 60. Steady-state fresh groundwater budget for recent conditions on Kaua‘i, O‘ahu, Maui, and Hawai‘i Island.

Hawai‘i. Groundwater discharge along the coasts of Hawai‘i has been studied on a local scale using direct measurements, geochemistry, and remote imagery (for example Garrison and others, 2003; Johnson and others, 2008; Dimova and others, 2012; Kelly, 2012) but regional-scale direct measurement of this discharge is currently not available. The best approach currently available for quantifying each of the two subcomponents of natural groundwater discharge from Hawai‘i’s aquifers is numerical modeling of the freshwater/saltwater systems of each island.

Conceptual Models of Groundwater Occurrence and Movement

As discussed in the *Introduction*, groundwater availability for human use is limited by whether or not the impacts of groundwater withdrawals are deemed acceptable. These impacts differ from one groundwater setting to another—they depend on how water enters, moves in, is stored in, and exits a given groundwater setting. On the basis of the hydrogeologic framework and groundwater budgets discussed above, groundwater occurrence and movement in Hawaiian volcanic aquifers can be discussed in terms of four principal conceptual models: (1) high-permeability lava-flow aquifers with freshwater lenses, (2) aquifers with groundwater impounded by dikes, (3) thickly saturated low-permeability aquifers made mostly of lava flows but also sediment, and (4) perched aquifers. The nonvolcanic (sedimentary) HGUs are included in this discussion only as they relate to the storage and movement of water in the volcanic aquifers.

High-Permeability Lava-Flow Aquifer with Freshwater Lens

Aquifers formed from thin, high-permeability lava flows (fig. 61) are the primary source of fresh groundwater for human use in Hawai‘i. Groundwater in these aquifers exists as a freshwater lens buoyantly overlying saltwater (fig. 62*A*,*B*). As discussed in the *Hydrogeologic Overview*, the freshwater lenses in Hawai‘i were referred to as “basal” groundwater in general conceptual models developed in the 20th century. The term “basal” reflected the characteristically low altitude (less than about 50 ft above sea level) and gentle seaward gradient of the water table in the high-permeability aquifer. Use of the term is not perpetuated in this report, however, because not all freshwater lenses have low-altitude or gently sloping water tables (see *Thickly Saturated Low-Permeability Lava-Flow Aquifers,* below).

In the freshwater lens, groundwater flows from inland areas toward discharge areas at or near the coast. Part of the groundwater that flows through the freshwater lens comes from groundwater recharge through the land surface. Recharge over the high-permeability lava-flow aquifers in Hawai‘i ranges widely, from less than an inch per year in arid leeward areas to hundreds of inches per year in wet windward areas (figs 47–54). In some places, isolated low-permeability layers within the stack of high-permeability lava flows intercept recharge and form perched groundwater bodies. The perched bodies may divert some of the recharge back to the surface, but much of the recharge water continues to seep down and eventually is incorporated in the freshwater lens. Part of the flow through the lens comes from subsurface inflow from adjacent up-gradient groundwater bodies. Because of the typical structure of Hawaiian shield volcanoes, this subsurface inflow in most cases comes, or is presumed to come, from dike-impounded groundwater (figs. 61 and 62*A*,*B*).

Near the coast, groundwater naturally discharges subaerially (by way of springs and stream seepage) as well as below sea level (by way of submarine groundwater discharge) (fig. 62). Because the freshwater lens lies buoyantly on the slightly denser saltwater in the aquifer, most of the thickness of the freshwater lens in a high-permeability aquifer is below sea level; in general, therefore, most of the groundwater discharge near the coast occurs below sea level. As will be discussed below, this may not be the case where substantial caprock resists the discharge of groundwater to the ocean, or in thickly saturated low-permeability lava-flow aquifers.

On younger islands, where there is little to retard groundwater flow through the high-permeability lava-flow aquifer except the small resistance offered by the aquifer itself, the freshwater lens is thin (fig. 62*B*). The lens is especially thin in arid areas—for example the lens on the western coast of Hawai‘i Island is so thin that the brackish transition zone emerges at the water table inland from the coast (Oki, 1999; Oki and others, 1999b). In some areas, however, low-permeability sediments, weathered rock, and rejuvenated-stage volcanic rocks along the coast form a semiconfining unit locally known as caprock (figs. 61 and 62*A*) that resists groundwater discharge to the ocean. In reality, the caprock is a heterogeneous mix of both high- and low-permeability rocks. Palmer (1927) suggested that low-permeability layers mixed with high-permeability layers throughout the caprock result in the overall low permeability of the unit, but others (for example, Stearns and Vaksvik, 1935; Hunt, 1996) suggest that low-permeability weathered basalt at the base of the caprock is chiefly responsible for the low-permeability behavior of the unit. In any case, the overall effect of the caprock is that of a semiconfining unit partly covering the permeable lava-flow aquifer (Oki and others, 1996). The caprock resists groundwater discharge to the ocean and allows the freshwater lens to thicken—by raising the water table and lowering the transition zone—despite the high-permeability of the aquifer (fig. 62*A*). If the caprock extends above sea level, it causes groundwater to discharge at higher altitudes and farther inland (figs. 62*A* and 63), resulting in an increase in the proportion of subaerial groundwater discharge. On O‘ahu for example, the Pearl Harbor Springs discharge substantial amounts of groundwater above sea level where the caprock overlying the high-permeability lava-flow aquifer pinches out landward; these springs support base flow in the lower reaches of streams. Groundwater also flows through the caprock and discharges both above and below sea level (Palmer, 1927, 1946).

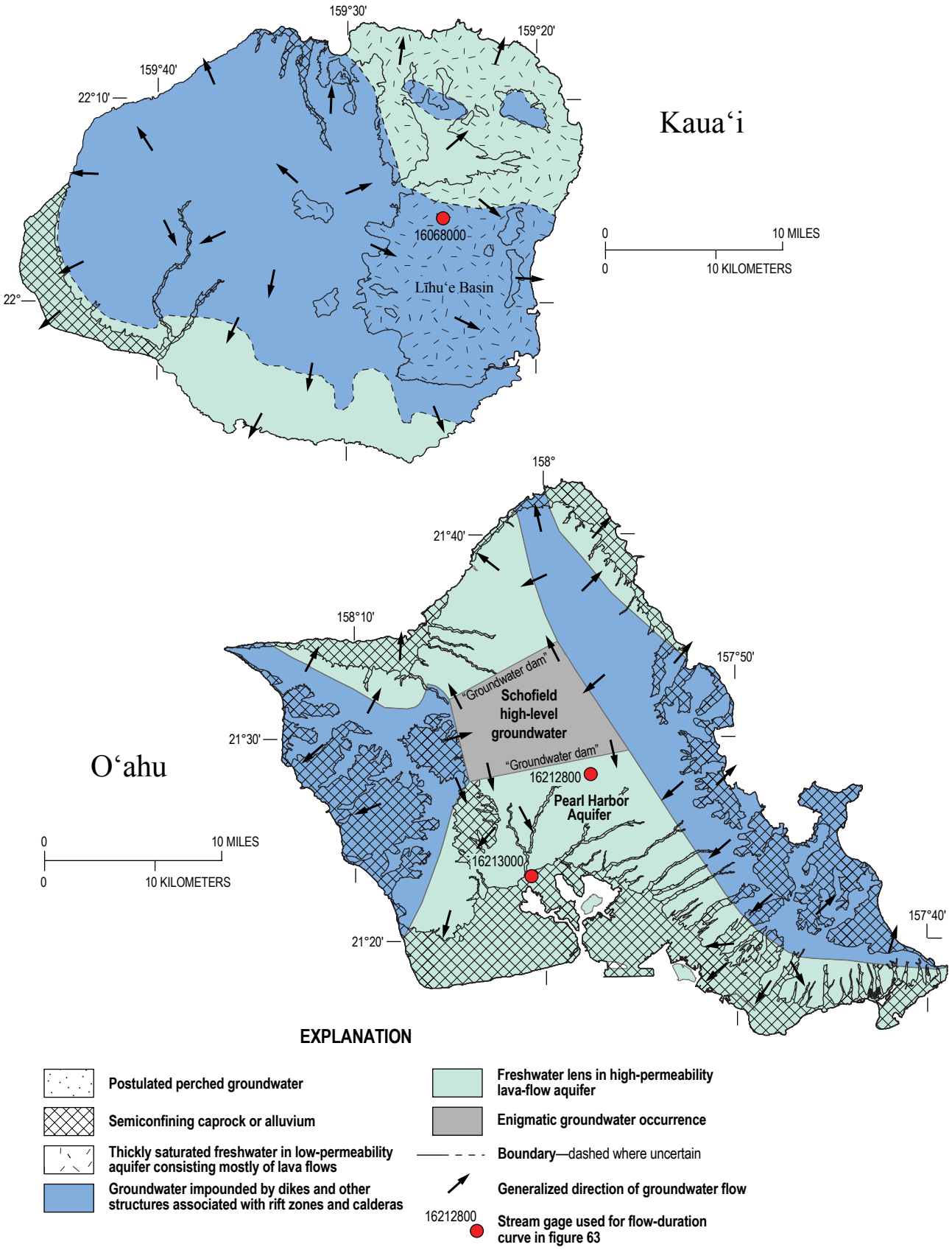

Figure 61. Maps of modes of groundwater occurrence and flow on Kaua‘i, O‘ahu, Maui, and Hawai‘i Island. Compiled and interpreted from Stearns (1939), Stearns and Macdonald (1942, 1946), Yamanaga and Huxel (1969, 1970), Takasaki and Mink (1985), Hunt (1996), Sherrod and others (2007), Gingerich (2008), Gingerich and Engott (2012), Flinders and others (2013), and water-level data in the National Water Inventory System database.

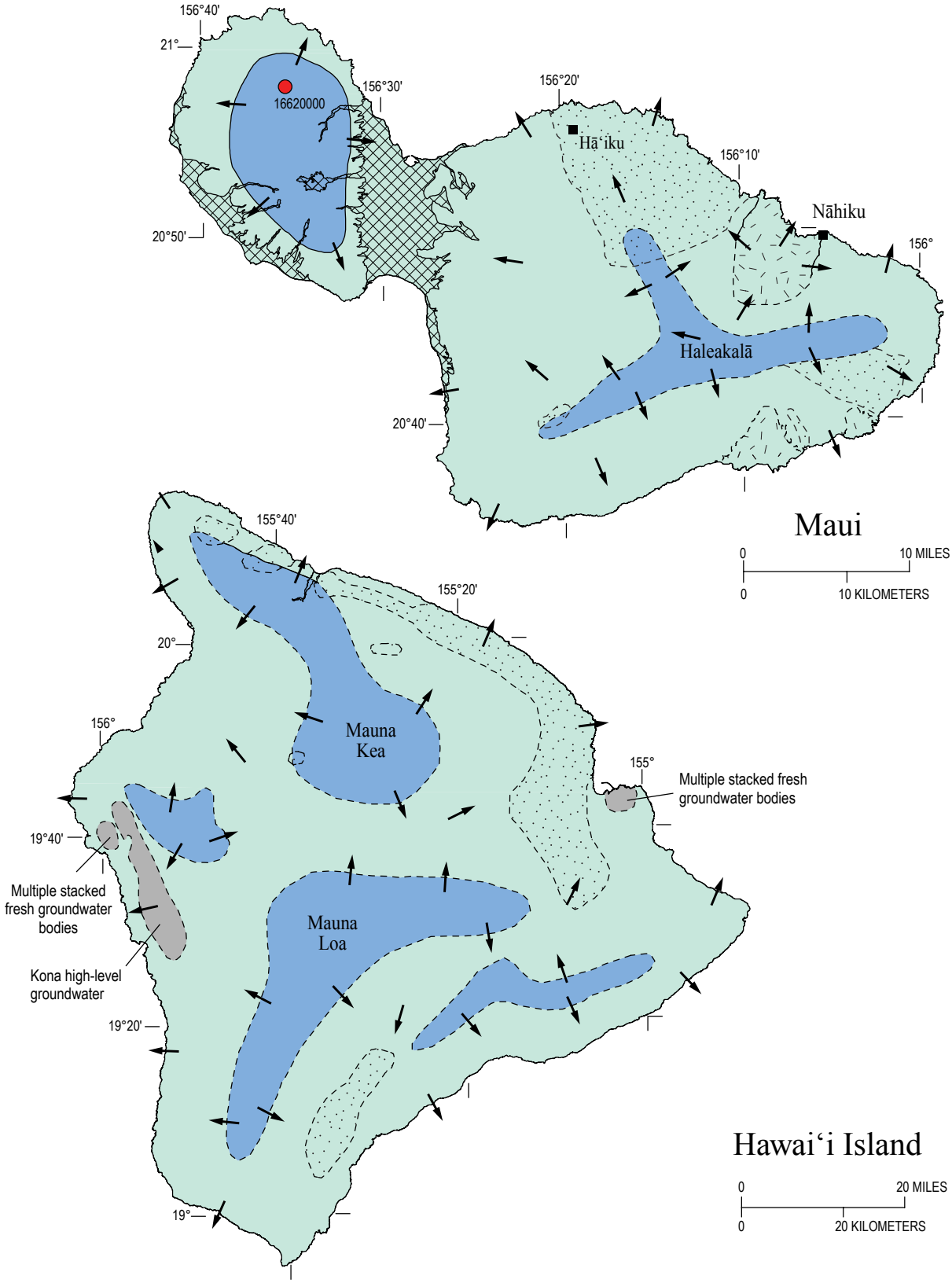

North American Datum 1983, Universal Transverse Mercator projection, zone 4N.

Figure 61. Maps of modes of groundwater occurrence and flow on Kaua‘i, O‘ahu, Maui, and Hawai‘i Island. Compiled and interpreted from Stearns (1939), Stearns and Macdonald (1942, 1946), Yamanaga and Huxel (1969, 1970), Takasaki and Mink (1985), Hunt (1996), Sherrod and others (2007), Gingerich (2008), Gingerich and Engott (2012), Flinders and others (2013), and water-level data in the National Water Inventory System database.—Continued

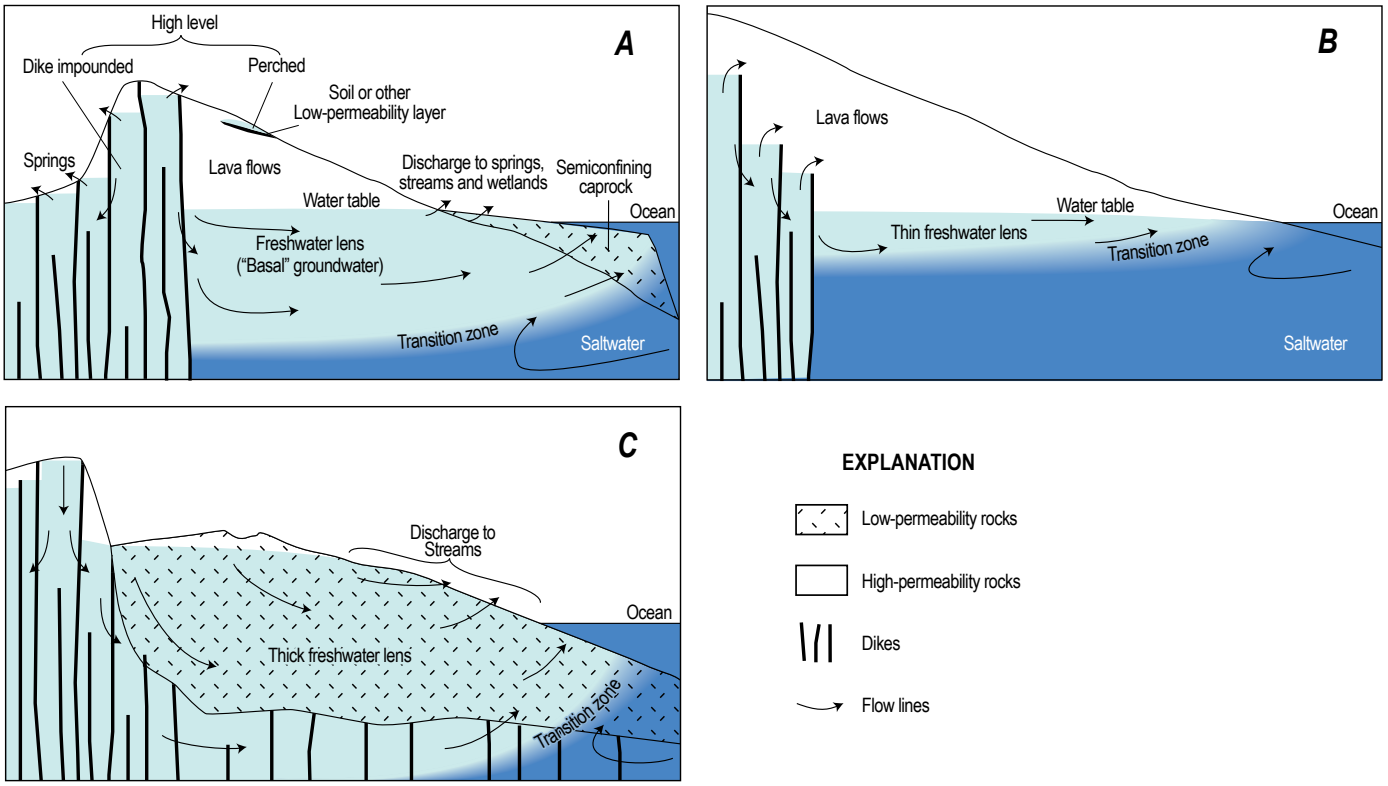

Figure 62. Conceptual models of groundwater occurrence and flow in Hawai'i. (*A*) General conceptual model from about the early to middle 20th century. On O'ahu, the low-permeability caprock is composed of coastal-plain sediments and rejuvenated volcanic rocks. (*B*) Conceptual model of a young shield volcano with no confining caprock, and where most dikes have not been exposed by erosion. (*C*) Conceptual model for areas with substantial low-permeability rock and a thick freshwater lens. In the Līhu'e basin, Kaua'i, the low-permeability rock is made of rejuvenated-stage lava flows and sediments that filled a pre-existing topographic depression, and the underlying shield-stage lava flows also have low permeability as a result of dike intrusion.

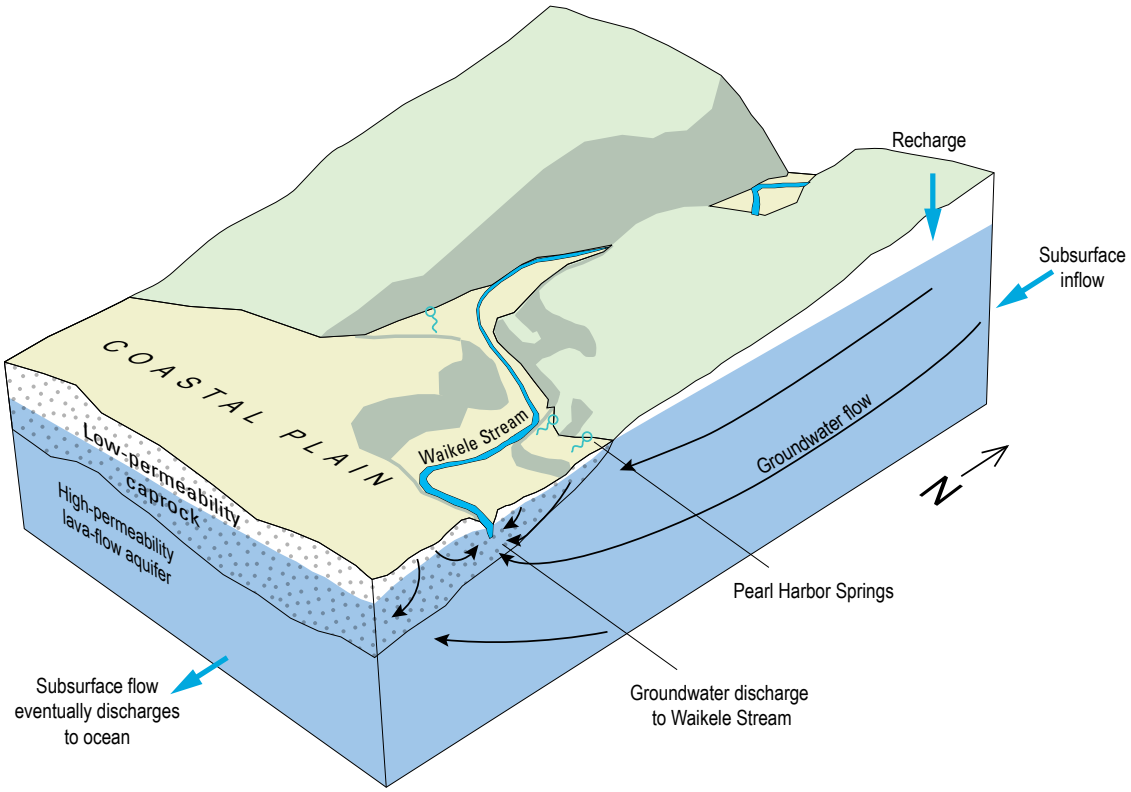

Figure 63. Block diagram showing relation between groundwater discharge in and near semiconfining caprock overlying the high-permeability lava-flow Pearl Harbor aquifer, O'ahu, Hawai'i. Modified from Anthony and others (2004).

Flow-duration curves from streamflow records are a convenient method for comparing stream reaches that do and do not receive substantial amounts of groundwater. The flow-duration curves in figure 64 were constructed from daily-mean discharge data from selected continuous-record stream gages representing various hydrogeologic settings in Hawai‘i. These cumulative-frequency curves show the percentage of time specified discharges were equaled or exceeded during a given period. Plotted on a log-probability graph, curves from gages where streamflow has a substantial groundwater component tend to have an elevated low-flow end (right side). In contrast, the low-flow end of curves from gages on reaches without a substantial groundwater component slope steeply downward. Comparison of the flow-duration curves of gages 16213000 and 16212800 show how groundwater discharge to a stream reach depends on location (fig. 61). Gage 16213000 on Waikele Stream is on the semiconfining caprock downstream from the Pearl Harbor Springs. The upward turn of the flow-duration curve for this gage indicates substantial groundwater discharge (the downward turn at the lowest part of the curve probably reflects small diversions upstream of the gage). On the other hand, gage 16212800 on Kīpapa Stream is several miles inland from the Pearl Harbor Springs on a losing reach high above the water table of the freshwater lens; its relatively straight, steep flow-duration curve indicates no substantial groundwater discharge.

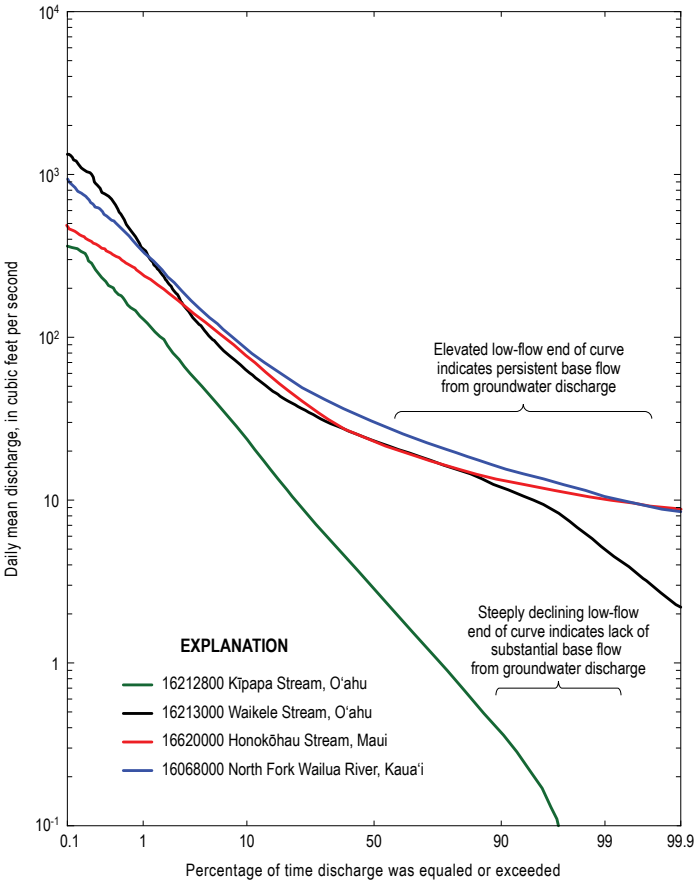

Figure 64. Flow-duration curves calculated from daily mean discharge data for the complete periods of record for selected stream gages in Hawai‘i. Gage locations are shown on figure 61.

The coastal aquifers of O‘ahu are classic examples of high-permeability lava-flow aquifers in which relatively thick freshwater lenses have developed behind extensive caprock—in this case, coastal-plain deposits that almost completely encircle the island (figs. 61 and 63). The combination of a thick freshwater resource in a high-permeability aquifer allows some wells to produce millions of gallons per day each with relatively little drawdown and reduced threat from saltwater intrusion—especially when shafts and galleries are used. These aquifers form the extensive groundwater resources on which O‘ahu’s large population, commerce, and military rely. The Pearl Harbor aquifer, the most heavily used aquifer in Hawai‘i (Oki, 2005), is an example of a freshwater lens in a high-permeability lava-flow aquifer whose groundwater resources are enhanced by the presence of caprock. High-permeability aquifers partly overlain by semiconfining caprock also occur in southwestern Kaua‘i, in the isthmus between West Maui volcano and Haleakalā, and on the southwestern coast of West Maui volcano.

Early workers on O‘ahu (for example, Palmer, 1927, 1946; Stearns and Vaksvik, 1935) referred to the parts of the groundwater resources overlain by caprock as “artesian” because wells penetrating through the caprock commonly had water levels above land surface and flowed without pumping. Water levels above land surface are also known from some wells drilled through the caprock in southwestern Kaua‘i and the Maui isthmus.

Some freshwater lenses on O‘ahu and Maui are subdivided by alluvial valley fill and weathered rock that form low-permeability flow barriers that partly penetrate the top of the freshwater lens (fig. 65*A*). In plan view, these barriers follow the radial pattern characteristic of stream erosion on Hawaiian shield volcanoes, which also roughly parallels the seaward direction of groundwater flow (fig. 65*B*). The barriers allow slight differences in water-table altitudes (and lens thickness) between adjacent areas, referred to as isopiestic areas in some literature (Palmer, 1927). The low-permeability alluvial fill also contains a small amount of groundwater that stands higher than groundwater in the freshwater lens.

Effects of Withdrawal and Limits to Groundwater Availability—The effects of new or increased withdrawals from a lens in a high-permeability lava-flow aquifer include (1) the lowering (drawing down) of the water table, (2) the rise of the transition zone and saltwater, and ultimately (3) a decrease in the natural groundwater discharge to springs, streams, wetlands and submarine seeps near the coast. Thin freshwater lenses in areas without caprock are particularly susceptible to saltwater intrusion, and the effects on well water quality may be a primary limiting factor on groundwater availability. Also in areas with no caprock, most of the groundwater commonly discharges below sea level, so the effects of reduced submarine groundwater discharge may be another limiting factor on groundwater availability. On the west coast of Hawai‘i Island, for example, concerns have been raised about the impact of groundwater development on ecosystems adapted to the brackish water that forms when freshwater from the lens mixes with seawater (Oki, 1999; Oki and others, 1999b).

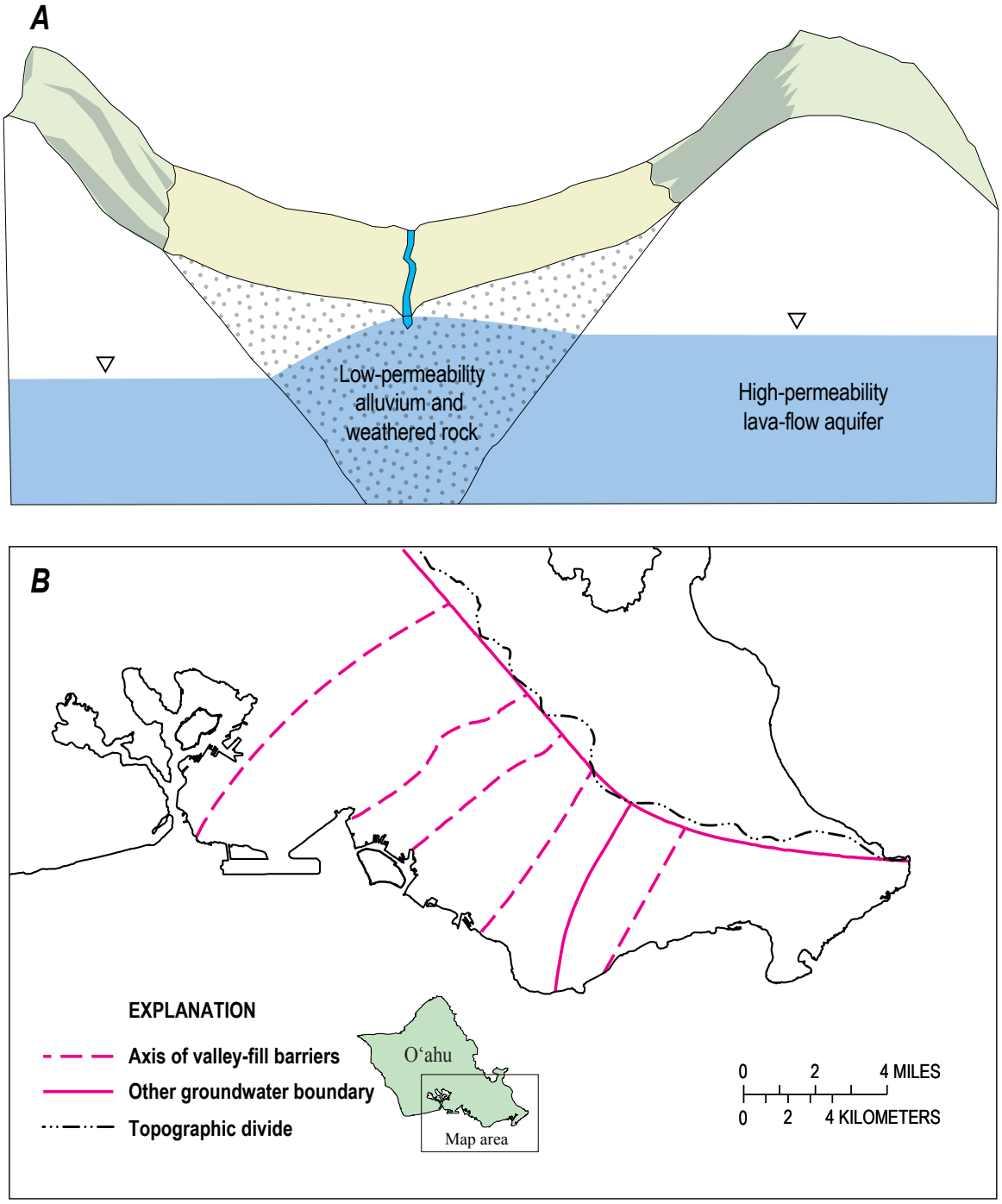

Figure 65. Groundwater barriers created by valley-filling alluvium in Hawai‘i. (*A*) Block diagram showing a groundwater flow barrier in the freshwater lens created by valley-filling alluvium and weathered rock. (*B*) Subdivisions within the freshwater lens of southern O‘ahu created by flow barriers composed of low-permeability valley fill. Modified from Oki (2005).

In areas with substantial caprock, effects related to water-table decline and saltwater rise are partly mitigated by the thicker freshwater lens that forms. In a thick freshwater lens, wells are less susceptible to saltwater intrusion even when pumped at high rates. Even so, the salinity of some wells has risen over decades of groundwater development (Hunt, 1996; Oki, 1999), and dozens of deep monitoring wells have been drilled to track the movement of the transition zone and underlying saltwater in heavily used aquifers on O‘ahu and Maui (Rotzoll, 2010). Data from these wells indicate that most freshwater lenses have been shrinking over the past 40 years (Rotzoll and others, 2010). Gingerich and Voss (2005) used a 3-dimensional numerical simulation to show how the freshwater lens in the Pearl Harbor aquifer changed in response to well withdrawals.

Where fresh groundwater discharges above sea level, the effects of reduced discharge to springs, streams, and wetlands may become a limiting factor on groundwater availability. Groundwater still discharges below sea level, however, so the effects of reduced coastal groundwater discharge remain a potential limiting factor.

Groundwater Impounded by Dikes

Groundwater occurrence and flow near the center of Hawaiian shield volcanoes is, or is presumed to be, affected by low-permeability dikes (figs. 61 and 62). Although high concentrations of dikes can substantially reduce the bulk permeability and storage of an aquifer, a few widely spaced dikes intruded into an otherwise porous, high-permeability aquifer can increase the storage of the aquifer by impounding groundwater to hundreds or thousands of feet above sea level. Most of the water moves and is stored in permeable lava flows between the dikes, but the dikes form vertical barriers of low-permeability rock behind which fresh groundwater is stored. The system of dikes and intervening porous, high-permeability lava flows is sometimes conceptualized as “dike compartments,” although a “compartment” may not be closed on all sides by dikes, and the dikes are leaky. The water resource in this setting is commonly referred to as dike-impounded groundwater (Takasaki and Mink, 1985).

Regions with dike-impounded groundwater usually have the highest groundwater levels in an island, and some are under high-rainfall areas. As a result, inflow to dike-impounded groundwater areas is mostly from recharge through the ground surface. Groundwater flows from higher compartments to lower compartments, and eventually flows out of the dike-impounded groundwater area to adjacent groundwater bodies—such as freshwater lenses—at lower altitudes (figs. 61 and 62). Dike-impounded water can also discharge directly into the ocean. In younger volcanoes where most dikes remain unexposed by erosion (fig. 62*B*), most of the groundwater exiting the dike compartments flows though the subsurface. Some water seeps through the dike rock itself, but most of the water probably flows over the top or around the dikes (Macdonald and others, 1960). In areas where erosion has carved into water-bearing dike compartments, groundwater not only exits through the subsurface, but also discharges to springs and streams, into overlying rocks such as sediments, and directly to the ocean. Groundwater levels in a dike compartment are thus limited by the altitude of the top of the dike, the altitude to which erosion has cut into the dike compartment, or the altitude of overlying semiconfining units such as alluvium.

Where erosion has cut into dike-impounded groundwater, streams typically have substantial base flow. For example, characteristics indicative of substantial groundwater discharge are evident in the flow-duration curve for stream gage 16620000 on Honokōhau Stream in the dike-impounded groundwater area of West Maui (figs. 61 and 64). Some longer streams originate in the dike-impounded groundwater areas, then flow over areas of high-permeability dike-free lava flows. These streams gain from groundwater seepage in the upper reaches where they incise saturated dike compartments, but lose water back into the ground over the dike-free aquifer where the water table of the freshwater lens is lower than the stream (fig. 66).

Most of the present knowledge of the relation between dikes and groundwater comes from the extensively exposed dike complexes on O‘ahu. The areas of dike-impounded groundwater for O‘ahu shown in figure 61 include the dike complexes, marginal dike zones, and dike-intruded areas beneath former calderas. The permeability of dike-intruded areas and their ability to store groundwater depend on the volume of the aquifer occupied by dikes relative to that occupied by high-permeability lava flows. Permeability and storage are low where dikes are densely clustered, such as in the center of the dike complexes and in the sites of former calderas. Permeability and storage are larger in the marginal dike zone, where there are fewer dikes and larger volumes of high-permeability lava flows between the dikes. Groundwater levels in the marginal dike zones of O‘ahu stand hundreds of feet higher than they would without the dikes, thereby increasing the volume of stored fresh groundwater by hundreds of billions of gallons (Takasaki and Mink, 1985). Because dikes on O‘ahu are oriented roughly parallel to each other and to the ancient rift zones, groundwater flow is preferential along the strike of the dikes (Hirashima, 1962).

Dike-impounded groundwater bodies exist on other islands, although they have not been developed for human use on these islands as much as on O‘ahu. The dikes on Kaua‘i and West Maui are not organized into linear rift zones. The areas of dike-impounded groundwater on these volcanoes are roughly ovate, although the boundary of the dike zone of Kaua‘i is uncertain because most of it is obscured by younger rocks (fig. 61). Macdonald and others (1960) attributed high-level groundwater along the Nāpali Coast and in the Makaleha Mountains of Kaua‘i (fig. 23) to groundwater impounded by dikes, but considered most of the island unfavorable for the existence of large volumes of dike-impounded water. Stearns and Macdonald (1942) described springs and water-development tunnels that tapped dike-impounded groundwater in West Maui, and speculated that large amounts of dike-impounded groundwater exist in the principal rift zones of Haleakalā. Stearns and Macdonald (1946) described springs and groundwater discharge to streams fed by dike-impounded groundwater in Kohala volcano on Hawai‘i Island, and a tunnel designed to tap those resources. Thomas and

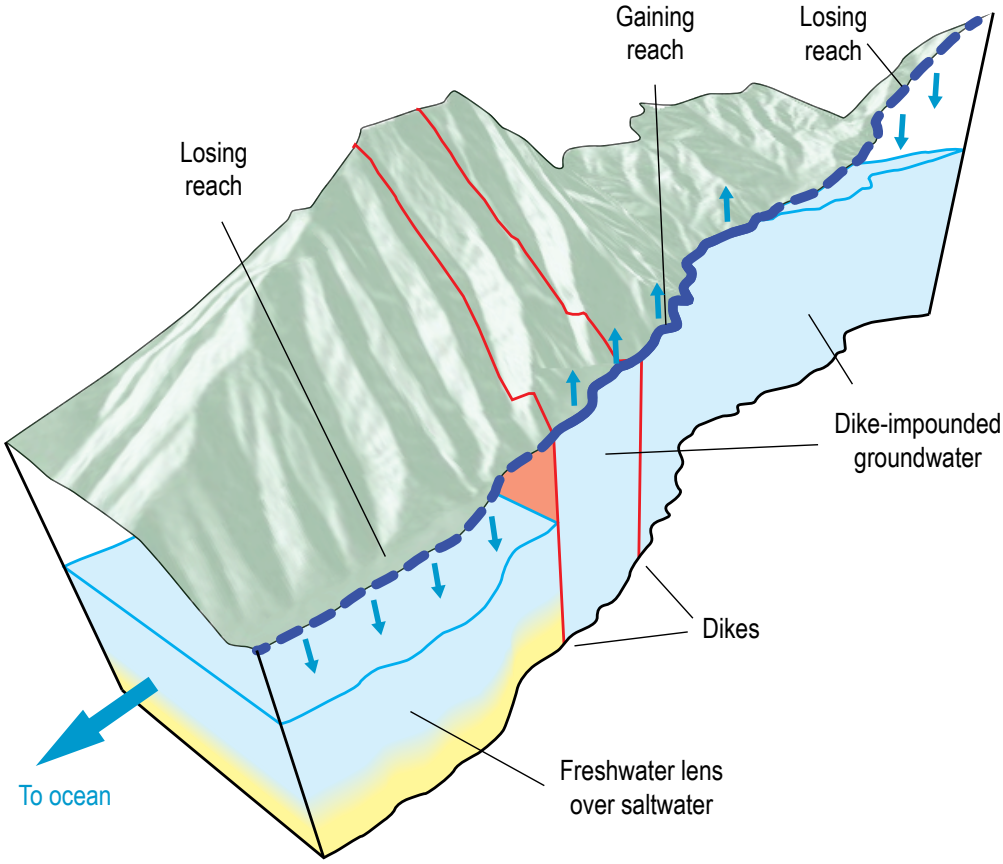

Figure 66. Block diagram, cut along the course of a stream, showing the relation between dike-impounded groundwater and losing reaches (dashed line and downward flow arrows) and gaining reaches (solid line and upward flow arrows) of a stream in Hawai‘i. Modified from Oki and others (2010).

Haskins (2013) interpreted a groundwater level at about 4,600-ft altitude in a deep scientific drill hole in the saddle between Mauna Loa and Mauna Kea on Hawai‘i Island (PTA in fig. 44) to be dike-impounded water. Pierce and Thomas (2009), interpreting electrical-resistivity data, suggested that groundwater exists a few hundred to a few thousand feet above sea level at other areas along the saddle, but whether these high water levels are the result of dike impoundment is not known.

How deep the dike-impounded freshwater extends below sea level is not known. Researchers have postulated that at some depth, effective porosity will diminish to zero for one or a combination of reasons, including (1) dikes will be so densely packed that the rock is effectively impermeable, (2) rocks erupted under water presumably have lower permeability, and (3) alteration and secondary mineralization will fill void spaces (Takasaki and Mink, 1985; Kauahikaua, 1993; Moore and Trusdell, 1993). In most conceptualizations of groundwater that is impounded to high altitudes by dikes in Hawai‘i, fresh groundwater is presumed to extend at least several thousand feet below sea level, through the entire depth that groundwater is significantly mobile.

Effects of Withdrawal and Limits to Groundwater Availability—The effects of new or increased withdrawal from dike-impounded groundwater include (1) depletion of storage, (2) depletion of natural spring flow and stream base flow, and (3) reduction of subsurface groundwater flow to adjacent aquifers. Saltwater encroachment is not likely to be a major limiting factor in this setting, except near the coast. However, whereas subsurface flow from dike-impounded groundwater can constitute a substantial part of the total flow thorough an adjacent freshwater lens, development of dike-impounded groundwater can reduce the flow in the freshwater lens, and in turn affect the salinity of water pumped from wells. These impacts may present limitations on groundwater availability from dike-impounded systems.

Development of dike-impounded groundwater by tunnels on the windward side of the Ko‘olau Range on O‘ahu has resulted in measurable depletion of groundwater storage and reductions in stream base flow (Hirashima, 1962, 1965, 1971; Yeung and Fontaine, 2007). Reductions in stream and spring flow are not only apparent immediately adjacent to the tunnels, but have been detected in streams as much as 2.5 mi away (Hirashima, 1962). Storage depletion has resulted in diminished yields from water-development tunnels (Hirashima, 1971); attempts to stem storage depletion by installing bulkheads have had limited success (Takasaki and Mink, 1985). The effects of storage depletion and reduced discharge to springs and streams may, therefore, constitute limiting factors to groundwater availability from dike-impounded groundwater systems, especially those that have been dissected by erosion and contribute substantially to stream base flow.

Thickly Saturated Low-Permeability Lava-Flow Aquifers

Some lava-flow aquifers have low permeability, even though they are not intruded by dikes. The Līhu‘e basin on Kaua‘i (and likely much of the eastern part of the island) has the most extensive and best known example of this mode of groundwater occurrence in Hawai‘i (Izuka and Gingerich, 1998b; 2003) (fig. 61). In general, well yield is low and drawdown is high in low-permeability aquifers; this is evident in eastern Kaua‘i, where measured hydraulic conductivities are typically lower than they are elsewhere on the island. Even so, the low-permeability aquifer in the Līhu‘e basin is an important source of water for the commerce and population in eastern Kaua‘i. Because of the low permeability and high groundwater-recharge rates on the wet, eastern side of Kaua‘i, groundwater thickly saturates the aquifer to hundreds of feet above sea level (fig. 62*C*)—much higher than in high-permeability dike-free lava flows discussed previously. The high water levels were once interpreted as part of perched groundwater systems, but several lines of evidence including numerical-modeling analysis showed that the high water levels are part of a thick freshwater lens. The Nāhiku area on the northeastern coast of Haleakalā volcano on Maui probably also has a thickly saturated low-permeability lava-flow aquifer (Gingerich, 1999c; Meyer, 2000; Scholl and others, 2002); however, the hydrogeologic reason for the low permeability in that area is not definitively known.

In the Līhu‘e basin (fig. 61), rejuvenated-stage lavas of the Kōloa Volcanics ponded in pre-existing depressions to form thick, low-permeability lava flows interbedded with lesser amounts of low-permeability sediment (Izuka and Gingerich, 1998b, 2003). The pile of thick lava flows and sediments (referred to as the Kōloa HGU in the *Hydrogeologic Framework* section of this report) has hydraulic conductivities that are several orders of magnitude lower than those of the high-permeability dike-free lava-flow aquifers that are more common in Hawai‘i. As a result, head gradients in both the horizontal and vertical directions are steep in the low-permeability aquifer of the Līhu‘e basin, and groundwater saturates nearly to the land surface (figs. 62*C* and 67). The water table is kept just below most of the land surface by the draining action of streams that have incised the saturated groundwater body. The shape of the top of the saturated groundwater body is thus dictated largely by the land-surface topography.

The fresh groundwater body in the Līhu‘e basin near the coast may be underlain by a transition zone and saltwater (fig. 62*C*), but whether mobile saltwater also exists farther inland beneath areas where the water table is hundreds of feet

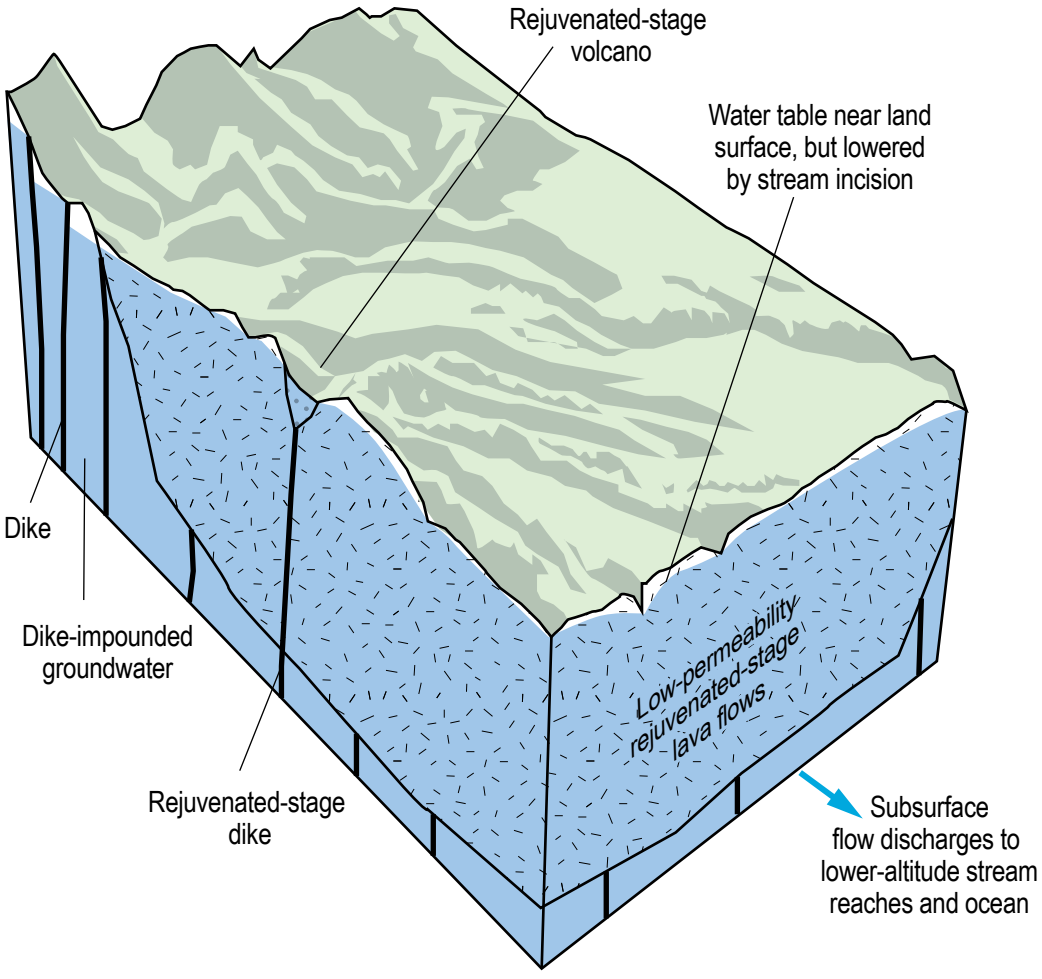

Figure 67. Block diagram showing the setting for thickly saturated low-permeability lava flows in the Līhu‘e basin, Kaua‘i, Hawai‘i.

above sea level is not known. The Ghyben-Herzberg relation indicates that a freshwater lens with such a high water table would reach tens of thousands of feet below sea level within five (horizontal) miles of the coast, but the relation is invalid here because vertical head gradients in the low-permeability aquifer are steep (Izuka and Gingerich, 1998a,b). In addition, the bottom of the thick freshwater body is likely to be limited by diminishing rock porosity with depth, as is dike-impounded groundwater. Numerical models of the Līhu‘e basin (for example, Izuka and Gingerich, 1998a) have placed a no-flow boundary at about 6,000 ft below sea level on the basis of drill-core porosity and geophysical data; a similar no-flow boundary, based on seismic data, has been used in numerical models of O‘ahu (Souza and Voss, 1987; Oki, 1998, 2005).

The thickly saturated low-permeability lava-flow aquifer in the Līhu‘e basin receives water from surface recharge and subsurface flow from dike-impounded groundwater (figs. 61 and 62*C*). The groundwater flows from recharge areas on land toward the coast, where it naturally discharges to streams and the ocean. Because the top of the saturated aquifer is drained by streams, most of the groundwater flowing though the aquifer discharges above sea level rather than below (Izuka and Gingerich, 1998b, 2003). The flow-duration curve for gage 16068000 on North Fork Wailua River, for example, shows an elevated low-flow end characteristic of streams receiving substantial groundwater (figs. 61 and 64). Streams thus provide the primary means by which groundwater discharges naturally from the thickly saturated aquifer.

Effects of Withdrawal and Limits to Groundwater Availability—Inasmuch as streams are the primary means by which groundwater discharges from the thickly saturated low-permeability system, increasing groundwater withdrawal from the aquifer is likely to have substantial effects on stream base flow. Numerical-model simulations of the Līhu‘e basin showed that the pumping effects of new wells will spread until they cause a reduction in natural groundwater discharge equal to the pumping rate, and 95 to 100 percent of this reduction will occur at streams (Izuka and Oki, 2002). The simulations also showed that the effects may take decades to develop fully, and, depending on the placement of wells and pumping rates, may be distributed among several streams. In any case, limitations placed on stream depletion can constitute a major limitation to groundwater availability from low-permeability aquifers.

Whereas drawdowns tend to be high in low-permeability aquifers, concerns over declining groundwater levels may also limit groundwater availability. Groundwater levels in the Līhu‘e basin declined after a number of new wells were constructed between the 1960s and 1980s, but the declines also coincided with decreased application of diverted stream water for irrigation and a prolonged period of low rainfall in the 1990s–2000s. Numerical simulations of the various factors that could have caused the groundwater-level decline indicated that increases in groundwater withdrawal had a small effect compared to the effects of irrigation reduction and low rainfall; however, the total simulated well withdrawal inside the basin was only 2.4 Mgal/d (Izuka, 2006).

Assessing the limitations to fresh groundwater availability related to pumping-induced rise or encroachment of saltwater is difficult because it is not known whether saltwater underlies the freshwater body except very near the coast. No wells in the central part of the Līhu‘e basin have reached brackish water or saltwater, and the inapplicability of the Ghyben-Herzberg relation in low-permeability aquifers makes it difficult to estimate how far below sea level the freshwater body extends. Numerical modeling indicates that fresh groundwater in most of the Līhu‘e basin extends down to thousands of feet below sea level (Izuka and Gingerich, 1998a). Meyer (2000) used an equation relating the freshwater-saltwater interface depth to water-level declines measured during well drilling (Izuka and Gingerich, 1998b) in order to estimate that freshwater in the Nāhiku area extends from about 400 to 1,000 ft below sea level. Considering the overall thick freshwater saturation in most areas of these low-permeability aquifers, saltwater rise or encroachment is less likely to constitute a major limitation to groundwater availability; however, because most fresh groundwater discharges to streams, the freshwater lens likely thins rapidly near the coast and saltwater intrusion can still limit productivity of wells near the coast.

Perched Groundwater

Perched groundwater is a body of saturated groundwater that is held up or “perched” by a low-permeability layer encased within a body of higher permeability rock (fig. 62*A*). By definition, perched groundwater is separated from underlying groundwater bodies—such as the freshwater lens—by unsaturated rock (Meinzer, 1923b). Confirming whether unsaturated rock exists beneath a suspected perched groundwater body is difficult, however. Seepage from a hillside spring may appear to be perched above unsaturated rock, but the apparent unsaturated zone may not extend very far into the hillside; deeper in the hill, the water body feeding the spring may be a part of a system that is fully saturated down to sea level. Water levels that appear to decline during well drilling as the hole is deepened (sometimes resulting in water cascading down the bore hole) have been cited as evidence of perching, but water-level declines—even abrupt ones—also can occur during well drilling in a fully saturated system if vertical head gradients are steep, such as in low-permeability aquifers (Izuka and Gingerich, 1998a, 2003; Gingerich, 1999b; Meyer, 2000). In some cases, high-altitude water levels in wells were assumed to be perched because conceptual models in existence at that time had no other mechanism to explain high-level groundwater in dike-free lava flows.

Because confirmation of the perched condition is problematic, the areas of perched water shown in figure 61 are only postulated, and only the largest areas are shown. Notable regions of presumed perched groundwater include the eastern flanks of Mauna Kea and Mauna Loa, where tunnels have been constructed to develop groundwater presumed to be perched on the Pāhala Ash (Stearns and Macdonald, 1946). A large area of perched groundwater is also postulated on the northern part of Haleakalā where it discharges to springs and supports perennial streamflow; outcrops and drilling data indicate the water is

perched on thick-bedded low-permeability lava flows underlain by thin-bedded high permeability flows (Gingerich, 1999b,c; Scholl and others, 2002). Even these larger perched groundwater bodies, however, are thin and store much less water than those in other modes of groundwater occurrence. Storage and flow in perched groundwater bodies is susceptible to variations in rainfall.

Inflows to perched groundwater bodies come from recharge through the surface. Natural outflows from perched groundwater bodies include discharge to high-altitude springs and stream seepage. Groundwater also passes though and around the low-permeability perching layer, travels downward through the unsaturated zone, and eventually contributes to underlying groundwater bodies such as freshwater-lens aquifers. Thus, even though perched groundwater bodies are thin and small, the water that passes through them may constitute a substantial part of the inflow to larger groundwater bodies. Gingerich (1999c) estimated that even though an extensive perched groundwater system exists in the northern part of Haleakalā, more than 90 percent of the recharge in the area near Ha‘ikū eventually flows down to the freshwater lens.

Effects of Withdrawal and Limits to Groundwater Availability—Whereas much of the perched groundwater is ultimately on its way to recharge the underlying freshwater lens, withdrawal of perched groundwater indirectly takes some of the water from the freshwater lens. If the perched groundwater body overlies a large part of a freshwater lens, withdrawing from the perched groundwater can substantially reduce the flow in the freshwater lens. Thus, concerns over reducing recharge to the freshwater lens, and the effects of such a reduction, can be a limiting factor to groundwater availability from perched systems. Also, withdrawal of perched groundwater can cause reductions in the natural spring discharge and stream seepage; thus, any limitations placed on streamflow depletion can constitute a limitation to the groundwater availability from perched aquifers.

Groundwater Enigmas

Groundwater occurrence and movement are not completely understood in a few areas of Hawai‘i. The lack of understanding limits the ability to assess the availability of groundwater resources in these settings. In some cases, such as the interior of Hawai‘i Island, the lack of understanding results from a lack of hydrologic data. But in other cases, hydrologic data are available but do not fit into one of the four conceptual models of groundwater occurrence presented above.

Schofield High-Level Groundwater

In 1936, a groundwater level of 276 ft was discovered beneath the Schofield Plateau in central O‘ahu (fig. 61). Data from subsequent well construction showed a remarkably uniform water table at about 270 to 290 ft altitude over a 36-mi^2 area. This high-altitude groundwater body has come to be known as the Schofield high-level groundwater. The high water levels are anomalous because they were not expected in what had been presumed to be a high-permeability dike-free lava-flow aquifer. North and south of the Schofield high-level groundwater, water levels decline steeply toward the lower water levels in adjacent freshwater lenses (fig. 34). To the east and west, the Schofield high-level groundwater is bounded by the dike-impounded groundwater of the Ko‘olau and Wai‘anae Ranges.

The Schofield high-level groundwater is not within any of the major rift zones of the Ko‘olau or Wai‘anae volcanoes. Also, the relatively high hydraulic conductivities indicated by the high specific capacities of wells over most of the area (Rotzoll and El-Kadi, 2008) are not consistent with low permeabilities associated with dike zones or thick low-permeability lava flows. Wells drilled to depths below sea level confirmed that the Schofield high-level groundwater was saturated to sea level, and thus was not perched (Stearns, 1940; Oki, 1998). Most conceptualizations suggest that vertical low-permeability “groundwater dams” form the north and south boundaries of the Schofield high-level groundwater (fig. 61), but the geologic nature of the dams, and their precise location if they exist, are not known. Oki (1998) summarized hypotheses offered in previous literature to explain the geologic origin of the dams; these hypotheses include stray dikes striking transversely to the trend of the main Ko‘olau and Wai‘anae rift zones, and former ridge spurs of the Wai‘anae Range that have been buried by younger Ko‘olau lava flows. He also cited aquifer-test data that indicate the dams have a “compartmental nature” that is similar to compartments in the marginal dike zone. Some hypotheses are unrelated to the dam conceptualization, attributing the high water levels to a low-permeability weathered horizon between the Wai‘anae and Ko‘olau lava flows.

Because of its intermediate water levels and location relative to other groundwater bodies, inflow to the Schofield high-level groundwater comes from recharge through the surface, and subsurface flow from the dike-impounded groundwater bodies in the Wai‘anae and Ko‘olau Ranges (fig. 61). The Schofield high-level groundwater is landlocked and the water table is hundreds of feet below the land surface, so the only means of natural outflow from the groundwater body is through the subsurface to adjacent freshwater lenses in high-permeability lava-flow aquifers to the north and south. To the south is the heavily used Pearl Harbor aquifer, which receives about 31 percent of its total flow from the Schofield high-level groundwater (Oki, 2005).

Effects of Withdrawal and Limits to Groundwater Availability—Withdrawal from the Schofield high-level groundwater will result not only in storage depletion within the high-level groundwater body, but also in the reduction of groundwater flow to adjacent aquifers to the north and south; ultimately affecting the groundwater availability from those aquifers. Whether the effects will spread more to the north or to the south, or be distributed relatively equally between them, depends on the nature of the geologic structures causing the high-level water. Inasmuch as the nature of the structures is uncertain, so are the effects on groundwater availability.

Kona High-Level Groundwater

Well drilling in the early 1990s discovered anomalously high groundwater levels on the west flank of Hualālai (figs. 46 and 61) (Oki, 1999; Bauer, 2003). Wells at a relatively short distance (about 2 to 5 mi) inland from the coast have water levels that are several tens to hundreds of feet above sea level—much higher than would be expected if the area was underlain by a high-permeability dike-free aquifer. The anomalously high water levels indicate the presence of buried low-permeability structures that locally impede seaward groundwater flow. The areal extent of the Kona high-level groundwater is not fully known. Well data indicate that its seaward boundary trends roughly north-northwest about 2 to 4 mi inland from the coast, but not enough data exist to indicate how far to the north and south, or how far inland, the Kona high-level groundwater extends. No relation has been identified between the Kona high-level groundwater and topography or any geologic features visible at the surface.

The impeding structures have not been identified, although some have been postulated, including intrusive bodies such as dikes, buried low-permeability layers such as ash or unusually dense lava flows, and buried deformation structures such as lava-draped faults (Oki, 1999; Bauer, 2003). Rift-zone traces interpreted from Hualālai's present topography do not come close to the Kona high-level groundwater, but interpretations of gravity data suggest the possibility of dense intrusive rocks in the vicinity of the Kona high-level groundwater (Fiske and Jackson, 1972; Kauahikaua and others, 2000; Flinders and others, 2013). Stearns and Macdonald (1946, p. 149) write that the lavas on Hualālai's west flank "have unusually steep slopes about a mile inland from Keahole Point," and suggest that this may be the result of "steep terminal margins of flows, ancient sea cliffs, or faults, smoothed by later flows," but these features would be west of the western boundary of the Kona high-level groundwater.

The relation between the Kona high-level groundwater and the adjacent coastal aquifer is not well understood. Water levels in the area seaward of the Kona high-level water are mostly less than about 10 ft above sea level (Bauer, 2003), which is consistent with a thin freshwater lens in a high-permeability dike-free aquifer. However, specific-electrical-conductance profiling of the water column in a well recently drilled in the area (fig. 61) indicated the presence of a shallower brackish-water layer and a deeper layer of freshwater separated by saltwater (Tillman and others, 2014). The geology causing brackish water and freshwater to be separated by saltwater, and the extent of hydrologic connection to the high level water, are not known.

Effects of Withdrawal and Limits to Groundwater Availability—Because the hydrogeology of the Kona high-level groundwater is unknown, the effects of groundwater development, and consequent limits to groundwater availability, are difficult to assess. Most conceptual models suggested so far and available geochemical data (Tillman and others, 2014) indicate that some groundwater probably flows from the Kona high-level groundwater body to the coastal freshwater lens in the adjacent high-permeability lava-flow aquifer; thus, withdrawal from the Kona high-level groundwater will affect the coastal freshwater lens. Specific flow rates and flow paths, however, depend on the nature of the structural boundary between the groundwater bodies.

Stacked Freshwater Bodies Near Hilo

The deep HSDP drill holes in Hilo, near the coast in the saddle between Mauna Kea and Mauna Loa on Hawai'i Island (figs. 44 and 61), showed that groundwater in dike-free high-permeability lava flows does not always form a single freshwater lens. Thomas and others (1996) reported that the first of the two holes drilled (HSDP1) penetrated not only a "basal lens" near sea level, but also a deeper freshwater body about 700-ft thick confined beneath a soil layer about 900 ft below sea level between overlying Mauna Loa and underlying Mauna Kea strata. The second, deeper drill hole HSDP2 penetrated several additional freshwater layers separated from each other by saltwater, and there was evidence for freshwater as deep as 7,000 ft below sea level (Stolper and others, 2009).

How the multiple stacked freshwater aquifers fit into the groundwater budget is not completely understood. Stable-isotope and carbon-14-age analyses led Thomas and others (1996) to conclude that the freshwater confined beneath the soil between Mauna Kea and Mauna Loa is part of an actively flowing groundwater system receiving recharge at an altitude of about 7,000 ft and discharging to deep submarine springs. Stolper and others (2009, p. 7) estimated that "flow through [the lower freshwater body] could represent as much as a third of the rainfall-recharge to the windward midlevel slopes of Mauna Kea," but did not describe the basis for this estimate. The estimate is probably high because the confining unit responsible for the lower freshwater body, if attributed correctly to the soil layer between Mauna Loa and Mauna Kea strata, can only exist where the two volcanoes meet—that is, in the saddle south of Mauna Kea—not along the volcano's northeastern windward flank. Even so, the point that some groundwater recharge can flow through freshwater bodies other than the commonly conceptualized freshwater lens is valid. The lack of information needed to quantify flow limits the ability to assess groundwater availability in coastal areas with multiple stacked freshwater bodies.

Study Limitations

This study relies on the availability of various types of physical and historical data. Lack of data or sparse, uneven distribution of data in space and time, and poor understanding of some hydrologically relevant processes limit the precision and accuracy of study results. This section reviews the limitations imposed by the present data availability and current understanding of processes that relate to groundwater availability, and discusses information that could advance future efforts to more accurately assess the availability of groundwater resources in the volcanic rock aquifers of Hawai'i.

Precipitation—Rainfall is an essential dataset for estimating inflow from recharge to the groundwater budget. Although Hawai‘i has a higher number of rain gages per square mile than most other places, the placement of gages and their periods of operation have been dictated by the water-supply needs of humans—particularly for agriculture (Giambelluca and others, 1986). One of the primary sources of rainfall data used in this study, the Rainfall Atlas of Hawai‘i by Giambelluca and others (2013), discusses limitations to rainfall regionalization related to the number and distribution of rain gages and the limited periods of record; these limitations translate to limitations in the recharge results of this study. The online version of the rainfall atlas provides maps of rain-gage locations and uncertainty in the extrapolated rainfall estimates. These maps indicate that rain gages are scarce in areas that are less populated or unfavorable for agriculture, such as in the high-altitude interiors of islands or areas that have rugged terrain. Rainfall estimates for these areas thus have a greater degree of uncertainty, yet these tend to be the wettest areas of the islands and the areas where most recharge occurs. Recharge estimates can be improved with rainfall data from these sparsely gaged areas. The number of rain gages, however, has decreased sharply in the past 30 years, particularly as a result of the discontinuation of gage networks that were maintained by large sugarcane and pineapple plantations and associated irrigation companies (Giambelluca and others, 2013).

Fog-interception data are particularly scant. Fog interception is believed to provide a substantial part of the water available for groundwater recharge over large areas of the Hawaiian Islands, but has been quantified by only a few studies in a few places. As a result, fog-drip distribution was applied in a very generalized fashion in the recharge calculation. Recharge estimates can be improved with a better quantification of the spatial and temporal variability of fog-interception rates, and the ability of different types of vegetation to intercept fog.

Evapotranspiration—An acknowledged limitation of the recharge model is that monthly reference ET is uniformly distributed among each day of the month, regardless of the daily rainfall distribution over the month. In reality, reference ET should be lower during cloudy, rainy days than during sunny days. Recharge estimates could be improved with more measurements of the daily variations of reference ET across the study area.

Another ET-related limitation of this study is the lack of data needed to more accurately differentiate ET parameters among native and alien plant species. Replacement of native forest by invasive alien plants like strawberry guava (*Psidium cattleianum*) is a problem on all of the islands, especially the windward side of Mauna Loa on Hawai‘i Island (Asner and others, 2008). More data could be used to develop better crop coefficients for native and alien plants. These improvements would help to better estimate the difference in recharge that could be expected in native- versus alien-dominated forests.

The accuracy of the modified Gash canopy-interception model used in this study (see appendix 1) is limited by the quantity, quality, and spatial distribution of data used to develop model parameters. Field measurements of one parameter, the ratio of the mean evaporation rate to the mean precipitation rate during saturated canopy conditions (E/R), are especially lacking. Additional measurements of canopy-evaporation and related parameters could be used to better confirm and calibrate the canopy-evaporation estimates of the modified Gash model.

Runoff—Runoff is perhaps the most uncertain parameter in the recharge analysis. The runoff-to-rainfall ratio method in the recharge model used in this study was improved by developing regression equations relating the ratio to drainage-basin characteristics, and using these equations to extrapolate the ratios from gaged to ungaged basins (appendix 1). However, because the number of ungaged basins was far greater than the number of gaged basins, ratios had to be extrapolated to some ungaged basins having characteristic values that were beyond the range of values used to develop the regression equations. Stream-gage data from more basins with a wider range of characteristic values are needed to improve the regression approach to regionalizing runoff ratios. The number of stream gages in Hawai‘i, however, has declined sharply since the 1970s (Oki, 2004b).

The runoff-to-rainfall ratio method used in the recharge model in this study varied the ratios on a seasonal basis with rainfall. Concurrent daily direct-runoff and high-resolution rainfall data could improve the understanding of the processes controlling temporal variability in runoff estimates.

Development of the regression equations suggested that runoff in windward and leeward basins differ statistically. Better understanding of the physical basis of this statistical difference would improve conceptualization of runoff processes.

The recharge model used in this study applies the runoff-to-rainfall ratios at the basin level, that is, ratios do not vary spatially within a basin, even though the basin may encompass a range of climates and a variety of land covers, soil types, and slopes. The basin-level application of runoff-to-rainfall ratios limits the model's ability to assess differences in runoff and groundwater recharge that may exist between different areas within the basin, such as between forested and deforested areas. Part of the limitation stems from the scarcity of studies assessing the variation in runoff rates for different vegetation, soil, and slope characteristics in Hawai‘i. In a study comparing adjacent deforested rangeland and reforested areas on the south slope of Haleakalā on Maui, Perkins and others (2012, 2014) found that the reforested areas had soil hydraulic properties that favored rapid and deep infiltration of water. This finding suggests that runoff would be lower from the forested area than from the deforested area of their study, but the study did not measure runoff. Better understanding of the processes and distribution of hydrogeological characteristics at the subbasin scale are important for answering questions that are often posed about watershed management, such as the effect of forest restoration on water resources.

Water Use—Quantification of groundwater withdrawals is a critical element for understanding the groundwater budget, the impacts of human activity, and the availability of groundwater resources from Hawai‘i's volcanic aquifers. Surface-water use also is relevant to the assessment of groundwater-resource availability because surface water used for irrigation can artificially enhance groundwater recharge. Records of reported water use are, however, known to be incomplete, particularly

for surface-water withdrawals and for withdrawals by users of small amounts of groundwater. Although various approaches have been used to reconcile the underreporting and improve estimates of water use for the periods of concern in this report, in many cases, reconciliations can only be made broadly at the island scale. Assessment of the effect of human activities on groundwater availability can be made much more accurate with complete location and withdrawal data for all wells, and surface-water use records that include withdrawal rates as well as the rates and locations of applied irrigation. Improving the completeness of water-use reporting is essential to improving the accuracy of groundwater-availability assessments.

Hydrogeology and Conceptual Models—Hydrogeologic understanding of Hawai‘i’s volcanic aquifers relies on surface and subsurface data. Surface geologic information is provided by the geologic maps and descriptions cited in this report, but the hydrologically relevant information that can be interpreted from surface geology may be limited—an example is identification of rift zones that have not been exposed by erosion. Subsurface information is available only in areas penetrated by wells, tunnels, or other excavations, or where geophysical surveys have been conducted. Most wells are near populated areas, and most of the populated areas are near the coast; thus, with the exception of O‘ahu, well data are sparse in island interiors. Geophysical surveys have helped fill the spatial gaps in the well data, but these surveys are also limited in areal extent or resolution, and interpretation of the geophysical data in terms of hydrogeologic structures is not always definitive. Very little subsurface information is available for large regions, especially the high-altitude regions of the less-densely populated islands. As a result, substantial uncertainty exists about the hydrology of parts of Maui and Kaua‘i, and for much of Hawai‘i Island.

The discovery of thick freshwater lenses in low-permeability dike-free aquifers in the Līhu‘e basin on Kaua‘i and the Nāhiku area on Maui, raises the question of whether other high-elevation groundwater bodies once interpreted as perched may be part of thickly saturated low-permeability aquifers. The Līhu‘e and Nāhiku occurrences of thickly saturated low-permeability aquifers are supported by multiple lines of evidence, including analysis of the change in water levels as well borings were deepened, the persistence of high water levels in wells penetrating below sea level, measurements of stream base flow, and determination of aquifer properties from aquifer-test data. Not all occurrences of high-level groundwater bodies have enough data to confirm if they are perched or part of a thickly saturated low-permeability aquifer, yet the distinction relates to the impacts of developing water from these bodies, and in turn the amount of groundwater available for use.

Some unresolved geologic enigmas, such as the origins of the Līhu‘e basin and the Olokele Member on Kaua‘i, have hydrologic implications. In some cases, subsurface information has led to discoveries of other enigmas, such as the high-level groundwater bodies in Schofield and Kona, and the stacked fresh groundwater bodies in Hilo. As long as these enigmas remain unresolved, uncertainty exists about the impacts of groundwater development and the quantity of groundwater available from Hawai‘i’s aquifers. The fact that some of these enigmas have been discovered relatively recently indicates that although much is known about the gross movement and storage of groundwater in Hawai‘i, many details are yet to be discovered. Future drilling and geophysical surveys, especially in areas where subsurface information is lacking, may help resolve these enigmas.

Summary

Volcanic aquifers supply freshwater that supports Hawai‘i’s residents and industries, a large component of the U.S. military in the Pacific, cultural practices, aesthetics and recreation, and aquatic habitats. Hawai‘i’s aquifers have limited capacity to store fresh groundwater because the islands are small and isolated from each other by seawater, and saltwater underlies much of the fresh groundwater resource. Fresh groundwater resources in Hawai‘i are therefore particularly vulnerable to the effects of human activity, short-term climate cycles, and long-term climate change. The availability of fresh groundwater for human use is constrained by the degree to which impacts of groundwater withdrawals are deemed acceptable. Any artificial groundwater withdrawal has effects, such as the lowering of the water table, the rise of saltwater, and the reduction in the natural discharge rate to springs, streams, wetlands, and submarine seeps.

Since humans arrived in Hawai‘i around A.D. 300–700, they have purposefully and inadvertently affected groundwater resources through the introduction of nonnative plants and animals, deforestation, crop irrigation, and groundwater withdrawal. One of the largest impacts during the 19th and 20th centuries came from sugarcane agriculture, which not only withdrew groundwater for irrigation, but also enhanced groundwater recharge by diverting streamflow for irrigation. Sugarcane agriculture declined substantially in the latter 20th century.

Hydrogeology— The principal aquifers of Hawai‘i were built by large shield volcanoes. The aquifers are composed primarily of thin lava flows that are highly permeable. In some areas, low-permeability dikes impede the horizontal flow of groundwater. Dikes are especially numerous beneath rift zones and calderas, and can reduce the bulk permeability and storage of aquifers. At the margins of rift zones, however, a few widely spaced dikes intruding an area of otherwise permeable lava flows can impound groundwater to high levels and thus increase the volume of stored groundwater. Low-permeability ash horizons interlayered within lava-flow aquifers can result in perched groundwater bodies. On some islands, sedimentary rocks and rejuvenated-stage volcanic rocks form a coastal plain. The costal plain deposits constitute a semiconfining unit, locally known as caprock, that impedes natural groundwater discharge to the ocean, thus allowing thicker freshwater lenses to form. In some regions, thick lava flows formed by ponding in preexisting depressions form aquifers that are much less permeable than aquifers formed by thin lava flows.

Groundwater Budget—Because each island in Hawai‘i is surrounded by seawater, fresh groundwater inflow comes almost solely through the surface as recharge. The source of most water for recharge is precipitation, but irrigation and water-system leaks also contribute to recharge. Waste-water injection contributes a small percentage to inflows. Outflows from the fresh groundwater system include withdrawals from wells and natural groundwater discharge to springs, streams, wetlands, and submarine seeps. Any new well withdrawal or increase in well withdrawals is eventually compensated by an equal reduction of natural groundwater discharge.

Precipitation distribution in Hawai‘i is influenced by the orographic effect, which results in a sharp contrast between dry leeward and low-elevation areas on one hand, and wet mountain peaks and windward slopes on the other. Orographic rainfall is limited to below 7,200 ft altitude by the trade-wind inversion; thus, the peaks of the highest mountains are arid. Occasional migratory storm systems also bring precipitation to the islands. The climate in Hawai‘i varies with multi-year cycles linked to the El-Niño-Southern Oscillation (ENSO) and the Pacific Decadal Oscillation (PDO), and monitoring data indicate a long-term-average drying trend over the last century. Climate change from anthropogenic greenhouse-gas emissions are likely to affect Hawai‘i’s precipitation in the future.

In this study, groundwater budgets (inflows and outflows) were estimated for predevelopment (1870) and recent (2010 land cover and 1978–2007 rainfall for Kaua‘i, O‘ahu, and Maui; 2008 land cover and 1916–1983 rainfall for Hawai‘i Island) conditions. Estimates of mean annual groundwater recharge for predevelopment conditions are 871 Mgal/d for Kaua‘i, 675 Mgal/d for O‘ahu, 1,279 Mgal/d for Maui, and 5,291 Mgal/d for Hawai‘i Island. In total, the four islands received 8,116 Mgal/d of groundwater recharge in predevelopment conditions. Estimates of mean annual groundwater recharge for recent conditions are 875 Mgal/d (33.2 in/yr) for Kaua‘i, 660 Mgal/d (23.3 in/yr) for O‘ahu, 1,308 Mgal/d (37.7 in/yr) for Maui, and 6,595 Mgal/d (34.4 in/yr) for Hawai‘i Island. Predevelopment and recent recharge values differ by only a few percent for all islands except Hawai‘i Island, where the substantial difference has been attributed to differences in forest cover. Recharge distributions under both predevelopment and recent conditions mimic that of rainfall—recharge is high on windward slopes and mountain tops below the top of the trade-wind inversion. The exception is where other sources of water, such as irrigated fields and leaky reservoirs and taro fields, contribute to recharge.

Groundwater withdrawal from wells for the recent period (2000–2010) averaged 19 Mgal/d on Kaua‘i, 209 Mgal/d on O‘ahu, 104 Mgal/d on Maui, and 103 Mgal/d on Hawai‘i Island (groundwater withdrawal during predevelopment conditions is assumed negligible). The total recent groundwater withdrawal for the four islands in this study is 435 Mgal/d, or only about 5 percent of total recharge (9,438 Mgal/d). About half of the total withdrawal, however, comes from O‘ahu, yet O‘ahu’s recharge constitutes only 7 percent of the total recharge. O‘ahu’s withdrawals constitute 32 percent of the island’s average recent recharge, whereas withdrawals on Kaua‘i, Maui, and Hawai‘i Island are each only 2 to 8 percent of their respective recharge values. Because no freshwater flows between islands, effects of high withdrawals on O‘ahu cannot be mitigated by the lower withdrawals on other islands. Even within an island, high withdrawals from one area cannot be completely mitigated by flow from adjacent areas, and effects will be focused in the areas close to the high withdrawal. If withdrawals are maintained until a steady state is achieved, natural groundwater discharge to springs, streams, wetlands, and submarine seeps will be reduced by an amount equal to the total groundwater withdrawal rate. Assessing the effects of unevenly distributed groundwater withdrawal requires a tool, such as a numerical groundwater model, that can comprehensively analyze spatially distributed factors.

Water-level data from selected wells in Hawai‘i’s volcanic aquifers indicate an overall reduction in storage for most areas where groundwater has been developed. Data from deep monitor wells have shown a general rise in the transition zone and diminished fresh groundwater storage. Declining groundwater storage is also evident in diminished streamflow.

Conceptual Models—Groundwater occurrence and movement in Hawaiian volcanic aquifers can be discussed in terms of four principal conceptual models: (1) fresh groundwater lenses in high-permeability lava-flow aquifers, (2) aquifers with groundwater impounded by dikes, (3) thickly saturated low-permeability aquifers formed mostly by lava flows but also sediment, and (4) perched aquifers. Much of Hawai‘i’s fresh groundwater resources exist in the dike-free high-permeability lava flows of the shield volcanoes, where freshwater lenses overlie saltwater. The water tables of the lenses have gentle gradients and are generally less than 50 ft above sea level. The aquifers receive inflow from groundwater recharge and adjacent up-gradient groundwater bodies (commonly dike-impounded groundwater). Groundwater naturally discharges at or near the coast to springs, streams, wetlands, and submarine seeps. Freshwater lenses can be thick where semiconfining caprock resists groundwater discharge near the coast, and thin where caprock is absent. The pairing of high-permeability lava-flow aquifers with extensive caprock is responsible for the highly productive aquifers of O‘ahu. The primary limiting factor on groundwater availability from freshwater lenses in high-permeability aquifers is saltwater intrusion and its effect on water quality. Other limitations may result from reduced groundwater discharge to springs, streams, and wetlands and submarine seeps.

Groundwater impounded by dikes commonly occurs near the center of Hawaiian shield volcanoes. Although high concentrations of dikes can substantially reduce the bulk permeability and storage of an aquifer, a few widely spaced dikes intruded into an otherwise high-permeability aquifer can impound groundwater to hundreds or thousands of feet above sea level and thereby increase the storage of the aquifer by hundreds of billions of gallons. Most of the water moves and is stored in permeable lava flows between the dikes. Inflow to dike-impounded groundwater regions comes almost entirely from recharge. Where dikes have not been exposed by erosion, groundwater flows from the dike compartments though

the subsurface to adjacent lower-altitude groundwater bodies—such as freshwater lenses. Where erosion has exposed water-bearing dike compartments, much of the groundwater discharges to springs and streams, into overlying sediments, and directly to the ocean. Major limiting factors to groundwater availability in areas of dike-impounded groundwater include impacts related to storage depletion, reduction of flow to adjacent aquifers such as freshwater lenses, and reduction of natural groundwater discharge to streams. Saltwater encroachment is not likely to be a major limiting factor except in dike compartments adjacent to the coast.

Thickly saturated, low-permeability dike-free lava-flow aquifers have been identified in some regions of Hawai‘i. The best known example is from eastern Kaua‘i, where rejuvenated-stage lavas ponded in pre-existing depressions to form thick, low-permeability lava flows interbedded with sediment; these deposits have hydraulic conductivities that are several orders of magnitude lower than those of the high-permeability dike-free lava flow aquifers. Groundwater thickly saturates the aquifer to hundreds of feet above sea level and streams provide the primary means by which groundwater discharges naturally from the aquifer. As a result, groundwater withdrawal from the aquifer is likely to have substantial effects on stream base flows. Limitations placed on streamflow depletion can constitute a major limitation to the availability of groundwater from low-permeability aquifers. Drawdowns tend to be high in low-permeability aquifers, therefore concerns over declining groundwater levels may also limit groundwater availability. Saltwater intrusion is less likely to constitute a major limitation to groundwater availability in most parts of these aquifers, but may limit freshwater yields in wells near the coast.

Perched groundwater is postulated to exist in some areas of Hawai‘i, although confirmation is problematic. However, even the largest suspected perched groundwater bodies are thin and store much less water than other modes of groundwater occurrence. Inflows to perched groundwater bodies come from recharge through the surface. Natural outflows include discharge to high-altitude springs and streams; groundwater also passes though the low-permeability perching layer, travels downward through the unsaturated zone, and eventually contributes to underlying groundwater bodies such as freshwater lenses. Withdrawal of perched groundwater by wells therefore takes some of the water from the freshwater lens, and the effects of reducing inflow to the freshwater lens can be limiting factors to groundwater availability from perched aquifers. Also, withdrawal of perched groundwater can cause reductions in natural spring discharge and stream seepage; thus, any limitations placed on streamflow depletion can in turn limit groundwater availability from perched aquifers.

Some groundwater systems in Hawai‘i, such as the Schofield and Kona high-level groundwater bodies, and the multiple stacked freshwater lenses beneath Hilo, are enigmatic. The lack of understanding about these systems, and the impact of developing groundwater from them, both limit assessment of groundwater availability.

Study Limitations—Lack of data or sparse, uneven distribution of data in space and time, and poor understanding of some hydrologically relevant processes limit the precision and accuracy of study results. Climate and streamflow data are essential for estimating groundwater recharge, but available data are sparse in some areas and commonly available only at a monthly frequency rather than the daily or greater frequency needed for accurate recharge quantification. Also, the numbers of rain and stream gages have decreased sharply in recent decades. A better understanding of processes such as evapotranspiration and runoff is also needed to improve groundwater-recharge quantification and assess commonly posed questions about watershed management. Quantification of water use by humans is critical for assessment of groundwater-resource availability, but records of reported groundwater and surface-water use are incomplete. Improving the completeness of water-use reporting is essential to improving the accuracy of groundwater-availability assessments.

Hydrogeologic understanding relies on surface and subsurface data. Although surface information is provided by the geologic maps, subsurface information from wells and geophysical surveys is sparse in some areas of Hawai‘i, especially island interiors. Some geologic and hydrologic enigmas remain unresolved; these enigmas translate to uncertainty about the impact of groundwater development and the quantity of groundwater available from some of Hawai‘i’s aquifers.

References Cited

Andrews, J.E., and Bainbridge, C., 1972, Submarine canyons off eastern Oahu: Pacific Science, v. 26, no. 1, p. 108–113.

Anthony, S.S., Hunt, Jr., C.D., Brasher, A.M., Miller, L.D., and Tomlinson, M.S., 2004, Water quality on the island of Oahu, Hawaii: U.S. Geological Survey Circular 1239, 37 p.

Asner, G.P., Hughes, R.F., Vitousek, P.M., Knapp, D.E., Kennedy-Bowdoin, T., Boardman, Joseph, Martin, R.E., Eastwood, M., and Green, R.O., 2008, Invasive plants transform the three-dimensional structure of rain forests: Proceedings of the National Academy of Sciences, v. 105, no. 11, p. 4,519–4,523.

Bassiouni, M., and Oki, D.S., 2013, Trends and shifts in streamflow in Hawai‘i, 1913–2008: Hydrological Processes, accessed May 24, 2012, at http://onlinelibrary.wiley.com/doi/10.1002/hyp.9298/full.

Bauer, G.R., 2003, A study of the ground-water conditions in North and South Kona and South Kohala districts Island of Hawaii, 1991–2002: State of Hawaii Department of Land and Natural Resources, Commission on Water Resource Management, PR-2003-01, 92 p.

Beeson, M.H., Clague, D.A., and Lockwood, J.P., 1996, Origin and depositional environment of clastic deposits in the Hilo drill hole, Hawaii: Journal of Geophysical Research, v. 101, no. b5, p. 11,617–11,629.

Burnham, W.L., Larson, S.P., and Cooper, H.H., 1977, Distribution of injected wastewater in the saline lava aquifer, Wailuku-Kahului wastewater treatment facility, Kahului, Maui, Hawaii: U.S Geological Survey Open File Report 77-469, 58 p.

Burt, R.J., 1979, Availability of ground water for irrigation on the Kekaha-Mana coastal plain, Island of Kauai, Hawaii: State of Hawaii Department of Land and Natural Resources Division of Water and Land Development Report R53, 50 p.

Cai, Junning, and Leung, PingSun, 2004, Economic impacts of shutting down Hawaii's sugar industry: University of Hawai'i at Manoa, College of Tropical Agriculture and Human Resources, Economic Issues 6, 4 p., accessed February 21, 2013, at http://www.ctahr.hawaii.edu/oc/freepubs/pdf/EI-6.pdf.

Camp Dresser & McKee, 1993, Groundwater modeling study—Review of existing data, Ewa marina project: Report to Haseko (Ewa), Inc., Honolulu, HI, variously paged.

Chu, P.-S., and Chen, H., 2005, Interannual and interdecadal rainfall variations in the Hawaiian islands: Journal of Climate, v. 18, p. 4,796–4,813.

Chu, P.-S., Chen, Y.R., Schroeder, T.A., 2010, Changes in precipitation extremes in the Hawaiian Islands in a warming climate: Journal of Climate, v 23, no. 18, p. 4,881–4,900.

Clague, D.A., and Dalrymple, G.B., 1987, The Hawaiian-Emperor volcanic chain, Part 1—Geologic evolution, *in* Decker, R.W., Wright, T.L, and Stauffer, P.H., eds., Volcanism in Hawaii: U.S. Geological Survey Professional Paper 1350, v. 1, p. 5–54.

Clague, D.A., and Sherrod, D.R., 2014, Growth and degradation of Hawaiian volcanoes, *in* Poland, M.P., Takahashi, J.T., and Landowski, C.M., eds., Characteristics of Hawaiian Volcanoes: U.S. Geological Survey Professional Paper 1801, p. 97–146.

Cooper, H.H., Jr., 1964, Relation of saltwater to fresh ground water, *in* Cooper, H.H., Jr., Kohout, F.A., Henry, H.R., and Glover, R.E., Seawater in coastal aquifers: U.S. Geological Survey Water Supply Paper 1613-C, p. C1–C12.

Coulbourn, W.T., Campbell, J.F., and Moberly, R., 1974, Hawaiian submarine terraces, canyons, and Quaternary history evaluated by seismic-reflection profiling: Marine Geology, v. 17, p. 215–234.

Cuddihy, L.W., and Stone, C.P., 1990, Alteration of Native Hawaiian vegetation—Effects of humans, their activities and introductions: Cooperative National Park Resources Studies Unit, University of Hawaii, Manoa, University of Hawaii Press, 138 p.

Dale, R.H., 1978, A ground-water inventory of the Waialua basal-water body, island of Oahu, Hawaii: U.S. Geological Survey Open-File Report 78–24, 76 p.

Denlinger, R.P., and Morgan, J.P., 2014, Instability of Hawaiian volcanoes, *in* Poland, M.P., Takahashi, J.T., and Landowski, C.M., eds., Characteristics of Hawaiian Volcanoes: U.S. Geological Survey Professional Paper 1801, p. 149–176.

Dimova, N.T., Swarzenski, P.W., Dulaiova, H., and Glenn, C.R., 2012, Utilizing multichannel electrical resistivity methods to examine the dynamics of the fresh water–seawater interface in two Hawaiian groundwater systems: Journal of Geophysical Research, v. 117, C02012, doi:10.1029/2011JC007509.

Dorrance, W.H., and Morgan, F.S., 2000, Sugar islands—the 165-year story of sugar in Hawai'i: Honolulu, Mutual Publishing, 259 p.

Duffield, W.A., 1975, Structure and origin of the Koae fault system, Kilauea Volcano, Hawaii: U.S. Geological Survey Professional Paper 856, 12 p.

Eakins, B.W., and Robinson, J.E., 2006, Submarine geology of Hana Ridge and Haleakala Volcano's northeast flank, Maui: Journal of Volcanology and Geothermal Research, v. 151, p. 229–250.

Eakins, B.W., Robinson, J.E., Kanamatsu, T., Naka, J., Smith, J.R., Takahashi, E., and Clague, D.A., 2003, Hawaii's volcanoes revealed: U.S. Geological Survey IMAP-2809, 1 sheet.

Engott, J.A., 2011, A water-budget model and assessment of groundwater recharge for the Island of Hawai'i: U.S. Geological Survey Scientific Investigations Report 2011–5078, 53 p.

Engott, J.A., and Vana, T.T., 2007, Effects of agricultural land-use changes and rainfall on ground-water recharge in central and west Maui, Hawai'i, 1926–2004: U.S. Geological Survey Scientific Investigations Report 2007–5103, 56 p.

Eyre, P.R., 1983, Investigation of Waikele Well No. 2401-01, Oahu, Hawaii—Pumping test, well logs and water quality: U.S. Geological Survey Water-Resources Investigations Report 83–4089, 38 p.

Eyre, P.R., Ewart, C.J., and Shade, P.J., 1986, Hydrology of the leeward aquifers, Southeast Oahu, Hawaii: U.S. Geological Survey Water-Resources Investigations Report 85–4270, 75 p.

Feigenson, M.D., Hofmann, A.W., and Spera, F.J., 1983, Case studies on the origin of basalt II. The transition from tholeiitic to alkalic volcanism on Kohala volcano, Hawaii: Contributions to Mineralogy and Petrology, v. 84, p 390–405.

Fiske, R.S., and Jackson, E.D., 1972, Orientation and growth of Hawaiian volcanic rifts—the effect of regional structure and gravitational stresses: Proceedings of the Royal Society of London, Series A, Mathematical and Physical Sciences, v. 329, p. 299–326.

Flinders, A.F., Ito, G., and Garcia, M.O., 2010, Gravity anomalies of the Northern Hawaiian Islands—Implications on the shield evolutions of Kauai and Niihau: Journal of Geophysical Research, v. 115, B08412, doi:10.1029/2009JB006877.

Flinders, A.F., Ito, G., Garcia, M.O., Sinton, J.M., Kauahikaua, J., and Taylor, B., 2013, Intrusive dike complexes, cumulate cores, and the extrusive growth of Hawaiian volcanoes: Geophysical Research Letters, v. 40, p. 3,367–3,373, doi:10.1002/grl.50633.

Fornari, D.J., 1987, The geomorphic and structural development of Hawaiian submarine rift zones, *in* Decker, R.W., Wright, T.L, and Stauffer, P.H., eds., Volcanism in Hawaii: U.S. Geological Survey Professional Paper 1350, v. 1, p.125–132.

Frazier, A.G., Giambelluca, T.W., Diaz, H.F., and Needham, H.L., 2016, Comparison of geostatistical approaches to spatially interpolate month-year rainfall for the Hawaiian Islands: International Journal of Climatology, v. 36, no. 3, p. 1459–1470, doi:10.1002/joc.4437.

Gandy, C.E., 2006, Volume and petrologic characteristics of the Koloa Volcanics, Kauaʻi, Hawaiʻi: Honolulu, University of Hawaiʻi, M.S. thesis, 107 p.

Garcia, M.O., Haskins, E.H., Stopler, E.M., and Baker, M., 2007, Stratigraphy of the Hawaiʻi Scientific Drilling Project core (HSDP2)—Anatomy of a Hawaiian shield volcano: Geochemistry Geophysics Geosystems, v. 8, no. 2, 37 p.

Garcia, M.O., Swinnard, L., Weis, D., Greene, A.R., Tagami, T., Sano, H., and Gandy, C.E., 2010, Petrology, geochemistry and geochronology of Kauaʻi lavas over 4.5 Myr—Implications for the origin of rejuvenated volcanism and the evolution of the Hawaiian plume: Journal of Petrology, v. 51, p. 1,507–1,540.

Garrison, G.H., Glenn, C.R., and McMurtry, G.M., 2003, Measurement of submarine groundwater discharge in Kahana Bay, Oʻahu, Hawaiʻi: Limnology and Oceanography, v. 48, p. 920–928.

Giambelluca, T.W., Chen, Q., Frazier, A.G., Price, J.P., Chen, Y.-L., Chu, P.-S., Eischeid, J.K., and Delparte, D.M., 2013, Online rainfall atlas of Hawaiʻi: Bulletin of the American Meteorological Society, doi: 10.1175/BAMS-D-11-00228.1, accessed April 2, 2013, at http://rainfall.geography.hawaii.edu/.

Giambelluca, T.W., Nullet, M.A., and Schroeder, T.A., 1986, Rainfall atlas of Hawaiʻi: Hawaiʻi Department of Land and Natural Resources Division of Water and Land Development Technical Report R76, 267 p.

Giambelluca, T.W., and Schroeder, T.A., 1998, Climate, *in* Juvik, S.P., and Juvik, J.O., eds., Atlas of Hawaiʻi (3d ed.): Honolulu, University Press of Hawaiʻi, 333 p.

Giambelluca, T.W., Shuai, Xiufu, Barnes, M.L., Alliss, R.J., Longman, R.J., Miura, Tomoaki, Chen, Qi, Frazier, A.G., Mudd, R.G., Cuo, Lan, and Businger, A.D., 2014, Evapotranspiration of Hawaiʻi: Final report submitted to U.S. Army Corps of Engineers–Honolulu District and Commission on Water Resource Management, State of Hawaiʻi, 178 p.

Gingerich. S.B., 1995, The hydrothermal system of the lower east rift zone of Kilauea Volcano— Conceptual and numerical models of energy and solute transport: Honolulu, University of Hawaiʻi, Ph.D. dissertation, 215 p.

Gingerich, S.B., 1999a, Estimating transmissivity and storage properties from aquifer tests in the Southern Lihue Basin, Kauai, Hawaii: U.S. Geological Survey Water-Resources Investigations Report 99–4066, 33 p.

Gingerich, S.B., 1999b, Ground-water occurrence and contribution to streamflow, Northeast Maui, Hawaii: U.S. Geological Survey Water-Resources Investigations Report 99–4090, 69 p. plus 1 plate.

Gingerich, S.B., 1999c, Ground-water and surface water in the Haiku area, East Maui, Hawaii: U.S. Geological Survey Water-Resources Investigations Report 98–4142, 38 p.

Gingerich, S.B., 2008, Ground-water availability in the Wailuku area, Maui, Hawaiʻi: U.S. Geological Survey Scientific Investigations Report 2008–5236, 95 p.

Gingerich, S.B., and Engott, J.A., 2012, Groundwater availability in the Lahaina District, west Maui, Hawaiʻi: U.S. Geological Survey Scientific Investigations Report 2012–5010, 90 p.

Gingerich, S.B., and Izuka, S.K., 1997, Construction, geologic log, and aquifer tests of the Northwest Kilohana monitor well (State Well 2–0126–01), Lihue, Kauai, Hawaii: U.S. Geological Survey Open-File Report 97–40, 20 p.

Gingerich, S.B., and Voss, C.I., 2005, Three-dimensional variable-density flow simulation of a coastal aquifer in southern Oahu, Hawaii, USA: Hydrogeology Journal, v. 13, p. 436–450.

Gregory, A.E.I., 1980, Reflection profiling studies of the 500-meter shelf south of Oahu—Reef development on a mid-oceanic island: Honolulu, University of Hawaii, M.S. thesis, 65 p.

Grigg, R.W., and Jones, A.T., 1997, Uplift caused by lithospheric flexure in the Hawaiian Archipelago as revealed by elevated coral deposits: Marine Geology, v. 141, p. 11–25.

Hawaii Agriculture Research Center [2014], Hawaii's Sugar Industry: Hawaii Agriculture Research Center Web page, accessed December 7, 2015, at http://www.hawaiiag.org/harc/HARCHS11.

Hawaii Marine Research, 1980, Refraction/reflection seismic survey of Kuou II well sites, Kaneohe, Hawaii: Prepared for the Department of Land and Natural Resources, 22 p.

Hawaii Water Authority, 1959, Water resources in Hawaii: Territory of Hawaii, Honolulu, Hawaii, 148 p.

Hirashima, G.T., 1962, Effect of the Haiku Tunnel on Kahaluu Stream, Oahu, Hawaii, *in* Short papers in geology and hydrology: U.S. Geological Survey Professional Paper 450C, p. C118–C117.

Hirashima, G.T., 1965, Effects of water withdrawals by tunnels, Waihee Valley, Oahu, Hawaii: State of Hawaii Department of Land and Natural Resources, Division of Water and Land Development, Report R28, 38 p.

Hirashima, G.T., 1971, Tunnels and dikes of the Koolau Range, Oahu, Hawaii, and their effect on storage depletion and movement of ground water: U.S. Geological Survey Water-Supply Paper 1999-M, 21 p.

Holcomb, R.T., Nelson, B.K., Reiners, P.W., and Sawyer, N., 2000, Overlapping volcanoes—The origin of Hilo Ridge, Hawaii: Geology, v. 28, no. 6, p 547–550.

Holcomb, R.T., Reiners, P.W., Nelson, B.K., and Sawyer, N.E, 1997, Evidence for two shield volcanoes exposed on the island of Kauai: Geology, v. 25, p. 811–814.

Hunt, C.D., Jr., 1996, Geohydrology of the Island of Oahu, Hawaii: U.S. Geological Survey Professional Paper 1412–B, 54 p.

Hunt, C.D., Jr., 2007, Ground-water nutrient flux to coastal waters and numerical simulation of wastewater injection at Kihei, Maui, Hawaii: U.S. Geological Survey Scientific Investigations Report 2006–5283, 69 p.

Hunt, C.D., Jr., and De Carlo, E.H., 2000, Hydrology and water and sediment quality at James Campbell National Wildlife Refuge near Kahuku, island of Oahu, Hawaii: U.S. Geological Survey Water-Resources Investigations Report 99–4171, 85 p.

Imada, J.A., 1984, Numerical modeling of the groundwater in the east rift zone of Kilauea Volcano, Hawaii: Honolulu, University of Hawai‘i, M.S. thesis, 102 p.

Ingebritsen, S.E., and Scholl, M.A., 1993, The hydrogeology of Kilauea Volcano: Geothermics, v. 22. no. 4. p. 255–270.

Intergovernmental Panel on Climate Change, 2013, Summary for Policymakers, *in* Stocker, T.F., Qin, D., Plattner, G.-K., Tignor, M., Allen, S.K., Boschung, J., Nauels, A., Xia, Y., Bex, V., Midgley, P.M., eds., Climate Change 2013—The physical science basis: Contribution of Working Group I to the Fifth Assessment Report of the Intergovernmental Panel on Climate Change, Cambridge University Press, Cambridge, UK and New York, USA.

Izuka, S.K., 1992, Geology and stream infiltration of North Halawa Valley, Oahu, Hawaii: U.S. Geological Survey Water-Resources Investigations Report 91–4197, 21 p.

Izuka, S.K, 2006, Effects of irrigation, drought, and ground-water withdrawals in ground-water levels in the southern Lihue Basin, Kauai, Hawaii: U.S. Geological Survey Scientific Investigations Report 2006–5291, 42 p.

Izuka, S.K., 2011, Potential effects of roadside dry wells on groundwater quality on the Island of Hawai‘i—Assessment using numerical groundwater models: U.S. Geological Survey Scientific Investigations Report 2011–5072, 30 p.

Izuka, S.K., 2012, Sources of suspended sediment in the Waikele watershed, O‘ahu, Hawai‘i: U.S. Geological Survey Scientific Investigations Report 2012–5085, 28 p.

Izuka, S.K., and Gingerich, S.B., 1997a, Construction, geologic log, and aquifer tests of the Hanamaulu monitor well (State Well 2–5923–08), Lihue, Kauai, Hawaii: U.S. Geological Survey Open-File Report 97–36, 23 p.

Izuka, S.K., and Gingerich, S.B., 1997b, Construction, geologic log, and aquifer tests of the Northeast Kilohana monitor well (State Well 2–0124–01), Lihue, Kauai: Hawaii: U.S. Geological Survey Open-File Report 97–37, 21 p.

Izuka, S.K., and Gingerich, S.B., 1997c, Construction and geologic log of the South Wailua monitor well (State Well 2–0121–01), Lihue, Kauai, Hawaii: U.S. Geological Survey Open-File Report 97–38, 14 p.

Izuka, S.K., and Gingerich, S.B., 1997d, Construction, geologic log, and aquifer tests of the Pukaki Reservoir monitor well (State Well 2–0023–01), Lihue, Kauai, Hawaii: U.S. Geological Survey Open-File Report 97–41, 22 p.

Izuka, S.K., and Gingerich, S.B., 1998a, Groundwater in the southern Lihue basin, Kauai, Hawaii: U.S. Geological Survey Water-Resources Investigations Report 98–4031, 71 p.

Izuka, S.K., and Gingerich, S.B., 1998b, Estimation of the depth to the fresh-water/salt-water interface from vertical head gradients in wells in coastal and island aquifers: Hydrogeology Journal, v. 6, p. 365–373.

Izuka, S.K., and Gingerich, S.B., 2003, A thick lens of fresh groundwater in the southern Lihue Basin, Kauai, Hawaii, USA: Hydrogeology Journal, v. 11, p. 240–248.

Izuka, S.K., and Oki, D.S., 2002, Numerical simulation of ground-water withdrawals in the southern Lihue Basin, Kauai, Hawaii: U.S. Geological Survey Water-Resources Investigations Report 01-4200, 54 p.

Izuka, S.K., Oki, D.S., and Chen, C., 2005, Effects of irrigation and rainfall reduction on ground-water recharge in the Lihue Basin, Kauai, Hawaii: U.S. Geological Survey Scientific Investigations Report 2005-5146, 48 p.

Izuka, S.K., and Resig, J.M., 2008, Evidence of Late Pliocene–Early Pleistocene marine environments in the deep subsurface of the Lihue basin, Kauai, Hawaii: Palaios, v. 23, p. 442–451.

Jagger, T.A., 1920, Seismometric investigation of the Hawaiian lava column: Geological Society of America Bulletin, v. 10, no, 4, p. 155–275.

Johnson, A.G., Glenn, C.R., Burnett, W.C., Peterson, R.N., and Lucey, P.G., 2008, Aerial infrared imaging reveals large nutrient-rich groundwater inputs to the ocean: Geophysical Research Letters, v. 35, 6 p.

Jones, S.B., 1938, Geomorphology of the Hawaiian Islands—A review: Journal of Geomorphology, v. 1, p. 55–61.

Juvik, J.O., and Ekern, P.C., 1978, A climatology of mountain fog on Mauna Loa, Hawaii Island: Honolulu, University of Hawai‘i, Water Resources Research Center Technical Report 118, 63 p.

Juvik, S.P., and Juvik, J.O., 1998, Atlas of Hawai‘i (3d ed.): Honolulu, University of Hawai‘i Press, 333 p.

Juvik, J.O., and Nullet, Dennis, 1995, Relationships between rainfall, cloud-water interception, and canopy throughfall in a Hawaiian montane forest, chap. 11 *of* Hamilton, L.S., Juvik, J.O., and Scatena, F.N., eds., Tropical montane cloud forests: New York, Springer-Verlag, p. 165–182.

Kauahikaua, J., 1993, Geophysical characteristics of the hydrothermal systems of Kilauea volcano, Hawai‘i: Geothermics, v. 22. no. 4. p. 271–299.

Kauahikaua, J., Duarte, K., and Foster, J., 1998, A preliminary gravity survey of the Kailua-Kona area, Hawai‘i, for delineation of a hydrologic boundary: U.S. Geological Survey Open-File Report 98–110, 21 p.

Kauahikaua, J., Hildenbrand, T., and Webring, M., 2000, Deep magmatic structures of Hawaiian volcanoes, imaged by three-dimensional gravity models: Geology, v. 28, p. 883–886.

Kelly, J.L, 2012, Identification and quantification of submarine groundwater discharge in the Hawaiian Islands: University of Hawai‘i at Mānoa, Ph.D. dissertation, 811 p.

Kinoshita, W.T., 1965, A gravity survey of the island of Hawaii: Pacific Science, v. 19, p. 339–340.

Kinoshita, W.T., and Okamura, R.T., 1965, A gravity survey of the island of Maui, Hawaii: Pacific Science, v. 19, p. 341–342.

Kirch, P.V., 1982, The impact of the prehistoric Polynesians on the Hawaiian ecosystem: Pacific Science, v. 36, no. 1, p. 1–14.

Kirch, P.V., 1998, Archaeology, *in* Juvik, S.P., and Juvik, J.O., eds., Atlas of Hawai‘i (3d ed.): Honolulu, University of Hawai‘i Press, p. 161–168.

Kirch, P.V., 2000, On the road of the winds—An archaeological history of the Pacific islands before European contact: Berkley, University of California Press, 424 p.

Konikow, L.F., 2013, Groundwater depletion in the United States (1900−2008): U.S. Geological Survey Scientific Investigations Report 2013−5079, 63 p.

Krivoy, H.L., Baker, M., and Moe, E.E., 1965, A reconnaissance gravity survey of the island of Kauai, Hawaii: Pacific Science, v. 19, p. 354–358.

Kruk, M.C., and Levinson, D.H., 2008, Evaluating the impacts of climate change on rainfall extremes for Hawaii and coastal Alaska: Proceedings of the 24th Conference on Severe Local Storms, American Meteorological Society, October 27-31, 2008, Savannah, Georgia, accessed January 6, 2015, at https://ams.confex.com/ams/pdfpapers/142172.pdf.

Langenheim, V.A.M., and Clague, D.A., 1987, The Hawaiian Emperor volcanic chain part II—Stratigraphic framework of volcanic rocks of the Hawaiian Islands, *in* Decker, R.W., Wright, T.L., and Stauffer, P.H., eds., Volcanism in Hawaii: U.S. Geological Survey Professional Paper 1350, v. 1, p. 55–84.

Langlas, C.M., 1998, History, *in* Juvik, S.P., and Juvik, J.O., eds., Atlas of Hawai‘i (3d ed.): Honolulu, University of Hawai‘i Press, p. 169–182.

Lau, L.S., and Mink, J.F., 2006, Hydrology of the Hawaiian Islands: Honolulu, University of Hawai‘i Press, 274 p.

Leone, Diana, 2009, Kauai sugar plantation prepares final harvest: Honolulu Advertiser, September 24, 2009, accessed June 24, 2014, at http://the.honoluluadvertiser.com/article/2009/Sep/24/ln/hawaii909240309.html.

Lipman, P.W., Lockwood, J.P. Okamura, R.T., Swanson, D.A., and Yamashita, K.M., 1985, Ground deformation associated with the 1975 magnitude-7.2 earthquake and resulting changes in activity of Kilauea Volcano, Hawaii: U.S. Geological Survey Professional Paper 1276, 45 p.

Lipman, P.W., Rhodes, J.M., and Dalrymple, G.B., 1990, The Ninole Basalt—Implications for the structural evolution of Mauna Loa volcano, Hawaii: Bulletin of Volcanology, v 53, p. 1–19.

Lipman, P.W., Sisson, T.W., Ui, T., and Naka, J., 2000, In search of ancestral Kilauea volcano: Geology, v. 28, no 12, p. 1,079–1,082.

Ludwig, K.R., Szabo, B.J., Moore, J.G., and Simmons, K.R., 1991, Crustal subsidence rate off Hawaii determined from $^{234}U/^{238}U$ ages of drowned coral reefs: Geology, v. 19, p. 171–174.

Macdonald, G.A., 1968, Composition and origin of Hawaiian lavas: Geological Society of America Memoir 116, p. 477–522.

Macdonald, G.A., 1972, Volcanoes: Englewood Cliffs, N.J., Prentice-Hall, 510 p.

Macdonald, G.A., Abbott, A.T., and Peterson, F.L, 1983, Volcanoes in the sea—The geology of Hawaii (2d ed.): Honolulu, University of Hawaii Press, 517 p.

Macdonald, G.A., Davis, D.A., and Cox, D.C., 1960, Geology and groundwater resources of the island of Kauai, Hawaii: Hawaii Division of Hydrography Bulletin 13, 212 p.

Macdonald, G.A., and Katsura, T., 1964, Chemical composition of Hawaiian lavas: Journal of Petrology, v. 5, part 1, p. 82–133.

Mark, R.K., and Moore, J.G., 1987, Slopes of the Hawaiian Ridge, *in* Decker, R.W., Wright, T.L, and Stauffer, P.H., eds., Volcanism in Hawaii: U.S. Geological Survey Professional Paper 1350, v. 1, p. 101–107.

Meinzer, O.E., 1923a, The occurrence of ground water in the United States: U.S. Geological Survey Water Supply Paper 489, 321 p.

Meinzer, O.E., 1923b, Outline of ground-water hydrology, with definitions: U.S. Geological Survey Water Supply Paper 494, 71 p.

Meinzer, O.E., 1930, Groundwater resources in the Hawaiian Islands, *in* Stearns, H.T., and Clark, W.O., Geology and groundwater resources of the Kau District, Hawaii: U.S. Geological Survey Water-Supply Paper 616, p. 1–28.

Meyer, W., 2000, A reevaluation of the occurrence of ground water in the Nahiku area, East Maui, Hawaii: U.S. Geological Survey Professional Paper 1618, 81 p.

Meyer, W., and Presley, T.K., 2000, The response of the Iao aquifer to ground-water development, rainfall, and land-use practices between 1940 and 1998, island of Maui, Hawaii: U.S. Geological Survey Water Resources investigations Report 00–4223, 60 p.

Meyer, W., and Souza, W.R., 1995, Factors that control the amount of water that can be diverted to wells in a high-level aquifer, *in* Hermann, R., Back, W., Sidle, R.C., and Johnson, A.I., eds., Water resources and environmental hazards—Emphasis on hydrologic and cultural insight in the Pacific Rim: Proceedings of the American Water Resources Association Annual Summer Symposium, June 25–28, p. 207–216.

Mink, J.F., 1980, State of the groundwater resources of southern Oahu: Honolulu Board of Water Supply, 83 p.

Mink, J.F., and Lau, L.S., 1980, Hawaiian groundwater geology and hydrology, and early mathematical models: University of Hawaii, Water Resources Research Center Technical Memorandum Report 62, 74 p.

Mink, J.F., and Lau, L.S., 1993, Aquifer identification and classification for the island of Hawai'i: Groundwater protection strategy for Hawai'i: University of Hawaii, Water Resources Research Center Technical Report 191, 108 p.

Moberly, R., Baver, L.D., and Morrison, M., 1965, Source and variation of Hawaiian littoral sand: Journal of Sedimentary Petrology, v. 35, p. 589–598.

Moore, J.G., 1970, Relationship between subsidence and volcanic load, Hawaii: Bulletin Volcanologique, v. 34, p. 562–576.

Moore, J.G., 1987, Subsidence of the Hawaiian Ridge, *in* Decker, R.W., Wright, T.L, and Stauffer, P.H., eds., Volcanism in Hawaii: U.S. Geological Survey Professional Paper 1350, v. 1, p. 85–100.

Moore, J.G., and Clague, D.A., 1992, Volcano growth and evolution of the island of Hawaii: Geological Society of America Bulletin, v. 104, p. 1,471–1,484.

Moore, J.G., Clague, D.A., Holcomb, R.T., Lipman, P.W., Normark, W.R., and Torresan, M.E., 1989, Prodigious submarine landslides on the Hawaiian Ridge: Journal of Geophysical Research, v. 94, no. B12, p. 17,465–17,484.

Moore, J.G., Clague, D.A., Ludwig, K.R., and Mark, R.K., 1990, Subsidence and volcanism of the Haleakala Ridge, Hawaii: Journal of Volcanology and Geothermal Research, v. 42, p. 273–284

Moore, J.G., and Fiske, R.S., 1969, Volcanic substructure inferred from dredge samples and ocean-bottom photographs, Hawaii: Geological Society of America Bulletin, v. 80, p. 1,191–1,202.

Moore, J.G., and Fornari, D.J., 1984, Drowned reefs as indicators of the rate of subsidence of the island of Hawaii: Journal of Geology, v. 92, p. 752–759.

Moore, R.B., Clague, D.A., Rubin, M., and Bohrson, W.A., 1987, Hualalai Volcano—A preliminary summary of geologic, petrologic, and geophysical data, *in* Decker, R.W., Wright, T.L, and Stauffer, P.H., eds., Volcanism in Hawaii: U.S. Geological Survey Professional Paper 1350, v. 1, p. 571–585.

Moore, R.B., and Trusdell, F.A., 1993, Geology of Kilauea volcano: Geothermics, v. 22, p. 243–254.

Newman, T.S., 1972, Man in the prehistoric Hawaiian ecosystem, *in* Kay, E.A., ed., Natural history of the Hawaiian Islands—Selected readings: Honolulu, University of Hawai'i Press, p. 559–603.

Nichols, W.D., Shade, P.J., and Hunt, C.D., 1996, Summary of the Oahu, Hawaii, Regional Aquifer-System Analysis: U.S. Geological Survey Professional Paper 1412-A, 61 p.

Oki, D.S., 1997, Modeling the effects of pumping, barometric pressure and ocean tides on ground-water levels in northern Oahu, Hawaii: Honolulu, University of Hawaii, Ph.D. dissertation, 321 p.

Oki, D.S., 1998, Geohydrology of the central Oahu, Hawaii, ground-water flow system and numerical simulation of the effects of additional pumping: U.S. Geological Survey Water-Resources Investigations Report 97–4276, 132 p.

Oki, D.S., 1999, Geohydrology and numerical simulation of the ground-water flow system of Kona, Island of Hawaii: U.S. Geological Survey Water-Resources Investigations Report 99–4070, 49 p.

Oki, D.S., 2002, Reassessment of ground-water recharge and simulated ground-water availability for the Hawi area of North Kohala, Hawaii: U.S. Geological Survey Water-Resources Investigations Report 02–4006, 62 p.

Oki, D.S., 2004a, Trends in streamflow characteristics at long-term gaging stations, Hawaii: U.S. Geological Survey Scientific Investigations Report 2004–5080, 116 p.

Oki, D.S., 2004b, Trends in streamflow characteristics in Hawaii, 1913–2002: U.S. Geological Survey Fact Sheet 2004–3104, 4 p.

Oki, D.S., 2005, Numerical simulation of the effects of low-permeability valley-fill barriers and the redistribution of ground-water withdrawals in the Pearl Harbor Area, Oahu, Hawaii: U.S. Geological Survey Scientific Investigations Report 2005–5253, 111 p.

Oki, D.S., Gingerich, S.B., and Whitehead, R.L., 1999a, Hawaii, *in* Ground water atlas of the United States, Segment 13, Alaska, Hawaii, Puerto Rico, and the U.S. Virgin Islands: U.S. Geological Survey Hydrologic Investigations Atlas 730-N, p. N12–N22, N36.

Oki, D.S., Souza, W.R., Bolke, E.L, and Bauer, G.R., 1996, Numerical analysis of ground-water flow and salinity in the Ewa area, Oahu, Hawaii: U.S. Geological Survey Open-File Report 96–442, 43 p.

Oki, D.S., Souza, W.R., Bolke, E.L., and Bauer, G.R., 1998, Numerical analysis of the hydrogeologic controls in a layered coastal aquifer system, Oahu, Hawaii, USA: Hydrogeology Journal, v. 6, no. 2, p. 243–263.

Oki, D.S., Tribble, G.W., Souza, W.R., and Bolke, E.L., 1999b, Ground-water resources in Kaloko Honokohau National Historical Park, Island of Hawaii, and numerical simulation of the effects of groundwater withdrawals: U.S. Geological Survey Water-Resources Investigations Report 99–4070, 49 p.

Oki, D.S., Wolff, R.H., and Perreault, J.A., 2006, Effects of surface-water diversion and ground-water withdrawal on streamflow and habitat, Punaluu stream, Oahu, Hawaii: U.S. Geological Survey Scientific Investigations Report 2006–5153, 104 p.

Oki, D.S., Wolff, R.H., and Perreault, J.A., 2010, Effects of surface-water diversion on streamflow, recharge, physical habitat, and temperature, Nā Wai ʻEhā, Maui, Hawaiʻi: U.S. Geological Survey Scientific Investigations Report 2010–5011, 154 p.

Palmer, H.S., 1927, The geology of the Honolulu artesian system: Supplement to the Report of the Honolulu Sewer and Water Commission, 68 p.

Palmer, H.S., 1946, Geology of the Honolulu ground-water supply: Board of Water Supply, Honolulu, 55 p.

Patrick, M.R., and Delparte, D., 2014, Tracking dramatic changes at Hawaii's only alpine lake: Eos, v. 95, no. 14, p. 117–118.

Perkins, K.S., Nimmo, J.R., and Medeiros, A.C., 2012, Effects of native forest restoration on soil hydraulic properties, Auwahi, Maui, Hawaiian Islands: Geophysical Research Letters, v. 39, L05405, doi:10.1029/2012GL051120.

Perkins, K.S., Nimmo, J.R., Medeiros, A.C., Szutu, D.J., and von Allmen, E., 2014, Assessing effects of native forest restoration on soil moisture dynamics and potential aquifer recharge, Auwahi, Maui: Ecohydrology, v. 7, no. 5, p. 1,437–1,451, doi: 10.1002/eco.1469.

Peterson, D.W., and Moore, R.B., 1987, Geologic history and evolution of concepts, island of Hawaii, *in* Decker, R.W., Wright, T.L, and Stauffer, P.H., eds., Volcanism in Hawaii: U.S. Geological Survey Professional Paper 1350, v. 1, p. 149–189.

Pierce, H.A., and Thomas, D.M., 2009, Magnetotelluric and audiomagnetotelluric groundwater survey along the Humu'ula Portion of Saddle Road near and around the Pohakuloa Training Area, Hawaii: U.S. Geological Survey Open-File Report 2009–1135, 160 p.

Porter, S.C., 1979a, Quaternary stratigraphy and chronology of Mauna Kea, Hawaii—A 380,000-yr record of mid-Pacific volcanism and ice-cap glaciation: Geological Society of America Bulletin, Part II, v. 90, p. 908–1093.

Porter, S.C., 1979b, Hawaiian glacial ages: Quaternary Research, v. 12, p. 161–187.

Presley, T.K., Sinton, J.M., and Pringle, M., 1997, Postshield volcanism and catastrophic mass wasting of the Waianae Volcano, Oahu, Hawaii: Bulletin of Volcanology, v. 58, p. 597–616.

Price, J.P., and Elliott-Fisk, D., 2004, Topographic history of the Maui Nui complex, Hawaiʻi, and its implications for biogeography: Pacific Science, v. 55, p. 27–45.

Quane S.L., Garcia, M.O., Guilloub, H., and Hulsebosch, T.P., 2000, Magmatic history of the East Rift Zone of Kilauea Volcano, Hawaii based on drill core from SOH 1: Journal of Volcanology and Geothermal Research, v. 102, p. 319–338.

Reilly, T.E., Dennehy, K.F., Alley, W.M., and Cunningham, W.L., 2008, Ground-water availability in the United States: U.S. Geological Survey Circular 1323, 70 p.

Reiners, P.W., Nelson, B.K., and Izuka, S.K., 1999, Structural and petrologic evolution of the Lihue basin, and eastern Kauai, Hawaii: Geological Society of America Bulletin, v. 111, p. 674–685.

Rhodes, J.M., 1996, Geochemical stratigraphy of lava flows sampled by the Hawaii Scientific Drilling Project: Journal of Geophysical Research, v. 101, no. B5, p 11,729–11,746.

Rhodes, J.M., and Vollinger, M.J., 2004, Composition of basaltic lavas sampled by phase-2 of the Hawaii Scientific Drilling Project—Geochemical stratigraphy and magma types: Geochemistry, Geophysics, Geosystems, v. 5, Q03G13, doi:10.1029/2002GC000434, accessed October 28, 2013, at http://onlinelibrary.wiley.com/doi/10.1029/2002GC000434/full.

Robinson, J.E., and Eakins, B.W., 2006, Calculated volumes of individual shield volcanoes at the young end of the Hawaiian Ridge: Journal of Volcanology and Geothermal Research, v. 151, p. 309–317.

Rosenau, J.C., Lubke, E.R., and Nakahara, R.H., 1971, Water resources of north-central Oahu, Hawaii: U.S. Geological Survey Water Supply Paper 1899–D, 40 p.

Rotzoll, K., 2010, Effects of groundwater withdrawal on borehole flow and salinity measured in deep monitor wells in Hawai‘i—Implications for groundwater management: U.S. Geological Survey Scientific Investigations Report 2010–5058, 42 p.

Rotzoll, K., 2012, Numerical simulation of flow in deep open boreholes in a coastal freshwater lens, Pearl Harbor Aquifer, O’ahu, Hawai’i: U.S. Geological Survey Scientific Investigations Report 2012–5009, 39 p.

Rotzoll, K., and El-Kadi, A.I., 2007, Numerical ground-water flow simulation for Red Hill fuel storage facilities, NAVFAC Pacific, Oahu, Hawaii: University of Hawaii, Water Resources Research Center prepared for TEC Inc., 74 p.

Rotzoll, K., and El-Kadi, A.I., 2008, Estimating hydraulic conductivity from specific capacity for Hawaii aquifers, USA: Hydrogeology Journal, v 16, p. 969–979.

Rotzoll, K., El-Kadi, A.I, and Gingerich, S.B., 2007, Estimating hydraulic properties of volcanic aquifers using constant-rate and variable-rate aquifer tests: Journal of the American Water Resources Association, v. 43, p. 334–345.

Rotzoll, K., and Fletcher, C.H., 2013, Assessment of groundwater inundation as a consequence of sea-level rise: Nature Climate Change, v. 3, no. 5, p. 477–481.

Rotzoll, K, Oki, D.S., and El-Kadi, A.I., 2010, Changes of freshwater-lens thickness in basaltic island aquifers overlain by thick coastal sediments: Hydrogeology Journal, v. 18, p. 1425–1436.

Ryan, M.P., Koyanagi, R.Y., and Fiske, R.S., 1981, Modeling the three-dimensional structure of macroscopic magma transport systems: application to Kilauea Volcano, Hawaii: Journal of Geophysical Research, v. 86, no. B8, p. 7,111–7,129.

Sager, W.W., Zhang. J., Korenaga, J., Sano, T., Koppers, A.A.P., Widdowson, M., and Mahoney, J.J., 2013, An immense shield volcano within the Shatsky Rise oceanic plateau, northwest Pacific Ocean: Nature Geoscience, v. 6, p. 976 –981.

Sato, H.T., Ikeda, W., Paeth, R., Smythe, R., and Yakehiro, M., 1973, Soil survey of the island of Hawaii, State of Hawaii: U.S. Department of Agriculture, Soil Conservation Service, 115 p. plus maps.

Schmitt, R.C., 1998, Population, *in* Juvik, S.P., and Juvik, J.O., eds., Atlas of Hawai‘i (3d ed.): Honolulu, University of Hawai‘i Press, p. 183–197.

Scholl, M.A., Gingerich, S.B., and Tribble, G.W., 2002, The influence of microclimates and fog on stable isotope signatures used in interpretation of regional hydrology—East Maui, Hawaii: Journal of Hydrology, v. 264, p. 170–184.

Shade, P.J., 1995, Water budget for the Kohala area, island of Hawaii: U.S. Geological Survey Water Resources Investigations Report 95–4114, 19 p.

Shade, P.J., and Nichols, W.D., 1996, Water budget and the effects of land-use changes on ground-water recharge, Oahu, Hawaii: U.S. Geological Survey Professional Paper 1412–C, 38 p.

Sharp, W.D., and Renne, P.R., 2005, The $^{40}Ar/^{39}Ar$ dating of core recovered by the Hawaii Scientific Drilling Project (phase 2), Hilo, Hawaii—Geochemical stratigraphy and magma types: Geochemistry, Geophysics, Geosystems, v. 6, Q04G17, doi:10.1029/2004GC000846, accessed October 28, 2013, at http://onlinelibrary.wiley.com/doi/10.1029/2004GC000846/full.

Sharp, W.D., Turrin, B.D. Renne, P.R. and Lanphere, M.A., 1996, The $^{40}Ar/^{30}Ar$ and K/Ar dating of lavas from the Hilo 1-km core hole, Hawaii Scientific Drilling Project: Journal of Geophysical Research, v. 101, no. B5, p 11,607–11,616.

Sherrod, D.R., Hagstrum, J.T., McGeehin, J.P., Champion, D.E., and Trusdell, F.A., 2006, Distribution, ^{14}C chronology, and paleomagnetism of latest Pleistocene and Holocene lava flows at Haleakalā volcano, Island of Maui, Hawai‘i—A revision of lava flow hazard zones: Journal of Geophysical Research, v. 111, 24 p.

Sherrod, D.R., Izuka, S.K., and Cousens, B.L., 2015, Onset of rejuvenated-stage volcanism and the formation of Līhu‘e Basin—Kaua‘i events that occurred 3–4 million years ago, *in* Carey, R., Cayol, V., Poland, M., and Weis, D., eds, Hawaiian Volcanoes—From source to surface: American Geophysical Union Geophysical Monograph 208, p. 105–123.

Sherrod, D.R., Nishimitsu, Y., and Tagami, T., 2003, New K-Ar ages and the geologic evidence against rejuvenated-stage volcanism at Haleakalā, East Maui, a postshield-stage volcano of the Hawaiian island chain: Geological Society of America Bulletin, v. 115, no. 6, p. 683–694.

Sherrod, D.R., Sinton, J.M., Watkins, S.E., and Brunt, K.M., 2007, Geologic map of the State of Hawai'i: U.S. Geological Survey Open-File Report 2007–1089, 83 p., 8 plates, scales 1:100,000 and 1:250,000, with GIS database.

Sinton, J.M., 1987, Revision of stratigraphic nomenclature of Waianae volcano, Oahu, Hawaii: U.S. Geological Survey Bulletin 1775–A, p. A9–A15.

Sinton, J.M., Eason, D.E., Tardona, M., Pyle, D., van der Zander, I., Guillou, H., Clague, D.A., and Mahoney, J.J., 2014, Ka'ena Volcano—A precursor volcano of the island of O'ahu, Hawai'i: Geological Society of America Bulletin, v. 126, no. 9/10, p. 1219–1244.

Soroos, R.L., 1973, Determination of hydraulic conductivity of some Oahu aquifers with step-drawdown test data: Honolulu, University of Hawaii, M.S. thesis, 239 p.

Souza, W.R., and Voss, C.I., 1987, Analysis of an anisotropic coastal aquifer system using variable-density flow and solute transport simulation: Journal of Hydrology, v. 92, p. 17–41.

Spengler, S.R., and Garcia, M.O., 1988, Geochemistry of the Hawi lavas, Kohala Volcano, Hawaii: Contributions to Mineralogy and Petrology, v. 99, p. 90–104.

State of Hawai'i, 2008a, State Water Code, Chapter 174C (2008 Amendment): Hawaii Revised Statutes, accessed February 6, 2014, at http://files.hi.gov/dlnr/cwrm/regulations/Code174C.pdf.

State of Hawai'i, 2008b, Water resource protection plan, June 2008: State of Hawai'i, Commission on Water Resource Management, 556 p., accessed February 20, 2014, at http://state.hi.us/dlnr/cwrm/planning/wrpp2008update/FINAL_WRPP_20080828.pdf.

State of Hawai'i, 2011, Hawaii facts and figures: State of Hawai'i, Department of Business, Economic Development, and Tourism, 20 p., accessed December 7, 2015, at http://files.hawaii.gov/dbedt/economic/databook/db2011/section19.pdf.

State of Hawai'i, 2012a, Increased food security and food self-sufficiency strategy; Volume II—A history of agriculture in Hawai'i and technical reference document: State of Hawai'i, Office of Planning, Department of Business, Economic Development, and Tourism, accessed February 5, 2014, at http://files.hawaii.gov/dbedt/op/spb/Volume_II_History_of_Agriculture_in_Hawaii_and_Technical_Reference_Document_FINAL.pdf.

State of Hawai'i, 2012b, Increased food security and food self-sufficiency strategy; Volume III—Assessment of irrigation systems in Hawaii: State of Hawai'i, Office of Planning, Department of Business, Economic Development, and Tourism, accessed February 5, 2014, at http://files.hawaii.gov/dbedt/op/spb/Volume_III_Assessment_of_Irrigation_Systems_in_Hawaii_FINAL.pdf.

State of Hawai'i, [2014a], What are the major industries in the State of Hawaii?: State of Hawai'i Department of Business, Economic Development and Tourism Web page, accessed June 4, 2014, at http://dbedt.hawaii.gov/economic/library/faq/faq08/.

State of Hawai'i, [2014b], Water-use reporting: State of Hawai'i, Commission on Water Resource Management Web page, accessed December 7, 2015, at http://dlnr.hi.gov/cwrm/info/waterusereport/.

State of Hawai'i [2014c], Hawaii census data: State of Hawai'i, Department of Business, Economic Development and Tourism Web page, accessed March 5, 2014, at http://census.hawaii.gov/.

Stearns, H.T., 1939, Geologic map and guide of the island of Oahu, Hawaii (with a chapter on mineral resources): Hawaii Division of Hydrography Bulletin 2, 75 p. and map.

Stearns, H.T., 1940, Supplement to the geology and groundwater resources of the island of Oahu, Hawaii: Hawaii Division of Hydrography Bulletin 5, 164 p.

Stearns, H.T., 1946, Geology of the Hawaiian Islands: Hawai'i Division of Hydrography Bulletin 8, 106 p.

Stearns, H.T., 1966, Geology of the State of Hawaii: Palo Alto, California, Pacific Books, 266 p.

Stearns, H.T., 1978, Submerged shorelines and shelves in the Hawaiian Islands and a revision of some of the eustatic emerged shorelines: Geological Society of America Bulletin, v. 85, p. 795–804.

Stearns, H.T., 1985, Geology of the State of Hawaii (2d ed.): Palo Alto, CA, Pacific Books, 335 p.

Stearns, H.T., and Clark, W.O., 1930, Geology and water resources of the Kau District, Hawaii: U.S. Geological Survey Water-Supply Paper 616, 194 p.

Stearns, H.T., and Macdonald, G.A., 1942, Geology and ground-water resources of the island of Maui, Hawaii: Hawai'i Division of Hydrography Bulletin 7, 344 p.

Stearns, H.T., and Macdonald, G.A., 1946, Geology and groundwater resources of the island of Hawaii: Hawaii Division of Hydrography Bulletin 9, 363 p.

Stearns, H.T., and Vaksvik, K.N., 1935, Geology and groundwater resources of the Island of Oahu, Hawaii: Hawaii Division of Hydrography Bulletin 1, 479 p.

Stolper, E.M., DePaolo, D.J., and Thomas, D.M., 1996, Introduction to special section—Hawaii Scientific Drilling Project: Journal of Geophysical Research, v. 101, no. B5, p. 11,593–11,598.

Stolper, E.M., DePaolo, D.J., and Thomas, D.M., 2009, Deep drilling into a mantle plume volcano—The Hawaii Scientific Drilling Project: Scientific Drilling, v. 4, p. 4–14.

Swanson, D.A., Duffield, W.A., and Fiske, R.S., 1976, Displacement of the south flank of Kilauea Volcano; the result of forceful intrusion of magma into the rift zones: U.S. Geological Survey Professional Paper 936, 39 p.

Takasaki, K.J., 1993, Ground water in Kilauea volcano and adjacent areas of Mauna Loa volcano, island of Hawaii: U.S. Geological Survey Open-File Report 93–82, 28 p.

Takasaki, K.J., Hirashima, G.T., and Lubke, E.R., 1969, Water resources of windward Oahu, Hawaii: U.S. Geological Survey Water-Supply Paper 1894, 119 p.

Takasaki, K.J., and Mink, J.F., 1982, Water resources of southeastern Oahu, Hawaii: U.S. Geological Survey Water-Resources Investigations Report 82–628, 89 p.

Takasaki, K.J., and Mink, J.F., 1985, Evaluation of major dike-impounded ground-water reservoirs, Island of Oahu: U.S. Geological Survey Water-Supply Paper 2217, 77 p.

Takasaki, K.J., and Yamanaga, G., 1970, Preliminary report on the water resources of Northeast Maui: State of Hawaii Department of Land and Natural Resources Division of Water and Land Development Circular C60, 41 p.

Takeguchi, A., Hollyer, J., Koga, W., Hakoda, M., Rohrbach, K., Bittenbender, H.C., Buckley, B., Friday, J.B., Bowen, R., Manshardt, R., Leary, J., Teves, G., Herring, E., Zaleski, H., Leonhardt, K., and Eger, B., 1999, History of agriculture in Hawaii: Hawaii Department of Agriculture Web page accessed January 28, 2014, at http://hawaii.gov/hdoa/agresources/history.

Tenorio, P.A., Young, R.H.F., Burbank, N.C.J., and Lau, L.S., 1970, Identification of irrigation return water in the sub-surface, Phase III—Kahuku, Oahu and Kahului and Lahaina, Maui: Water Resources Research Center and Honolulu Board of Water Supply Technical Report 44, 53 p.

Theis, C.V., 1940, The source of water derived from wells—Essential factors controlling the response of an aquifer to development: Civil Engineering v. 10, p. 277–280.

Thomas, D.M., and Haskins, E., 2013, Analysis of the hydrologic structures within an ocean island volcano using diamond wireline core drilling: Poster, American Geophysical Union 2013 Fall Meeting, San Francisco, USA.

Thomas, D.M., Paillet, F.L., and Conrad, M.E., 1996, Hydrogeology of the Hawaii Scientific drilling project borehole KP-1—2. Groundwater geochemistry and regional flow patterns: Journal of Geophysical Research, v. 101, p. 11,683–11,694.

Tilling, R.I., Heliker, C., and Swanson, D.A., 2010, Eruptions of Hawaiian volcanoes—Past, present, and future: U.S. Geological Survey General Information Product 117, 63 p.

Tillman, F.D., Oki, D.S., Johnson, A.G., Barber, L.B., and Beisner, K., 2014, Investigation of geochemical indicators to evaluate the connection between inland and coastal groundwater systems near Kaloko-Honokōhau National Historical Park, Hawai'i: Applied Geochemistry, v. 51, p. 278–292.

Timm, O.E., Giambelluca, T.W., and Diaz, H.F., 2015, Statistical downscaling of rainfall changes in Hawai'i based on the CMIP5 global model projections: Journal of Geophysical Research Atmospheres, v. 120, p. 92–112, doi:10.1002/2014JD022059.

Todd, D.K., and Meyer, C.F., 1971, Hydrology and geology of the Honolulu aquifer: Proceedings of the American Society of Civil Engineers, Journal of the Hydraulics Division, v. 97, no. HY2, p. 233–256.

U.S. Census Bureau, 2011, 2010 Census—Hawaii Profile: U.S. Census Bureau Web page, accessed February 10, 2012, at http://www2.census.gov/geo/maps/dc10_thematic/2010_Profile/2010_Profile_Map_Hawaii.pdf.

U.S. Department of Agriculture, 2006a, Soil survey geographic (SSURGO) database for the island of Maui: U.S. Department of Agriculture, Natural Resources Conservation Service, accessed October 3, 2011, at http://SoilDataMart.nrcs.usda.gov/.

U.S. Department of Agriculture, 2006b, Soil survey geographic (SSURGO) database for the island of Kauai: U.S. Department of Agriculture, Natural Resources Conservation Service, accessed September 4, 2012, at http://SoilDataMart.nrcs.usda.gov/.

U.S. Department of Agriculture, 2006c, Soil survey geographic (SSURGO) database for the island of Oahu: U.S. Department of Agriculture, Natural Resources Conservation Service, accessed June 8, 2011, at http://SoilDataMart.nrcs.usda.gov/.

U.S. Geological Survey, 2012a, LandsatLook Viewer, scenes LE70630472001006EDC00, LE70630462001006EDC00, LE70620472001031EDC00, and LE70620462000365EDC01: U.S. Geological Survey Web page, accessed November 6, 2013, at http://landsatlook.usgs.gov/.

U.S. Geological Survey, 2012b, The National map, National hydrography dataset: U.S. Geological Survey Web page, accessed February 12, 2013, at http://nhd.usgs.gov/data.html;ftp://nhdftp.usgs.gov/DataSets/Staged/States/FileGDB_C/.

U.S. Geological Survey, 2013, Hawaiian Volcano observatory: U.S. Geological Survey Web page, accessed November 25, 2014, at http://hvo.wr.usgs.gov/kilauea/summary/.

U.S. Geological Survey, 2014, Water Use in the United States: U.S. Geological Survey Web page, accessed February 25, 2014, at http://water.usgs.gov/watuse/50years.html.

Underwood, M.R., Meyer, W., and Souza, W.R., 1995, Groundwater availability from the Hawi aquifer in the Kohala area, Hawaii: U.S. Geological Survey Water-Resources Investigations Report 95–4113, 57 p.

University of Hawai‘i, 2011, Main Hawaiian Islands Multibeam Bathymetry Synthesis: Hawaii Mapping Research Group, School of Ocean and Earth Science and Technology, University of Hawai‘i at Mānoa, accessed March 22, 2013, at http://www.soest.hawaii.edu/hmrg/multibeam/grids.php.

Visher, F.N., and Mink, J.F., 1964, Ground-water resources in southern Oahu, Hawaii: U.S. Geological Survey Water Supply Paper 1778, 133 p.

Voss, C.I., and Souza, W.R., 1987, Variable density flow and solute transport simulation of regional aquifers containing a narrow freshwater-saltwater transition zone: Water Resources Research, v. 23, no. 10, p. 1,851–1,866.

Walker, G.P.L., 1987, The dike complex of Koolau volcano, Oahu—Internal structure of a Hawaiian rift zone, *in* Decker, R.W., Wright, T.L, and Stauffer, P.H., eds., Volcanism in Hawaii: U.S. Geological Survey Professional Paper 1350, v. 2, p. 961–993.

Wanless, V.D., Garcia, M.O., Rhodes, J.M., Weis, D., and Norman, M.D., 2006, Shield-stage alkalic volcanism on Mauna Loa Volcano, Hawaii: Journal of Volcanology and Geothermal Research, v. 151 p. 141–155.

Webster, J.M., Wallace, L.M., Clague, D.A., and Braga, J.C., 2007, Numerical modeling of the growth and drowning of Hawaiian coral reefs during the last two glacial cycles (0–250 kyr): Geochemistry Geophysics Geosystems, v. 8, no. 3, p. 1–23.

Wentworth, C.K., 1928, Principles of stream erosion in Hawaii: Journal of Geology, v. 36, no. 5, p. 385–410.

Wentworth, C.K., 1938, Geology and ground-water resources of the Palolo-Waialae district: Honolulu Board of Water Supply, 274 p.

Wentworth, C.K., 1951, Geology and ground-water resources of the Honolulu-Pearl Harbor area, Oahu, Hawaii: Honolulu Board of Water Supply, 111 p.

Whittier, R.B., Rotzoll, K., Dhal, S., El-Kadi, A.I., Ray, C., and Chang, D., 2010, Groundwater source assessment program for the state of Hawaii, USA—Methodology and example application: Hydrogeology Journal, v. 18, no. 3, p. 711–723.

Whittier, R.B., Rotzoll, K., Dhal, S., El-Kadi, A.I., Ray, C., Chen, G., and Chang, D., 2004, Hawaii source water assessment program report—Volume II, Island of Hawaii source water assessment program report: Water Resources Research Center, University of Hawai‘i at Mānoa, Honolulu, Hawai‘i, 65 p.

Wilcox, Carol, 1996, Sugar water—Hawaii’s plantation ditches: Honolulu, University of Hawai‘i Press, 191 p.

Williams, J.A., and Soroos, R.L., 1973, Evaluation of methods of pumping test analysis for application to Hawaiian aquifers: University of Hawaii, Water Resources Research Center Technical Report 70, 159 p.

Wilson Okamoto Corporation, 2008, Hawaii water plan—Water resource protection plan: State of Hawaii Department Of Land And Natural Resources, Commission On Water Resource Management, 556 p.

Wolfe, E.W., and Morris, Jean, 1996, Geologic map of the Island of Hawaii: U.S. Geological Survey IMAP Series I–2524–A, scale 1:100,000.

Wolfe, E.W., Wise, W.S., and Dalrymple, G.B., 1997, The geology and petrology of Mauna Kea Volcano, Hawaii—A study of postshield volcanism: U.S. Geological Survey Professional Paper 1557, 129 p.

Woodcock, A.H., 1974, Permafrost and climatology of a Hawaii volcano crater: Arctic and Alpine Research, v. 6, no. 1, p. 49–62.

Woodcock, D., 2003, To restore the watersheds—Early twentieth-century tree planting in Hawai‘i: Annals of the Association of American Geographers, v. 93, p. 624–635.

Yamanaga, G., and Huxel, C.J., Jr, 1969, Preliminary report on the water resources of the Lahaina District, Maui: State of Hawaii Department of Land and Natural Resources Division of Water and Land Development Circular C51, 47 p.

Yamanaga, G., and Huxel, C.J., Jr, 1970, Preliminary report on the water resources of the Wailuku area, Maui: State of Hawaii Department of Land and Natural Resources Division of Water and Land Development Circular C61, 43 p.

Yeung, C.W., and Fontaine, R.A., 2007, Natural and diverted low-flow duration discharges for streams affected by the Waiāhole Ditch System, windward O‘ahu, Hawai‘i: U.S. Geological Survey Scientific Investigations Report 2006–5285, 75 p.

Ziegler, A.C., 2002, Hawaiian natural history, ecology and evolution: Honolulu, University of Hawai‘i Press, 477 p.

Zohdy, A.A.R., and Jackson, D.B., 1969, Application of deep electrical soundings for groundwater exploration in Hawaii: Geophysics, v. 34, no. 4, p. 584–600.

Appendixes

Appendix 1. Calculation of Groundwater Recharge

Groundwater recharge in this study was estimated using a daily "threshold-type" or "reservoir" model based on a modification of the soil water-balance concepts of Thornthwaite and Mather (1955). In this water balance, part of the water that falls or is applied to the land surface runs off to the ocean and the remainder infiltrates the soil. The infiltrated water is temporarily stored in the plant-root zone where it is subject to evapotranspiration (ET) (fig. 1-1). Recharge to the aquifer occurs when more water infiltrates than can be held in the plant-root zone given its water-storage capacity, antecedent water content, and losses from ET. The excess infiltrated water is then passed to the underlying aquifer and becomes groundwater recharge. The method thus constitutes a balance of input (precipitation and irrigation), output (runoff, ET, and groundwater recharge), and water storage in the plant-soil system. The capacity of the plant-root zone reservoir is calculated on the basis of plant and soil properties. In the recharge model used for this study, water entering, leaving, and being stored within the plant-root zone reservoir is accounted for on a daily basis. A small amount of water from septic-system leaching is also subject to the processes in the plant-root zone.

The recharge model used in this study also includes temporary water storage in the forest canopy, where the water is subject to evaporation (fig. 1-1). Unlike in the plant-root zone, however, water is not stored in the canopy for more than a day. Rainfall and fog (precipitation) intercepted by the forest canopy on a given day either evaporates from the canopy or reaches the soil surface and becomes inflow to the plant-root zone. Inflow to the plant-root zone is called net precipitation. In nonforested areas, there is no canopy; therefore, net precipitation is simply the sum of fog interception and rainfall.

FOR NONFOREST LAND COVERS:

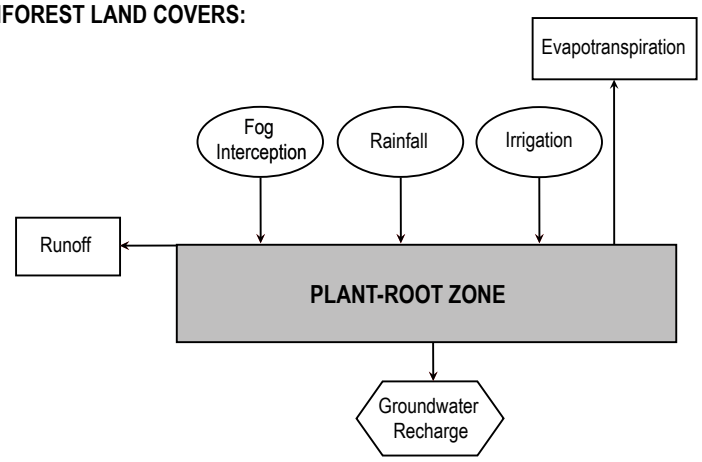

FOR FOREST LAND COVERS:
(modified from McJannet and others, 2007)

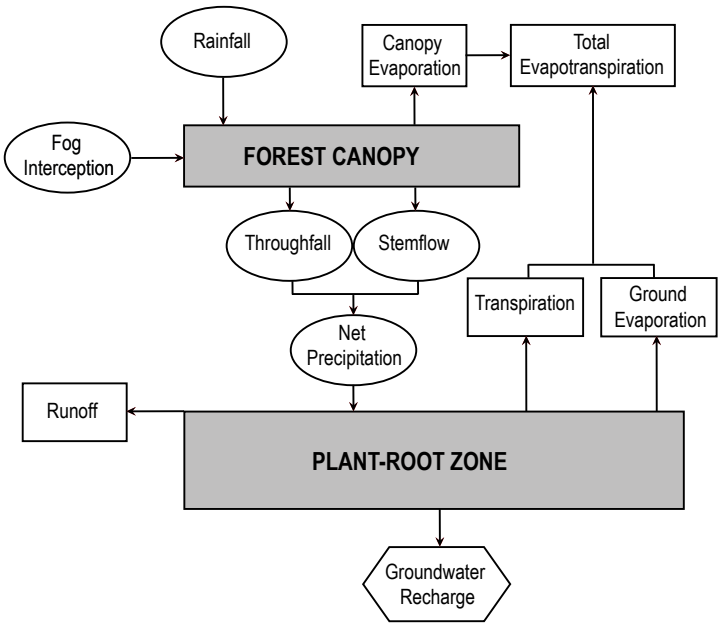

Figure 1-1. Conceptualizations of water flow in the recharge models used in this study.

Recharge from other sources, such as leaks from water systems and cesspools, is also incorporated in the model. These sources are considered "direct recharge," that is, they do not contribute to surface runoff and are not subject to evaporation or transpiration in either the forest canopy or plant-root zone reservoirs. Recharge from streambed seepage is not explicitly considered in the model.

Groundwater Recharge Model Calculations for Kaua'i, O'ahu, and Maui

Groundwater recharge was calculated using the model and input data that quantify the spatial and temporal distribution of rainfall, fog interception, irrigation, evaporation, runoff, soil type, and land cover. Areas of homogeneous properties, termed "subareas," are generated by merging datasets that characterize the spatial and temporal distributions of rainfall, fog, irrigation, potential ET, runoff, soil type, and land cover in a geographic information system (GIS). The model calculates recharge for each subarea independently; there is no transfer of water between subareas in the model calculations. At the end of a simulation period, results for the subareas are summed over larger areas of interest. Generally, the models for each island consist of several hundred thousand subareas with an average area of about 1 to 5 acres.

For each subarea at the start of each day, the model calculates interim moisture storage. Interim moisture storage is the amount of water that enters the plant-root zone for the current day plus the amount of water already in the zone from the previous day. For the first day of the simulation, a value for the amount of water already in the zone from the previous day (initial soil moisture) is assigned. For subareas with nonforest land covers, interim moisture storage is given by the equation

$$X_i = R_i + F_i + I_i + L_i + W_i - U_i + M_{i\text{-}1}, \quad (1a)$$

where

X_i is interim moisture storage for the current day [L],
R_i is rainfall for the current day [L],
F_i is fog interception for the current day [L],
I_i is irrigation for the current day [L],
L_i is septic-system leachate for the current day [L],
W_i is excess water from the impervious fraction of a subarea distributed over the pervious fraction of the subarea [L],
U_i is direct runoff for the current day [L],
$M_{i\text{-}1}$ is moisture storage at the end of the previous day (i-1) [L], and
i is a subscript designating the current day.

For subareas with forest land cover, interim moisture storage is given by the equation

$$X_i = (NP)_i + L_i + W_i - U_i + M_{i\text{-}1}, \quad (1b)$$

where

$(NP)_i$ is net precipitation for the current day [L].

For subareas with forest land cover, net precipitation is calculated as precipitation minus canopy evaporation, which is the amount of precipitation that is intercepted by and evaporates from the leaves, stems, and trunks of a forest. Precipitation is the sum of rainfall and fog:

$$P_i = R_i + F_i \quad (2)$$

where

P_i is precipitation for the current day [L].

Net precipitation is calculated as:

$$(NP)_i = P_i - (CE)_i, \quad (3)$$

where

$(CE)_i$ is canopy evaporation [L].

For this study, canopy evaporation is estimated using a method based on Gash and others (1995) (see *Evapotranspiration* section, below).

For each subarea with impervious surfaces, such as paved roads and buildings, the interim moisture-storage equations (equations 1a,b) include the factor W_i, which is a function of the proportion of the subarea that is impervious and the rainfall-retention capacity, N. For subareas that have no impervious surfaces, W_i is zero. The fraction of the subarea that is impervious, z, is estimated from a digital map of impervious surfaces (National Oceanic and Atmospheric Administration, 2008) using GIS software. This fraction, z, is used to separate, from the total rain that falls in a subarea, a depth of water that is treated mathematically as though it fell on an impervious surface. Water in excess of the rainfall-retention capacity, N, of the impervious surface is considered excess water, W_i (equations 4 and 5). For subareas without storm-drain systems, W_i is added to the water budget of the pervious fraction of the model subarea (equations 1a,b). For subareas with storm-drain systems, which in this study are subareas with medium- and high-intensity developed land covers (fig. 6 in main report), this excess water, W_i, is assumed to be captured by storm-drain systems.

For subareas with impervious surfaces, excess water, W_i, and water storage (ponded water) on the surface of impervious areas were determined using the following equations:

$$X1_i = P_i - U_i + T_{i\text{-}1}, \quad (4)$$

for $X1_i \le N$, $W_i = 0$, and $X2_i = X1_i$,

for $X1_i > N$, $W_i = (X1_i - N)z/(1 - z)$, and $X2_i = N$, (5)

where

$X1_i$ is the first interim moisture storage on the surface of impervious area for the current day [L],

$X2_i$ is the second interim moisture storage on the surface of impervious area for the current day [L],
T_{i-1} is the water storage (ponded water) on the surface of impervious area at the end of the previous day (i –1) [L],
N is the rainfall-retention capacity (maximum amount of water storage on the surface of impervious area) [L], and
z is the fraction of area that is impervious [dimensionless].

The water storage on the surface of the impervious area at the end of the current day, T_i, is determined from the equation

for $X2_i > G_i$, $T_i = X2_i - G_i$, and

for $X2_i \leq G_i$, $T_i = 0$, (6)

where

G_i is reference ET for the current day [L], and
T_i is the water storage (ponded water) on the surface of impervious area at the end of the day [L].

The next step in the water-budget calculation is to determine the amount of water that will be removed from the plant-root zone by ET. Actual ET is a function of potential ET and interim moisture, X_i. The plant-root zone loses water to the atmosphere at the potential-ET rate if sufficient water is available. The potential ET rate, $(PET)_i$, is calculated as the product of (1) reference ET, G_i, which is the potential ET of a grass reference surface, and (2) crop coefficient, which is a factor that depends on vegetation and land cover. For moisture contents greater than or equal to a threshold value, C_i, the rate of ET is assumed to be equal to the potential-ET rate. For moisture contents less than C_i, ET is assumed to occur at a reduced rate that declines linearly with soil-moisture content:

for $M \geq C_i$, $E = (PET)_i$, and

for $M < C_i$ and $C_i > 0$, $E = M \times (PET)_i / C_i$, (7)

where

E is the instantaneous evapotranspiration rate [L/T],
$(PET)_i$ is the potential-evapotranspiration rate for the current day [L/T],
M is the instantaneous moisture storage [L], and
C_i is the threshold moisture storage for the current day below which evapotranspiration is less than the potential-evapotranspiration rate [L].

The threshold moisture storage, C_i, was estimated using the model of Allen and others (1998) for soil moisture. In this model, a depletion fraction, d, which ranges from 0 to 1, is defined as the fraction of maximum moisture storage that can be depleted from the plant-root zone before moisture stress causes a reduction in ET. The threshold moisture, C_i, is estimated from d by the equation

$$C_i = (1 - d) \times M_m \,, \quad (8)$$

where

M_m is the moisture-storage capacity of the plant-root zone [L], and
d is the depletion fraction [dimensionless].

The moisture-storage capacity of the plant-root zone, M_m, expressed as a depth of water, is equal to the plant root depth, D, multiplied by the available water capacity of the soil, φ. Available water capacity is the difference between the volumetric field-capacity moisture content and the volumetric wilting-point moisture content:

$$M_m = D \times \varphi \,, \quad (9)$$

where

D is the plant root depth [L],
φ is the available water capacity, $\theta_{fc} - \theta_{wp}$ [L^3/L^3],
θ_{fc} is the volumetric field-capacity moisture content [L^3/L^3], and
θ_{wp} is the volumetric wilting-point moisture content [L^3/L^3].

Values for d depend on vegetation type and can be adjusted to reflect different potential-ET rates. In this study, d values were based on data in Allen and others (1998) and Fares (2008).

In the recharge model, the ET rate from the plant-root zone may be (1) equal to the potential-ET rate for part of the day and less than the potential-ET rate for the remainder of the day, (2) equal to the potential-ET rate for the entire day, or (3) less than the potential-ET rate for the entire day. The total ET from the plant-root zone during a day is a function of the potential-ET rate, $(PET)_i$, interim moisture storage, X_i, and threshold moisture content, C_i. By recognizing that $E = -dM/dt$, the total depth of water removed by ET during a day, E_i, was determined as follows:

for $X_i > C_i$ and $C_i > 0$, $E_i = (PET)_i t_i + C_i\{1 - \exp[-(PET)_i(1-t_i) / C_i]\}$,

for $X_i > C_i$ and $C_i = 0$, $E_i = (PET)_i t_i$,

for $X_i \leq C_i$ and $C_i > 0$, $E_i = X_i\{1 - \exp[-(PET)_i / C_i]\}$, and

for $X_i = C_i$, and $C_i = 0$, $E_i = 0$, (10)

where

E_i is the evapotranspiration from the plant-root zone during the day [L], and
t_i is the time during which moisture storage is above C_i [T].

The value of t_i ranges from 0 to 1 day and is calculated as follows:

for $(X_i - C_i) < (PET)_i$(1 day), $t_i = (X_i - C_i) / (PET)_i$, and

for $(X_i - C_i) \geq (PET)_i(1\ \text{day}),\ \ t_i = 1.$ (11)

After accounting for runoff (equations 1a,b), ET from the plant-root zone for a given day was subtracted from the interim moisture storage, and any moisture remaining above the maximum moisture storage was assumed to be recharge. The daily rate of direct recharge from anthropogenic sources is also added to daily recharge at this point. Recharge and moisture storage at the end of a given day were assigned according to the following conditions:

for $X_i - E_i \leq \mathrm{M}_m$, $\mathrm{Q}_i = DR$, $M_i = X_i - E_i$, and

for $X_i - E_i > M_m$, $Q_i = (X_i - E_i - M_m) + DR$, $M_i = M_m$, (12)

where Q_i is the groundwater recharge during the day [L],
M_i is the moisture storage at the end of the current day (i) [L], and
DR is the daily rate of direct recharge (a constant) [L].

Iteration

To mitigate possible effects of arbitrary starting values and random selection of monthly rainfall fragment sets (see *Rainfall* section, below), the recharge models were run multiple times and the results were averaged. To determine the appropriate number of simulations to run, the recharge model for each island—Kaua‘i, O‘ahu, and Maui—was run 50 times and the absolute percentage change in cumulative mean recharge for each island was computed for each successive simulation (fig. 1-2). The average percentage change did not exceed 0.002 percent after 15 simulations for each island. This very small value, 0.002 percent, was determined to be adequate for this study. Accordingly, for each model scenario, the recharge model was run for at least 15 simulations (16 simulations for Kaua‘i and 25 simulations for O‘ahu and Maui), and the results were averaged.

Model Input

The recharge model for this study uses spatial information from GIS coverages and user-defined parameter values that may be linked to the spatial information. The recharge model requires information that is briefly described below.

Land-Cover Maps

For estimating recharge during recent conditions on Kaua‘i, O‘ahu, and Maui, base land-cover maps representative of 2010 land cover were developed using the LANDFIRE Existing Vegetation Type (EVT) dataset (U.S. Geological Survey, 2010a). Base maps were modified in GIS and included converting from raster datasets to vector datasets and combining similar land-cover categories. Additional categories were created to account for hydrologically important land covers that were not included in the LANDFIRE EVT dataset, such as kiawe/phreatophytes, reservoirs, golf courses, and specific agricultural crops (table 1-1). To delineate kiawe/phreatophytes, the Hawai‘i Gap Analysis Program (GAP) dataset (U.S. Geological Survey, 2006), which includes this land-cover category, was used. Reservoirs, which

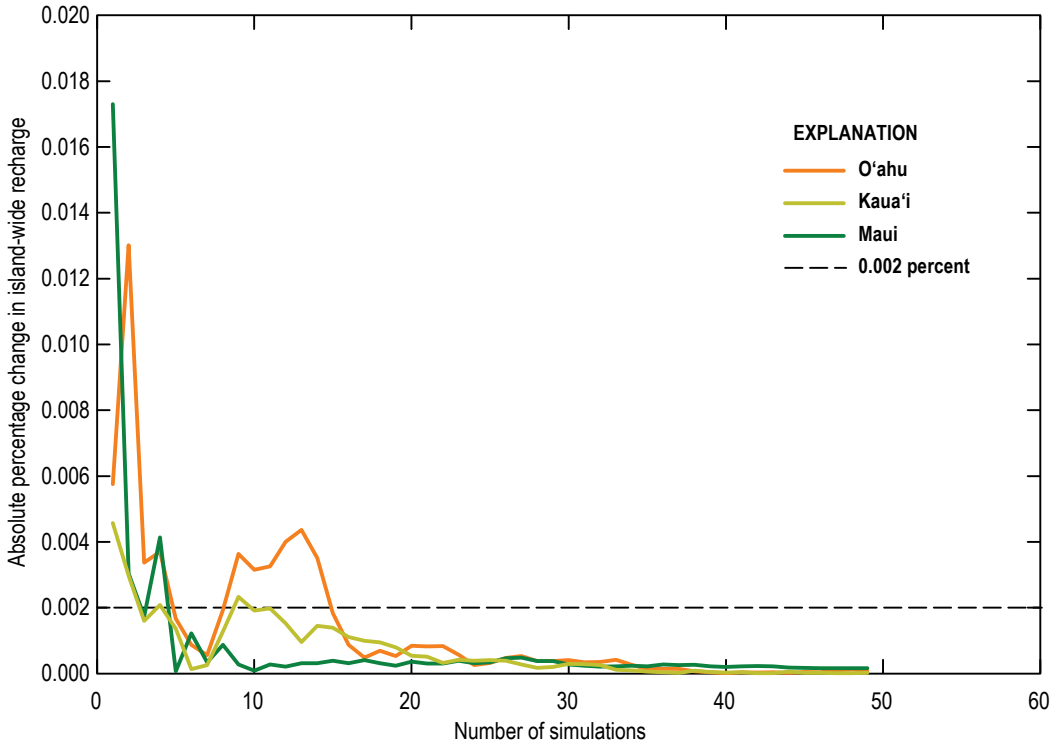

Figure 1-2. Graph of the absolute percentage change in island-wide recharge with each successive recharge-model simulation for Kaua‘i, O‘ahu, and Maui.

Table 1-1. Land-cover parameters used in the water-budget calculations for Kauaʻi, Oʻahu, and Maui, Hawaiʻi Island.

[–, not applicable. Crop coefficients for forest land covers are used to calculate the sum of transpiration and ground evaporation. Canopy evaporation is calculated separately. Crop coefficients for nonforest land covers are used to calculate the sum of all evaporative components. Sugarcane crop coefficients vary with time according to the different stages of the sugarcane crop cycle and are between 0.31 and 1.25]

Land-cover category	Root depth (inches)	Depletion fraction	Crop coefficient	Fog-catch efficiency	Irrigation method	Irrigation-method efficiency	Irrigation-estimation multiplier
Forest land covers							
Alien forest	60	0.50	0.33[a], 0.44[b]	1	–	–	–
Native forest	30	0.50	0.30	1	–	–	–
Tree plantation	60	0.50	0.33[a], 0.44[b]	1	–	–	–
Kiawe/phreatophytes	71	1.00	0.84	1	–	–	–
Open native forest[c]	27	0.53	0.68	1	–	–	–
Nonforest land covers							
Coffee	48	0.40	0.91	0.5	Micro-spray	0.80	1
Diversified agriculture	10	0.35	1.00	0	Drip	0.85	0.41[e], 0.55[f,g]
Fallow/grassland	39	0.60	0.95	0	–	–	–
Macadamia	60	0.50	0.91	1	Micro-spray	0.80	1
Pineapple	18	0.50	0.30	0	Drip	0.85	1
Corn	18	0.60	0.29–1.20	0	Drip	0.85	1
Sugarcane	24	0.65	0.31–1.25	0	Drip	0.80[e], 0.85[f]	1
Taro[d]	10	1.00	1.05	0	Flood	0.50	1
Developed, open space	12	0.50	1.18	0	–	–	–
Developed, low-intensity	12	0.50	1.18	0	–	–	–
Developed, medium-intensity	12	0.50	1.18	0	Sprinkler	0.70	0.37
Developed, high-intensity	12	0.50	1.18	0	Sprinkler	0.70	0.37
Golf course	30	0.50	0.85	0	Sprinkler	0.70	1
Shrubland	12	0.50	1.00	0.5	–	–	–
Grassland	39	0.60	0.95	0	–	–	–
Sparsely vegetated	5	0.50	1.18	0	–	–	–
Water body	0	1.00	1.05	0	–	–	–
Reservoir	0	1.00	1.05	0	–	–	–
Estuarine/near-coastal water body	0	1.00	1.05	0	–	–	–
Wetland	39	0.50	1.18	0	–	–	–
Grass/shrubland[c]	26	0.55	0.98	0.25	–	–	–
Sparse grassland[c]	22	0.55	1.07	0	–	–	–

[a]Value used for forests inside the fog zone, which is between altitudes of 2,000 and 8,200 ft.

[b]Value used for forests outside the fog zone.

[c]Category used for predevelopment (1870) scenario only.

[d]Method of estimating water-budget components is different than other agriculture.

[e]Value used on Maui.

[f]Value used on Kauaʻi.

[g]Value used on Oʻahu.

have different seepage rates than natural water bodies, were identified and recategorized. Agricultural parcels in the base map were separated into individual crop types or into fallow/grassland. Crop types considered were sugarcane, pineapple, corn, coffee, macadamia, taro, and diversified agriculture. Boundaries were defined on the basis of satellite imagery in Google Earth (google.com/earth), recent orthoimagery (U.S. Department of Agriculture, 2007a), digital and paper field maps from Gay and Robinson, Inc., Hawai‘i Agribusiness Development Corporation, Hawaiian Commercial & Sugar Company, and reported crop acreages (U.S. Department of Agriculture, 2007b). Areas of significant taro cultivation (Gingerich and others, 2007) and golf courses also were identified and delineated using satellite imagery from Google Earth (google.com/earth).

For estimating recharge during the predevelopment period on Kaua‘i, O‘ahu, Maui, and Hawai‘i Island, maps of generalized 1870 land cover at low and middle elevations (Samuel Gon, III, The Nature Conservancy, written commun., 2014, and James Jacobi, USGS, written commun., 2014) were superimposed on LANDFIRE Biophysical Settings (BPS) base map datasets (U.S. Geological Survey, 2010b). The 1870 land-cover maps include areas of wetland taro cultivation. For this study, 14 percent of the wetland taro areas delineated by the 1870 land-cover maps were considered to be irrigated and cultivated in 1870. This percentage was estimated by dividing the tons of demand per year (0.0025 tons/person/day × 365 days/yr × 77,932 people) by the estimated tons of yield per year (25 tons/hectare/yr × the mapped hectares of taro in 1870). The taro yield of 25 tons per hectare per year is from Ladefoged and others (2009); the taro demand of 5 pounds per person per day is from Coulter (1931); and the estimated 1870 population for the state as 77,932 is from Schmitt (1973).

Rainfall

Digital maps of 1978–2007 monthly rainfall (Frazier and others, 2016) for Kaua‘i, O‘ahu, and Maui were used to define the spatial and temporal rainfall distributions in the recharge-model calculations (fig. 1-3). This base period was used in the recharge model because it is consistent with the mean monthly rainfall datasets of the Rainfall Atlas of Hawai‘i (Giambelluca and others, 2013). The digital rainfall maps are formatted as 8.1-arcsecond grids, with cell sizes approximately 770 by 820 ft. Each cell has an estimated rainfall value for each month during 1978–2007 (360 total months). Using GIS software, the monthly rainfall maps were converted from raster to polygon format for use in the recharge model.

Cell-by-cell comparisons of the mean monthly rainfall calculated for 1978–2007 from the Frazier and others (2016) dataset and the mean monthly values in Giambelluca and others (2013) showed small differences. For consistency, the monthly rainfall values from Frazier and others (2016) were adjusted to produce the same mean monthly rainfall values for 1978–2007 as Giambelluca and others (2013). A total of 12 monthly adjustment factors for each grid cell were determined as the ratio of the 1978–2007 mean monthly rainfall from Giambelluca and others (2013) to the 1978–2007 mean monthly rainfall calculated from Frazier and others (2016). In this study, the monthly rainfall for each grid cell was determined by multiplying the value in Frazier and others (2016) by the appropriate monthly adjustment factor.

For the purposes of calibrating crop coefficients for forests (see *Crop Coefficients* section, below), a separate rainfall-distribution dataset that included available monthly rainfall-distribution grids for 2001–2007 (Frazier, 2012) was assembled for Kaua‘i, O‘ahu, and Maui for 2001–2010. At the time of the calibration, monthly rainfall-distribution grids for 2008–2010 were not available; therefore, the following method was used to estimate monthly rainfall distribution for these three years. Rain gages used in Giambelluca and others (2013) that had complete (or nearly complete) monthly records from 2008 through 2010 were identified. From among these gages, a subset was selected on the basis of spatial distribution (table 1-2). Thiessen polygons were created around the locations of the selected gages in a GIS, and mean monthly rainfall for each selected gage during 1978–2007 was determined using data from Giambelluca and others (2013). The ratio of observed to mean monthly rainfall for each month during 2008 through 2010 was calculated for each selected gage, creating a time series of 36 ratios. For all grid cells with a centroid within a given Thiessen polygon, the time series of ratios from that associated gage was applied to the mean monthly rainfall for that grid cell.

Daily-rainfall data were needed for the recharge model. Estimates of the spatial distribution of daily rainfall on Kaua‘i, O‘ahu, and Maui during 1978–2007 were not available and were not developed as part of this study. Instead, daily rainfall was synthesized by disaggregating the monthly values of the 1978–2007 rainfall distribution maps using the method of fragments (see, for example, Oki, 2002). The method of fragments creates a synthetic sequence of daily rainfall from monthly rainfall by imposing the rainfall pattern from a nearby rain gage with daily data. The synthesized daily rainfall data approximate the long-term average character of daily rainfall, such as frequency, duration, and intensity, but may not reproduce the true historical daily rainfall record for 1978–2007.

Daily rainfall measurements at 66, 47, and 52 rain gages on Kaua‘i, O‘ahu, and Maui, respectively, were used to disaggregate monthly rainfall into daily rainfall for the recharge model (fig. 1-3). Rain gages were selected on the basis of completeness of daily record and location. Daily rainfall data for the rain gages were obtained from the National Climatic Data Center (NCDC), the U.S. Geological Survey, and the Remote Automated Weather System (RAWS) network. Thiessen polygons were drawn around each of the rain gages using a GIS. These Thiessen polygons were used to spatially extrapolate the daily rainfall patterns indicated by the gages.

Daily rainfall fragments were created by dividing each daily rainfall measurement for a particular month by the total rainfall for that month. This resulted in a set of fragments for that particular month in which the total number of fragments was equal to the number of days in the month, and the sum of the fragments was equal to 1. Fragment sets were created for

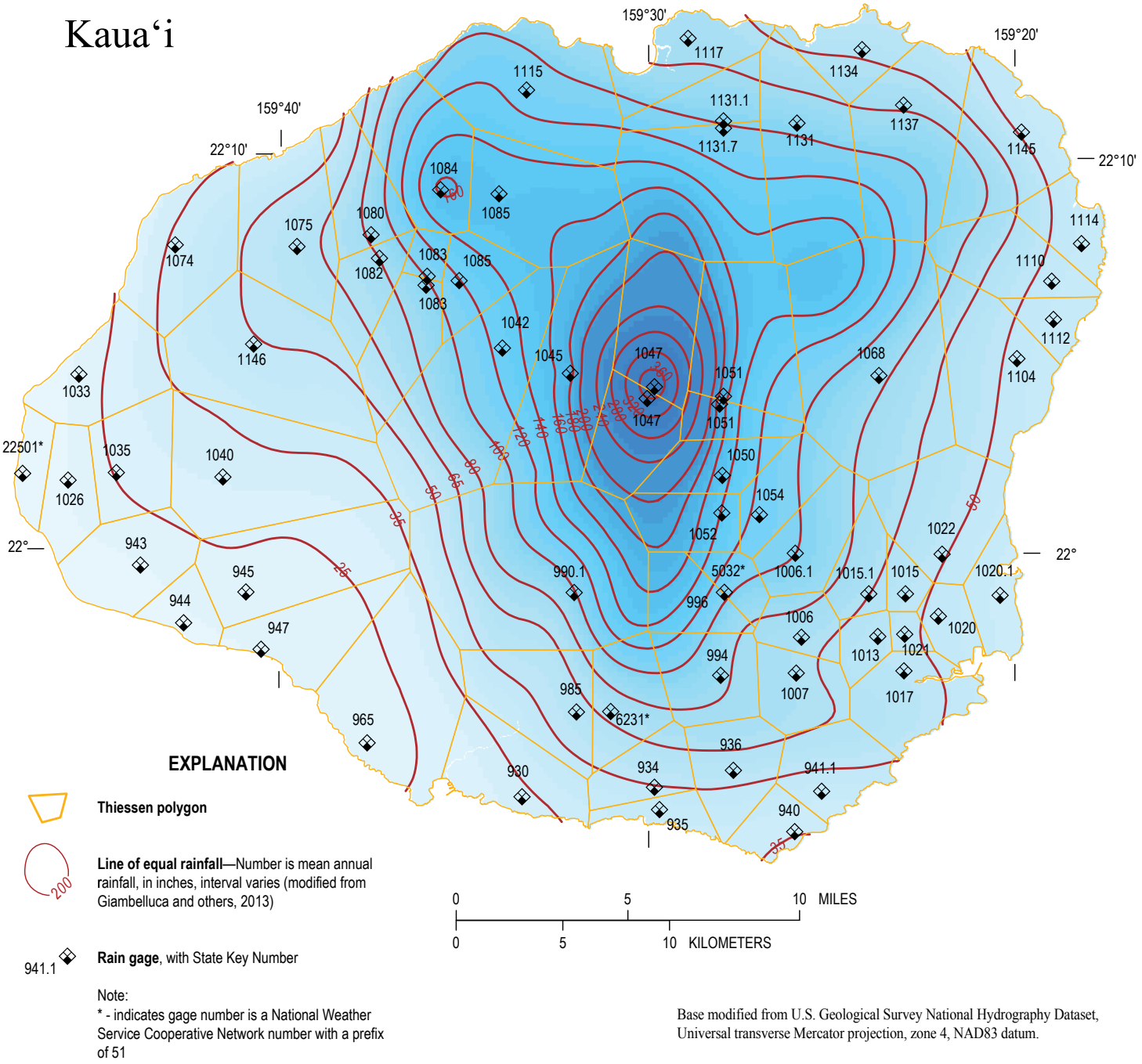

Figure 1-3. Map of mean annual rainfall, rain-gage locations, and Thiessen polygons generated for recharge calculation for Kaua‘i, O‘ahu, and Maui.

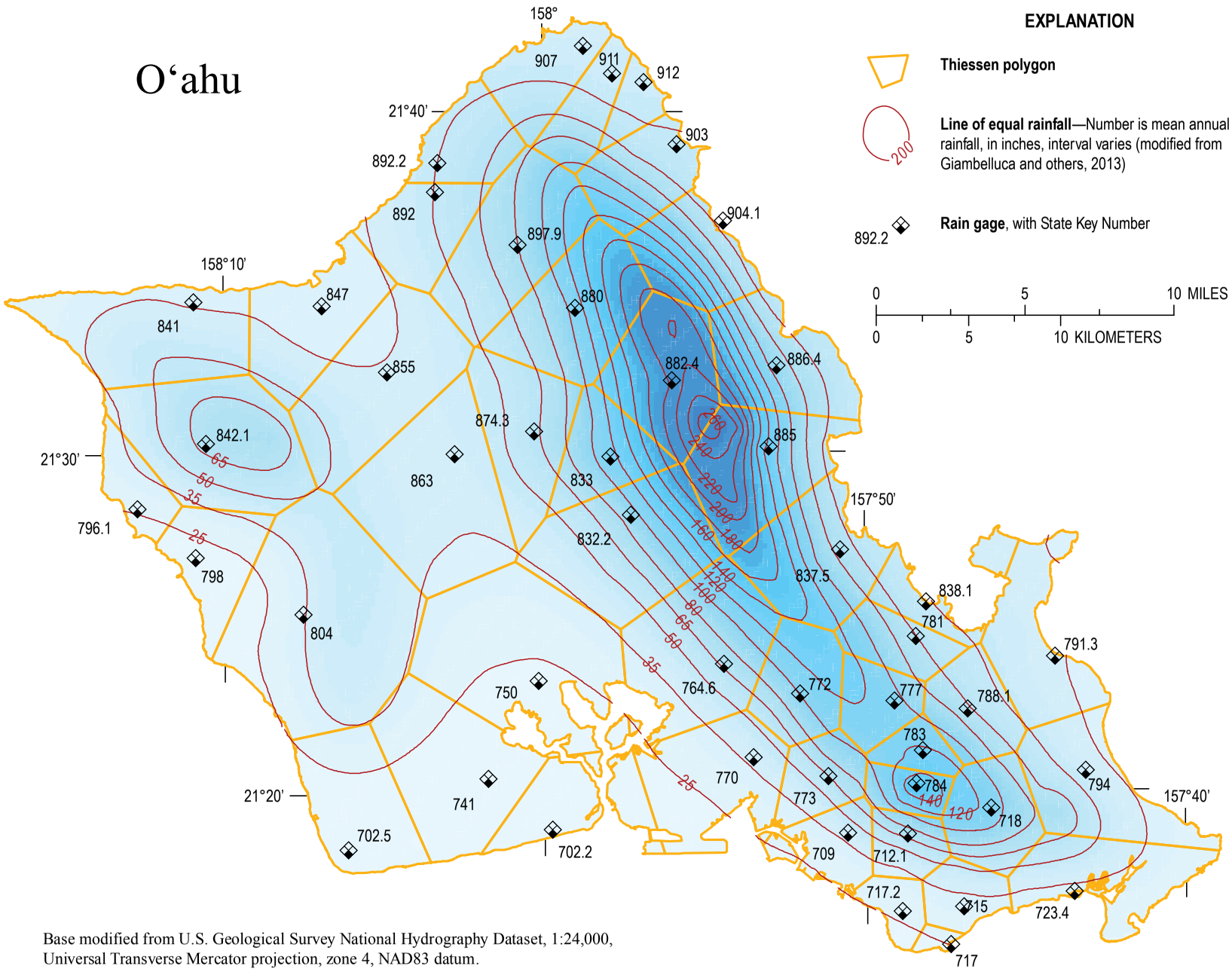

Base modified from U.S. Geological Survey National Hydrography Dataset, 1:24,000, Universal Transverse Mercator projection, zone 4, NAD83 datum.

Figure 1-3. Map of mean annual rainfall, rain-gage locations, and Thiessen polygons generated for recharge calculation for Kaua'i, O'ahu, and Maui.—Continued

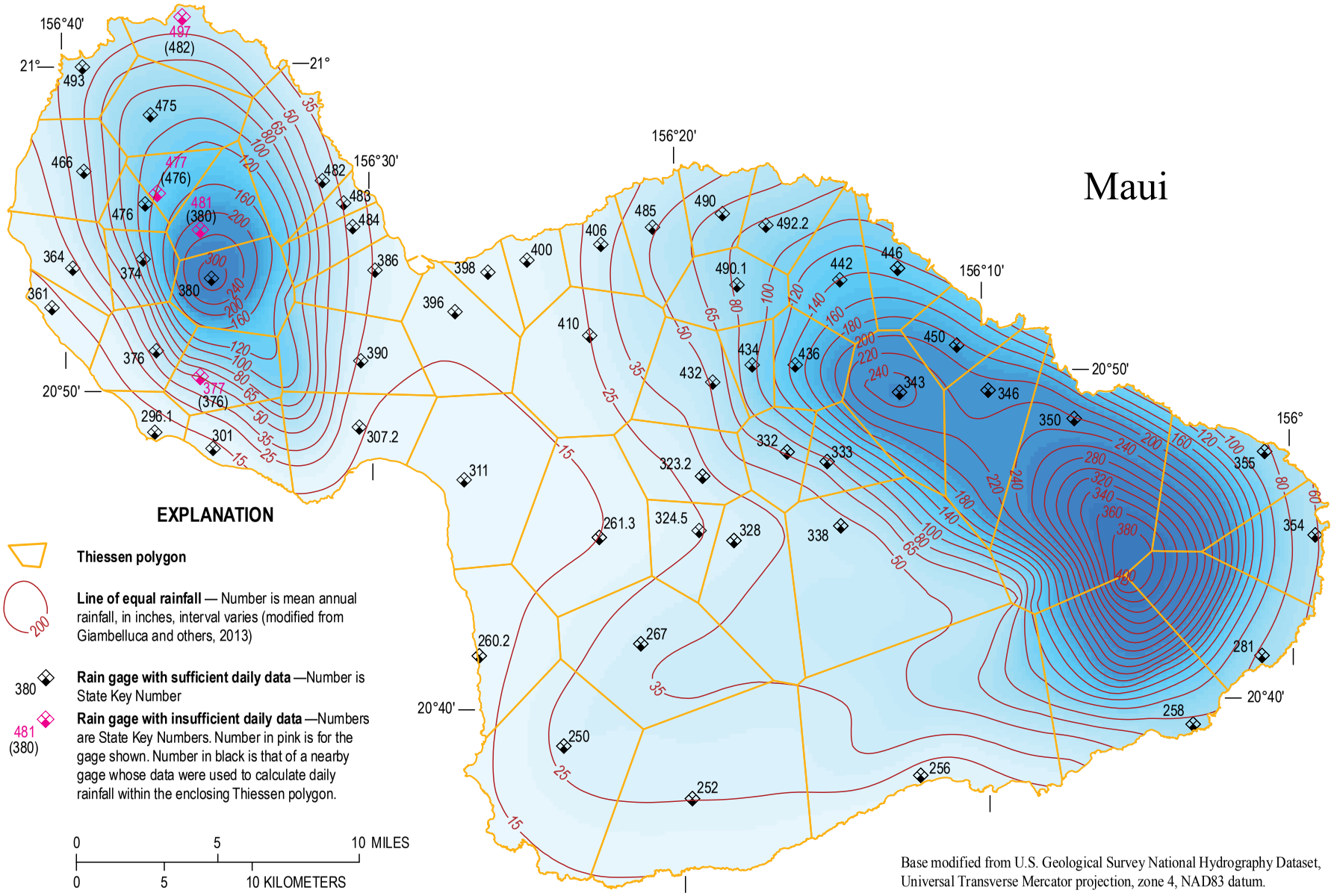

Figure 1-3. Map of mean annual rainfall, rain-gage locations, and Thiessen polygons generated for recharge calculation for Kaua'i, O'ahu, and Maui.—Continued

Table 1-2. Rain gages used to estimate rainfall during 2008–10 on Kaua‘i, O‘ahu, and Maui.

[Rain gages are listed by State Key Number; see fig. 1-3 for gage locations]

Kaua‘i	O‘ahu	Maui
927	702.5	249.1
930	703	250
931	709	255
936	717.2	258.6
941.1	718	266
947	723.4	267
965	764.6	297
985	777	307.2
1006	795.1	311
1013	798	324.5
1020.1	837.5	338
1042	886.4	348.5
1047	892.2	355
1051	911	372
1062.1	--	380
1068	--	396
1075	--	400
1083	--	410
1084	--	432
1115	--	446
1117	--	462
1131.7	--	477
1134	--	482
1137	--	484
--	--	485

every gage for every month in which complete daily rainfall measurements were available. Fragment sets were grouped by month of the year and by rain gage. In the recharge calculation, the fragment set to be used for a given gage for a given month was selected randomly from among all available sets for that gage for that month of the year. Daily rainfall for a given month was synthesized by multiplying total rainfall for that month (from the rainfall map) by each fragment in the set, thereby providing daily rainfall, R_i, for equation 1a or 1b.

Owing to insufficient daily records, fragment sets for each of the 12 calendar months could not be calculated for rain gages on Maui with State Key Numbers 497, 477, 481, and 377 (fig. 1-3). These four gages were assigned fragment sets from nearby gages with similar amounts of mean rainfall. Gage 497 was assigned the gage 482 fragment set, gage 477 the gage 476 fragment set, gage 481 the gage 380 fragment set, and gage 377 the gage 376 fragment set.

Fog Interception

Fog is often persistent on the mid-elevation mountain slopes of Hawai‘i, occurring during periods of onshore, upsloping winds favorable for orographic cloud formation. Fog may be persistent at elevations as low as about 2,000 to 3,000 ft (Juvik and Ekern, 1978). Orographic cloud formation is often limited or capped by the base of the trade-wind inversion, which commonly occurs between 5,000 and 10,000 ft (Giambelluca and Schroeder, 1998). This limitation on cloud formation hinders the growth of large raindrops and produces high ratios of fog to rain near, or at, the inversion-base altitude (Juvik and Ekern, 1978). Above the base of the inversion, fog tends to dissipate quickly in the drier air regime.

Where fog is persistent, the interception of this moisture by vegetation has been shown to be a significant component of the water budget (Ekern, 1964; Juvik and Ekern, 1978; Juvik and others, 1993; Juvik and Nullet, 1995; Scholl and others, 2007). Fog interception occurs through the processes of turbulent diffusion and gravitational sedimentation of droplets onto vegetative surfaces, mainly leaves or needles (Bruijnzeel and others, 2005). Fog-interception rates are highly site dependent and influenced by both meteorological and biotic variables, including the duration and frequency of fog periods, wind speed and direction, fog liquid water content, location within a forest, and forest structural characteristics, such as height, size, spatial pattern, and physical characteristics of leaves and epiphytes (Walmsley and others, 1996; Bruijnzeel and others, 2005; Villegas and others, 2007). The quantification of fog interception is a complex endeavor and is the subject of continuing research, both in Hawai‘i and worldwide.

Fog interception was calculated in the recharge model using fog-to-rainfall ratios. Fog-to-rainfall ratios for Kaua‘i and Maui were calculated using mean fog-interception rates (table 1-3) and mean rainfall from the Rainfall Atlas of Hawai‘i (Giambelluca and others, 2013). The mean annual fog-interception rates were obtained from a summary of Hawaiian fog studies (DeLay and Giambelluca (2010). The “fog zone,” which is an altitudinal range in which fog occurrence is common, was defined for this study as 2,000 to 8,200 ft, on the basis of DeLay and Giambelluca (2010). Below the fog zone, fog interception was assumed to be zero. Within the fog zone, fog interception was assumed to be 14 and 30 in/yr for the leeward and windward forests of each island, respectively. These are mid-range values taken from DeLay and Giambelluca (2010). Above the fog zone, fog interception was assumed to decrease with altitude. Between 8,200 and 9,000 ft, fog interception was set to 10 and 18 in/yr, for the leeward and windward aspects, respectively. Rates of 10 and 18 in/yr are averages of the assumed rates for forests within the fog zone and 6 in/yr, the assumed rate for both windward and leeward forests above 9,000 ft. A rate of 6 in/yr is based on two fog studies conducted at 11,200 ft on Mauna Loa (Juvik and Ekern, 1978; Juvik and Perreira, 1974) and summarized in DeLay and Giambelluca (2010). Monthly fog-to-rainfall ratios for Kaua‘i and Maui were calculated for each rainfall grid cell as the quotient of (1) mean annual fog interception divided by 12, and (2) mean monthly rainfall from Giambelluca and others (2013). For a given subarea in the recharge model, daily fog interception was calculated as the product of daily rainfall and the monthly fog-to-rainfall ratio for the corresponding month.

Owing to a dearth of monthly fog data, fog-to-rainfall ratios for Kaua‘i and Maui were calculated using the assumption that mean monthly fog-interception rates were the same each month of the year. This assumption is acceptable for this study because

Table 1-3. Fog-interception rates used to calculate fog-to-rainfall ratios for the recharge model for Kaua‘i and Maui.

[See figures 1-5 and 1-7 for boundaries between windward and leeward aspects; <, less than; >, greater than]

Altitude range (feet above mean sea level)		Location relative to fog zone	Fog-interception rate (inches per year)	
From	To		Leeward aspect	Windward aspect
0	<2,000	Below	0	0
2,000	8,200	Within	14	30
>8,200	<9,000	Above	10	18
9,000 and higher		Above	6	6

mean annual fog-interception estimates of the recharge model are consistent with fog-interception measurements in Hawai‘i. Additionally, the seasonal variation of the fog-to-rainfall ratios derived for use in the recharge model is consistent with that in a generalized model of seasonal fog on the windward slope of Mauna Loa, Hawai‘i Island (fig. 9 in Juvik and Ekern, 1978).

Fog-to-rainfall ratios for O‘ahu were derived from fog-interception and rainfall measurements in the Ko‘olau Range on O‘ahu and previous studies. For leeward O‘ahu above 2,000 ft, monthly ratios of fog interception to rainfall were calculated from data given in Ekern (1983) (table 1-4). The lowest ratio, 0.01, occurs in October, and the highest ratio, 0.15, occurs in February. For windward O‘ahu above 2,000 ft, a relatively small area where no fog studies have been conducted, a ratio of 0.20 was used. This is the same fog-interception to rainfall ratio used in Engott and Vana (2007) for the windward West Maui volcano.

Fog interception is primarily a phenomenon associated with trees and other tall vegetation, because the magnitude of fog interception is directly related to the height of the vegetated surface (Walmsley and others, 1996; Bruijnzeel and others, 2005). To account for the differences in fog collecting ability among land-cover types, a fog-catch efficiency factor is used in this study (table 1-1). The factor is a ratio of the amount of fog intercepted by the land cover to the amount of fog in a given area. For all forested areas, including tree and macadamia plantations, the fog-catch efficiency factor is 1. For shrubland and coffee, the factor is 0.5. For grass/shrubland, which is a land cover used only for the predevelopment simulation, the factor is 0.25. For all other land covers, the factor is 0, meaning no fog interception occurs.

Irrigation

Irrigation was applied to golf courses and agricultural land covers including coffee, diversified agriculture, pineapple, sugarcane, corn, and taro (figs. 5 and 6 in main report). Irrigation was also applied to medium- and high-intensity developed subareas to simulate the watering of lawns and other landscapes. Irrigation rates were calculated using a demand-based approach that is similar to that used in the Hawai‘i Agricultural Water Use and Development Plan (University of Hawai‘i, 2008). Irrigation demand for a given subarea is estimated on the basis of monthly rainfall, runoff, potential evapotranspiration, and irrigation method:

$$\text{for } (PE)_m + U_m > R_m, \qquad I_m = [(PE)_m + U_m - R_m] / g$$

$$\text{for } (PE)_m + U_m \leq R_m, \qquad I_m = 0 \tag{13}$$

where $(PE)_m$ is the potential evapotranspiration for month m (varies by location) [L],
U_m is the amount of runoff for month m [L],
R_m is the amount of rainfall for month m [L],
I_m is the amount of irrigation for month m [L], and
g is the irrigation efficiency (varies by irrigation method) [dimensionless].

Irrigation-method efficiencies used in this study are shown in table 1-1. Diversified agriculture, pineapple, corn, and Kaua‘i sugarcane were assumed to use drip irrigation, which has an irrigation-method efficiency of 0.85 (University of Hawai‘i, 2008). Coffee was assumed to use micro-spray irrigation, which has an irrigation efficiency of 0.80 (University of Hawai‘i, 2008). Golf courses and medium- and high-intensity developed land cover were assumed to use sprinkler irrigation, which has an irrigation efficiency of 0.70 (University of Hawai‘i, 2008). On Maui, Hawaiian Commercial & Sugar Company (HC&S) uses drip irrigation for its sugarcane fields and estimates an irrigation efficiency of 0.80 (Engott and Vana, 2007). On the basis of this information, 0.80 was used for Maui sugarcane in the recharge calculations for this report.

For all irrigated land covers other than sugarcane and pineapple, monthly irrigation calculated using equation 13 was allocated in equal amounts for each day of a given month. To simulate the sugarcane growth cycle, irrigation rates for sugarcane were varied throughout the cultivation cycle. The methods used by Engott and Vana (2007) to estimate sugarcane irrigation also were used for this study, and are briefly summarized here. Sugarcane was assumed to have a 24-month

Table 1-4. Ratios of fog interception to rainfall used in the recharge model for O‘ahu.

[See fig. 1-6 for boundaries between windward and leeward aspects]

Month	Aspect	
	Leeward	Windward
January	0.12	0.20
February	0.15	0.20
March	0.08	0.20
April	0.08	0.20
May	0.02	0.20
June	0.12	0.20
July	0.09	0.20
August	0.06	0.20
September	0.05	0.20
October	0.01	0.20
November	0.05	0.20
December	0.11	0.20

cultivation cycle in which the crop coefficient changes depending on the stage of growth (fig. 1-4). For a given sugarcane field, irrigation water was applied during the first 20 months of the cycle; monthly irrigation was calculated using equation 13 and was uniformly distributed on days 1, 2, 3, 8, 9, 10, 15, 16, 17, 22, 23, 24, and 28 of each month. No irrigation was applied to the field during the last 4 months of the 24-month cycle. At the end of the 24-month cycle, the sugarcane was assumed to be harvested, and the field left fallow until the next cycle began. The cultivation cycles of sugarcane fields were staggered such that about half the fields would be harvested in any one year. Similar to the approach taken in Engott and Vana (2007), the monthly irrigation volume calculated for pineapple using equation 13 was uniformly distributed on days 1, 2, 3, 8, 9, 10, 15, 16, 17, 22, 23, 24, and 28 of each month. Simulation of the pineapple cultivation cycle was not attempted in this study.

Corn irrigation for this study is based on a cultivation cycle of two crops per year. Only 25 percent of the corn land cover is cultivated at any one time, leaving the remaining 75 percent fallow/grassland. This approach was developed on the basis of general practices on Moloka‘i (Ray Foster, Monanto Company, written commun., 2012), which are assumed to be generally applicable elsewhere in Hawai‘i.

Irrigation rates for taro were not calculated using the demand-based approach (equation 13) because the crop is grown in flooded pond fields. The irrigation rate used in the water-budget model for taro is not meant to reflect the actual rate of water flow through the pond fields, but was assumed to equal the recharge rate, which was set equal to a constant rate representing pond-field seepage. For recent conditions on O‘ahu and Maui, all subareas mapped as taro (fig. 6) were assigned a recharge rate of 455 in/yr, which is equal to the average of the estimated seepage rates from four water-use studies for taro pond fields in Hawai‘i (Miles, 1931; Watson, 1964; de la Peña and Melchor, 1984; Berg and others, 1997). For recent conditions on Kaua‘i, only half of the area mapped as taro was assumed to have active cultivation; because the locations of the actual cultivated taro areas are not known, half the taro-recharge rate (227.5 in/yr) was applied to all subareas mapped as taro. For predevelopment conditions, only 14 percent of the subareas mapped as taro on Kaua‘i, O‘ahu, and Maui (fig. 5) were assumed to have active taro cultivation; therefore, a recharge rate of 63.7 in/yr was applied to these subareas.

An irrigation-estimation multiplier (table 1-1) was used to adjust the irrigation estimate (equation 13) for the diversified agriculture land-cover category because of its relatively large total area (fig. 6 in main report) combined with the large uncertainty involved in selecting crop parameters given the variety of crops represented by this category. For the Kaua‘i and O‘ahu recharge models, an irrigation-estimation multiplier of 0.55, derived by Engott and others (2017), was used on the basis of irrigation-supply information for fields served by the Waiāhole Ditch in central and southern O‘ahu. For Maui, the irrigation-estimation multiplier for diversified agriculture, 0.41, was derived by Johnson and others (2018) on the basis of water supplied to Kula Agricultural Park. An irrigation-estimation multiplier, 0.37, also was used for the medium- and high-intensity land-cover categories to calibrate the irrigation estimates from equation 13 to the rates used in Giambelluca (1983) and Giambelluca and others (2014) for urban irrigation in southern O‘ahu. The remaining irrigated land covers were assigned an irrigation-estimation multiplier of 1, meaning no adjustments were made to the irrigation estimates from equation 13. Sugarcane was assigned an irrigation-estimation multiplier of 1 because its mean annual irrigation rate, estimated by the recharge model for recent conditions on Maui, was less than the average amount of water available for irrigating sugarcane on Maui, as described in Johnson and others (2018).

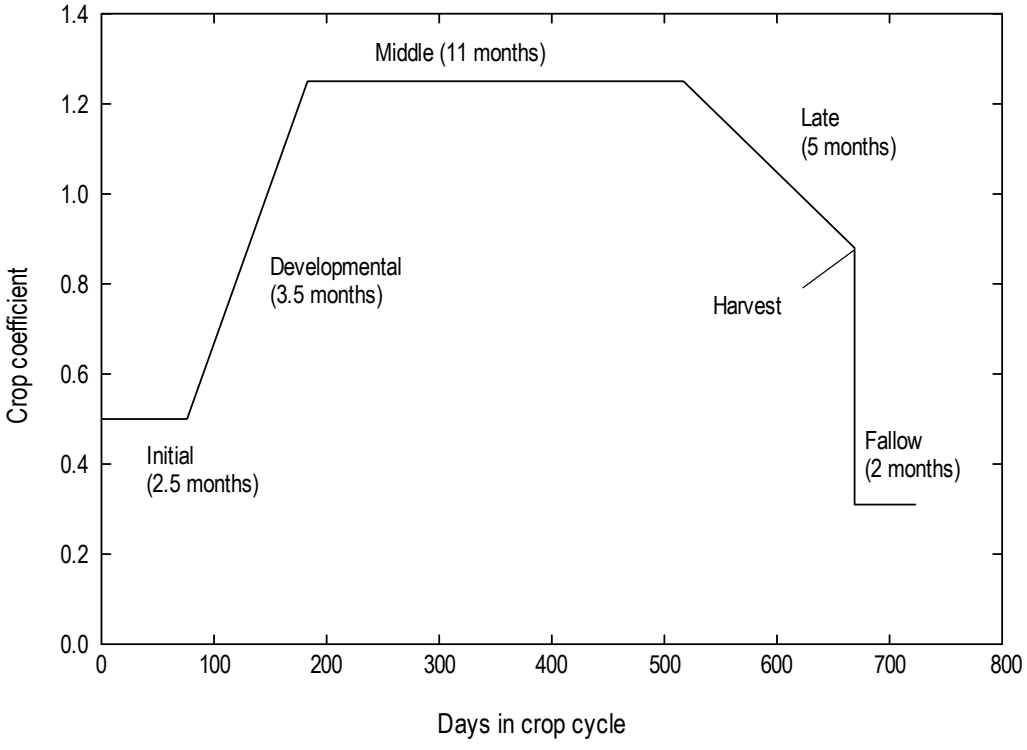

Figure 1-4. Graph of crop coefficients used in the water-budget calculation for different growth stages of sugarcane (based on data from Fukunaga, 1978).

Septic-System Leaching

For tax map key (TMK) parcels with septic systems, the effluent flux was added to the plant-root zone (equations 1a,b). Whittier and El-Kadi (2009; 2013) compiled an inventory of on-site wastewater-disposal systems on Kaua‘i, O‘ahu, and Maui. For each TMK parcel, Whittier and El-Kadi (2009; 2013) specify the number and type (class) of on-site disposal systems and the total estimated wastewater effluent flux. For the recharge calculation, all effluent flux was applied daily and uniformly across each TMK parcel area. For parcels with cesspools, the effluent flux was assumed to be direct recharge (see *Direct Recharge section).*

Direct Runoff

Direct runoff is the fraction of rainfall that does not contribute to net moisture gain within the plant-root zone (fig. 1-1). Direct runoff consists of overland flow and subsurface storm flow that rapidly returns infiltrated water to streams (Oki, 2003). In the water-budget calculation, direct runoff was estimated as a fraction of rainfall using runoff-to-rainfall ratios. This approach was used also in previous water-budget studies for Hawai‘i and other Pacific islands (for example, Izuka and others, 2005; Engott and Vana, 2007; Engott, 2011; Gingerich and Engott, 2012; Johnson, 2012) and was shown to provide reasonable estimates of regional average direct runoff using a minimal level of complexity.

The spatial variability of runoff-to-rainfall ratios depends on numerous factors including geology, climate, soil type, topography, and land use. Runoff-to-rainfall ratios are expected to be highest where the rainfall amount and intensity are high, permeability of the soils and substrate is low, slopes are steep, and soil moisture is high (Oki, 2003). The temporal variability in runoff-to-rainfall ratios reflects event characteristics, such as antecedent soil moisture and rainfall intensity. In Hawai‘i, runoff-to-rainfall ratios generally follow a seasonal pattern; runoff-to-rainfall ratios are highest during the wet season and lowest during the dry season.

In the water-budget model, daily direct runoff, U_i, was calculated by multiplying daily rainfall, R_i, with seasonal (wet and dry season) runoff-to-rainfall ratios assigned to catchment zones. Catchment zones were delineated by Rea and Skinner (2012). For this study, each catchment zone was assigned two attributes: (1) gaged or ungaged, and (2) windward or leeward (figs. 1-5, 1-6, and 1-7). The boundaries of the drainage basins of selected stream-gaging stations are from Rosa and Oki (2010), and the boundary between windward and leeward regions is based on topographic divides and is generally consistent with previous studies (Yamanaga, 1972; Oki and others, 2010). On Maui, the 20-in. mean annual isohyet was used as the boundary between the windward region on the West Maui volcano and the leeward region on the isthmus. The runoff-to-rainfall ratio assigned to each catchment zone and used to calculate direct runoff was selected as one of the following: (1) the observed seasonal runoff-to-rainfall ratio for the season, year, and location of interest, if available, (2) the observed mean seasonal runoff-to-rainfall ratio for the location of interest, or (3) the mean seasonal runoff-to-rainfall ratio estimated using a regression equation for the location of interest. A description of the approach used to calculate the ratios is presented below. For this study, November through April was considered the wet season; May through October was considered the dry season.

Seasonal runoff-to-rainfall ratios assigned to catchment zones in the water-budget model were calculated from data for drainage basins of stream-gaging stations. These drainage basins consist of one or more catchment zones. For gaged drainage basins consisting of a single catchment zone, observed seasonal or mean seasonal runoff-to-rainfall ratios for the gaged basin were assigned to the catchment zone. For gaged drainage basins consisting of multiple catchment zones, observed seasonal or mean seasonal runoff-to-rainfall ratios for the gaged drainage basin were spatially disaggregated to each catchment zone within the gaged basin. Catchment zones in ungaged areas were assigned mean seasonal runoff-to-rainfall ratios derived from regional-regression models.

Calculation of Seasonal Runoff-to-Rainfall Ratios

Runoff and rainfall data for the drainage basins of 55 stream-gaging stations (25 on Maui, 13 on Kaua‘i, and 17 on O‘ahu) were used to estimate seasonal runoff-to-rainfall ratios for the water-budget model (table 1-5). Stream-gaging stations selected for the runoff analysis had (1) at least eight complete years of daily mean discharge records between 1920 and 2007, (2) a drainage-basin area greater than 0.2 mi^2, and (3) unregulated streamflow or regulated streamflow with complete and reliable records of daily mean diverted flow available to reconstruct total streamflow at the gage. Criterion (1) is based on an analysis of average runoff-to-rainfall ratios calculated for stream-gaging stations with 30 years of record during 1978-2007 using subsets ranging from 1 to 30 years. Criterion (2) is based on the spatial uncertainty of the drainage-basin boundaries, which were delineated using a 10-m digital elevation model. Criterion (3) is based on guidance in Fontaine (1995). For drainage basins with more than one stream-gaging station, only the station at the lowest altitude was used in the runoff analysis because it had the largest drainage basin and doing so reduced redundancy in the regression. Additionally, concurrent streamflow data for two stations within a drainage basin was generally absent or insufficient for improving direct runoff estimates. The drainage basins of the selected stream-gaging stations were delineated using the USGS StreamStats application for Hawai‘i (Rosa and Oki, 2010). Rainfall within each drainage basin was calculated using gridded maps of monthly rainfall (Frazier and others, 2016).

Because streamflow measured at most gaging stations consists of direct runoff and base flow, the base-flow component was estimated and subtracted from the total streamflow. Streamflow at stations 16500100 and 16660000 on Maui, and station 16013000 on Kaua‘i, was ephemeral and was assumed to have no base flow. Base flow at the other gaged basins was estimated using a computerized base-flow separation method (Wahl and Wahl, 1995). This method

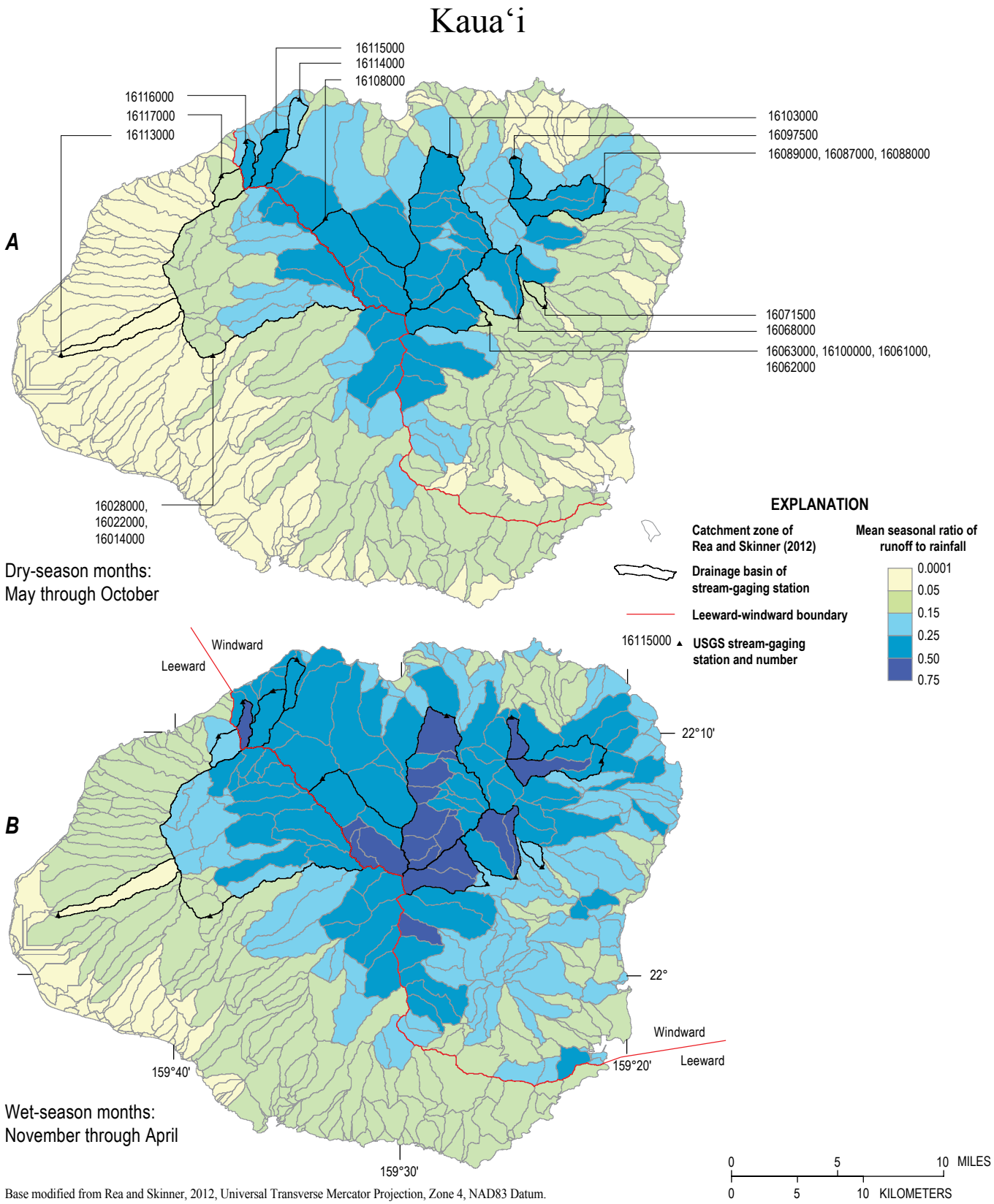

Figure 1-5. Map of mean runoff-to-rainfall ratios for the (A) dry-season months (May through October), and (B) wet-season months (November through April) for drainage basins of selected stream-gaging stations and catchment zones on Kaua‘i, Hawai‘i (modified from Rea and Skinner, 2012).

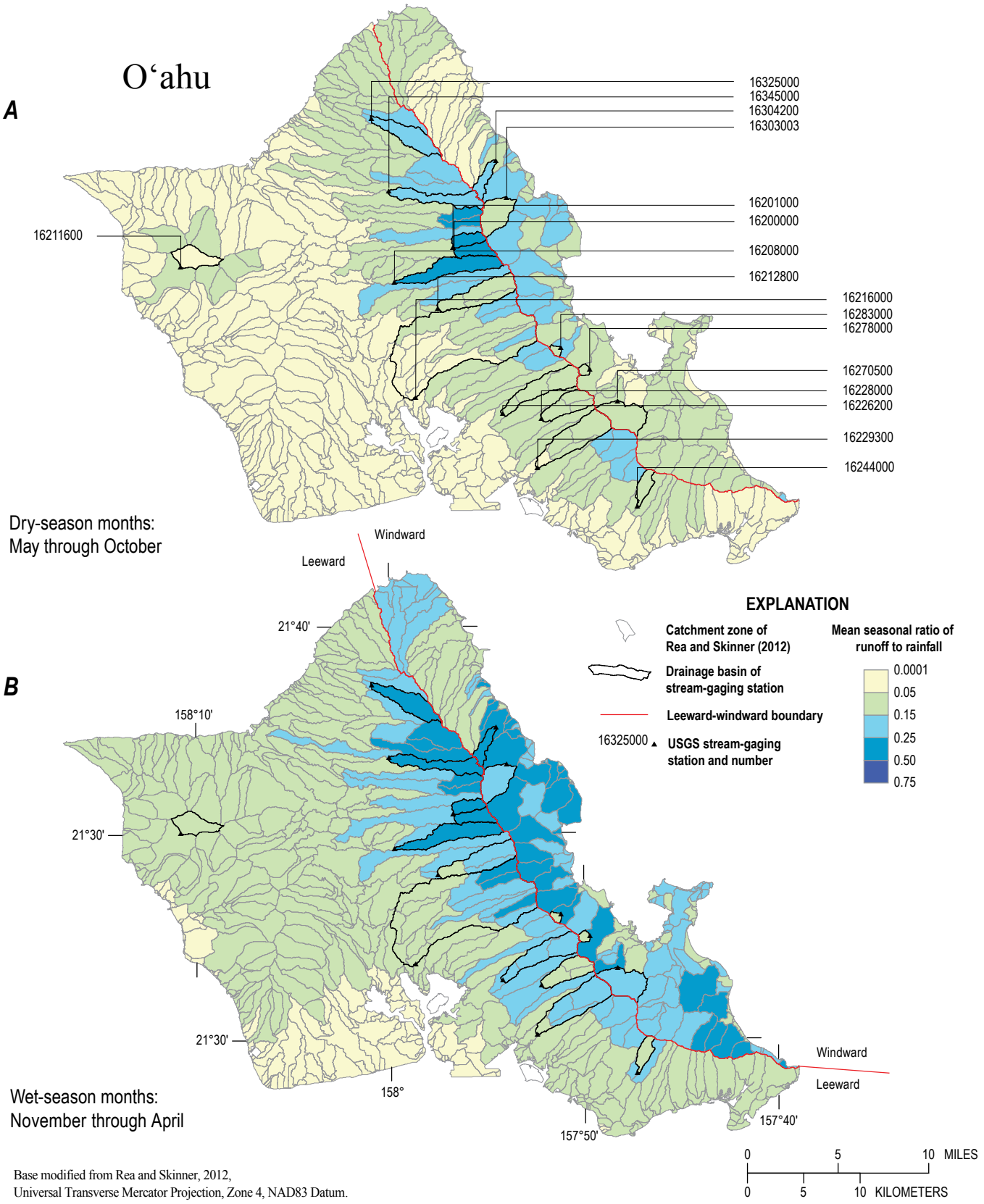

Figure 1-6. Map of mean runoff-to-rainfall ratios for the (*A*) dry-season months (May through October), and (*B*) wet-season months (November through April) for drainage basins of selected stream-gaging stations and catchment zones on O‘ahu, Hawai‘i (modified from Rea and Skinner, 2012).

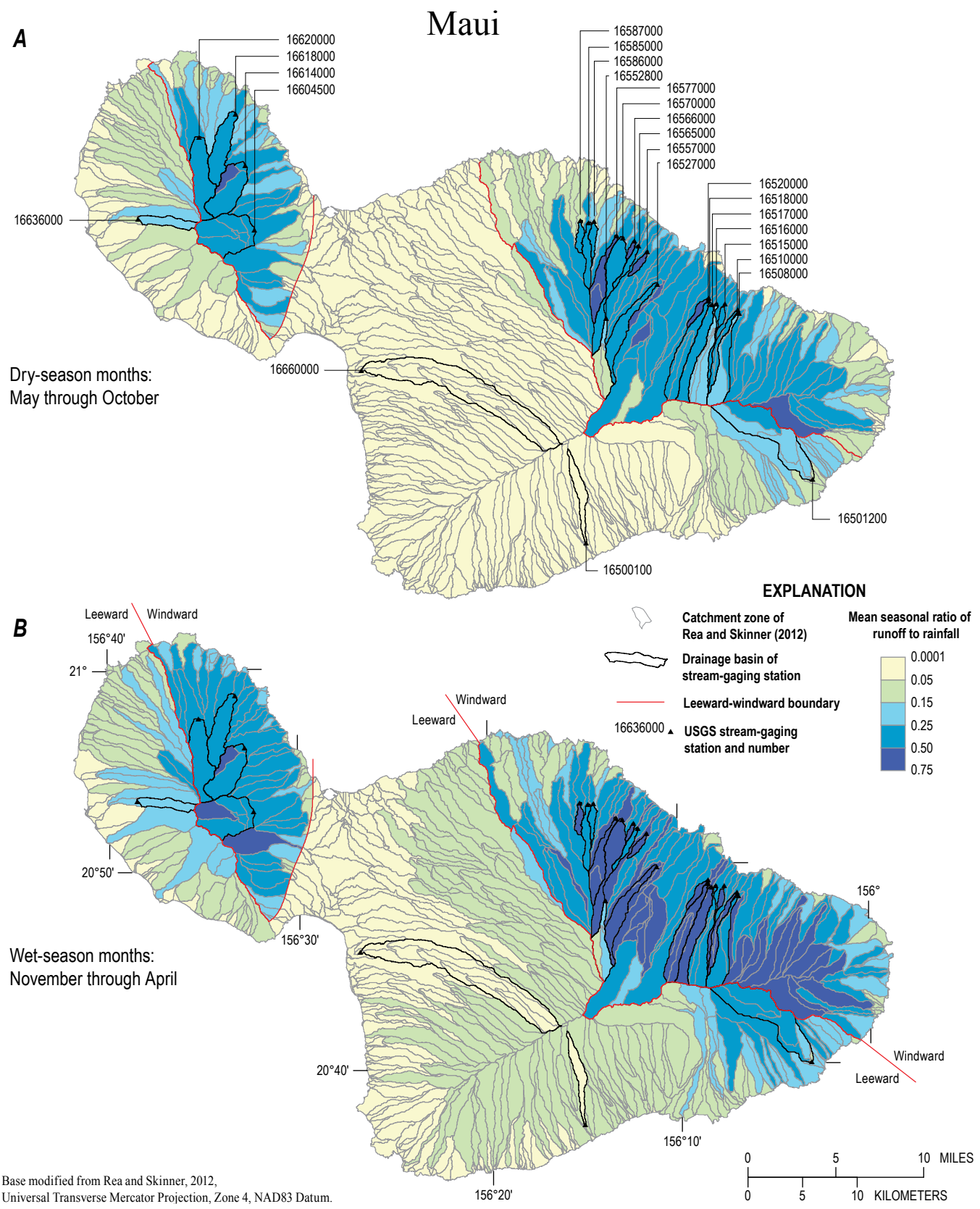

Figure 1-7. Map of mean runoff-to-rainfall ratios for the (*A*) dry-season months (May through October), and (*B*) wet-season months (November through April) for drainage basins of selected stream-gaging stations and catchment zones on Maui, Hawai'i (modified from Rea and Skinner, 2012).

Table 1-5. Mean seasonal runoff-to-rainfall ratios and characteristics for drainage basins of stream-gaging stations on Kauaʻi, Oʻahu, and Maui.

[See figs. 1-5, 1-6, and 1-7 for locations of drainage basins; *n*, number of days used for determining minimum flows in the base flow-separation program (Wahl and Wahl, 1995); E, the base flow-separation program (Wahl and Wahl, 1995) was not used to estimate direct runoff because the streamflow measured at station was ephemeral and was assumed to equal direct runoff; mean annual rainfall estimated from Giambelluca and others (2013) and Frazier and others (2016)]

[1]Gaging-station number	Stream	Island	Aspect	Drainage-basin area (square miles)	*n*	Period of record selected to calculate mean runoff-to-rainfall ratios			Mean runoff-to-rainfall ratio		Mean annual rainfall	
						Start	End	Number of years	Wet season: November through April	Dry season: May through October	During 1978–2007 (inches)	[2]Percentage difference in mean annual rainfall during selected period and 1978-2007 period
16028000 (16022000, 16014000)	Waimea River	Kauaʻi	Leeward	43.68	5	1927	1947	21	0.29	0.22	89.0	5.6
16063000 (16100000, 16062000, 16061000)	North fork Wailua River	Kauaʻi	Windward	5.34	4	1957	1984	28	0.63	0.48	199.8	7.4
16068000	East bank of north fork Wailua River	Kauaʻi	Windward	6.24	4	1978	2007	30	0.50	0.27	129.0	0.0
16071500	Left branch ʻŌpaekaʻa Stream	Kauaʻi	Windward	0.75	4	1978	2007	30	0.22	0.09	100.5	0.0
16089000 (16088000, 16087000)	Anahola Stream	Kauaʻi	Windward	5.45	4	1956	1985	30	0.48	0.35	108.4	5.2
16097500	Halaulani Stream	Kauaʻi	Windward	1.20	4	1978	2007	30	0.62	0.41	115.0	0.0
16103000	Hanalei River	Kauaʻi	Windward	18.51	4	1993	2007	15	0.57	0.34	175.4	-8.1
16108000	Wainiha River	Kauaʻi	Windward	10.44	5	1978	2007	30	0.54	0.39	207.6	0.0
16114000	Limahuli Stream	Kauaʻi	Windward	1.37	4	1995	2005	11	0.35	0.21	116.5	-2.3
16115000	Hanakāpīʻai Stream	Kauaʻi	Windward	2.75	5	1941	1949	9	0.41	0.28	128.7	1.2
16116000	Hanakoa Stream	Kauaʻi	Windward	1.09	5	1939	1947	9	0.53	0.31	105.8	1.9
16117000	Kalalau Stream	Kauaʻi	Leeward	1.60	5	1932	1948	17	0.24	0.09	80.5	4.4
16130000	Nahomalu Valley	Kauaʻi	Leeward	3.79	E	1964	1971	8	0.04	0.01	36.6	26.7
16200000	North fork Kaukonahua Stream	Oʻahu	Leeward	1.38	4	1978	2007	30	0.48	0.49	232.4	0.0
16201000	Right bank of north fork Kaukonahua Stream	Oʻahu	Leeward	1.15	4	1940	1951	12	0.34	0.36	213.4	4.6
16208000	South fork Kaukonahua Stream	Oʻahu	Leeward	4.10	5	1978	2007	29	0.32	0.28	168.9	0.0
16211600	Mākaha Stream	Oʻahu	Leeward	2.12	5	1978	2007	30	0.13	0.04	71.2	0.0
16212800	Kīpapa Stream	Oʻahu	Leeward	4.25	4	1978	2004	27	0.19	0.13	178.3	0.3
16216000	Waiawa Stream	Oʻahu	Leeward	25.19	4	1978	2004	27	0.21	0.12	93.7	0.3
16226200	North Hālawa Stream	Oʻahu	Leeward	4.02	5	1983	2007	24	0.19	0.10	111.8	-2.8
16228000	Moanalua Stream	Oʻahu	Leeward	2.71	4	1949	1978	30	0.15	0.07	117.8	3.1
16229300	Kalihi Stream	Oʻahu	Leeward	5.21	4	1978	2003	26	0.21	0.11	97.6	-1.1
16244000	Pūkele Stream	Oʻahu	Leeward	1.15	5	1953	1982	30	0.14	0.08	114.6	3.6
16270500	Kamoʻoaliʻi Stream	Oʻahu	Windward	3.20	3	1967	1976	9	0.18	0.06	82.8	2.9
16278000	ʻIolekaʻa Stream	Oʻahu	Windward	0.32	3	1944	1968	25	0.09	0.07	95.8	0.4

Table 1-5. Mean seasonal runoff-to-rainfall ratios and characteristics for drainage basins of stream-gaging stations on Kaua'i, O'ahu, and Maui.—Continued

[1]Gaging-station number	Stream	Island	Aspect	Drainage-basin area (square miles)	*n*	Period of record selected to calculate mean runoff-to-rainfall ratios			Mean runoff-to-rainfall ratio		Mean annual rainfall	
						Start	End	Number of years	Wet season: November through April	Dry season: May through October	During 1978–2007 (inches)	[2]Percentage difference in mean annual rainfall during selected period and 1978-2007 period
16283000	Kahalu'u Stream	O'ahu	Windward	0.28	3	1941	1970	30	0.11	0.08	119.2	2.9
16303000 (16302000)	Punalu'u Stream	O'ahu	Windward	2.78	4	1978	2006	29	0.21	0.13	186.6	0.4
16304200	Kaluanui Stream	O'ahu	Windward	1.09	4	1978	2007	30	0.34	0.25	168.4	0.0
16325000	Kamananui Stream	O'ahu	Leeward	3.15	4	1971	2000	30	0.29	0.15	132.0	0.0
16345000	'Ōpae'ula Stream	O'ahu	Leeward	3.00	4	1978	2007	30	0.37	0.24	164.6	0.0
16500100	Kepuni Gulch	Maui	Leeward	1.93	E	1963	1972	10	0.04	0.01	33.1	35.1
16501200	'Ohe'o Gulch	Maui	Leeward	8.53	4	1990	1997	8	0.38	0.25	249.4	0.7
16508000	Hanawī Stream	Maui	Windward	3.29	4	1978	2007	30	0.42	0.24	248.7	0.0
16510000	Kapā'ula Gulch	Maui	Windward	1.35	4	1933	1962	30	0.61	0.38	257.3	1.2
16515000	Waiohue Gulch	Maui	Windward	0.74	4	1933	1962	30	0.52	0.32	247.9	1.3
16516000	Kopiliula Stream	Maui	Windward	3.56	4	1938	1957	20	0.43	0.24	197.8	3.4
16517000	East Wailuaiki Stream	Maui	Windward	3.14	4	1928	1957	30	0.58	0.35	201.2	4.7
16518000	West Wailuaiki Stream	Maui	Windward	3.59	4	1978	2007	30	0.64	0.39	183.5	0.0
16520000	East Wailuanui Stream	Maui	Windward	0.53	4	1928	1957	30	0.75	0.55	228.1	5.4
16527000	Honomanū Stream	Maui	Windward	2.94	4	1939	1963	25	0.55	0.45	149.8	3.7
16552800	Waikamoi Strream	Maui	Windward	2.50	4	1957	1967	11	0.17	0.12	62.9	3.5
16557000	Alo Stream	Maui	Windward	0.47	4	1928	1957	30	0.75	0.65	209.3	2.0
16565000	Ka'aiea Gulch	Maui	Windward	0.68	4	1933	1962	30	0.50	0.44	216.5	-0.5
16566000	'O'opuola Stream	Maui	Windward	0.25	4	1931	1957	27	0.64	0.54	189.4	-0.8
16570000	Na'ili'ilihaele Stream	Maui	Windward	3.69	5	1945	1974	30	0.60	0.50	181.9	-1.7
16577000	Kailua Stream	Maui	Windward	2.41	4	1928	1957	30	0.75	0.53	203.4	1.8
16585000	Ho'olawanui Stream	Maui	Windward	1.34	5	1942	1971	30	0.50	0.32	174.9	-0.7
16586000	Ho'olawali'ili'i Stream	Maui	Windward	0.62	4	1931	1957	27	0.43	0.33	160.2	4.8
16587000	Honopou Stream	Maui	Windward	0.59	4	1978	2007	30	0.57	0.38	145.6	0.0
16604500	'Īao Stream	Maui	Windward	6.13	4	1983	2007	24	0.48	0.40	178.1	-3.8
16614000	Waihe'e River	Maui	Windward	4.27	3	1984	2007	24	0.49	0.45	184.6	-2.4
16618000	Kahakuloa Stream	Maui	Windward	3.40	4	1978	2007	30	0.43	0.33	127.0	0.0
16620000	Honokōhau Stream	Maui	Windward	4.18	4	1978	2007	28	0.35	0.31	200.3	0.0
16636000	Kanahā Stream	Maui	Leeward	1.57	3	1920	1931	11	0.17	0.16	141.8	3.1
16660000	Kūlanihāko'i Gulch	Maui	Leeward	15.03	E	1963	1970	8	0.01	0.00	22.4	38.6

[1]Data for gaging-station numbers in parentheses were used to reconstruct streamflow at the gaging station whose number is not in parentheses.

[2]For example, mean annual rainfall on the drainage basin of station 16500100 was 35 percent greater during 1963–1972 than that during 1978–2007.

has been used in numerous other studies in Hawai‘i (for example, Izuka and others, 2005, Engott and Vana, 2007, Engott, 2011) and provides a reasonable estimate of base flow for perennial streams in Hawai‘i. The method defines local streamflow minimums within consecutive, nonoverlapping *n*-day periods and requires two parameters (1) *f*, the turning-point test factor, and (2) *n*, the number of days in a test window. In this study, the *f* value used for all stations was 0.9. The *n* values were determined for each station using the method described by Wahl and Wahl (1995) and ranged from 3 to 5 days (table 1-5). Daily base flow was subtracted from daily streamflow to determine daily direct runoff.

Observed seasonal runoff-to-rainfall ratios were calculated for gaged drainage basins that were operational during 1978–2007, but are not presented in this report. Each observed seasonal runoff-to-rainfall ratio for the gaged drainage basins was calculated as the quotient of cumulative direct runoff and cumulative rainfall during the season. For example, the observed runoff-to-rainfall ratio for a gaged basin during the dry season of 2001 was calculated as the quotient of cumulative direct runoff and cumulative rainfall during May–October 2001.

For each of the 55 selected gaged drainage basins on Kaua‘i, O‘ahu, and Maui, mean seasonal runoff-to-rainfall ratios were calculated for a period with rainfall and runoff conditions generally representative of those during 1978–2007 (table 1-5). Each mean seasonal runoff-to-rainfall ratio for the gaged drainage basins was calculated as the quotient of cumulative direct runoff and cumulative rainfall during the appropriate season of the selected period. For example, the mean dry-season runoff-to-rainfall ratio for stream-gaging station 16228000 was calculated as the quotient of cumulative direct runoff and cumulative rainfall during May–October between 1949 and 1978.

Criteria for selecting periods of record were determined by examining temporal variations in seasonal runoff-to-rainfall ratios for stream-gaging stations that were operational during 1978–2007. For these stations, mean seasonal runoff-to-rainfall ratios calculated for 1978–2007 were compared with those calculated for smaller subset periods during 1920–2007. The results of these comparisons show that the difference between mean seasonal runoff-to-rainfall ratios calculated for 1978–2007 and those calculated for subset periods decreases with increasing record length of the subset period, and with decreasing differences between mean annual rainfall during 1978–2007 and that of the subset period. Accordingly, the period of record selected to calculate mean seasonal runoff-to-rainfall ratios was (1) the entire period during 1978–2007 for stream-gaging stations with at least 24 complete years of record during that time, (2) the longest continuous period during 1920–2007 that had less than a 5-percent difference in mean annual rainfall, relative to rainfall for 1978–2007, for all remaining stream-gaging stations on perennial streams with base flow, and (3) the entire period of record for three stream-gaging stations on ephemeral streams. Despite the relatively high rainfall during their periods of record (table 1-5), the latter three stations were included in the analysis owing to the sparseness of runoff data for areas with ephemeral streams.

Runoff-to-Rainfall Ratios Assigned to Ungaged Catchment Zones

Ungaged catchment zones are outside of the drainage basins of the 55 selected stream-gaging stations on Kaua‘i, O‘ahu, and Maui (figs. 1-5, 1-6, and 1-7). Direct runoff for ungaged catchment zones was calculated using mean seasonal runoff-to-rainfall ratios determined from four regional-regression equations (table 1-6) derived from mean seasonal runoff-to-rainfall ratios and basin characteristics for the 55 stream-gaging stations (table 1-5). Separate windward and leeward regression equations were derived for the wet and dry seasons. The regional-regression equations relate mean seasonal runoff-to-rainfall ratios and basin characteristics, and were developed with methods consistent with the discussion given in Helsel and Hirsch (1992).

To derive the regional-regression equations, 30 basin characteristics—including those related to climate, soil, and vegetation—were evaluated as possible explanatory variables (not shown). The regional regressions (table 1-6) were selected because they had the lowest residual sum of squares and met the following criteria: (1) all regression coefficients were statistically significant at a 5-percent significance level, (2) the sign and magnitude of the fitted coefficients were physically meaningful, and (3) the cross-validated results indicated less than 10 percent bias. For leeward catchment zones, wet-season runoff-to-rainfall ratios were estimated on the basis of mean wet-season rainfall during 1978–2007 (Giambelluca and others, 2013); dry-season

Table 1-6. Regional regression models used to estimate mean seasonal runoff-to-rainfall ratios in ungaged areas on Kaua‘i, O‘ahu, and Maui.

[See figs. 1-5, 1-6, and 1-7 for locations of windward and leeward regions; wet season, November-April; dry season, May-October; rainfall is from Giambelluca and others (2013) in inches; ETo, reference evapotranspiration is from Giambelluca and others (2014) in inches; % HSG C, percentage of area with soil in hydrologic soil group C as defined by U.S. Department of Agriculture (2006a,b,c); % HSG D, percentage of area with soil in hydrologic soil group D as defined by U.S. Department of Agriculture (2006a,b,c)]

Region	Season	Regression used to calculate runoff-to-rainfall ratio	Root-mean-square error				Percentage bias			
			Overall	Kaua‘i	O‘ahu	Maui	Overall	Kaua‘i	O‘ahu	Maui
Leeward	Wet	0.00320 [wet-season rainfall]	**0.06**	0.07	0.06	0.06	**0.6**	-21	-3	38
Leeward	Dry	0.00293 [dry-season rainfall]	**0.07**	0.08	0.07	0.03	**3.8**	-39	6	24
Windward	Wet	$[\%\ HSG\ C]^{0.185}\ [\%\ HSG\ D]^{0.247}\ [annual\ ETo]^{-0.590}$	**0.12**	0.13	0.13	0.12	**-4.8**	-20	28	-1
Windward	Dry	$[\%\ HSG\ C]^{0.186}\ [\%\ HSG\ D]^{0.346}\ [dry\text{-}season\ ETo]^{-0.947}$	**0.11**	0.09	0.10	0.12	**-5.8**	-15	23	-5

runoff-to-rainfall ratios were estimated on the basis of mean dry-season rainfall during 1978–2007. For windward catchment zones, wet-season runoff-to-rainfall ratios were estimated on the basis of mean annual reference ET (Giambelluca and others, 2014) and the percentage of the catchment zone's area containing hydrologic soil groups C and D (U.S. Department of Agriculture, 2006a,b,c); dry-season runoff-to-rainfall ratios were estimated on the basis of mean dry-season reference ET and the percentage of the zone's area containing hydrologic soil groups C and D. The performance statistics of the regression equations (table 1-6) are used to examine the sensitivity of recharge to runoff-to-rainfall ratios (see *Sensitivity Analysis)*.

Runoff-to-Rainfall Ratios Assigned to Gaged Basins with a Single Catchment Zone

For stream-gaging stations having drainage basins with a single catchment zone (fig. 1-5, 1-6, and 1-7) that were not operational during 1978–2007 (table 1-5), the recharge model calculated direct runoff for the drainage basins by using mean seasonal runoff-to-rainfall ratios. For stream-gaging stations having drainage basins with a single catchment zone that were operational during part or all of 1978–2007 (table 1-5), the model calculated direct runoff for the drainage basins by using (1) observed seasonal runoff-to-rainfall ratios, for seasons when observed ratios were available, and (2) mean seasonal runoff-to-rainfall ratios for seasons when observed ratios were not available.

Runoff-to-Rainfall Ratios Assigned to Gaged Basins with Multiple Catchment Zones

For stream-gaging stations having drainage basins containing multiple catchment zones (fig. 1-5, 1-6, and 1-7), the model calculated direct runoff for each of the catchment zones by using adjusted seasonal runoff-to-rainfall ratios determined from equation 14:

$$\widetilde{rr}_{a,t} = \widetilde{RR}_a \times \frac{rr_{b,t} \times rf_{b,t}}{\sum_{i=1}^{j} \widetilde{RR}_i \times rf_{i,t}} \qquad (14)$$

where

$\widetilde{rr}_{a,t}$ is the adjusted runoff-to-rainfall ratio for catchment zone a during season t [dimensionless],

$\widetilde{RR}_a$ is the mean runoff-to-rainfall ratio for catchment zone a estimated using the appropriate regional-regression equation (table 1-6) [dimensionless],

j is the number of catchment zones in the gaged basin b [dimensionless],

$\widetilde{RR}_i$ is the mean runoff-to-rainfall ratio for catchment zone i estimated using the regional-regression equations [dimensionless],

$rf_{i,t}$ is the rainfall for catchment zone i during season t [L^3],

$rr_{b,t}$ is the observed runoff-to-rainfall ratio for the gaged basin b during season t. If the observed runoff-to-rainfall ratio for gaged basin b is not available during season t, the mean seasonal runoff-to-rainfall ratio is used (table 1-5) [dimensionless], and

$rf_{b,t}$ is the rainfall for gaged basin b during season t [L^3].

Equation 14 uses the regional-regression models and seasonal rainfall to spatially disaggregate observed seasonal and mean seasonal runoff-to-rainfall ratios of a gaged basin for each catchment zone within a gaged basin. Hence, seasonal runoff-to-rainfall ratios were allowed to be spatially variable, instead of spatially uniform, across the catchment zones within gaged drainage basins containing multiple catchment zones.

Evapotranspiration

Evapotranspiration (ET) is a collective term for all of the evaporative and plant-transpiration processes in a plant-soil system. These processes can be grouped into three main types: (1) canopy evaporation, which is evaporation of intercepted rain and fog from the vegetation surface; (2) ground evaporation, which is evaporation from the soil surface and overlying litter and mulch layers; and (3) transpiration, the process by which soil moisture taken up by vegetation is eventually evaporated as it exits at plant pores (Viessman and Lewis, 2003, p. 143). These processes are difficult to quantify individually and are commonly combined together in water budgets. A more rigorous treatment of ET is often appropriate for some areas because ET processes tend to operate on much different time scales and vary in relative importance according to prevailing meteorological conditions and land-cover setting. Canopy and ground evaporation operate on the order of hours, whereas transpiration operates on the order of weeks or longer, depending on soil depth (Savenije, 2004).

Canopy evaporation can be very important in forests. Because of the height of trees, turbulent diffusion is much more efficient at removing intercepted water from forests than from other land-cover types, and this enhanced rate of evaporation from a wet canopy makes realistic estimates of ET from forests possible only if transpiration and canopy evaporation are evaluated separately (Shuttleworth, 1993). In the recharge model, ET in forests is calculated by separately estimating canopy evaporation and combined ground evaporation and transpiration. These two terms are then added together to yield a total ET rate. For all other land covers, ET is calculated using a more traditional approach, commonly used in agricultural practice, in which canopy evaporation and combined ground evaporation and transpiration are not separately estimated. The concept of potential ET, combined with soil-moisture limiting, is used to estimate ground

evaporation and transpiration in forests and total ET for all other land covers. Canopy evaporation in forests is estimated using a method based on Gash and others (1995), modified for this study to include fog interception.

Forest Canopy Evaporation and Net Precipitation

As rain falls on a vegetated surface, some of the droplets will strike and collect on the leaves, trunks, or stems of the vegetation in a process known as canopy interception. Additional moisture from fog interception may also enhance the volume of this collected water, which is called canopy storage. Canopy storage is partitioned into three fractions: (1) that which remains on the vegetation and is evaporated after or during rainfall, called canopy evaporation in this study; (2) that which flows to the ground along trunks or stems, called stemflow; and (3) that which drips from the canopy and falls to the ground between the various components of the vegetation (Crockford and Richardson, 2000). The fraction of rain that does not contact vegetation on the way to the ground combined with the fraction described in (3) is called throughfall. The amount of water that reaches the soil surface, called net precipitation, is the sum of throughfall and stemflow. Canopy interception occurs in all vegetated land covers, but research primarily has been limited to forests. Direct measurements of canopy evaporation are very difficult to obtain and rarely attempted. Instead, it is far more common for researchers to collect net precipitation on the forest floor, beneath the canopy, and compare it to rainfall collected contemporaneously above the forest canopy or in a nearby open field. Therefore, net precipitation typically is reported as a percentage of rainfall, regardless of whether or not fog interception is occurring in the forest. In areas with fog interception, it is possible for net precipitation to be greater than 100 percent of rainfall.

For this study, net precipitation in forests was calculated as rainfall plus fog interception minus canopy evaporation (equation 3). In nonforested areas, net precipitation was calculated as rainfall plus fog interception. Canopy evaporation was estimated using a precipitation-interception model modified from Gash and others (1995). In the recharge calculation, the first step is to determine P', which is the minimum depth of precipitation necessary to saturate the forest canopy:

$$P' = -(S/(c \times E/R)) \times \ln(1 - E/R), \quad (15)$$

where

- P' is the precipitation necessary to saturate the canopy [L],
- S is the canopy capacity per unit of ground area [L] (a constant),
- c is the canopy cover per unit of ground area [dimensionless], and
- E/R is the ratio of mean evaporation rate to mean precipitation rate during saturated conditions [dimensionless].

Depending on P' and the amount of precipitation for a given day, P_i, canopy evaporation $(CE)_i$ is calculated as:

for $P_i \le P'$, $(CE)_i = c \times P_i$,

for $P_i \ge P'$ and $P_i \le k/p$, $(CE)_i = c \times P' + c \times E/R \times (P_i - P') + p \times P_i$,

for $P_i \ge P'$ and $P_i > k/p$, $(CE)_i = c \times P' + c \times E/R \times (P_i - P') + k$, (16)

where

- k is the trunk-storage capacity [L] (a constant), and
- p is the fraction of precipitation diverted to stem flow [dimensionless].

Canopy capacity per unit ground area, S, is the depth of water left on the canopy in zero evaporation conditions when rainfall and throughfall have ceased (Gash and Morton, 1978). Canopy capacity was set at 0.05 in., which is the average of the mean values reported for six forested sites in Hawai‘i (DeLay, 2005, p. 42; Takahashi and others, 2011, Safeeq and Fares, 2012). Canopy cover per unit ground area, c, is the fraction of a forested subarea that is covered by leaves, stems, and branches of trees. The canopy cover of each forested subarea in the recharge model was estimated from maps of mean annual vegetation cover fraction (Giambelluca and others, 2014). These maps quantify the vegetation cover fraction at a spatial resolution of about 14 acres. The calculated canopy-cover values for forested subareas in the recharge model range from 0.03 to 1. Trunk storage capacity, k, was set at 0.01 inches, which is the average of the values reported for four forest sites in Hawai‘i (DeLay, 2005, p. 42; Safeeq and Fares, 2012). The fraction of precipitation diverted to stem flow, p, was assumed to be 0.04, which is the average of the reported values for eight forest sites in Hawai‘i (Gaskill, 2004; DeLay, 2005; Takahashi and others, 2011; Safeeq and Fares, 2012). Some forest sites in Takahashi and others (2011) and Safeeq and Fares (2012) that had an abundance of *Psidium cattleianum* (strawberry guava) were excluded from the average because of very high stem-flow rates relative to the other sites.

Very little published data exist from which to estimate E/R for Hawaiian forests. For this study, subareas with forested land covers on Kaua‘i, O‘ahu, and Maui were selected and average annual canopy-evaporation rates were estimated for 2001 to 2010 for each subarea using equation 16 and a range of E/R values. For each subarea, the value of E/R that resulted in a calculated canopy-evaporation rate that most closely matched a map of mean annual wet canopy evaporation for the Hawaiian Islands (Giambelluca and others, 2014) was selected. Relations between these calibrated E/R values and various other parameters of the selected subareas, including mean annual rainfall, reference ET, Penman-Monteith ET from Giambelluca and others (2014), and estimates of mean annual wind speed from AWS Truewind, LLC (2004) were determined.

Estimates of *E/R* from a linear regression (equation 17) relating *E/R* to the quotient of mean annual wind speed and mean annual rainfall resulted in the best agreement with the calibrated *E/R* values, in terms of bias and root-mean-square error.

$$\text{For } w < 0.009, \quad E/R = 0.01,$$

$$\text{for } 0.009 \le w \le 0.192, \quad E/R = 2.677 \times w - 0.014, \text{ and}$$

$$\text{for } w > 0.192, \quad E/R = 0.50, \qquad (17)$$

where

w is the mean annual wind speed divided by mean annual rainfall (m/s/in).

Equation 17 was used to estimate the spatial distribution of *E/R* for the recharge model. The variable *w* is the quotient of (1) mean annual wind speed, in m/s, which was derived from a map of mean annual wind speed at a height of about 100 ft above the land surface (AWS Truewind, LLC, 2004), and (2) 1978–2007 mean annual rainfall, in inches (Giambelluca and others, 2013). In general, estimates of *E/R* for wet areas are less than those for dry areas. A range of 0.01–0.50 was established for this analysis on the basis of the range of mean *E/R* estimates in published reports. The low end of the range, 0.01, was determined by Hutjes and others (1990) for a humid, tropical forest site in the Ivory Coast. The high end of the range, 0.50, is the mean value reported by Safeeq and Fares (2012) for a forest site on leeward O‘ahu. A similar range of mean *E/R* estimates (about 0.03–0.40) was determined for 54 sites in various climate zones across Australia (Wallace and others, 2013). Subareas with calibrated *E/R* values that were outside the range of 0.01–0.50 were excluded from the derivation of equation 17.

Potential Evapotranspiration

Potential evapotranspiration (ET) is the maximum rate that water can be removed from the plant-root zone by ET if soil moisture is nonlimiting (Giambelluca, 1983). The actual-ET rate is a function of potential ET, soil-moisture content, and threshold-moisture content (see equation 10). The actual-ET rate becomes less than the potential rate with the onset of soil-moisture stress. As the soil dries, capillary and adsorptive forces bind the remaining water to the soil matrix, reducing water flow to roots. Soil-moisture stress occurs when the decreasing flow of water to the root system induces a response in the plant to slow down transpiration and prevent desiccation. The threshold-moisture content at which a plant begins to react to soil drying varies with the type of plant.

Potential ET is controlled by atmospheric conditions, topography, and land-cover characteristics (Giambelluca, 1983). Maps of mean monthly reference ET produced by Giambelluca and others (2014) were used in the water-budget model to estimate the influence of atmospheric conditions (radiation, air temperature, air humidity, and wind speed) on potential ET. Crop coefficients were used to estimate the integrated effects of land-cover and vegetation characteristics on potential ET. Potential ET for each subarea was calculated in the water-budget model as the product of mean monthly reference ET and the crop coefficient assigned to the land cover, and was assumed to be constant within a given month.

Reference Evapotranspiration

Reference ET, as defined in this study, is the potential ET of a hypothetical grass surface with specific characteristics and optimum soil-water conditions for given climatic conditions, and is equivalent to FAO Penman-Monteith ET (Allen and others, 1998). Reference ET is conceptually similar to pan evaporation, which has been used in previous water budgets for Maui and other Hawaiian Islands. Both pan evaporation and reference ET provide an index of the energy that is available for ET for a given area.

Maps of mean monthly grass-reference ET (Giambelluca and others, 2014) for Kaua‘i, O‘ahu, and Maui were used in the recharge model (figs. 1-8, 1-9, and 1-10). These maps have the same grid resolution as the monthly rainfall maps. Mean annual reference ET ranges from about 25 to 113 inches across the three islands. In general, mean annual reference ET is highest in dry lowland areas, and is lowest in wet upland areas within the cloud zone. In the water-budget calculation, monthly reference ET was not varied from year to year, and was assumed to equal mean monthly reference ET. Reference ET was assumed to be the same each day of a given month.

Crop Coefficients

A crop coefficient is an empirically derived ratio of the potential ET of a given land-cover type to reference ET. Crop coefficients, assigned to each land-cover category, provide an index of the integrated effect of vegetation characteristics (reflectance, roughness, and plant physiology) on potential ET (table 1-1). Crop coefficients were assumed to be temporally constant for all categories except sugarcane and corn. For nonforest land-cover categories, crop coefficients incorporate transpiration, ground evaporation, and canopy evaporation. For forest land-cover categories, crop coefficients incorporate only transpiration and ground evaporation; canopy evaporation is accounted for separately.

The crop coefficients for coffee and macadamia are the average of the monthly crop coefficients in Fares (2008). The range of monthly coefficients is 0.85 to 0.95 for both crops. Crop coefficients for shrubland and diversified agriculture were derived from pan coefficients used in several previous recharge reports for Hawai‘i (Izuka and others, 2005; Engott and Vana, 2007; Engott, 2011), using a ratio of FAO Penman-Monteith ET to pan evaporation of 0.85, which was derived in Engott (2011). A pan coefficient for a given land-cover category is the ratio of potential ET to pan evaporation. Crop coefficients for fallow/grassland, pineapple, taro, golf course, grassland, water body, reservoir, estuarine/near-coastal water body, and wetland are based on Allen and others (1998). The golf-course crop coefficient is based on the warm-season turf-grass value. Crop coefficients for

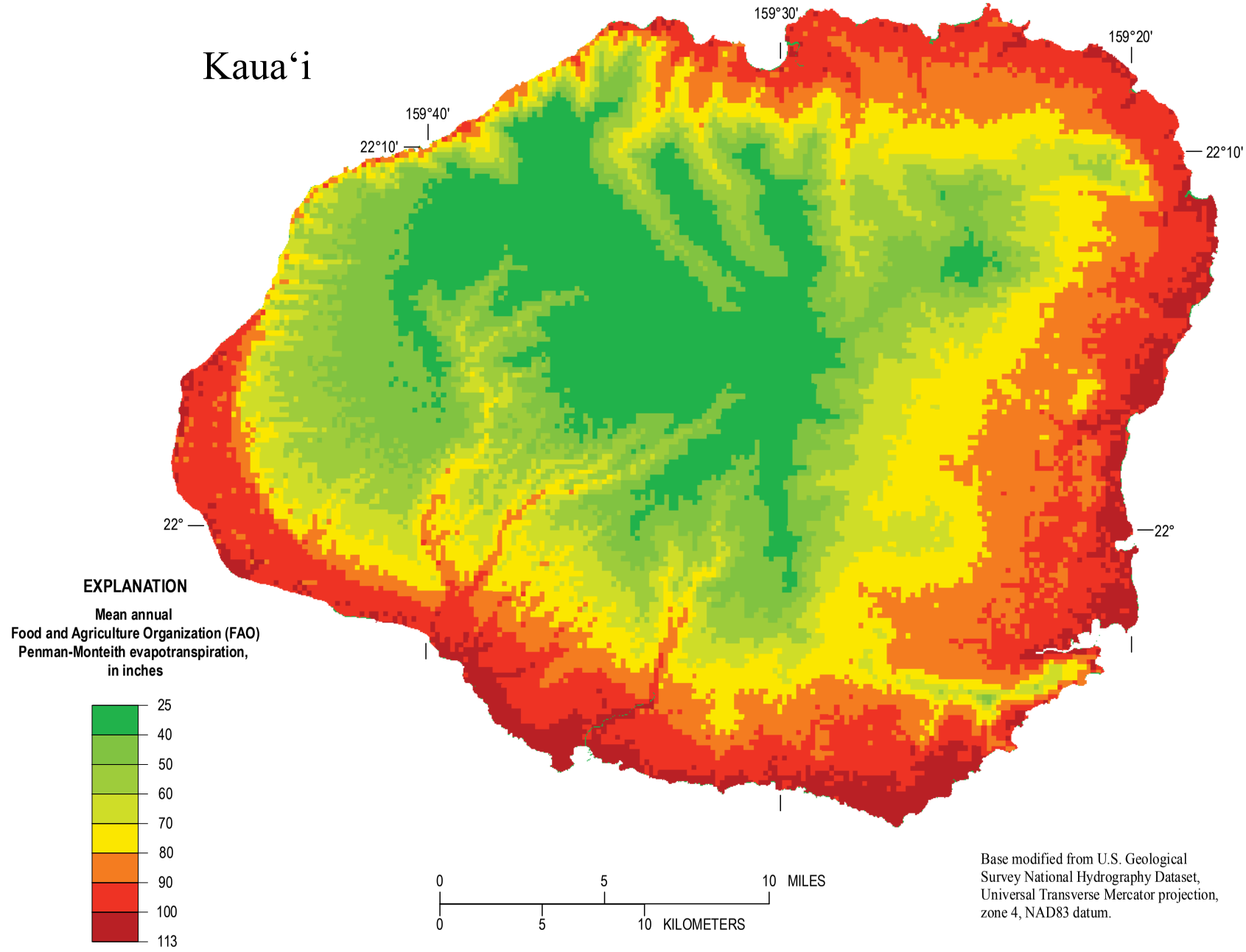

Figure 1-8. Map of mean annual reference evapotranspiration on Kaua'i (modified from grass-reference evapotranspiration in Giambelluca and others, 2014).

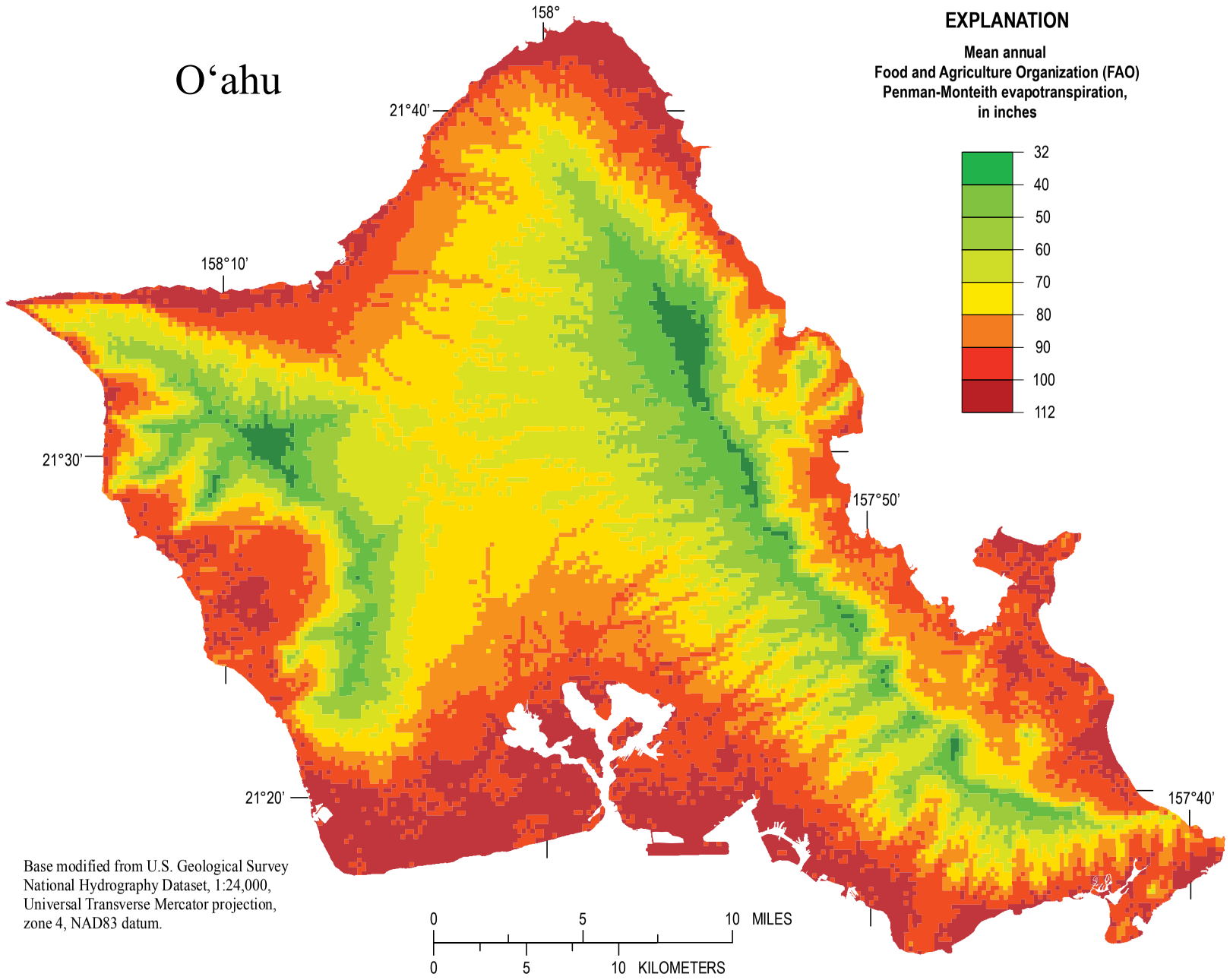

Figure 1-9. Map of mean annual reference evapotranspiration on O‘ahu (modified from grass-reference evapotranspiration in Giambelluca and others, 2014).

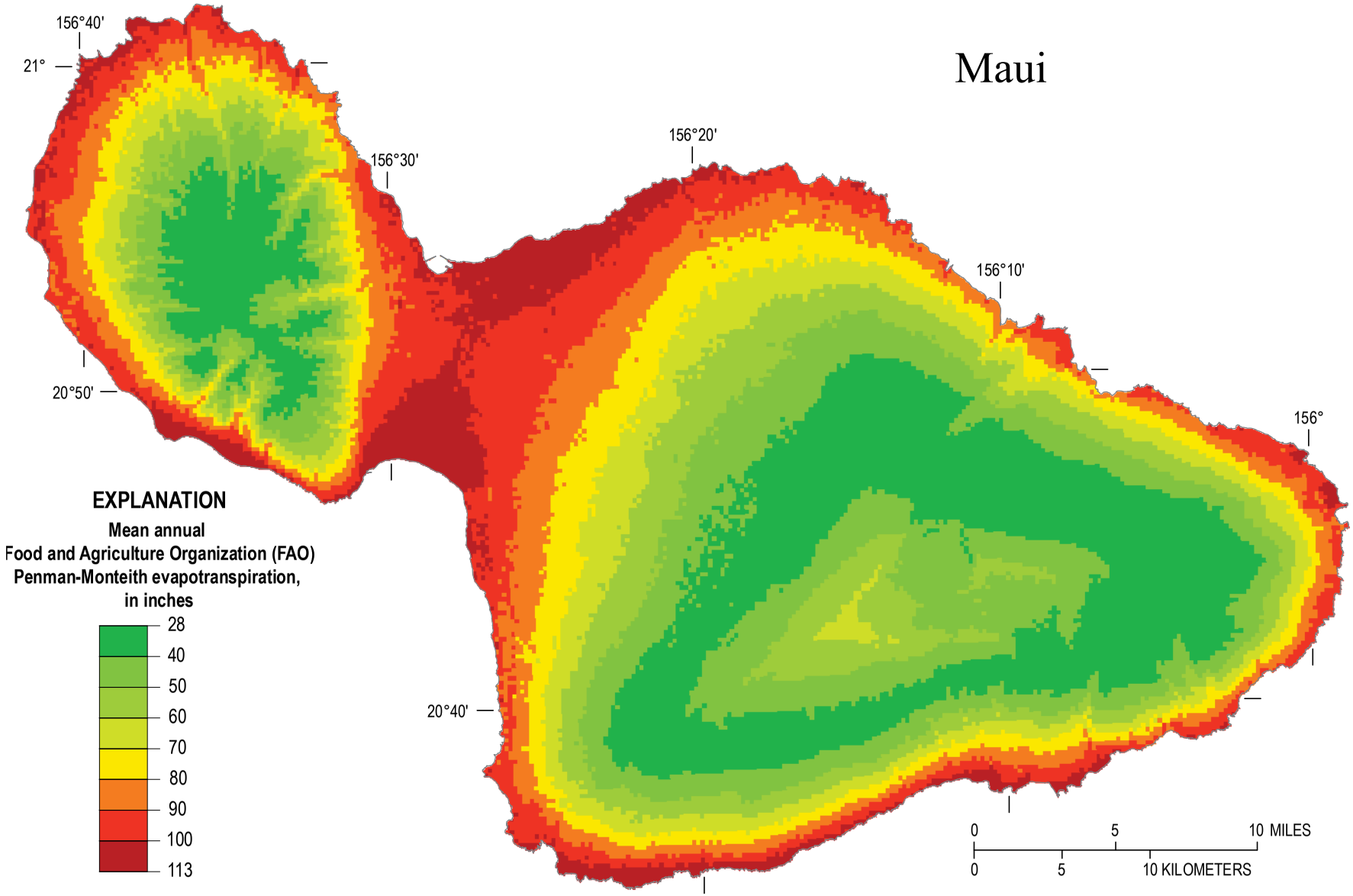

Base modified from U.S. Geological Survey National Hydrography Dataset, Universal Transverse Mercator projection, zone 4, NAD83 datum.

Figure 1-10. Map of mean annual reference evapotranspiration on Maui (modified from grass-reference evapotranspiration in Giambelluca and others, 2014).

taro, water body, reservoir, and estuarine/near-coastal water body are based on the tropical open-water value. Crop coefficients for the developed land-cover categories are based on the urban category in Giambelluca (1983). The crop coefficient for sparsely vegetated land cover is based on the pan coefficient used in Engott (2011). The crop coefficients for corn vary monthly and are based on information in the Hawai‘i Agricultural Water Use and Development Plan (University of Hawai‘i, 2008). The crop coefficients used are 0.85, 0.50, 0.29, 0.40, 0.80, 1.20, 0.85, 0.50, 0.29, 0.40, 0.80, and 1.20 for the months of January through December, respectively.

The sugarcane crop coefficients vary with time according to the different stages of the sugarcane cultivation cycle (fig. 1-4). These crop coefficients were based on temporally variable pan coefficients that were derived from Fukunaga (1978) and were used to estimate the potential ET of sugarcane in previous water budgets for Hawai‘i (Izuka and others, 2005; Engott and Vana, 2007). For the recharge calculations of this study, the sugarcane cultivation cycle was divided into the same growth stages used by Engott and Vana (2007). The pan coefficients for the different growth stages of the sugarcane cultivation cycle, which range between 0.25 and 1.0, were converted to crop coefficients by dividing them by 0.80. The factor 0.80 is the ratio of the pan coefficient from Fukunaga (1978) to the crop coefficient from Allen and others (1998) for mid-growth sugarcane.

Crop coefficients for alien and native forest land covers, both in and out of the fog zone, were calibrated to produce the closest match between mean annual transpiration and ground evaporation simulated by the recharge model and ET data from Giambelluca and others (2014) for Kaua‘i, O‘ahu, and Maui combined. The calibration used 2010 land-cover conditions and a separate 2001–2010 rainfall distribution dataset (see *Rainfall* section, above). (A subsequent check showed that the difference between coefficients produced using this dataset and coefficients produced using data from Frazier and others [2016] ranged from 0.00 to 0.02, which affects overall recharge in forested areas by less than 0.4 percent.) Several previous studies have provided some evidence that transpiration of native trees in foggy areas or conditions may be less than in drier areas or conditions (Santiago and others, 2000; Giambelluca and others, 2009); however, this distinction did not manifest in the crop-coefficient calibration for this study. One possible reason for this is that much of the native forest does not occur in the fog zone, the lower boundary of which is set at 2,000 ft for this study, but largely occurs in relatively high rainfall areas not far below the boundary. Therefore, the distinction between fog and non-fog native forest, in terms of crop coefficient, is not as pronounced as is the case for alien forest. Alien forest tends to occur in greater abundance in lower and drier areas compared to native forest. Crop coefficients for tree plantations were set equal to the alien forest category. Crop coefficients for kiawe/phreatophytes were derived from ET data for a kiawe (*Prosopis pallida*) relative, velvet mesquite (*Prosopis velutina*), in a study in Arizona (Leenhouts and others, 2006).

To estimate the crop coefficients of the land-cover categories for predevelopment land-cover conditions in 1870, combinations of other land covers were used (James Jacobi, USGS, written commun., 2014). These combination land covers are open native forest (grass/shrub), grass/shrubland, and sparse grassland (table 1-1). The percentage of canopy cover for open native forest was set at 45 percent (James Jacobi, USGS, written commun., 2014). The crop coefficient for open native forest (grass/shrub) was determined by combining the crop coefficients for area open to the sky and area beneath canopy. First, the crop coefficient of area open to the sky was calculated as 10 percent of the crop coefficient for sparsely vegetated, plus 40 percent of the crop coefficient for shrubland, plus 50 percent of the crop coefficient for grassland. The combined crop coefficient for area open to the sky and area beneath canopy was then calculated as 55 percent of the crop coefficient for area open to the sky plus 45 percent of the crop coefficient for native forest. The crop coefficient for grass/shrubland was calculated as the average of the grassland and shrubland crop coefficients. The crop coefficient for sparse grassland was calculated as the average of the sparsely vegetated and grassland crop coefficients.

Soil-Moisture Storage Capacity

The soil-moisture storage capacity of the plant-root zone (figs. 1-11, 1-12, and 1-13) was calculated as the product of available water capacity and root depth (equation 9). The U.S. Department of Agriculture (USDA) (2006a,b,c) soil maps and corresponding tables of available water capacities at various depth intervals were used to calculate a depth-weighted mean available water capacity for each subarea in the water-budget model. The soil unit “rock outcrop” has zero available water capacity at all depths according to tables of USDA (2006a,b,c). For this study, zero available water capacity for the “rock outcrop” soil unit was considered too low because many areas with this soil unit were mapped as grassland or shrubland. Therefore, for the water-budget calculations, available water-capacity values for the “rock land” soil unit were used for all subareas with the “rock outcrop” soil unit. The soil unit “rock land” was selected because it generally was mapped near “rock outcrop” soils and because its available water capacity exceeds zero in the top eight inches of soil.

Root depth varies by land-cover category (table 1-1). In this study, assignments of root depths were based on previously published information. The root depth for sugarcane is the same as that used by Engott and Vana (2007). The root depth for pineapple is the middle of the ranges reported in Fares (2008) and Allen and others (1998). The root depth for diversified agriculture is the middle of the range reported in Fares (2008) for typical diversified agriculture crops in Hawai‘i. The root depth for corn is the final root depth reported in Fares (2008). The root depth for kiawe/phreatophytes is based on Pasiecznik and others (2001) for the lower extent of the lateral root zone. The root depth for wetland assumes that grass is the dominant vegetation. For all other land-cover categories, the root depths are the same as those used by Engott (2011). The root depth used in this report for native forest, 30 inches, is the root depth used by Engott (2011) for closed native forest. For the predevelopment (1870) land covers, calculation of the root depths was done using the same weighted averaging process described for calculating crop coefficients in the *Crop Coefficients* section of this appendix.

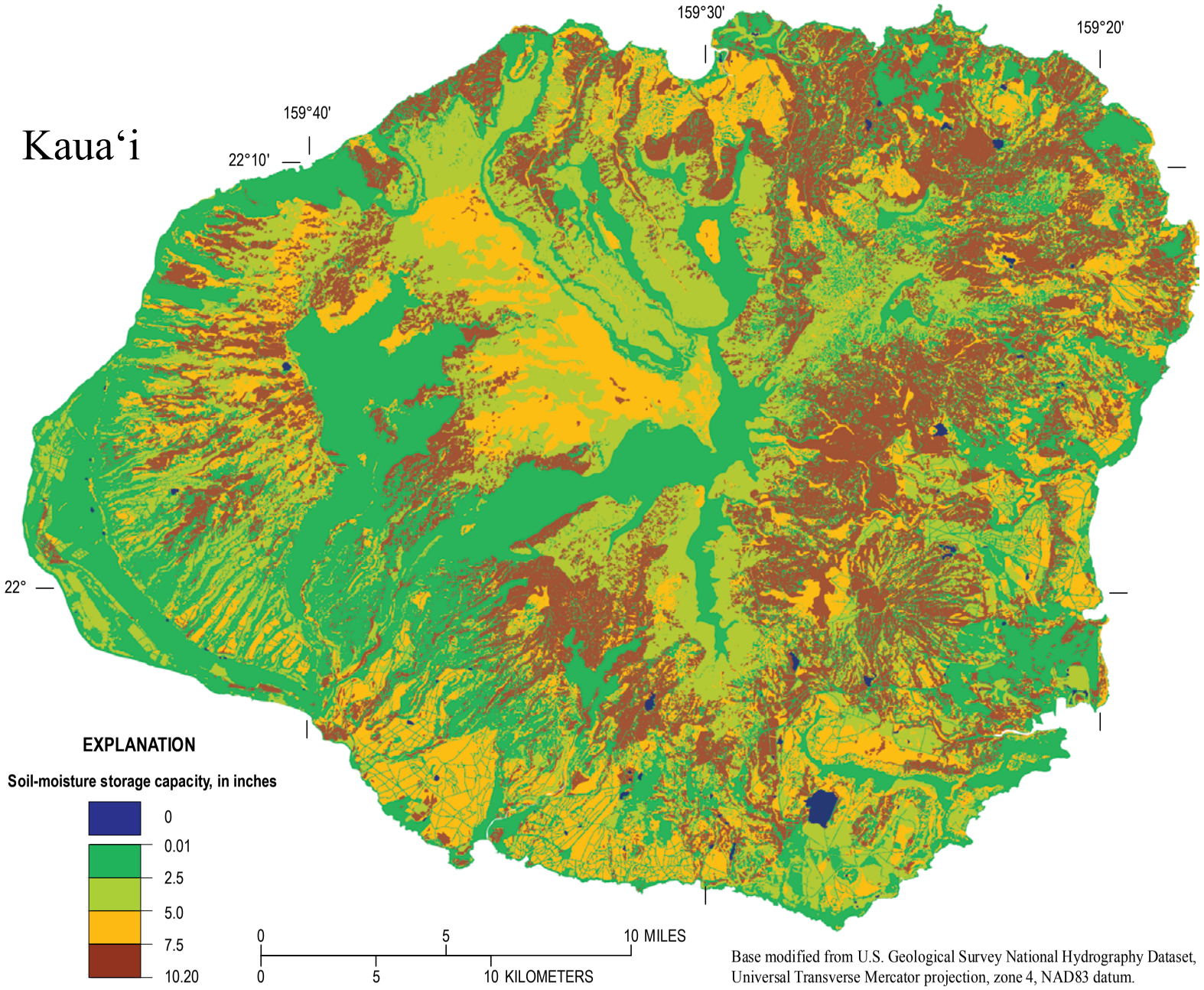

Figure 1-11. Map of soil-moisture storage capacity on Kaua‘i, calculated using 2010 land cover.

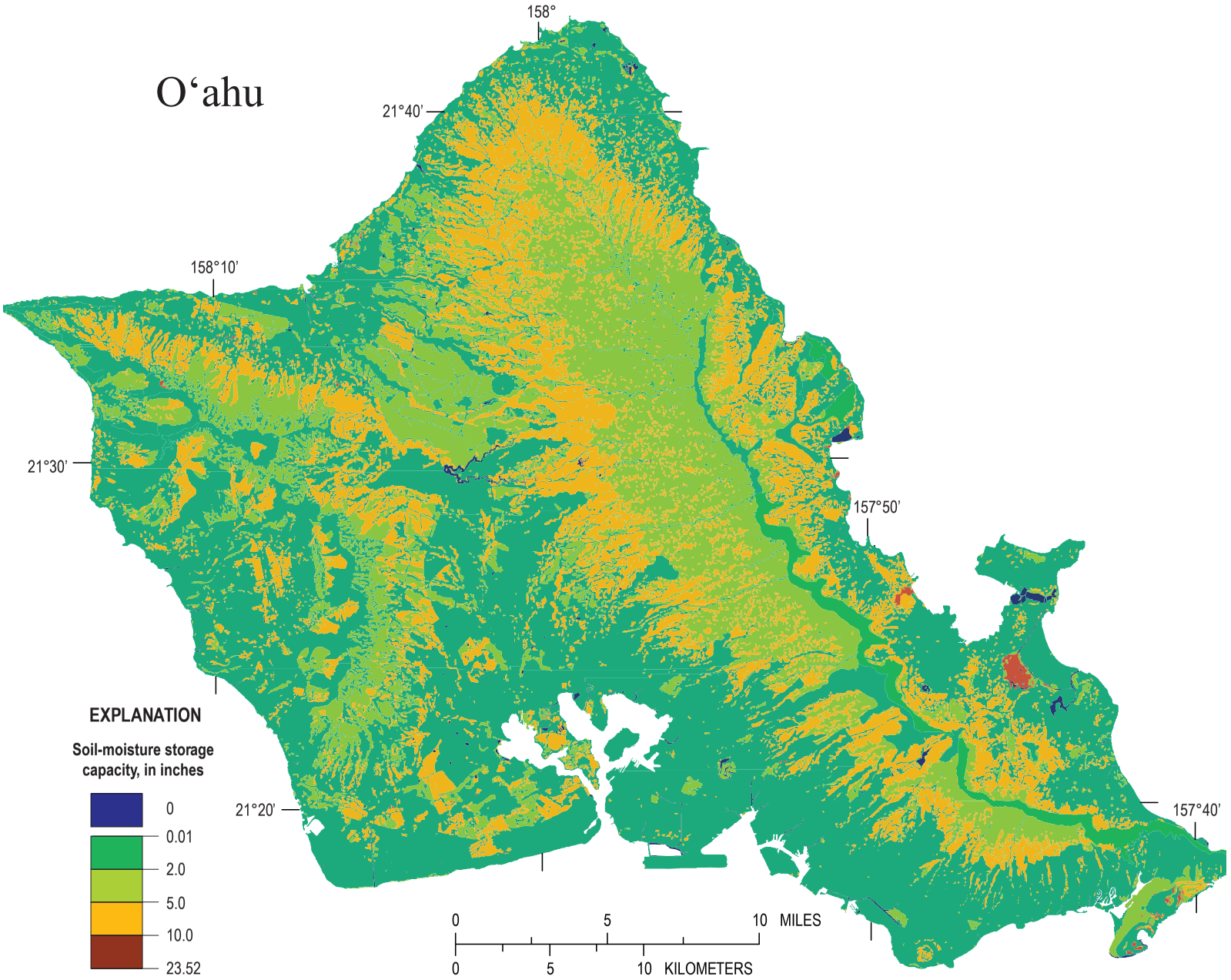

Base modified from U.S. Geological Survey National Hydrography Dataset, 1:24,000, Universal Transverse Mercator projection, zone 4, NAD83 datum.

Figure 1-12. Map of soil-moisture storage capacity on O‘ahu, calculated using 2010 land cover.

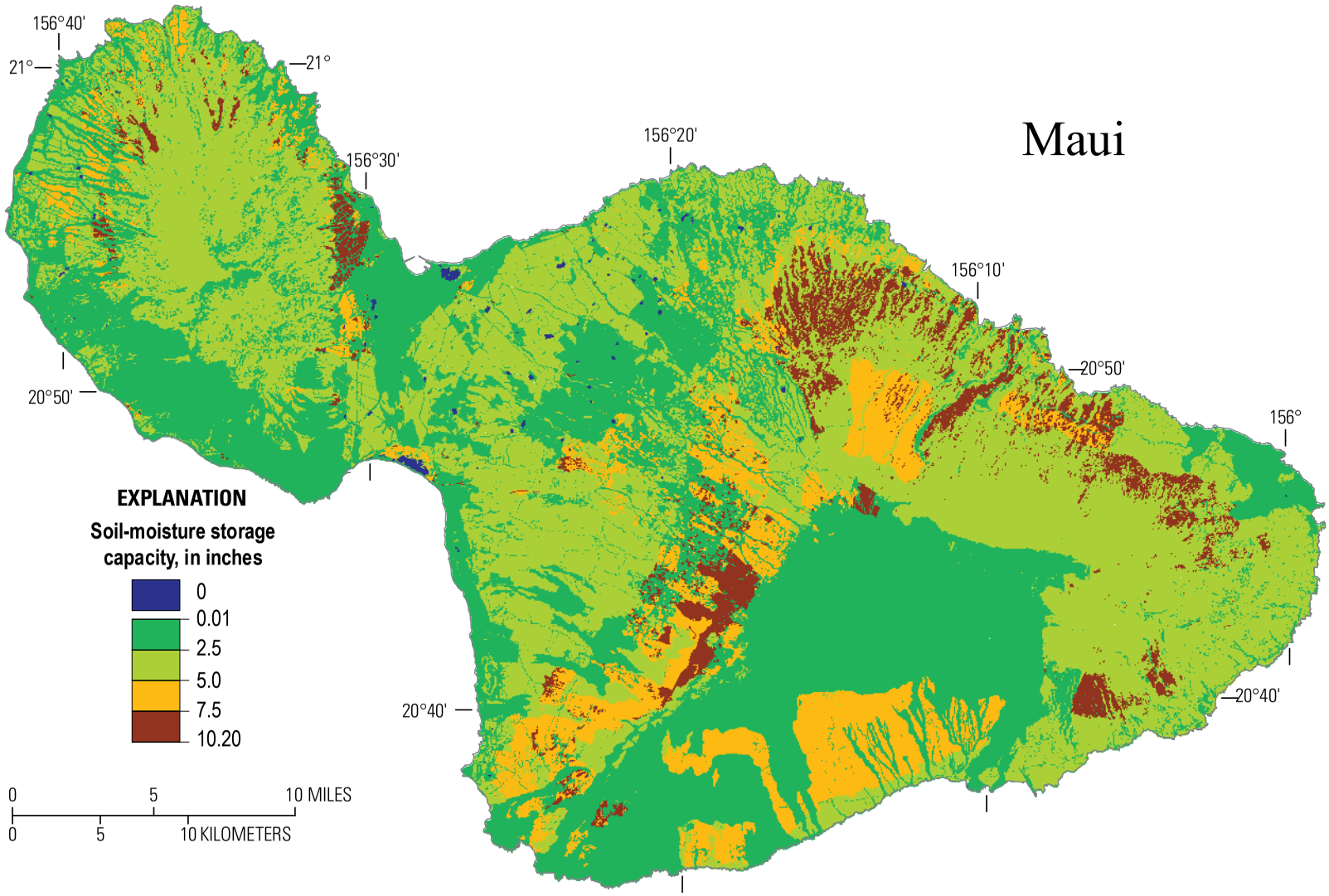

Base modified from U.S. Geological Survey National Hydrography Dataset, Universal Transverse Mercator projection, zone 4, NAD83 datum.

Figure 1-13. Map of soil-moisture storage capacity on Maui, calculated using 2010 land cover.

Direct Recharge

In this study, direct recharge is defined as water that passes directly to the groundwater system, completely bypassing the plant-soil zone (equation 12). Direct recharge is not subject to runoff or ET. Direct recharge was estimated for subareas with water mains, cesspools and land covers that are typically saturated—taro, water bodies, reservoirs, and estuarine/near-coastal water bodies (figs. 5 and 6 in main report). For subareas with cesspools, the wastewater effluent fluxes estimated by Whittier and El-Kadi (2009, 2013) were applied as direct recharge (see *Septic-System Leaching* section). For O‘ahu, the direct recharge rates for subareas with “Water body” and “Near-coastal or estuarine water body” land cover were set to 64 and 0 in/yr, respectively, on the basis of seepage estimates in Dugan and others (1975), consistent with the rates used by Engott and others (2017). For Maui, the direct recharge rate for subareas with “Water body” land cover was set to 0 in/yr, consistent with the rate used by Johnson and others (2018) because these subareas were located near the coast. For estuarine/near-coastal water bodies, the recharge rate was set to zero, because these water bodies were assumed to produce no net recharge. For reservoirs on Maui, the Hawaiian Commercial & Sugar Company estimates that the total seepage rate is between about 23 and 31 Mgal/d for 31 of its easternmost reservoirs (State of Hawai‘i, 2010, p. C-2). To reproduce the middle of this range (27 Mgal/d) for these reservoirs in the water budget, a direct recharge rate of 1,268 in/yr is needed. Accordingly, a direct recharge rate of 1,268 in/yr was used in the water budget for all reservoirs in the central isthmus of Maui (fig. 6 in main report). For the other reservoirs on Maui and all of the reservoirs on Kaua‘i and O‘ahu, the direct recharge was set to 528 in/yr, which has been used in recent water budgets for Hawai‘i (Engott and Vana, 2007; Engott, 2011). This rate was estimated from water-use data for 1998–2004 supplied by the Wailuku Water Co. (Clayton Suzuki, written commun., 2005). Seepage rates for reservoirs vary substantially. In addition to the variation in leakage attributable to the permeability of the substrate in which they are constructed, reservoirs generally leak less as they get older because of siltation.

Water-main leakage is another source of direct recharge. Water-main leakage on Kaua‘i and O‘ahu was estimated on the basis of maps and information supplied by the Kaua‘i Department of Water and the Honolulu Board of Water Supply, respectively. A detailed spreadsheet of water-main leaks on O‘ahu in 2007 (Carolyn Sawai, Honolulu Board of Water Supply, written commun., 2012) was used to estimate an average annual rate of water-main leakage. The total amount of water-main leakage on O‘ahu was estimated to be about 1.75 Mgal/d and was applied at a uniform rate, 0.01 in/day, along the length of each water main. This same uniform daily rate was used for water mains on Kaua‘i. A leakage rate of 1.75 Mgal/d is about 1.2 percent of the average system flow rate for O‘ahu, which is substantially lower than the typical average rate for a municipal water system—about 10 percent (State of California, 2014). However, using the lower rate is conservative with regard to recharge estimation, and on O‘ahu, some of the leakage is over the caprock and will not contribute to recharge of the volcanic aquifer. About 4.7 Mgal/d of water-main leakage was estimated for Maui from data supplied by the Maui Department of Water Supply, but this leakage was not included in the recharge model for Maui. Although the approach differs from the one taken for Kaua‘i and O‘ahu, the leakage rate is very small compared to other water inputs for the island and excluding it from the recharge calculation is conservative.

Other sources of direct recharge include (1) seepage from dry wells that are used to dispose of runoff from paved surfaces, and (2) injection of treated sewage. The drainage area of each dry well and the volumetric rate of water disposed are largely unknown. Hence, estimation of direct recharge from dry wells is not attempted in this report; however, it could be important to the local quality and quantity of recharge. For example, on Hawai‘i Island, there are an estimated 2,052 dry wells (Izuka and others, 2009). Injection of treated sewage also is not included as direct recharge in this study owing to a lack of information on injection rates and the close proximity of most injection facilities to the coast.

Other Inputs

In addition to the recharge-model inputs already discussed, several other inputs are required. The initial soil-moisture storage was set at 50 percent of capacity and the rainfall-retention capacity for impervious surfaces was set at 0.25 in. The values assigned to these parameters are consistent with those for other recent Hawai‘i water budgets (Izuka and others, 2005; Engott and Vana, 2007; Engott, 2011). The effects of these parameters on regional-scale recharge generally are minor because they either pertain to only a small area or are applicable during only a short time.

Sensitivity Analysis

To analyze the effect that uncertainty in model inputs has on estimated recharge, the recharge model was run repeatedly, changing one input value at a time within a reasonable range. For each island, the resulting recharge estimates were compared to recharge estimates for recent conditions (table 3 in main report). The parameters tested were (1) available water capacity, (2) fog-interception rates, (3) root depth, (4) ratio of runoff to rainfall, (5) crop coefficient, (6) ratio of the mean evaporation rate to mean precipitation rate during saturated conditions, E/R, which is used in the calculation of canopy evaporation, (7) canopy capacity, and (8) inclusion/exclusion of storm-drain capture.

For available water capacity, the range chosen for testing was between the high and low values published by the U.S. Department of Agriculture (2006a,b,c). For fog-interception rates and root depth, baseline values were increased by 50 percent and decreased by 50 percent. Runoff-to-rainfall ratios in ungaged areas were adjusted according to regression-model biases specific to each island, region, and season (table 1-6). Baseline runoff-to-rainfall ratios in ungaged areas were also increased and decreased by the root-mean-square error associated with the regression models for each island, region, and season (table 1-6). For crop coefficients, baseline values were increased by 20 percent and decreased by 20 percent. Values of E/R were increased by 0.1

and decreased by 0.1, within a range of 0.6 and 0.01. For canopy capacity, the range of values chosen for testing was between the highest, 0.08 in., and lowest, 0.02 in., published values for Hawai‘i sites. The model also was run without storm-drain capture.

For all three islands tested, recharge estimates were most sensitive to the ratio of runoff to rainfall and *E/R* (table 1-7). Island-wide recharge estimates were between 11.9 and 13.8 percent lower with the root-mean-square error added to the runoff-to-rainfall ratios generated using the regression described in the *Direct Runoff* subsection of the *Model Input* section (above), and island-wide recharge estimates were between 11.5 and 14.0 percent higher with the root-mean-square error subtracted from the ratios. These results demonstrate the need for accurate runoff estimates in the recharge model.

Island-wide recharge estimates were between 12.8 and 13.5 percent lower when *E/R* was increased by 0.1, and island-wide recharge estimates were between 4.8 and 10.4 percent higher when *E/R* was decreased by 0.1. These results indicate not only the importance of this parameter, but the entire canopy-evaporation estimation, to the recharge model. Adjusting other parameters produced less than a 10-percent change in estimated recharge.

Eliminating storm-drain capture did not have a large effect on island-wide recharge for any of the three islands. The largest difference in recharge was 5.6 percent higher for Oahu, which is expected because it is the most urbanized of the three islands. The difference in recharge was substantial, however, for the medium- and high-intensity developed subareas on all three islands in which storm-drain capture was excluded. This shows the importance of storm drains with regard to urban-area recharge.

Recharge Model, Input and Estimates for Hawai‘i Island

Recent and predevelopment recharge scenarios are also presented for Hawai‘i Island, but differ from those for Kaua‘i, O‘ahu, and Maui. Recent (1978–2007 rainfall and 2010 land cover) recharge estimate was not calculated for Hawai‘i Island in this study; instead, the estimate is taken from the results of Engott (2011), who used an earlier, slightly different version of the recharge model that also featured a daily time step. Recharge for a predevelopment scenario was calculated as part of this study, but to allow comparison between the scenarios for Hawai‘i Island, the predevelopment scenario was calculated using the same version of the recharge model that Engott used in his 2011 study. As in Engott (2011), the recharge model for Hawai‘i Island was run for 20 iterations, and the results were averaged. A full description of the methods and input datasets used to estimate recharge on Hawai‘i Island is given in Engott (2011); important differences in the methods and input datasets for Hawai‘i Island relative to the other islands are described here.

In the Hawai‘i Island study (Engott, 2011), net precipitation in forests was estimated using data from published studies in the Hawaiian Islands and similar tropical locations from which a linear regression model relating fog interception and net precipitation was developed. Canopy evaporation was then back-calculated as net precipitation subtracted from the sum of rainfall and fog. In this study, the Gash model was selected to estimate canopy evaporation for Kaua‘i, Maui, and O‘ahu instead of the linear regression model. The Gash model is preferred because it is physically based and sufficient data have become available since

Table 1-7. Results of sensitivity testing for selected recharge-model parameters

[RMSE, root-mean-square error; %, percent; recharge estimates for recent conditions are shown in table 3 of the main report]

Parameter	Adjusted parameter value	Percentage difference in recharge relative to recharge estimate for recent conditions		
		Kaua‘i	O‘ahu	Maui
Available water capacity	Low reported value	1.1	1.4	1.2
	High reported value	-0.4	-1.1	-0.8
Fog-interception rates	150% of baseline	5.4 (9.8)[a]	0.7 (5.5)[a]	6.4 (9.4)[a]
	50% of baseline	-5.4 (-9.7)[a]	-0.7 (-5.4)[a]	-6.4 (-9.4)[a]
Root depth	150% of baseline	-2.3	-3.1	-1.9
	50% of baseline	4.9	6.7	4.7
Ratio of runoff to rainfall (see table 1-5)	Regression bias adjustment	-6.6	2.3	-1.9
	Plus regression RMSE	-13.3	-11.9	-13.8
	Minus regression RMSE	13.5	11.5	14.0
Crop coefficient	120% of baseline	-6.7	-6.4	-3.2
	80% of baseline	8.2	7.9	4.3
Ratio of the mean evaporation rate to mean precipitation rate during saturated conditions, *E/R*	Increase by 0.1 unit	-13.5 (-19.4)[b]	-13.5 (-18.9)[b]	-12.8 (-18.9)[b]
	Decrease by 0.1 unit	8.3 (11.9)[b]	10.4 (14.4)[b]	4.8 (7.1)[b]
Canopy capacity	Increase by 0.03 inch	-6.0 (-8.6)[b]	-5.2 (-7.3)[b]	-3.9 (-5.8)[b]
	Decrease by 0.03 inch	7.0 (10.2)[b]	4.0 (5.5)[b]	4.3 (6.4)[b]
Storm-drain capture (on/off)	Storm-drain capture excluded	0.3 (94.9)[c]	5.6 (249.5)[c]	0.3 (60.1)[c]

[a]Value in parentheses is for areas within the fog zone only.

[b]Value in parentheses is for areas with forest land covers only.

[c]Value in parentheses is for areas with high- and medium-intensity developed land covers only.

the Engott (2011) study, from which to parameterize the model (for example, Giambelluca and others, 2014).

The Hawai‘i Island recharge study (Engott, 2011) used mean monthly rainfall during the period from 1916–83 (Giambelluca and others, 1986), because the monthly rainfall time series from Frazier and others (2016) and the mean monthly rainfall during the period 1978–2007 (Giambelluca and others, 2013) used in this study for Kaua‘i, Maui, and O‘ahu were not yet available. Runoff in the Hawai‘i Island study was estimated using runoff-to-rainfall ratios that were developed using a variety of methods that were selected to accommodate the amount of streamflow data available. In this study, regression equations were developed to calculate runoff-to-rainfall ratios for areas outside of gaged basins or basins lacking adequate streamflow data. Finally, the Hawai‘i Island study by Engott (2011) used pan evaporation reported by Ekern and Chang (1985) for reference ET, whereas this study for Kaua‘i, O‘ahu, and Maui used maps of mean monthly grass-reference ET reported by Giambelluca and others (2014) for reference ET.

Although Engott (2011) used slightly different methods and data sets to calculate recharge for Hawai‘i Island, his results are considered comparable to the recharge calculated for Kaua‘i, O‘ahu, and Maui for the purposes of this study. Recharge in Hawai‘i is strongly correlated with rainfall (Izuka and others, 2010), and mean island-wide rainfall on Hawai‘i Island for the period 1978–2007 (Giambelluca and others, 2013) is only 4.4 percent higher than the mean rainfall (Giambelluca and others, 1986) used in the Hawai‘i Island recharge study.

References Cited

Allen, R.G., Pereira, L.S., Raes, Dirk, and Smith, Martin, 1998, Crop evapotranspiration; guidelines for computing crop water requirements: Food and Agriculture Organization of the United Nations, FAO Irrigation and Drainage Paper 56, 300 p.

AWS Truewind, LLC, 2004, Wind energy resource maps of Hawaii: Prepared for Hawai‘i Department of Business, Economic Development, and Tourism Strategic Industries Division, Honolulu, Hawai‘i, 17 p., accessed January 25, 2012, at http://planning.hawaii.gov/gis/download-gis-data-expanded/.

Berg, N., McGurk, B., and Calhoun, R.S., 1997, Hydrology and land use effects in the Hanalei National Wildlife Refuge, Kauai, Hawai‘i, Final Report, Interagency Agreement 14-48-0001-94588: Albany, California, United States Department of Agriculture Forest Service, Pacific Southwest Research Station, 62 p.

Bruijnzeel, L.A.S., Eugster, Werner, and Burkard, Reto, 2005, Fog as a hydrologic input, chap. 38 of Anderson, M.G., ed., Encyclopedia of Hydrological Sciences: Hoboken, New Jersey, John Wiley and Sons, Ltd., p. 559–582.

Coulter, J.W., 1931, Population and utilization of land and sea in Hawaii, 1853: Honolulu, Bernice Pauahi Bishop Museum, Bulletin 88, 33 p., illus.

Crockford, R.H., and Richardson, D.P., 2000, Partitioning rainfall into throughfall, stemflow and interception; effect of forest type, ground cover and climate: Hydrological Processes, v. 14, p. 2,903–2,920.

de la Peña, R.S., and Melchor, F.M., 1984, Water use and efficiency in lowland taro production: Proceedings, Sixth Symposium of the International Society for Tropical Root Crops, Lima, Peru, February 21–26, 1983.

DeLay, J.K., 2005, Canopy water balance on an elfin cloud forest at Alakahi, Hawai‘i: Honolulu, University of Hawai‘i, M.S. thesis, 78 p.

DeLay J.K., and Giambelluca, T.W., 2010, History of fog and cloud water interception research in Hawai‘i, *in* Bruijnzeel, L.A., Scatena, F.N., and Hamilton, L.S., eds., Tropical montane cloud forests—Science for conservation and management: New York, Cambridge University Press, p. 332–341.

Dugan, G.L., Lau, L.S., and Yamauchi, H., 1975, Eutrophication and fish toxicity potentials in a multiple-use reservoir: University of Hawai‘i Water Resources Research Center Technical Report no. 89, 175 p.

Ekern, P.C., 1964, Direct interception of cloud water on Lanaihale, Hawaii: Soil Science Society of America Proceedings, v. 28, no. 3, p. 419–421.

Ekern, P.C., 1983, Measured evaporation in high rainfall areas, leeward Ko‘olau Ranges, O‘ahu, Hawai‘i: University of Hawai‘i Water Resources Research Center Technical Report no. 156, 60 p.

Ekern, P.C., and Chang, J.H., 1985, Pan evaporation; State of Hawai‘i, 1894–1983: State of Hawai‘i, Department of Land and Natural Resources, Division of Water and Land Development, Report R74, 172 p.

Engott, J.A., 2011, A water-budget model and assessment of groundwater recharge for the Island of Hawai‘i: U.S. Geological Survey Scientific Investigations Report 2011–5078, 53 p.

Engott, J.A., Johnson, A.G., Bassiouni, Maoya, Izuka, S.K., and Rotzoll, Kolja, 2017, Spatially distributed groundwater recharge for 2010 land cover estimated using a water-budget model for the Island of O‘ahu, Hawai‘i (ver. 2.0, December 2017): U.S. Geological Survey Scientific Investigations Report 2015–5010, 49 p., https://doi.org/10.3133/sir20155010.

Engott, J.A., and Vana, T.T., 2007, Effects of agricultural land-use changes and rainfall on ground-water recharge in central and west Maui, Hawai‘i, 1926–2004: U.S. Geological Survey Scientific Investigations Report 2007–5103, 56 p.

Fares, Ali, 2008, Water management software to estimate crop irrigation requirements for consumptive use permitting in Hawai‘i: State of Hawai‘i, Commission on Water Resource Management, 61 p., accessed March 13, 2009, at http://dlnr.hawaii.gov/cwrm/info/publications/.

Fontaine, R.A., 1995, Evaluation of the surface-water quantity, surface-water quality, and rainfall data-collection programs in Hawai‘i, 1994: U.S. Geological Survey Water-Resources Investigation Report 95–4212, 125 p.

Frazier, Abby, 2012, Month-year rainfall maps of the Hawaiian Islands: Honolulu, University of Hawai‘i, M.A. thesis, 81 p.

Frazier, A.G., Giambelluca, T.W., Diaz, H.F., and Needham, H.L., 2016, Comparison of geostatistical approaches to spatially interpolate month-year rainfall for the Hawaiian Islands: International Journal of Climatology, v. 36, no. 3, p. 1459–1470, doi: 10.1002/joc.4437.

Fukunaga, L.K., 1978, Some agroclimatic, economic, ecological, and site considerations that condition the practice of drip irrigation in Hawaii’s sugar industry: Honolulu, University of Hawai‘i, M.S. thesis, 181 p.

Gash, J.H.C., Lloyd, C.R., and Lachaud, G., 1995, Estimating sparse forest rainfall interception with an analytical model: Journal of Hydrology, v. 170, p. 79–86.

Gash, J.H.C., and Morton, A.J., 1978, An application of the Rutter model to the estimation of the interception loss from Thetford Forest: Journal of Hydrology, v. 38, p. 49–58.

Gaskill, T.G.R., 2004, Hydrology of forest ecosystems in the Honouliuli Preserve; implications for groundwater recharge and watershed restoration: Honolulu, University of Hawai‘i, Ph.D. dissertation, 177 p.

Giambelluca, T.W., 1983, Water balance of the Pearl Harbor-Honolulu basin, Hawai‘i, 1946–1975: University of Hawai‘i Water Resources Research Center Technical Report no. 151, 151 p.

Giambelluca, T.W., Chen, Q., Frazier, A.G., Price, J.P., Chen, Y.-L., Chu, P.-S., Eischeid, J.K., and Delparte, D.M., 2013, Online Rainfall Atlas of Hawai‘i: Bulletin of the American Meteorological Society v. 94, p. 313–316, doi: 10.1175/BAMS-D-11-00228.1, accessed October 24, 2011, at http://rainfall.geography.hawaii.edu/.

Giambelluca, T.W., Martin, R.E., Asner, G.P., Huang, Maoyi, Mudd, R.G., Nullet, M.A., DeLay, J.K., and Foote, David, 2009, Evaporation and energy balance of native wet montane cloud forest in Hawai‘i: Agricultural and Forest Meteorology, v. 149, no. 2, p. 230–243.

Giambelluca, T.W., Nullet, M.A., and Schroeder, T.A., 1986, Rainfall atlas of Hawai‘i: Hawai‘i Department of Land and Natural Resources, Division of Water and Land Development Report R76, 267 p.

Giambelluca, T.W., and Schroeder, T.A., 1998, Climate, *in* Juvik, S.P., and Juvik, J.O., eds., Atlas of Hawai‘i, (3d ed.): Honolulu, University of Hawai‘i Press, p. 49–59.

Giambelluca, T.W., Shuai, Xiufu, Barnes, M.L., Alliss, R.J., Longman, R.J., Miura, Tomoaki, Chen, Qi, Frazier, A.G., Mudd, R.G., Cuo, Lan, and Businger, A.D., 2014, Evapotranspiration of Hawai‘i: Final report, submitted to U.S. Army Corps of Engineers–Honolulu District and Commission on Water Resource Management, State of Hawai‘i, 178 p.

Gingerich, S.B, and Engott, J.A., 2012, Groundwater availability in the Lahaina District, West Maui, Hawai‘i: U.S. Geological Survey Scientific Investigations Report 2012–5010, 90 p.

Gingerich, S.B., Yeung, C.W., Ibarra, Tracy-Joy N., and Engott, J.A., 2007, Water Use in Wetland Kalo Cultivation in Hawai‘i: U.S. Geological Survey Open-File Report 2007–1157, 68 p.

Helsel, D.R., and Hirsch, R.M., 1992, Statistical methods in water resources: Amsterdam, Elsevier, 522 p.

Hutjes, R.W.A, Wierda, A., and Veen, A.W.L., 1990, Rainfall interception in the Tai Forest, Ivory Coast—Application of two simulation models to a humid tropical system: Journal of Hydrology, v. 114, p. 259–275.

Izuka, S.K., Oki, D.S., and Chen, C., 2005, Effects of irrigation and rainfall reduction on ground-water recharge in the Lihue Basin, Kauai, Hawaii: U.S. Geological Survey Scientific Investigations Report 2005–5146, 48 p.

Izuka, S.K., Oki, D.S., and Engott, J.A., 2010, Simple method for estimating groundwater recharge on tropical islands: Journal of Hydrology, v. 387. p. 81–89.

Izuka, S.K., Senter, C.A., and Johnson, A.G., 2009, Reconnaissance assessment of the potential for roadside dry wells to affect water quality on the island of Hawai‘i: U.S. Geological Survey Scientific Investigation Report 2009–5249, 55 p.

Johnson, A.G., 2012, A water-budget model and estimates of groundwater recharge for Guam: U.S. Geological Survey Scientific Investigations Report 2012–5028, 53 p.

Johnson, A.G., Engott, J.A., Bassiouni, Maoya, and Rotzoll, Kolja, 2018, Spatially distributed groundwater recharge estimated using a water-budget model for the Island of Maui, Hawai`i, 1978–2007 (ver. 2.0, February 2018): U.S. Geological Survey Scientific Investigations Report 2014–5168, 53 p., https://doi.org/10.3133/sir20145168.

Juvik, J.O., and Ekern, P.C., 1978, A climatology of mountain fog on Mauna Loa, Hawaii Island: University of Hawai‘i Water Resources Research Center Technical Report no. 118, 63 p.

Juvik, J.O., and Nullet, D., 1995, Relationships between rainfall, cloud-water interception, and canopy throughfall in a Hawaiian montane forest, chap. 11 of Hamilton, L.S., Juvik, J.O., and Scatena, F.N., eds., Tropical montane cloud forests: New York, Springer-Verlag, p. 165–182.

Juvik, J.O., Nullet, D., Banko, P., and Hughes, K., 1993, Forest climatology near the tree line in Hawai‘i: Agricultural and Forest Meteorology, v. 66, nos. 3–4, p. 159–172.

Juvik, J.O., and Perreira, D.J., 1974, Fog interception on Mauna Loa, Hawai‘i: Proceedings of the Association of American Geographers, v. 6, p. 22–24.

Ladefoged, T.N., Kirch, P.V., Gon, S.O., Chadwick, O.A., Hartshorn, A.S., and Vitousek, P.M., 2009, Opportunities and constraints for intensive agriculture in the Hawaiian archipelago prior to European contact: Journal of Archaeological Science, v. 36, no. 10, p. 2,374–2,383.

Leenhouts, J.M., Stromberg, J.C., and Scott, R.L., 2006, Hydrologic requirements of and evapotranspiration by riparian vegetation along the San Pedro River, Arizona: U.S. Geological Survey Fact Sheet 2006–3027.

McJannet, David, Wallace, Jim, Fitch, Peter, Disher, Mark, and Reddell, Paul, 2007, Water balance of tropical rainforest canopies in north Queensland, Australia: Hydrological Processes, v. 21, p. 3473–3484.

Miles, K., 1931, Report on study of water requirements of taro in Hanapēpē Valley, cooperative study by the Territory of Hawai‘i and McBryde Sugar Co.: ‘Ele‘ele, Hawai‘i, 52 p.

National Oceanic and Atmospheric Administration, 2008, Coastal Change Analysis Program (C-CAP) Land Cover, Maui, Hawaii 2006: National Oceanic and Atmospheric Administration Coastal Services Center, accessed October 3, 2011, at http://www.csc.noaa.gov/digitalcoast/dataregistry/#/.

Oki, D.S., 2002, Reassessment of ground-water recharge and simulated ground-water availability for the Hāwī area of North Kohala, Hawai‘i: U.S. Geological Survey Water Resources Investigations Report 02-4006, 62 p.

Oki, D.S., 2003, Surface water in Hawaii: U.S. Geological Survey Fact Sheet 045-03.

Oki, D.S., Rosa, S.N., and Yeung, C.W., 2010, Flood-frequency estimates for streams on Kaua‘i, O‘ahu, Moloka‘i, Maui, and Hawai‘i, State of Hawai‘i: U.S. Geological Survey Scientific Investigations Report 2010–5035, 121 p.

Pasiecznik, N.M., Felker, P., Harris, P.J.C., Harsh, L.N., Cruz, G., Tewari, J.C., Cadoret, K., and Maldonado, L.J., 2001, The Prosopis juliflora–Prosopis pallida complex—A monograph: Coventry, U.K., HDRA, 172 p.

Rea, A., and Skinner, K.D., 2012, Geospatial datasets for watershed delineation and characterization used in the Hawaii StreamStats web application: U.S. Geological Survey Data Series 680, 12 p., accessed November 19, 2013, at http://water.usgs.gov/GIS/metadata/usgswrd/XML/ds680_archydrohucs.xml#stdorder.

Rosa, S.N. and Oki, D.S., 2010, Hawaii StreamStats—A web application for defining drainage-basin characteristics and estimating peak-streamflow statistics: U.S. Geological Survey Fact Sheet 2010–3052, 4 p., accessed June 12, 2012, at http://water.usgs.gov/osw/streamstats/hawaii.html.

Safeeq, Mohammad, and Fares, Ali, 2012, Interception losses in three non-native Hawaiian forest stands: Hydrological Processes, DOI: 10.1002/hyp.9557.

Santiago, L.S., Goldstein, Guillermo, Meinzer, F.C., Fownes, J.H., and Muller-Dombois, Dieter, 2000, Transpiration and forest structure in relation to soil waterlogging in a Hawaiian montane cloud forest: Tree Physiology, v. 20, no. 10, p. 673–681.

Savenije, H.H.G., 2004, The importance of interception and why we should delete the term evapotranspiration from our vocabulary: Hydrological Processes, v. 18, p. 1,507–1,511.

Schmitt, R.C., 1973, The missionary censuses of Hawai‘i: Honolulu, Department of Anthropology, Bernice Pauahi Bishop Museum, 49 p.

Scholl, M.A., Giambelluca, T.W., Gingerich, S.B., Nullet, M.A., and Loope, L.L., 2007, Cloud water in windward and leeward mountain forests; the stable isotope signature of orographic cloud water: Water Resources Research, v. 43, W12411, 13 p.

Shuttleworth, W.J., 1993, Evaporation, chap. 4 of Maidment, D.R., ed., Handbook of hydrology: New York, McGraw-Hill, p. 4.1–4.53.

State of California, 2014, Leak detection: State of California, Department of Water Resources, accessed April 24, 2014, at http://www.water.ca.gov/wateruseefficiency/leak/.

State of Hawai‘i, 2010, Compilation of Data Submissions, Part II, PR-2010-01: Department of Land and Natural Resources, Commission on Water Resource Management.

Takahashi, Mami, Giambelluca, T.W., Mudd, R.G, DeLay, J.K., Nullet, M.A., and Asner, G.P., 2011, Rainfall portioning and cloud water interception in native forest and invaded forest in Hawai‘i Volcanoes National Park: Hydrological Processes, v. 25, no. 3, p. 448–464, doi: 10.1002/hyp.7797.

Thornthwaite, C.W., and Mather, J.R., 1955, The water balance: Publications in Climatology, v. 8, no. 1, p. 1–104.

U.S. Department of Agriculture, 2006a, Soil survey geographic (SSURGO) database for the island of Maui: U.S. Department of Agriculture, Natural Resources Conservation Service, accessed October 3, 2011, at http://SoilDataMart.nrcs.usda.gov/.

U.S. Department of Agriculture, 2006b, Soil survey geographic (SSURGO) database for the island of Kauai: U.S. Department of Agriculture, Natural Resources Conservation Service, accessed September 4, 2012, at http://SoilDataMart.nrcs.usda.gov/.

U.S. Department of Agriculture, 2006c, Soil survey geographic (SSURGO) database for the island of Oahu: U.S. Department of Agriculture, Natural Resources Conservation Service, accessed June 8, 2011, at http://SoilDataMart.nrcs.usda.gov/.

U.S. Department of Agriculture, 2007a, Natural color orthophoto mosaic of the Island of Maui, Maui County, Hawai‘i: U.S. Department of Agriculture, Natural Resources Conservation Service.

U.S. Department of Agriculture, 2007b, Quick Stats: U.S. Department of Agriculture, National Agricultural Statistics Service, accessed August 2, 2013, at http://quickstats.nass.gov.

U.S. Geological Survey, 2006, A GAP analysis of Hawai‘i: U.S. Geological Survey, The Hawai‘i GAP analysis project, accessed February 25, 2008, at http://gapanalysis.nbii.gov/portal/community/GAP_Analysis_Program/ Communities/GAP_Home.

U.S. Geological Survey, 2010a, LANDFIRE Existing Vegetation Type (Refresh08): U.S. Geological Survey Wildland Fire Science, Earth Resources Observation and Science Center Web page, accessed June 8, 2011, at http://landfire.cr.usgs.gov/viewer/.

U.S. Geological Survey, 2010b, LANDFIRE Biophysical Settings (Refresh08): U.S. Geological Survey Wildland Fire Science, Earth Resources Observation and Science Center Web page, accessed December 16, 2014, at http://landfire.cr.usgs.gov/viewer/.

University of Hawai‘i, 2008, Hawaii agricultural water use and development plan: report submitted to Hawai‘i Department of Agriculture by College of Tropical Agriculture and Human Resources, Department of Natural Resources and Environmental Management, University of Hawai‘i at Mānoa, Honolulu, Hawai‘i, 108 p.

Viessman, Warren, Jr., and Lewis, G.L., 2003, Introduction to hydrology (5th ed.): Upper Saddle River, N.J., Prentice Hall, 612 p.

Villegas, J.C., Tobon, Conrado, and Breshears, D.D., 2007, Fog interception by non-vascular epiphytes in tropical montane cloud forests; dependencies on gauge type and meteorological conditions: Hydrological Processes, v. 22, no. 14, p. 2,484–2,492.

Wahl, K.L., and Wahl, T.L., 1995, Determining the flow of Comal Springs at New Braunfels, Texas: Proceedings of Texas Water ’95, A Component Conference of the First International Conference on Water Resources Engineering, American Society of Civil Engineers, August 16–17, 1995, San Antonio, Texas, p. 77–86.

Wallace, J., Macfarlane, C., McJannet, D., Ellis, T., Grigg, A., and van Dijk, A., 2013, Evaluation of forest interception estimation in the continental scale Australian Water Resources Assessment – Landscape (AWRA-L) model: Journal of Hydrology, v. 499, p. 210–223.

Walmsley, J.L., Schemenauer, R.S., and Bridgman, H.A., 1996, A method for estimating the hydrologic input from fog in mountainous terrain: Journal of Applied Meteorology, v. 35, no. 12, p. 2,237–2,249.

Watson, L.J., ed., 1964, Observations made with respect to irrigation and growth of taro at certain patches at Waiāhole and Kahaluu: Honolulu, Hawai‘i, City & County of Honolulu Board of Water Supply Water Resources Division in Reppun v. Board of Water Supply, variously paginated.

Whittier, R.B., and El-Kadi, A.I., 2009, Human and environmental risk ranking of onsite sewage disposal systems: Department of Geology and Geophysics, University of Hawai‘i at Mānoa, Honolulu, Hawai‘i, 72 p.

Whittier, R.B., and El-Kadi, A.I., 2013, Human and environmental risk ranking of onsite sewage disposal systems for the Hawaiian Islands of Kauai, Maui, Molokai, and Hawaii (draft report January 2013): Department of Geology and Geophysics, University of Hawai‘i at Mānoa, Honolulu, Hawai‘i, 201 p.

Yamanaga, George, 1972, Evaluation of the streamflow-data program in Hawaii: U.S Geological Survey Open-File Report 72–453, 37 p.

Appendix 2. Annual Groundwater Recharge, 2001–2010

In addition to the predevelopment and recent scenarios discussed in the main report, annual groundwater recharge estimates for 2001–2010 were calculated for Kaua‘i, O‘ahu, and Maui (figure 2-1). The estimates were calculated using the recharge model described in appendix 1, with monthly rainfall for 2001–2010 from Frazier and others (2016), and varying land cover for the same period. All other input parameters used in the recharge model for this scenario were the same as those used to calculate recharge for recent conditions, as described in appendix 1. Geospatial datasets of 2001–2010 recharge for each island can be accessed online: doi:10.5066/F79021VS (Kaua‘i), doi:10.5066/F72F7KH4 (O‘ahu), and doi:10.5066/F7P8490T (Maui).

On average, Kaua‘i received 808 Mgal/d, O‘ahu received 586 Mgal/d, and Maui received 1,098 Mgal/d of recharge in 2001–2010 (table 2-1). On a depth basis, Maui (31.7 in/yr) had the highest average rate of recharge, followed by Kaua‘i (30.6 in/yr) and O‘ahu (20.6 in/yr) (table 2-2). For individual islands, mean recharge calculated for 2001–2010 differs from that for the “recent” scenario of the main report (2010 land cover and mean rainfall during the period 1978–2007) by as much as 19 percent; these differences are consistent with differences in rainfall and agricultural land cover between the two periods. On all three islands, recharge for the 2001–2010 period was lower than that for the recent scenario. On an annual basis, the estimated 2001–2010 recharge is highly correlated with rainfall—the correlation coefficient (Pearson’s r; Helsel and Hirsch, 1992) for each island is greater than 0.98.

Reference Cited

Helsel, D.R., and Hirsch, R.M., 1992, Statistical methods in water resources: Amsterdam, Elsevier, 522 p.

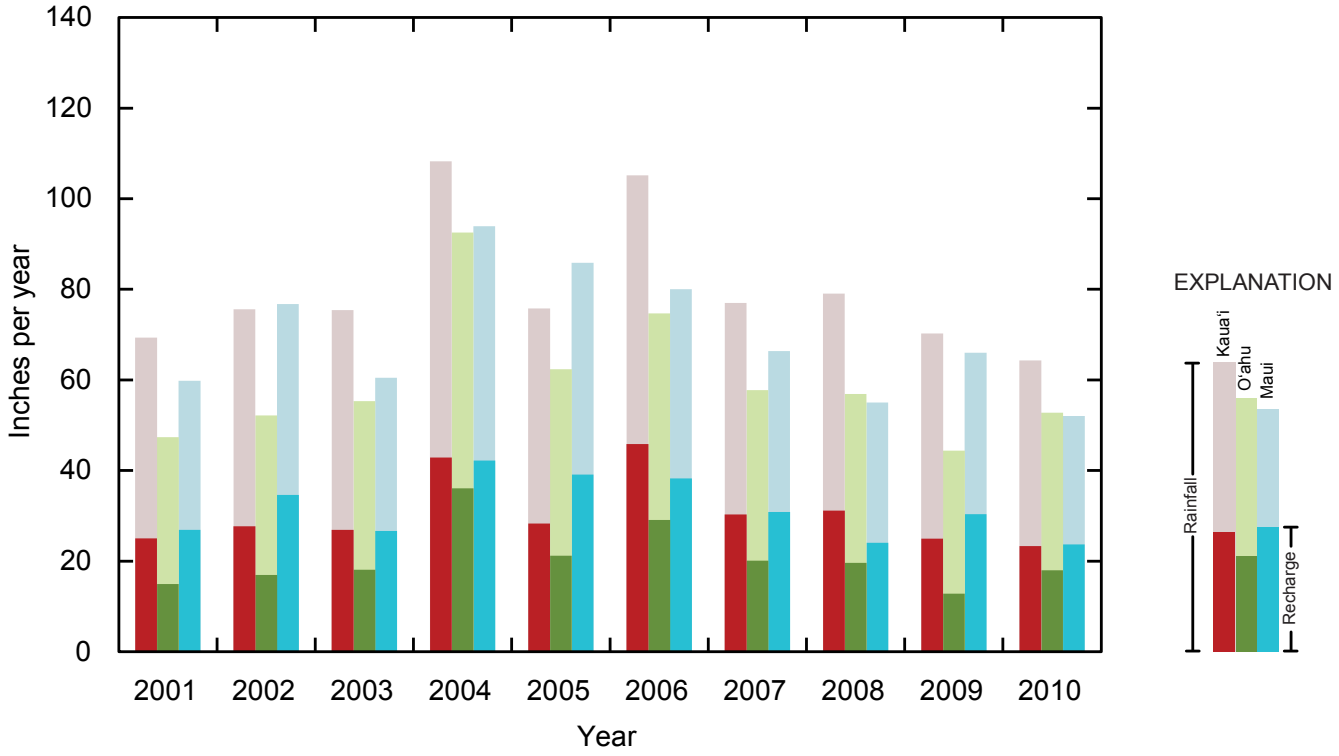

Figure 2-1. Graph of rainfall and estimated groundwater recharge from 2001 to 2010 on Kaua‘i, O‘ahu, and Maui.

Table 2-1. Mean annual water-budget components by volume.

[Septic, septic-system leachate;Total ET, total evapotranspiration, which includes canopy evaporation; net precipitation, rainfall plus fog for most areas, rainfall plus fog minus canopy interception for forested areas. Components may not balance because of rounding and direct recharge]

Island	Period	Water-budget estimate (million gallons per day)											
		Rainfall	Fog	Irrigation	Septic	Direct recharge	Runoff	Canopy evaporation	Actual ET	Total ET	Net precipitation	Storm-drain capture	Recharge
Kaua‘i	2001	1,829.01	91.97	105.14	1.93	55.54	425.56	248.91	734.98	983.90	1,672.07	1.69	660.32
	2002	1,993.78	95.74	91.66	1.93	55.54	484.83	262.25	758.23	1,020.49	1,827.26	2.43	730.72
	2003	1,989.88	99.01	91.88	1.93	55.54	450.89	269.71	786.31	1,056.02	1,819.19	2.38	710.15
	2004	2,855.51	137.29	78.08	1.93	55.54	763.03	328.89	865.52	1,194.41	2,663.92	4.17	1,130.40
	2005	1,999.04	101.69	92.78	1.93	55.54	528.01	258.88	726.25	985.14	1,841.85	2.46	747.10
	2006	2,773.26	120.35	81.73	1.93	55.54	716.19	314.82	784.28	1,099.10	2,578.79	5.69	1,209.34
	2007	2,031.61	92.09	85.21	1.93	55.54	439.42	266.19	723.31	989.50	1,857.51	3.36	799.47
	2008	2,085.11	102.15	85.41	1.93	55.54	511.61	267.83	691.66	959.49	1,919.43	3.04	821.76
	2009	1,853.30	86.04	88.23	1.93	55.54	486.75	242.67	694.85	937.52	1,696.68	1.97	658.11
	2010	1,696.86	83.74	53.15	1.93	55.54	395.19	239.44	613.16	852.60	1,541.16	1.83	616.04
	Mean 2001–10	2,110.74	101.01	85.33	1.93	55.54	520.15	269.96	737.86	1,007.82	1,941.78	2.90	808.34
O‘ahu[1]	2001	1,342.51	7.89	125.80	1.30	20.63	157.45	199.14	705.05	904.18	1,151.26	19.96	423.18
	2002	1,478.41	8.36	121.08	1.30	20.63	199.55	208.25	735.39	943.64	1,278.52	27.91	479.60
	2003	1,569.11	10.01	117.14	1.30	20.63	210.80	216.39	737.91	954.31	1,362.72	32.21	513.40
	2004	2,624.56	14.91	82.37	1.30	20.63	426.31	303.37	905.17	1,208.54	2,336.09	74.93	1,021.75
	2005	1,767.60	9.45	111.89	1.30	20.63	270.97	232.70	786.89	1,019.59	1,544.35	38.61	599.98
	2006	2,118.40	11.82	110.95	1.32	20.72	327.71	255.64	804.41	1,060.05	1,874.57	59.65	824.06
	2007	1,636.54	9.87	118.81	1.32	20.72	208.71	222.19	740.63	962.82	1,424.22	36.14	569.25
	2008	1,612.91	9.80	121.29	1.32	20.72	218.88	220.26	724.94	945.20	1,402.45	33.79	556.03
	2009	1,257.95	7.28	128.92	1.32	20.72	164.47	189.26	695.69	884.95	1,075.96	20.76	363.20
	2010	1,495.22	8.52	126.98	1.32	20.72	187.99	210.21	702.14	912.36	1,293.52	33.93	508.45
	Mean 2001–10	1,690.32	9.79	116.52	1.31	20.68	237.28	225.74	753.82	979.56	1,474.37	37.79	585.89
Maui	2001	2,072.42	138.15	305.99	3.78	54.58	585.21	199.55	838.39	1,037.95	2,011.01	1.61	933.90
	2002	2,659.16	170.31	256.92	3.78	54.58	753.77	227.61	966.47	1,194.08	2,601.86	4.24	1,198.82
	2003	2,095.16	135.62	286.80	3.78	54.58	553.39	202.30	873.22	1,075.51	2,028.49	2.18	924.13
	2004	3,252.46	194.95	236.03	3.78	54.58	1,010.95	253.86	1,003.50	1,257.37	3,193.55	5.21	1,462.36
	2005	2,973.58	196.42	259.59	3.78	54.58	925.43	241.59	971.20	1,212.80	2,928.41	3.79	1,355.00
	2006	2,770.94	170.64	274.46	3.78	54.58	745.58	229.40	961.62	1,191.01	2,712.18	3.82	1,326.90
	2007	2,298.89	139.89	300.11	3.78	54.58	622.74	208.06	863.67	1,071.73	2,230.72	3.35	1,069.28
	2008	1,906.24	127.08	300.98	3.78	54.58	523.11	187.89	823.85	1,011.74	1,845.44	1.55	835.08
	2009	2,285.43	149.63	286.40	3.78	54.58	614.40	210.44	899.21	1,109.65	2,224.62	2.06	1,053.49
	2010	1,803.07	112.58	300.89	3.78	54.58	420.71	190.73	822.78	1,013.50	1,724.93	1.26	822.39
	Mean 2001–10	2,411.74	153.53	280.82	3.78	54.58	675.53	215.14	902.39	1,117.53	2,350.12	2.91	1,098.13

[1]Excludes Sand Island and Ford Island.

Table 2-2. Mean annual water-budget components by depth.

[Septic, septic-system leachate;Total ET, total evapotranspiration, which includes canopy evaporation; net precipitation, rainfall plus fog for most areas, rainfall plus fog minus canopy interception for forested areas. Components may not balance because of rounding and direct recharge]

Island	Period	Water-budget estimate (inches per year)											
		Rainfall	Fog	Irrigation	Septic	Direct recharge	Runoff	Canopy evaporation	Actual ET	Total ET	Net precipitation	Storm-drain capture	Recharge
Kaua‘i	2001	69.34	3.49	3.99	0.07	2.11	16.13	9.44	27.86	37.30	63.39	0.06	25.03
	2002	75.59	3.63	3.47	0.07	2.11	18.38	9.94	28.75	38.69	69.27	0.09	27.70
	2003	75.44	3.75	3.48	0.07	2.11	17.09	10.23	29.81	40.04	68.97	0.09	26.92
	2004	108.26	5.21	2.96	0.07	2.11	28.93	12.47	32.81	45.28	100.99	0.16	42.85
	2005	75.79	3.86	3.52	0.07	2.11	20.02	9.81	27.53	37.35	69.83	0.09	28.32
	2006	105.14	4.56	3.10	0.07	2.11	27.15	11.94	29.73	41.67	97.77	0.22	45.85
	2007	77.02	3.49	3.23	0.07	2.11	16.66	10.09	27.42	37.51	70.42	0.13	30.31
	2008	79.05	3.87	3.24	0.07	2.11	19.40	10.15	26.22	36.38	72.77	0.12	31.15
	2009	70.26	3.26	3.35	0.07	2.11	18.45	9.20	26.34	35.54	64.32	0.07	24.95
	2010	64.33	3.17	2.01	0.07	2.11	14.98	9.08	23.25	32.32	58.43	0.07	23.36
	Mean 2001–10	80.02	3.83	3.23	0.07	2.11	19.72	10.23	27.97	38.21	73.62	0.11	30.65
O‘ahu[1]	2001	47.32	0.28	4.43	0.05	0.73	5.55	7.02	24.85	31.87	40.58	0.70	14.92
	2002	52.11	0.29	4.27	0.05	0.73	7.03	7.34	25.92	33.26	45.07	0.98	16.91
	2003	55.31	0.35	4.13	0.05	0.73	7.43	7.63	26.01	33.64	48.03	1.14	18.10
	2004	92.51	0.53	2.90	0.05	0.73	15.03	10.69	31.91	42.60	82.34	2.64	36.02
	2005	62.31	0.33	3.94	0.05	0.73	9.55	8.20	27.74	35.94	54.44	1.36	21.15
	2006	74.67	0.42	3.91	0.05	0.73	11.55	9.01	28.35	37.37	66.08	2.10	29.05
	2007	57.69	0.35	4.19	0.05	0.73	7.36	7.83	26.11	33.94	50.20	1.27	20.07
	2008	56.85	0.35	4.28	0.05	0.73	7.72	7.76	25.55	33.32	49.43	1.19	19.60
	2009	44.34	0.26	4.54	0.05	0.73	5.80	6.67	24.52	31.19	37.93	0.73	12.80
	2010	52.70	0.30	4.48	0.05	0.73	6.63	7.41	24.75	32.16	45.59	1.20	17.92
	Mean 2001–10	59.58	0.35	4.11	0.05	0.73	8.36	7.96	26.57	34.53	51.97	1.33	20.65
Maui	2001	59.79	3.99	8.83	0.11	1.57	16.88	5.76	24.19	29.95	58.02	0.05	26.95
	2002	76.72	4.91	7.41	0.11	1.57	21.75	6.57	27.88	34.45	75.07	0.12	34.59
	2003	60.45	3.91	8.27	0.11	1.57	15.97	5.84	25.19	31.03	58.53	0.06	26.66
	2004	93.84	5.62	6.81	0.11	1.57	29.17	7.32	28.95	36.28	92.14	0.15	42.19
	2005	85.79	5.67	7.49	0.11	1.57	26.70	6.97	28.02	34.99	84.49	0.11	39.09
	2006	79.95	4.92	7.92	0.11	1.57	21.51	6.62	27.74	34.36	78.25	0.11	38.28
	2007	66.33	4.04	8.66	0.11	1.57	17.97	6.00	24.92	30.92	64.36	0.10	30.85
	2008	55.00	3.67	8.68	0.11	1.57	15.09	5.42	23.77	29.19	53.25	0.04	24.09
	2009	65.94	4.32	8.26	0.11	1.57	17.73	6.07	25.94	32.02	64.19	0.06	30.40
	2010	52.02	3.25	8.68	0.11	1.57	12.14	5.50	23.74	29.24	49.77	0.04	23.73
	Mean 2001–10	69.58	4.43	8.10	0.11	1.57	19.49	6.21	26.04	32.24	67.81	0.08	31.68

[1]Excludes Sand Island and Ford Island.

Menlo Park Publishing Service Center, California
Manuscript approved for publication February 21, 2018
Edited by Katherine Jacques
Layout by Cory Hurd

ISSN 2328-0328 (online)
https://doi.org/10.3133/sir20155164